Université de Montréal

The roles of EPHs/EFNs in chromaffin cell biology

Par

Wei Shi

Département de Sciences Biomédicales

Faculté de Médecine

Thèse présentée à la Faculté des études supérieures en vue de l'obtention du grade de Philosophiae Doctor (Ph.D.) en sciences biomédicales

Février 2021

Université de Montréal

Département de Sciences Biomédicales, Faculté de Médecine

Cette thèse intitulée

The roles of EPHs/EFNs in chromaffin cell biology

Présentée par

Wei Shi

A été évaluée par un jury composé des personnes suivantes

Julie Lavoie
Président-rapporteur

Jiangping Wu
Directeur de recherche

Hongyu Luo
Codirecteur

Madhu Anand-Srivastava
Membre du jury

Nicolas Bisson
Examinateur externe

Résumé

Les récepteurs Erythropoietin-producing hepatocyte (EPH) constituent la plus grande famille de récepteurs à activité tyrosine kinase transmembranaires. Leur activité kinase peut être induite par leurs ligands, les éphrines (EFN). Une fois activés, ces récepteurs sont impliqués dans la régulation de la fonction cellulaire par transduction antérograde ou rétrograde du signal EPH-EFN. Au cours de la dernière décennie, nos études ont démontré que les EPH / EFN jouent un rôle important dans la régulation de la pression artérielle par la modulation de la contractilité des cellules musculaires lisses vasculaires (VSMC). EPHB6, EFNB1 et EFNB3 ont un effet négatif sur la contractilité des VSMC et la pression artérielle, tandis que EPHB4 et EFNB2 montrent un effet positif. La famille EPH / EFN est donc un nouveau système *yin* et *yang* qui ajuste finement l'homéostasie de la pression artérielle. Nous avons également constaté que les catécholamines urinaires de 24 h sont réduites chez les souris mâles EPHB6 knockout (KO), suggérant que l'EPHB6 régule la pression artérielle non seulement via les VSMC mais aussi par la sécrétion de catécholamine (CAT). La régulation de CAT par l'EPHB6 dépend de la testostérone car (1) les niveaux réduits de CAT ne sont pas observés chez les souris femelles EPHB6 KO ; et (2) la castration chez les souris mâles EPHB6 KO ramène la CAT à des niveaux normaux. Durant ma thèse, nous avons étudié le mécanisme impliqué dans la régulation de la sécrétion et de la synthèse des catécholamines chez les cellules chromaffines des glandes surrénales (AGCC) par la voie de signalisation de l'EPHB6. En *ex vivo*, la teneur totale en épinéphrine et la sécrétion d'épinéphrine déclenchée par l'acétylcholine (ACh) sont toutes deux réduites dans les glandes surrénales venant des souris KO mâles mais pas dans celles venant des femelles ou de mâles castrés. Ensuite, nous avons observé une diminution de l'afflux de Ca^{2+} dépendant de l'ACh dans les AGCC venant des souris mâles EPHB6 KO, ce qui découle de l'effet non-génomique de la testostérone. En appliquant le *patch clamping* de cellules entières sur les AGCC, nous avons démontré que la diminution d'afflux de Ca^{2+} dans ces cellules est causée par l'augmentation des courants de potassium à grande conductance activé par le calcium (BK). En utilisant l'enregistrement ampérométrique, nous avons constaté que la sécrétion de CAT par les AGCC est compromise en l'absence d'EPHB6. Nous avons également observé une diminution du

désassemblage de la F-actine corticale dans les AGCC venant de souris mâles KO associée à une diminution de l'exocytose des vésicules contenant es catécholamines. Ces deux phénomènes n'ont pas été observés chez les femelles KO ni chez les mâles castrés. Des études complémentaires ont montré que le désassemblage défectueux de la F-actine dans les AGCC est régulé par la signalisation inverse de l'EPHB6 à l'EFNB1 via deux voies de signalisations différentes : la voie du membre A de la famille des homologues Ras (RHOA) et la voie de la tyrosine kinase proto-oncogène de la famille Src (FYN) / proto-oncogène c-ABL / la calponine monooxygénase associée aux microtubules et le domaine LIM contenant 1 (MICAL-1). En outre, nous avons observé que la diminution de la teneur totale en épinéphrine dans la glande surrénale venant des souris mâles KO est causée par une expression altérée de la tyrosine hydroxylase (TH), qui est l'enzyme limitant la vitesse dans la biosynthèse des CAT. L'effet non génomique de la testostérone a également participé dans ce processus. Nous avons révélé que la signalisation inverse d'EPHB6 à EFNB1 contribue à la surexpression de TH dans les AGCC par l'augmentation de son niveau de transcription. La voie en aval de cette signalisation inverse implique la petite famille Rac GTPase 1 (RAC1) / MAP kinase kinase 7 (MKK7) / c-Jun N-terminal kinase (JNK) / proto-oncogène c-Jun / activator protein 1 (AP1) / réponse de croissance précoce 1 (EGR1).

Ces travaux démontrent pour la première fois un rôle spécifique de la famille EPH / EFN dans la régulation de la biologie médullaire de la glande surrénale. La signalisation rétrograde d'EPHB6 via EFNB1 régule la synthèse et la sécrétion des catécholamines de concert avec la testostérone dans les AGCC.

Mots-clés : Erythropoietin-producing hepatocyte (EPH), éphrines (EFN), cellules chromaffines des glandes surrénales, catécholamine, testostérone.

Abstract

Erythropoietin-producing hepatocyte (Eph) receptors are the largest family of cell surface transmembrane receptor tyrosine kinases. Their kinase activity can be activated by their ligands, ephrins (EFNs), and involved in cell function regulation through either EPH-EFN forward or reverse signaling transduction. In the last decade, we have revealed the previously unknown function of EPHs/EFNs in the regulation of blood pressure by modulating the contractility of vascular smooth muscle cells (VSMCs). EPHB6, EFNB1, and EFNB3 have a negative effect on the VSMCs contractility and blood pressure, while EPHB4 and EFNB2 show a positive effect instead. Thus, EPH/EFN family is a novel yin and yang system that finely tunes blood pressure homeostasis. EPHB6 also targets cells responsible for catecholamine (CAT) secretion in addition to the VSMCs, since we found that the 24-h urine catecholamines are reduced in male EPHB6 knockout (KO) mice. This phenotype in EPHB6 KO mice is testosterone-dependent because the reduced CAT levels are not observed in female KO mice; castration in KO male mice reverts the CAT levels to a normal range. In this research, we investigated the mechanism for the regulation of catecholamine secretion and synthesis in adrenal gland chromaffin cells (AGCCs) by EPHB6 signaling. In *ex vivo*, the total content of epinephrine and the acetylcholine (ACh)-triggered epinephrine secretion were both reduced in the adrenal gland from KO male but not female or castrated mice. Then, we found a reduced ACh-dependent Ca^{2+} influx in AGCCs from male EPHB6 KO mice, and this effect depended on the non-genomic effect of testosterone. The results of whole-cell patch clamping on AGCCs indicated that the enhanced large-conductance calcium-activated potassium (BK) currents were responsible for the reduced Ca^{2+} influx in these cells. Using amperometry recording, we found that CAT secretion by AGCCs was compromised in the absence of EPHB6. The cortical F-actin disassembly in AGCCs from KO male but not female or castrated mice was reduced, accompanied by decreased catecholamine vesicle exocytosis. Further study showed such defective F-actin disassembly in AGCCs was regulated by the reverse signaling from EPHB6 to EFNB1 via the Ras homolog family member A (RHOA) and proto-oncogene Src family tyrosine kinase (FYN)/proto-oncogene c-ABL/microtubule-associated monooxygenase calponin and LIM domain containing 1 (MICAL-1) pathways. Further, we observed that the reduced total content of epinephrine in the

adrenal gland from male KO mice was caused by impaired expression of tyrosine hydroxylase (TH), the rate-limiting enzyme in CAT biosynthesis. The non-genomic effect of testosterone was also involved in this process. We revealed that the reverse signaling from EPHB6 to EFNB1 contributed to the up-regulation of TH expression in AGCCs by enhancing its transcription. The downstream pathway of this reverse signaling involved Rac family small GTPase 1 (RAC1)/MAP kinase kinase 7 (MKK7)/c-Jun N-terminal kinase (JNK)/ proto-oncogene c-Jun/activator protein 1 (AP1)/early growth response 1 (EGR1).

The present research, for the first time, revealed the specific role of the EPH/EFN family on the regulation of the adrenal gland medullary biology. The EPHB6 reverse signaling through EFNB1 in concert with testosterone regulates the catecholamine synthesis and secretion in AGCCs.

Keywords: Erythropoietin-producing hepatocyte (EPH), ephrins (EFN), adrenal gland chromaffin cell, catecholamine, testosterone.

.

Table des matières

Liste des figures

Liste des sigles et abréviations

ABPs: Actin-binding proteins

ACE: Angiotensin-converting enzyme

ACh: Acetylcholine

aFGF: Acidic fibroblast growth factor

AGCCs: Adrenal gland chromaffin cells

AP1: Activator protein 1

AR: Androgen receptor

AREs: Androgen response elements

ARF1: ADP-ribosylation factor 1

ARP: Actin-related protein

AT1: Angiotensin II type 1

AT2: Angiotensin II type 2

BH4: Tetrahydrobiopterin

BK: Big potassium

BSA: Bovine serum albumin

CaMKII: Ca2+/calmodulin-dependent protein kinase II

CAPS: Ca2+-activated dependent activator protein for secretion

CAT: Catecholamine

CNS: Central nervous system

COMT: Catechol-O-methyltransferases

CRD: Cysteine rich domain

CRE/CaRE: Cyclic AMP/Ca2+ responsive element

CREB: cAMP-responsive element-binding protein

DA: Dopamine

DBD: DNA binding domain

DHT: Dihydrotestosterone

EFNs: Ephrins

EGF: Epidermal growth factor

EGR1: Early growth response 1

EPH: Erythropoietin-producing hepatocyte

Epi: Epinephrine

ER: Estrogen receptor

ERE: Estrogen response element

ERK1/2: Extracellular-signal-regulated kinase 1/2

ET-1: Endothelin-1

FCG: Four Core Genotype

FGF: Fibroblast growth factor

GAPs: GTPase-activating proteins

GDI: Guanine nucleotide dissociating inhibitor

GEFs: Guanine nucleotide exchange factors

GI: Gastrointestinal

GPCR: G protein-coupled receptor

GPER: G protein-coupled membrane estrogen receptor

GRB: Growth factor receptor-bound protein

GRE: Glucocorticoid response element

Grip: Glutamate receptor-interacting protein

HRE: Hypoxia-responsive element

HVA: Homovanillic acid

IGF: Insulin-like growth factor

IP-3: Inositol triphosphate

IRP: Immediately releasable pool

JAK2: Janus kinase 2

JNK: c-Jun N-terminal kinase

KO: Knockout

LBD: Ligand binding globular domain

LD: Linkage disequilibrium

LIMKs: LIM-kinase proteins

LPS: Lipopolysaccharide

MAO: Monoamine oxidases

MAPK: Mitogen-activated protein kinase

MAPKAPK-2: Mitogen-activated protein kinase-activating protein kinase II

MICAL-1: Microtubule-associated monooxygenase calponin and LIM domain containing 1

miRNAs: MicroRNAs

MKK7: MAP kinase kinase 7

MLCK: Myosin light chain kinase

MLCP: Myosin light chain phosphatase

MMP-8: Matrix metalloproteinase-8

MUNC: Mammalian uncoordinated

mTORC1: Mammalian Target of Rapamycin complex 1

nAChR: Nicotinic ACh receptor

NCK: Non-catalytic region of tyrosine kinase adaptor protein

NE: Norepinephrine

NF-kB: Nuclear factor κB

NO: Nitric oxide

NPF: Nucleation promoting factors

NPY: Neuropeptide Y

NTD: N-terminal transcriptional regulation domain

PACAP: Pituitary adenylate cyclase-activating polypeptide

PAK: Serine/threonine-protein kinase

PBS: Phosphate-buffered saline

PCBP: Poly (C) binding protein

PCOS: Polycystic ovary syndrome

PCR: Polymerase chain reaction

PDCC: Phospho-dependent depolarizing cation conductance

PICK1: Protein Interacting with C Kinase-1

PIP2: Phospholipid phosphoinositol 4,5-bisphosphate

PI3K: Phosphatidylinositol 3-kinase

PKC: Protein kinase C

PLC: Phospholipase C

PP2A: Phosphoprotein phosphatases 2A

PSA: Prostate-specific antigen

PSF: Pre-spike feet

RAAS: Renin-angiotensin-aldosterone system

RAC1: Rac family small GTPase 1

Redox: Reduction-oxidation

RHOA: Ras homolog family member A

ROS: Reactive oxygen species

RRP: Readily releasable pool

RTKs: Receptor tyrosine kinases

SAM: Sterile alpha motif

SFK: Src family kinase

SH2: Src-homology-2

SNAP-25: Synaptosomal-associated protein 25

SNP: Single nucleotide polymorphism

Sp1: Specificity protein 1

SREs: Serum-responsive elements

SRP: Slow releasable pool

SRY: Sex-determining region Y

STAT3: Signal transducer and activator of transcription 3

TCR: T cell receptor

TH: Tyrosine hydroxylase

TIAM1: TIAM Rac1 Associated GEF 1

TMPRSS2: Transmembrane serine protease 2

TRKB: Tropomyosin receptor kinase B

TRT: Testosterone replacement therapy

T-β4: Thymosin β4

UTR: Untranslated region

VGCCs: Voltage-gated Ca2+ channels

VMA: Vanillylmandelic acid

VSMCs: Vascular smooth muscle cells

WASH: WASP and SCAR homologue

WASP: Wiskott–Aldrich syndrome protein

WAVE: WASP family verprolin-homologous protein

WT: Wild type

Remerciements

Throughout the whole PH.D. program and thesis writing, I have received a lot of support and assistance.

I would first like to thank my supervisor, Dr. Jiangping Wu, who provides me a rare opportunity to study at the University of Montreal for the PH.D. degree. When I first came, I have no scientific research experience at all, just like a blank sheet of paper. Your careful guidance helps me establish a set of scientific research thinking, improve my experimental skills, and push my work to a high level. Your words and deeds guide me to learn how to be an excellent scientist in my future career. It's a great honor for me to be your student. I would also like to thank my co-supervisor, Dr. Hongyu Luo. Thank you for teaching me various experimental techniques. You always strive for excellence in any work and make dauntless and persistent efforts to pursue goals. I am full of respect for your spirit and attitude.

To my thesis committee members, Professor Julie Lavoie, Professor Madhu Anand-Srivastava, and Professor Nicolas Bisson, I would like to thank you for your valuable opinions and suggestions on my thesis. Your generous help would make my work more excellent.

I would like to acknowledge my colleagues and friends in CRCHUM. Without your wonderful collaboration and support, I can't successfully finish my PH.D. program. Special thanks are given to Linjiang Lao, my best friend in Montreal. I benefit a lot from discussing with you.

Finally, I would especially like to thank my family. Your generous financial support allows me to complete my study without worry. No matter sorrow or joy, you are always with me.

Sincere thanks to everyone who helped me!

Wei Shi, February 2021

Chapitre 1 – INTRODUCTION

1.1 Function and signal pathways of EPHs/EFNs

Erythropoietin-producing hepatocyte (EPH) receptors are the largest family of cell surface transmembrane receptor tyrosine kinases (RTKs), which can transduce the extracellular signals to the cell interior through activating their kinase activity after ligand binding (Lisabeth et al., 2013). In 1987, Hirai et al. (Hirai et al., 1987) first described an EPH protein as a novel cell surface tyrosine kinase receptor and its potential role in the neoplastic process of some tumors. After that, many other members of the EPH family and their ligands (named Ephrins (EFNs)) were identified. (Lindberg and Hunter, 1990; Sajjadi et al., 1991; Bohme et al., 1993; Cerretti et al., 1995; Fox et al., 1995; Gurniak and Berg, 1996; Lee et al., 1996; Stein et al., 1996)

1.1.1 EPH/EFN family members and structure

According to sequence similarity and ligand affinity of the EPH receptors, they are subdivided into "A" and "B" subfamilies (Lisabeth et al., 2013). To date, 14 EPH receptors (EPHA1-EPHA8, EPHA10, and EPHB1-B4, EPHB6) and 8 EFNs (EFNA1-EFNA5, EFNB1-EFNB3) have been identified in mammals (Alfaro et al., 2020). In most cases, EPHA receptors promiscuously bind to EFNA ligands and EPHB receptors to EFNB ligands (Murai and Pasquale, 2004; Pasquale, 2005). However, Some EPHs such as EPHA2, EPHA3, EPHA4, and EPHB2 can also bind to the different subclasses of EFNs. Unlike other EPH receptors, EPHA10 and EPHB6 are tyrosine-kinase-defective receptors because their conserved kinase domains have been mutated, resulting in a lack of kinase activity (Lisabeth et al., 2013).

The EPH receptors are transmembrane proteins. The extracellular regions of EPHs are composed of a ligand-binding globular domain (LBD), a cysteine-rich domain (CRD), and two fibronectin-type III repeats. Their cytoplasmic part comprises a juxtamembrane domain, a tyrosine kinase domain, a sterile alpha motif (SAM), and a PDZ-binding motif (Fig. 1) (Kullander and Klein, 2002). Both EFN

subfamilies have a conserved EPH receptor-binding domain in the extracellular region. EFNAs connect to the cell membrane via a glycosylphosphatidylinositol anchor, while EFNBs are composed of a transmembrane segment and a short cytoplasmic tail (Fig. 1).

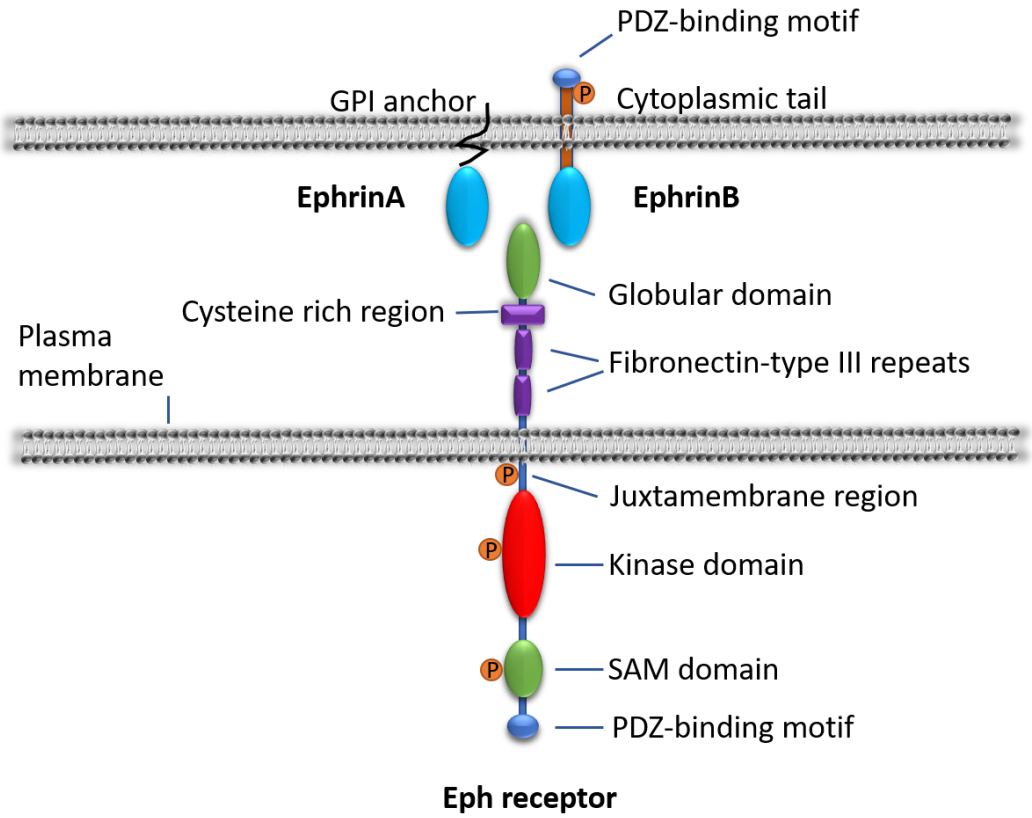

Figure 1. – Domain structure of EPH receptors and EFNs. Image modified from Kullander and Klein, 2002 (Kullander and Klein, 2002).

1.1.2 EPH/EFN Binding and Receptor Activation

EPH/EFN signaling is triggered by direct cell-cell contact and molecule clustering. EPH receptors and EFNs can carry out both *trans* (cell-cell interaction) and *cis* (within the same cell) signal transduction (Dravis and Henkemeyer, 2011). The binding of EFNs to the EPH receptors leads to aggregation of these two molecules in different clusters in the corresponding plasma membrane,

thus forming the bidirectional signaling center in which activated EPH receptors send the forward signaling into the EPH receptor-expressing cell, while EFNs are responsible for the reverse signaling sent into the EFN ligand-expressing cell (Himanen et al., 2001).

According to crystallography studies, the EPH/EFN clusters are formed via broad EPH/EPH, EPH/EFN, and EFN/EFN interactions. Before cell-cell contact, the EPH molecules are pre-clustered with each other on the cell surface through some extracellular domains, most probably in the LBD region and CRD region called the clustering interface (Himanen et al., 2010). EFNs can also form low-affinity EFN-EFN homodimers (Toth et al., 2001). Upon ligand binding, EPH receptors and EFNs can form high-affinity EPH-EFN heterodimers at a 1:1 ratio. This reorients these two molecules and creates a complementary interaction surface to make their homodimers more stable. Then these two pairs of EPH-EFN heterodimers can join into a ring-like tetrameric complex via EPH-EPH interactions in the clustering interface (Murai and Pasquale, 2003)（Fig. 2）. The process will continue, and hundreds of receptors will be recruited to generate large-sized clusters (Himanen et al., 2010; Xu et al., 2013). This EPH/EFN tetrameric complex is critical for bidirectional signaling. It fixes the orientation of the receptors and ligands and unleashes the tyrosine kinase domains of paired EPH receptors into an active conformation, and further trans-autophosphorylate each other and launch the forward signaling. While the EFNs are phosphorylated at their cytoplasmic tail and activated upon the repositioning of the EFN transmembrane and cytoplasmic domains to launch the reverse signaling (Himanen et al., 2001). What's more, the degree of EPH receptors activation depends on the oligomerization state of the EFNs and vice versa. *In vitro*, soluble EFN-Fc fusion proteins or anti-EPH antibodies require pre-clustering into oligomers to induce strong EPH receptor phosphorylation and downstream biological reactions. This feature is also unique in ligand-receptor interaction in the EPH/EFN signaling system (Davis et al., 1994).

Interestingly, this EPH/EFN complex can also recruit unliganded EPHs to participate in this assembly via homotypic EPH LBD-FNIII interaction, which can significantly expand the size of the signaling site on the cell surface during the EPH/EFN contact (Xu et al., 2013). This observation indicates the EPH receptors can be activated without direct ligand binding. This ligand-independent EPH receptor activation is also mentioned in Wimmer-Kleikamp's research. They

have found that EPHA3 mutants with impaired EFN-binding capacity can be recruited to the wild-type EPHA3/EFNA5 clusters and be phosphorylated (Wimmer-Kleikamp et al., 2004). Janes et al. even suggest that EPHA and EPHB receptors can be recruited to a cluster complex and phosphorylated upon ligand activation of one or the other receptor class via EPH heterologous interaction (Janes et al., 2011). Furthermore, the kinase-inactive mutant EPHA3 receptor can be cross-activated with wild-type EPHB2 receptor upon EFNB1 binding. Besides EPH/EPH receptor interactions, there are other cell-surface molecules that can be recruited to EPH clusters, such as EPH/C-X-C chemokine receptor type 4 interactions (Salvucci et al., 2006), EPH/ N-Methyl-D-aspartic acid or N-Methyl-D-aspartate interactions (Drescher, 2000), or EPH/FGFR (fibroblast growth factor receptors) interactions (Fukai et al., 2008), regulating their respective signaling. Such evidence shows that both ligand-induced and ligand-independent EPH receptor activation are important in the EPH/EFN signaling modulation.

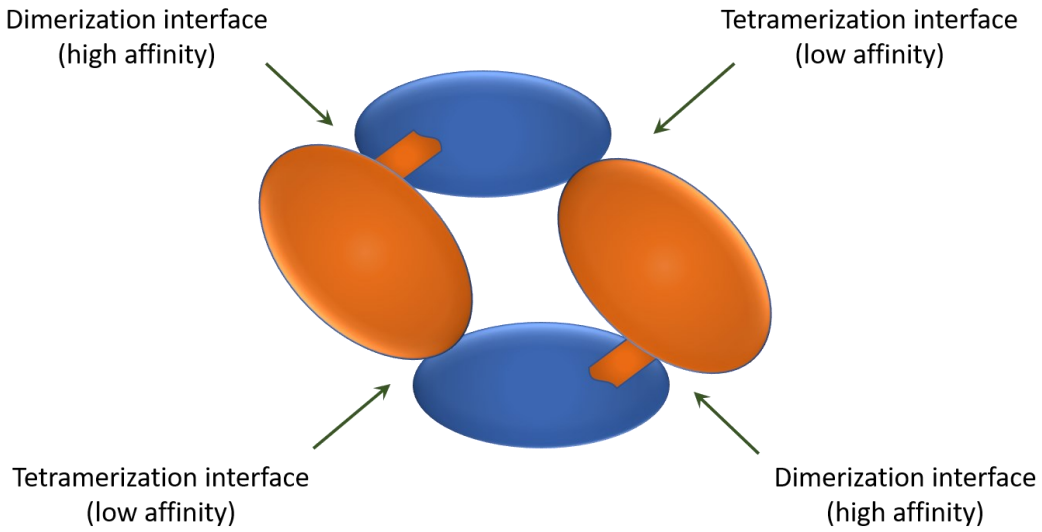

Figure 2. – EPH/EFN tetramer formation. Image modified from Murai and Pasquale, 2003 (Murai and Pasquale, 2003).

1.1.3 EPH/EFN forward signaling

Like the prototypical RTK signaling, the EPH/EFN forward signaling is triggered by the binding of the extracellular ligand EFNs to EPHs to activate the latter's cytoplasmic kinase domain. Upon the EFN binding, the EPH/EFN clusters recruit more liganded or unliganded EPH receptors to form oligomers and then amplify the signaling. This signaling autophosphorylates several tyrosine residues in the cytoplasmic region of the receptors, including the juxtamembrane domain and kinase domain. Autophosphorylation of two conserved tyrosines in the juxtamembrane domain is considered a critical step to fully activate the receptor's tyrosine kinase domain (Binns et al., 2000; Wybenga-Groot et al., 2001). To understand the role of the juxtamembrane domain in the tyrosine kinase receptor activation, Binns modified the EPHA4 cytoplasmic part by replacing the two conserved juxtamembrane tyrosine residues with phenylalanine and found this mutant causes significantly defective catalytic activation. This result indicates the inhibitory role of the juxtamembrane domain in EPH receptor kinase activation (Binns et al., 2000). Structural studies further explain this inhibitory role. The helical conformation of the juxtamembrane domain distorts the kinase domain, preventing the formation of an active conformation. Once the two conserved juxtamembrane tyrosine residues are phosphorylated, the interaction between the juxtamembrane domain and kinase domain is disturbed, allowing the kinase domain to escape from the inhibition to get fully activated (Wybenga-Groot et al., 2001).

The autophosphorylation not only results in kinase activation but also provides docking sites for cytoplasmic signaling molecules which contain an Src-homology-2 (SH2) domain, recruiting nonreceptor tyrosine kinases of the Src or Abl families and adaptors such as growth factor receptor-bound protein (Grb) 2, non-catalytic region of tyrosine kinase adaptor protein (Nck) (Kullander and Klein, 2002), and SH2 domain-containing adapter protein B (Wagner et al., 2020). The SAM domain will interact with some downstream effectors, such as the guanine nucleotide exchange factor VAV3 (Fang et al., 2008). The PDZ binding domain also recruits the PDZ domain-containing proteins, including actin cytoskeleton regulators, Ras and Rho family GTPases (Linnemann et al., 1999; Noren and Pasquale, 2004), and adaptors, such as protein Interacting with C Kinase-1 (PICK1) and glutamate receptor-interacting protein (Grip) (Torres et al., 1998). These interactions of the molecules are pivotal for signaling transduction.

EPH/EFN signaling is well-known in regulating cell morphology, adhesion, migration, invasion, proliferation, and differentiation upon cell-cell contact-dependent communication (Pasquale, 2005). The downstream signaling pathways of EPH/EFN signaling have been widely studied after the discovery of EPH/EFN. The most classic signaling pathway is the connection between EPH/EFN and the Rho and Ras GTPases (Noren and Pasquale, 2004). The EFN-induced EPH forward signaling acts as a switch to activate or inactivate the GTPases through regulating both guanine nucleotide exchange factors (GEFs) and GTPase-activating proteins (GAPs). There are three prominent members in Rho family GTPases, RhoA, Rac1, and Cdc42. The EFN-induced cell repulsion requires the activation of Rho family GTPases, particularly Rac1 and RhoA (Wahl et al., 2000; Jurney et al., 2002). The internalization of EPH/EFN complexes mainly depends on Rac activity, while RhoA is thought to promote disassembly of filamentous actin (F-actin) and actomyosin contractility. EFNA-induced forward signaling modulates the activity of Ephexin, a GEF for Rho GTPases, enhancing RhoA activity and inhibiting Cdc42 and Rac1 activity. Such effects regulate growth cone motility in retinal ganglion cells (Shamah et al., 2001). Apart from Ephexin, Rho family GEF Vav2 also activates RhoA when EPHA receptors are activated (Batson et al., 2014). Furthermore, Rac1-dependent EPH-EFN endocytosis is critical in cell repulsion. Rho family GEF Vav2 is first revealed as a link between the activated EPH receptors and Rac-dependent endocytosis, which switches the EPH forward signaling from adhesion to repulsion (Cowan et al., 2005). In addition to the Vav family GEFs, TIAM Rac1 Associated GEF 1 (Tiam1) can be recruited to the EPHA2 receptor upon the soluble EFNA1 stimulation. This further activates Rac1 GTPase, causing actin cytoskeletal remodeling and cortical neurons to extend neuritis (Tanaka et al., 2004). A similar effect of Tiam1-Rac on dendritic spine morphogenesis is found in the EPHB2 forward signaling pathway (Gaitanos et al., 2016). EPHB receptor activation leads to Rac1-dependent dendritic spine formation induced by Rac-GEF Tiam1. At the same time, the Rac-GAP is activated to prevent Rac1-mediated receptor from internalization to maintain an optimal level of Rac1 activity (Um et al., 2014). Therefore, the forward migration of the growth cone depends on the dynamic balance among RhoA, Rac1, and Cdc42 activities. Besides cell repulsion, EPH forward signaling also mediated many other cellular processes through the Rho GTPases. EFNB2-induced EPHA4 forward signaling regulates the Rho-dependent actin-filament polymerization to help monocytes to adhere to endothelial cells (Poitz

et al., 2015). EPHB3 and EPHB4 forward signaling induced by EFNB2 activate Cdc42 GTPase in metastatic PC-3 cells promotes their migration towards fibroblasts (Astin et al., 2010). Rho GEF kalirin is recruited to EPHB receptors, triggered by the EFN/EPH trans-synaptic signaling, and sequentially activates Rac1 and its effector Serine/threonine-protein kinase (PAK) to regulate the morphological development of the dendritic spines (Penzes et al., 2003). There are some other studies showing the extensive role of the EPH forward signaling and Rho family GTPases in physiology. For example, EFNA1-induced EPHA4 activity modulates blood-brain barrier injury in a RhoA activity-dependent way (Chen et al., 2018). EPH receptors work with Rho GTPases to regulate glioblastoma invasion (de Gooijer et al., 2018).

Like the Rho family GTPases, the Ras family GTPases are also widely regulated by the EPH receptor forward signaling. As opposed to other RTK members, EPH receptor forward signaling inhibits the Ras-mitogen-activated protein kinase (MAPK) pathway during cell physiological process regulation. In many cell lines, EPH forward signaling inhibits the extracellular-signal-regulated kinase 1/2 (ERK1/2) activity (Elowe et al., 2001; Miao et al., 2001; Minami et al., 2011). Such an inhibitory effect is dependent on p120RasGAP, which can inhibit Ras activity by elevating the intrinsic rate of GTP hydrolysis. For example, during the ascidian embryonic differentiation, the fibroblast growth factor (FGF)-dependent activation of ERK1/2 is attenuated by EPH/EFN forward-signaling through p120RasGAP (Haupaix et al., 2013).

EPHB6 forward signaling recruits the adaptor protein GRB2 and triggers the activation of Ras GTPase to enhance cell proliferation through the Ras-ERK pathway (Toosi et al., 2018). In PC12 cells, EPHA4 induces an increase of MAPK activity upon EFNA5 treatment (Shin et al., 2008). Furthermore, there are some other reports indicating that the inactivation of Rap1, another member of Ras family GTPase, by activating RapGAP or inhibiting the GEF C3G is critical for EFNs-induced cell retraction (Riedl et al., 2005; Richter et al., 2007). In addition to the negative effect of the EPH forward signaling on the Ras-ERK pathway, EPH receptors activate Ras GTPases in some sporadic studies (Vindis et al., 2003; Bush and Soriano, 2010).

Similar to their effects on the Ras family, EPHs mainly inactivate kinase Akt, which is involved in apoptosis, cell proliferation, and cell migration, but sometimes they activate it. In PC3 prostate

cancer cells, EFNA1-induced EPHA2 activity dephosphorylates Akt at T308 and S473 through a phosphatase, leading to the inactivation of the Akt-mTORC1 (mammalian Target of Rapamycin complex 1) oncogenic pathway to decrease cell growth and migration (Yang et al., 2011). This observation is also reported in other cancer cell types (Miao et al., 2009; Lin et al., 2015). The EPH receptor can act both upstream and downstream of Akt (Shi and Wang, 2018; Stallaert et al., 2018). However, the positive effect of EPH forward signaling on Akt activity through the phosphatidylinositol 3-kinase (PI3K) - Akt signaling axis in cell migration is also demonstrated in some studies (Chang et al., 2008; Jiang et al., 2015).

1.1.4 EPH/EFN reverse signaling

The EFNs also can transmit "reverse signaling" into the cell after the stimulation from EPH receptors during cell-cell contact. Because of the big difference in structure, EFNA and EFNB have different signal transmission methods. Due to the lack of an enzymatic domain, EFNB activation depends on Src family kinase (SFK)-mediated tyrosine phosphorylation in its intracellular domain, which contains five conserved tyrosine residues. EFNB1 has one more tyrosine residue than other EFNBs in the domain. The engagement of EPHBs and EFNBs rapidly recruits the SFKs to the cytoplasmic tyrosine sites of EFNBs, leading to the transient SFKs activation, which further transphosphorylates the EFNBs (Palmer et al., 2002). In the *Xenopus* oocyte system, EPHB receptors can trigger tyrosine phosphorylation of EFNB1 at Tyr298 (Tyr 304 in murine) by SFK and create a binding site for adaptor GRB4/NCK2 to transduce signals (Bong et al., 2004). Another SH2-containing protein, signal transducer and activator of transcription 3 (STAT3), can be recruited by the cytoplasmic domain of EFNB1 after the domain being phosphorylated by Janus kinase 2 (JAK2) (Bong et al., 2007). The downstream STAT3 phosphorylation is observed in the EPHB2-induced EFNB reverse signaling in regulating tumor angiogenesis (Sato et al., 2019). The phosphorylation of EFNB1 at Tyr310 leads to the dissociation of the EFNB1/ Par polarity complex protein-6 complex and the rescue of atypical protein kinase C (PKC) activity by active FGF receptor 1, resulting in the proper establishment of tight junction (Lee et al., 2008).

In addition to the phosphorylation-dependent signaling, EFNB ligands can recruit signaling proteins containing PDZ domains to their carboxyl terminus to transduce signals. According to the PDZ Base, there are approximately 300 PDZ domain-mediated protein-protein interactions involved in cell regulation (Beuming et al., 2005). Transcriptional coactivator with a PDZ-binding motif, TAZ, can bind to the PDZ domain of the EFNB ligand and interact with other transcription factors to regulate cell differentiation and organogenetic development (Strakova et al., 2010; Xing et al., 2010). PDZ-RGS3 is a binding partner of EFNB ligands. It mediates the EFNB reverse signaling and regulates G-protein-related responsiveness to neuronal guidance cues (Lu et al., 2001). GRIP binds to the cytoplasmic part of EFNB1 upon the stimulation of the soluble EPHB2 receptor and provides a scaffold for the assembly of the downstream signaling cluster. Moreover, other kinases are also recruited to form the EFN-GRIP complex, linking EFNB reverse signaling to cellular kinase cascades to transduce signals (Bruckner et al., 1999). Our previous research also reveals the essential role of GRIP1 in EFNB3 reverse signaling mediated blood pressure regulation (Wang et al., 2016b). The EFNB1 reverse signaling promotes cell invasion by activating ADP-ribosylation factor 1 (Arf1) GTPase and increases the secretion of matrix metalloproteinase-8 (MMP-8), which induces extracellular matrix degradation (Tanaka et al., 2007). In the activation of SFK and EFNB induced by EPHB receptors, PTP-BL, a cytoplasmic PDZ domain-containing protein tyrosine phosphatase, is recruited to the EFNB ligands PDZ domain, dephosphorylating both SFK and EFNB to turn off the reverse signaling (Palmer et al., 2002). This is a mechanism to convert phosphotyrosine/SFK-dependent signaling to PDZ-dependent signaling. PTP-BL is well known for its interaction with PTPL1-associated RhoGAP1, and they can work together to inactivate the Rho signaling in actin cytoskeleton dynamics, while the GTPase-activating protein p190RhoGAP acts as the main Src substrate in evoking Rho-mediated actin reorganization (Saras et al., 1997; Brouns et al., 2001). These results demonstrate that the rearrangement of actin cytoskeleton is regulated by EFNB reverse signaling in both phosphotyrosine-dependent and PDZ domain-dependent manners. EPHB2-induced EPH/EFN reverse signaling in hippocampal neurons initiates a negative regulation effect on axonal outgrowth through the RhoA/Rock pathway (Takeuchi et al., 2015). EFNB3 reverse signaling coupled with the SH2/SH3 adaptor protein Grb4/NCK2 mediates axon pruning via the GEFDock180-Rac/Cdc42-PAK pathway (Xu and Henkemeyer, 2009). EPHB reverse

signaling activates Rac-GEF Tiam and Rac GTPase to promote actin polymerization at the EPHB2 internalization site during the cell repulsion process (Gaitanos et al., 2016). These evidences demonstrate the extensive participation of the Rho GTPases in the EFN reverse signaling.

Since the EFNAs lack a cytoplasmic domain, the EFNA reverse signaling is transduced through interaction with non-EFN intracellular partners. A study on retinal ganglion cell axons shows that EFNA can interact *in cis* with the tropomyosin receptor kinase B (TrkB) receptor and enhance the retinal axon branching through the PI-3 kinase/Akt pathway (Xu and Henkemeyer, 2012). In retinal axons, p75 neurotrophin receptors form a complex with EFNA within caveolae along the retinal axons. This results in Fyn-mediated phosphorylation of EFNA to transduce reverse signaling into the cell, leading to axon repulsion (Lim et al., 2008). The reverse signaling through EFNA4 in T cells initiates the phosphorylation of SFKs, such as Lck, Fyn, Syk, and Akt, causing an antiapoptotic effect (Holen et al., 2008). Fyn protein tyrosine kinase is also reported to be activated by EFNA5 reverse signaling to regulate cellular architecture and adhesion (Davy et al., 1999). In addition to the SFKs, MAPKs ERK1/2 is also activated in EFNA5 reverse signaling, regulating axon morphogenesis and guidance (Davy and Robbins, 2000). Although more and more molecules are revealed to be involved in regulating EFNA reverse signaling, the mechanism of which still needs further clarification.

1.1.5 EPHB6

1.1.5.1 Unique feature of EPHB6 signaling

EPHB6 is an innately kinase-dead member of the EPH family. It's widespread in most tissues, and the highest expression is observed in the thymus and brain (Hafner et al., 2004). The sequence analysis of EPHB6 revealed that several key amino acid residues within its kinase domain were absent. This abolishes the kinase activity of EPHB6, so EPHB6 is classified as a pseudokinase (Gurniak and Berg, 1996). Although the tyrosine residues in the conserved activation loop of EPHB6 are missing, the two conserved tyrosine residues in the juxtamembrane region are still retained. The phosphorylation of these two tyrosine residues provides binding sites to SH2

domain-containing proteins or phosphotyrosine binding domain-containing proteins and further triggers the downstream signals to regulate cell function. Thus, unlike most EPH receptors that transduce signals through their kinase activation, EPHB6 participates in the EPH/EFN signaling network mainly via its kinase-independent activity. Many evidences have revealed the specificity of EPHB6 in the EPH/EFN signal transduction. Under the stimulation of EFNB1, EPHB1 could form a stable hetero-complex with EPHB6 resulting in increased EPHB6 phosphorylation, which subsequently recruited the proto-oncogene c-Cbl into EPH receptor complexes without changing the phosphorylation of Cbl for the downstream events. Such kind of cross-talk between EPHs was also reported in the interaction of EPHB6 with EPHB4 (Truitt et al., 2010), EPHB2, and EPHA2 (Fox and Kandpal, 2011). In addition, when exposed to EFNB2, EPHB6 could be phosphorylated by Src family kinase Fyn activity based on their constitutive association (Matsuoka et al., 2005). In these cases, EPHB6 exerted its non-catalytic functions via scaffolding or recruiting other EPHs, SH2 domain-containing proteins, and the adapter proteins. To further understand how EPHB6 functions, a structural analysis of EPHB6 and its oligomerization on the cell surface is required.

So far, we still know little about the complete three-dimensional protein structure of EPHB6. Until very recently, Emilia O. Mason determined the structural organization of the extracellular domain of EPHB6 by X-ray crystallography (Mason et al., 2021). Most parts of the EPHB6 ectodomain were very similar to those observed in the EPHAs. However, some unique structural features of EPHB6 were also revealed to be closely related to its potential functions. For instance, an insert of 11 serine residues within the J-K loop was found inside the LBD of EPHB6, which was not observed in other EPHs. It is speculated that this special structure might interfere with ligand binding, thereby reducing the affinity of EPHB6 for EFNBs. Another unique serine-rich short loop opposite to LBD of EPHB6 was potentially related to the EPH-EPH interactions during the formation of EPH/EFN signaling assemblies on the cell surface. These unique characteristics of EPHB6 determine its distinct mechanism of action in the EPH/EFN signaling pathways. The application of more advanced structural research techniques, such as cryo-electron microscopy, will help us to understand the structure of EPHB6 and its correlation with EPHB6 function more deeply.

1.1.5.2 EPHB6 biological effects

Despite the lack of intrinsic kinase activity, EPHB6 still plays an important role in many biological responses in both normal physiology and malignancy. For example, EPHB6 was reported to regulate the permeability of the tubule cells together with EPHB2, which affected the reabsorption ability of the kidney. A study of inflammatory pain and hyperalgesia showed the expression of EPHB6 in the spinal dorsal horn sensory neurons was important for pain signal transmission (King, 2014). Most recently, EPHB6 was demonstrated to be involved in the regulation of gut homeostasis (Li et al., 2020).

The role of EPHB6 in cancer seems more attractive. EPHB6 is described as a malignancy-suppressing factor due to its preventive effect on aggressive malignancies. The expression of EPHB6 was reported lower in various cancers, such as neuroblastoma, non-small cell lung cancer, and breast cancer (Truitt and Freywald, 2011). Such downregulation of EPHB6 in these cancers was caused by modification of multiple factors at the gene level and posttranscriptional levels, such as mutation, promoter hypermethylation, and transcript destabilization (Truitt and Freywald, 2011). The defective EPHB6 expression showed closely related to the increase of cancer invasion and distant metastasis (Tang et al., 2000; Muller-Tidow et al., 2005; Fox and Kandpal, 2009). This anti-invasive property of EPHB6 was further proved by the evidence that restoration of EPHB6 expression suppressed the metastasis of lung cancer, breast cancer, and colorectal cancer (Yu et al., 2010;Mateo-Lozano et al., 2017;Toosi et al., 2018). The underlying mechanism of EPHB6 anti-invasive action might be related to the enhanced adhesion of the cancer cells caused by EPHB6-induced actin cytoskeleton rearrangements, and the decreased level of metalloproteinases by the EPHB6 signaling (Fox and Kandpal, 2009;Truitt et al., 2010). Interestingly, overexpression of EPHB6 in the cancer cells was also conducive to reducing drug resistance during cancer therapies (El Zawily et al., 2017;Toosi et al., 2018).

In the last 20 years, our lab revealed some novel roles of EPHB6 in the immune system. We first showed the EPHB6 function in T cells in vitro. The proliferation of Jurkat cells was inhibited and turned to apoptosis upon the co-cross-linking of EPHB6 and cluster of differentiation 3 (Luo et al., 2001). While in the normal resting human T cells, the EPHB6 crosslinking by mAb resulted in the co-localization of EPHB6 and T cell receptor (TCR) and further stimulated the T cell proliferation,

which was accompanied by the increased production of lymphokines and the enhanced T cell responses to antigen (Luo et al., 2002). Similar effects on the T cells were also observed upon the stimulation of solid-phase EFNB2 and EFNB3, which are the ligands of EPHB6. The function of EPHB6 in T cells was further clarified in the EPHB6-null mutant mouse model. The absence of EPHB6 led to reduced T cell proliferation and compromised T cell response to TCR stimulation both in vitro and in vivo (Luo et al., 2004). In addition to T cells, the EPHB6 also contributed to the monocyte chemotaxis, which was involved in the development of atherosclerosis (Sakamoto et al., 2011). The critical roles of EPHB6 in the immune system will gradually emerge with the deepening of research.

When we studied the roles of EPHs/EFNs in the cardiovascular system, EPHB6 showed its powerful effect on blood pressure regulation (Luo et al., 2012). The reverse signaling from EFNBs to EPHB6 dampened the VSMCs contraction in vitro. The VSMCs are found within the wall of blood vessels, and their contraction or relaxation determines the vascular tone. Thus, it's supposed to see the enhanced blood vessel contractility and hence the elevated blood pressure when EPHB6 was absent. Surprisingly, the blood pressure presented no significant difference between WT and EPHB6 KO male or female mice. However, after castration, the KO male mice manifested higher blood pressure than their WT counterparts. It indicated that EPHB6 in concert with sex hormones contributed to the blood pressure regulation, and some compensatory feedback mechanisms should be involved in this process. Additional experiments revealed the 24-h urine catecholamines were reduced in EPHB6 KO male mice, which might compensatively offset the VSMCs contraction caused by EPHB6 deletion and keep blood pressure normal in KO male mice. However, such compensation was abolished after castration since the catecholamine levels of castrated KO male mice rose to normal, which might be the reason for the observed increased blood pressure in these mice. As we know, the majority of catecholamines are produced in adrenal gland chromaffin cells in mammals. So, these interesting phenotypes in EPHB6 KO mice indicated that EPHB6 should also target the adrenal gland chromaffin cells and exerted a testosterone-dependent catecholamine regulatory effect. In the next section, we will review the basic knowledge of catecholamines and chromaffin cell biology to explore further the roles of EPHBs/EFNs in this new field.

1.2 Catecholamines

Catecholamines, including dopamine (DA), epinephrine (Epi), and norepinephrine (NE), are very important monoamine neurotransmitters and hormones involved in the physiological regulation of the body. They are mainly produced by the postganglionic fibers of the sympathetic nervous system, adrenal gland, and chromaffin cells. Over 90% of circulating Epi is released by the adrenal medulla, but only 7% of circulating NE is contributed by it. In contrast, NE is widely produced as a neurotransmitter in the central nervous system (CNS), where Epi is much less abundant. Most circulating NE is derived from neurotransmission, whereas the circulating Epi exerts its main effect as a hormone. They together play important roles in the fight-to-flight response by accelerating the heart and lung action, increasing the blood flow to the muscles, and liberating the metabolic energy source for muscular action (Tank and Lee Wong, 2015). DA mainly acts as a neurotransmitter of the CNS. Therefore, it is mainly produced in the dopaminergic neurons in many areas of the brain, particularly the hypothalamus, the substantia nigra, and the ventral tegmental area (Juarez Olguin et al., 2016). It performs crucial neuromodulation tasks in the brain, including reward, movement regulation, motivation, and cognitive function (Klein et al., 2019). Catecholamines are essential signal mediators in normal physiological processes, being responsible for transmitting physiological signals and maintaining body homeostasis. Their serum levels can be used to assist in the diagnosis of endocrine-related diseases, such as hypertension, hyperthyroidism, pheochromocytoma, and neuroblastoma.

1.2.1 Catecholamine biosynthesis and regulation

1.2.1.1 Catecholamine biosynthesis

The catecholamines biosynthesis starts from L-tyrosine. Tyrosine hydroxylase (TH) is the rate-limiting enzyme in the synthesis of catecholamines. It catalyzes the conversion of the L-tyrosine to L-DOPA in the cytoplasm. Then the L-DOPA can be transformed into DA in the presence of DOPA decarboxylase. The DA is transported into the neurotransmitter vesicles and is converted

into NE by DA β-hydroxylase. In the adrenal gland chromaffin cells and some neurons containing phenylethanolamine N-methyltransferase, NE can be converted into Epi (Fig.3).

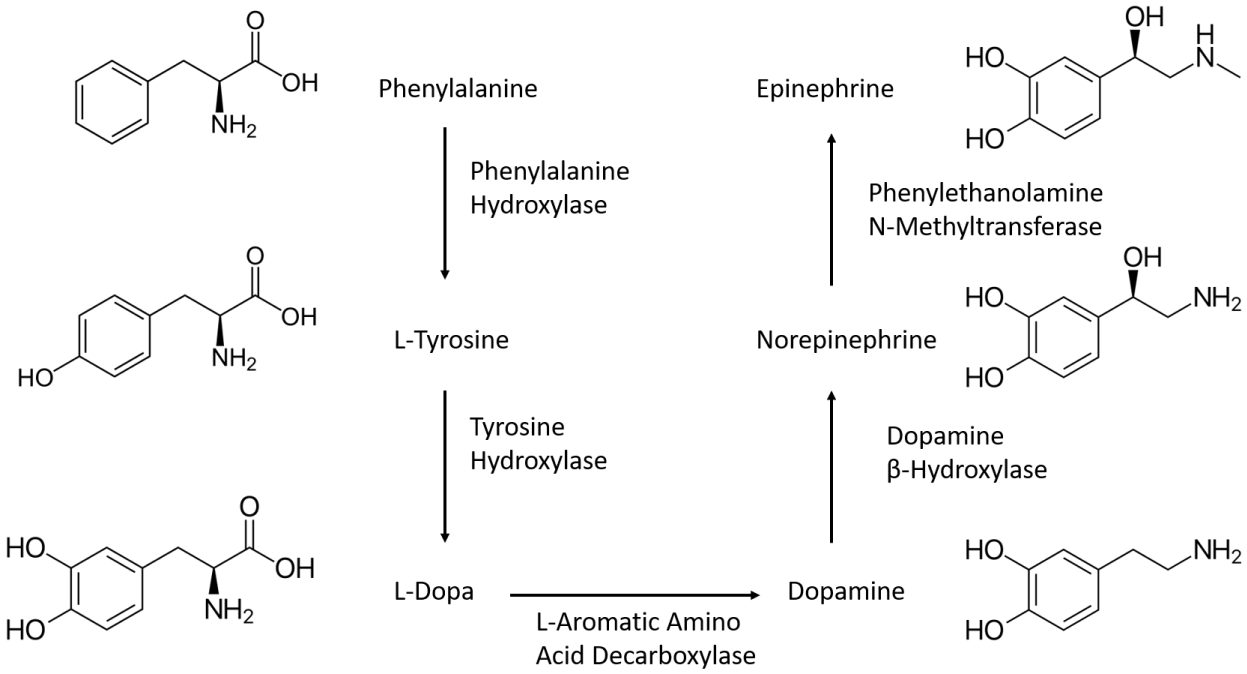

Figure 3. – Pathway of catecholamine biosynthesis. Image modified from Vegh et al. 2016 (Vegh et al., 2016).

1.2.1.2 Catecholamine biosynthesis regulation

From the process of catecholamine biosynthesis, we can identify at least four enzymes (TH, DOPA decarboxylase, DA β-hydroxylase, and phenylethanolamine N-methyltransferase) involved in the various steps of the synthesis of the different components (Fig.3). A large number of regulatory mechanisms for these four enzymes can affect the final catecholamine production. However, hydroxylation of the phenyl ring in tyrosine to form L-DOPA is the rate-limiting step in the catecholamine biosynthesis, so the regulation of TH is the most important event in the production of the catecholamines (Udenfriend, 1966). Our review of the catecholamine biosynthesis will mainly focus on TH synthesis and activity regulation.

1.2.1.2.1 Regulation of TH synthesis

TH exists as a tetramer of four identical subunits, including an N-terminal regulatory domain, a catalytic domain, and a C-terminal tetramerization domain. It uses the tetrahydrobiopterin (BH_4) as a substrate, and together with molecular oxygen and ion, converting tyrosine into L-DOPA. The TH synthesis is controlled by many regulatory factors at the transcriptional and post-transcriptional levels. The TH activity is also essential for catecholamine production and is regulated by multiple modes, including phosphorylation, protein-protein interactions, and catecholamine feedback inhibition. These regulatory mechanisms will be detailed discussed in the following sections.

1.2.1.2.2 Transcriptional regulation of TH

The transcriptional regulation of TH mainly depends on transcription factors' delicate work and other co-factors to finely produce the right amount of mRNA, just like they regulate all other genes. The role of *trans*-acting factors in regulating TH expression relies on their binding with *cis*-regulatory elements in the TH gene, such as promoters, enhancers, silencers, and insulators. This regulatory mechanism is responsible for developing and maintaining tissue-specific TH expression and regulating the expression level of TH responding to stimulus. Our discussion below will focus on the latter part.

As early as 1996, Kumer and Vrana already had a good description of the *TH* promoter's cis-regulatory elements (Kumer and Vrana, 1996). With additional research, more and more cis-regulatory elements of *TH* promoter have been discovered (Fig.4).

Cyclic AMP/Ca^{2+} responsive element (CRE/CaRE), located between -45 and -38 bp in the rat *TH* promoter, regulates TH expression primarily by responding to the intracellular concentration change of Ca^{2+} and the second messengers cAMP (Lenartowski and Goc, 2011). It is a critical regulatory element for both basic and induced TH synthesis, which many studies have proved. In the cAMP-responsive element-binding protein (CREB)-deficient PC12 cell lines, *TH* gene proximal promoter and CRE element activity are impaired under cAMP stimulation, resulting in a total arrest of *TH* mRNA transcription. The PKA signaling cascade is responsible for signal transmission

(Piech-Dumas and Tank, 1999). Long-term stimulation of nicotine elevates *TH* mRNA level in PC12 cell lines, and this depended on the activity of the cAMP-PKA-CREB axis (Hiremagalur et al., 1993). In addition to the cAMP-mediated pathway, short-term stimulation of nicotine induces the elevation of the intracellular Ca^{2+} concentration, which activates calmodulin kinase and in turn phosphorylates CREB, promoting *TH* transcription at its CRE/CaRE site (Gueorguiev et al., 1999). Moreover, membrane depolarization or ionomycin is also found to strengthen *TH* promoter activity via the CRE/CaRE (Kilbourne et al., 1992; Nankova et al., 1996). At a position further upstream (between -97 and -90 bp in the rat *TH* promoter), there is a second CRE2 site identified as a cAMP-responsive element to increase TH expression upon phorbol ester treatment (Best and Tank, 1998). It is worth noting that some studies also show that the binding of transcription factors with CRE and the flanking sequences of AP1 and pDSE are needed to form a complex to promote full activation of the rat *TH* gene (Patankar et al., 1997).

The AP1 element, located at about 200 bp upstream of the rat *TH* promoter's transcriptional start site and overlapping with E-box, is also important for TH expression (Yoon and Chikaraishi, 1994). The deletion of the AP1 binding site in the *TH* promoter on PC12 cells leads to the reduction of basal and enhanced expression of the *TH* gene (Gizang-Ginsberg and Ziff, 1990;1994). The AP1 element–dependent activation of *TH* gene expression can be induced by Ca^{2+}, phorbol esters, nerve growth factor, or hypoxia. AP1 transcription factor is a dimeric complex formed by members from the FOS, JUN, ATF, or MAF families, which is the major protein complex binding with the AP1 site. These protein families can form homodimers or heterodimers and bind to the AP1 site with different affinities. In research to study the induction of different TH–AP1 complexes in striatal neurons by acidic fibroblast growth factor (aFGF) and co-activator, gel shift assays revealed that aFGF stimulation leads to qualitative changes in the components of AP1 complexes binding to the AP1 site from low-affinity dimers (such as ATF/CREB) to high-affinity dimers (such as Fos/Jun), and these changes may depend on the signal transmission via MAPK pathway (Hai and Curran, 1991; Guo et al., 1998). Similar to CRE/CaRE, the protein complexes binding with AP1 often recognize the CRE site. The full *TH* gene activity induced by the AP1 element also requires the CRE element regulation (Piech-Dumas et al., 2001; Suzuki et al., 2004).

Specificity protein 1 (Sp1) element, located from -124 to -107 bp upstream of the transcription start site, was first identified by Yang in 1998 (Yang et al., 1998). This new *cis*-regulatory motif is identified using DNase I footprinting analysis in the rat *TH* gene's 503-bp proximal area. It may activate *TH* transcription in concert with the CRE element. The Sp1 site in the TH promoter region overlaps with the Egr1 site in a study about the immobilization stress on rat adrenal medulla (Papanikolaou and Sabban, 1999). The ability of transcription factor Egr1 to upregulate the activity of rat *TH* promoter induced by phorbol ester or stress may need not only the Sp1/Egr1 motif but also the AP1 element (Papanikolaou and Sabban, 2000; Nakashima et al., 2003).

Gender also involves in the regulation of TH expression by activating the specific elements in the *TH* promoter. Estrogen response element (ERE), located between -43 and -29 bp upstream of the *TH* promoter, together with the overlapping CRE/CaRE site, are essential for the elevated *TH* promoter activity in PC12 cells expressing estradiol receptor-alpha caused by 17beta-estradiol (Maharjan et al., 2005). This effect depends on the PKA/MEK signaling activating the CREB by phosphorylation and further increasing the CRE-driven promoter activity (Maharjan et al., 2010). The sex-determining region Y (SRY) binds to the site close to the AP1 site in the TH promoter and significantly increases TH gene expression.

Some other cis-regulatory elements in the *TH* promoter region help to regulate the expression of the *TH* gene. For instance, the glucocorticoid response element (GRE) (5734-5728 upstream), whose sequence is TGACTAA, resembling the AP1 element (so it is called GRE/AP1 site), involves in the regulation of *TH* gene expression induced by glucocorticoid stimulation. The hypoxia-responsive element (HRE) (226-221 upstream), when interacting with hypoxia-inducible transcription factors induced by hypoxia in oxygen-sensitive cells, increases *TH* gene expression (Schnell et al., 2003).

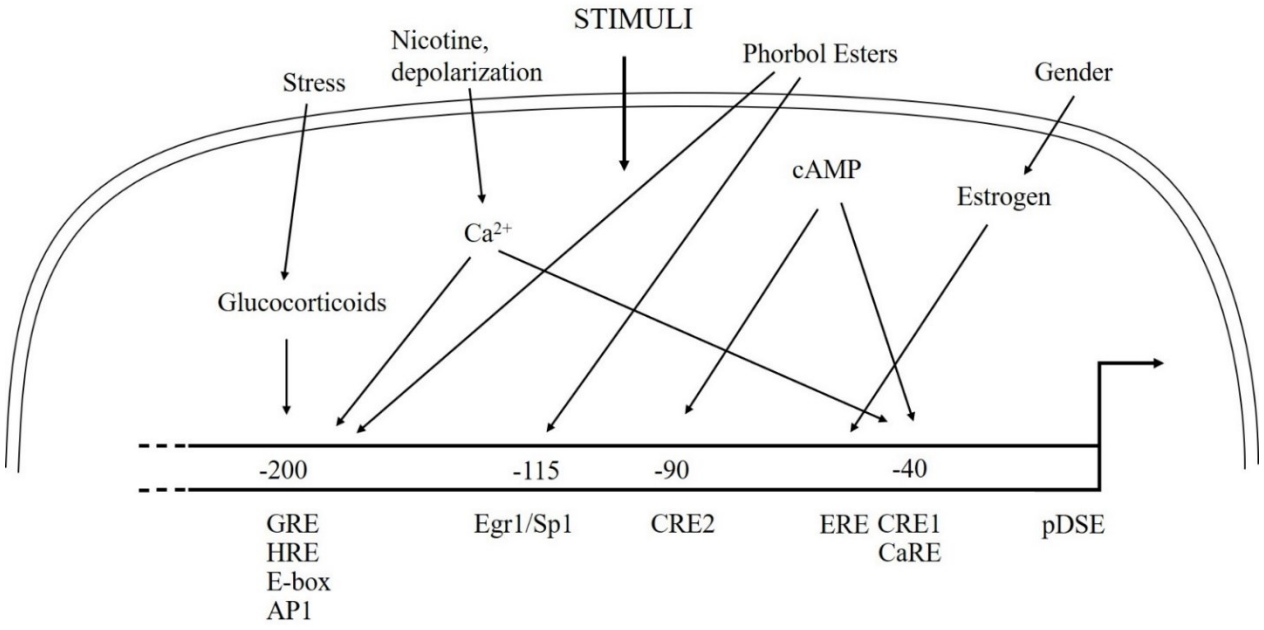

Figure 4. – A schematic diagram and overview of the regulation of the TH promoter. Image modified from Tekin et al. 2014 (Tekin et al., 2014).

1.2.1.2.3 Epigenetic regulation of TH

Research on the epigenetic regulation of gene expression developed rapidly in the past 20 years. More and more evidence has demonstrated that epigenetic factors are also important for TH expression. For example, TH protein expression in rat brain tissues is downregulated due to the decreased histone H3 acetylation level at the promoter after *Staphylococcus aureus* infection (Choudhury et al., 2019). It revealed that the TH expression would be restrained if the histone acetylation at the promoter region is impaired, and multiple other animal and human studies also provided similar evidence (Romano et al., 2007; Liu et al., 2014a; Qiao et al., 2019). The reason may be related to the destabilization of the *TH* mRNA after histone acetylation is inhibited (Aranyi et al., 2007). In addition to histone acetylation, methylation of histone also regulates the expression of *TH*. Exposure to methylmercury leads to a significantly increased tri-methylation of histone H3 lysine 27 levels at the *TH* promoter, resulting in repressed *TH* gene expression (Go et al., 2018). In recent years, many epigenetic types of research based on microRNAs (miRNAs) have further enriched the study of *TH* epigenetic regulation. A study in rat adrenal medulla revealed

miRNA-375 negatively regulates the biosynthesis of TH by targeting Sp1 and results in the decrease of catecholamine synthesis and secretion (Gai et al., 2017). The potential role of miRNA on the *TH* regulation is also reported by an *in silico* target gene prediction program based on the investigation of the miRNA expression in the brains of schizophrenic and bipolar disorder patients (Kim et al., 2010). Along with the development of epigenetics, we believe the picture of epigenetic regulation of TH will be more and more colorful.

1.2.1.2.4 Post-transcriptional regulation of TH

After transcription, the *TH* mRNA undergoes many post-transcriptional modifications to produce TH protein. The stability of *TH* mRNA, which is very important for subsequent translation, is mainly regulated by interacting with specific modulators. Under the hypoxia stimulation, the *TH* gene transcription level and *TH* mRNA stability are both increased in PC12 cells (Czyzyk-Krzeska et al., 1994b). Further study reveals that the *TH* mRNA stability depends on the interaction of the poly (C) binding protein (PCBP) with hypoxia-inducible protein binding sequence at the 3'-untranslated region (UTR) of rat *TH* mRNA (Czyzyk-Krzeska et al., 1994a; Czyzyk-Krzeska and Beresh, 1996). The half-life of *TH* mRNA increases four-fold in AGCCs stimulated with nicotinic agonist, and this elevation is also related to the binding of the protein to the 3`UTR (Roe et al., 2004). Similar results are found in the PC12 cells treated with cAMP analogs or phorbol esters; the RNA-protein interaction contributed to the stability of *TH* mRNA (Vyas et al., 1990; Fossom et al., 1992). In addition to maintaining *TH* mRNA stability, this manner of RNA-protein interaction also contributes to mRNA translation regulation. The increased *TH* mRNA translation level in dopaminergic neurons induced by cAMP is regulated by the binding of PCBP2 to the polypyrimidine-rich site in the *TH* mRNA 3′ -UTR (Xu et al., 2009). The vital role of RNA-protein interaction in TH translation regulation may also give a good explanation for the disproportionate change of TH protein level and *TH* mRNA level in adrenal medulla induced by short-term stressors (Xu et al., 2007).

1.2.1.2.5 Regulation of TH activity

The activity of the TH enzyme largely determines the output of catecholamine. TH synthesis is mainly responsible for the long-term TH activity regulation, while the short-term TH activity regulation depends mostly on the phosphorylation state of the TH enzyme. The principle of TH catalytic reaction is that it performs hydroxylation reaction on the aromatic amino acid in L-tyrosine using Fe^{2+}, oxygen, and BH4. The active site of TH protein is occupied by the iron atom. The catalysis can only proceed when the iron atom is in a ferrous state. The three-dimensional structure study of TH protein shows that when TH is in an inactive state, the regulatory domain will cover the active site, thereby restricting access to the active site. Phosphorylation in the regulatory domain relieves its inhibitory effect on the active site, while dephosphorylation restores it to the blocking position (Daubner et al., 2011).

1.2.1.2.6 Regulation of TH by phosphorylation and dephosphorylation

Many *in vivo* or *in vitro* studies reveal that four serine residues (Ser8, Ser19, Ser31, and Ser40) in the regulatory domain of TH protein primarily contribute to TH phosphorylation regulation. In response to different stimuli, single or multiple serine residues will be phosphorylated by multiple protein kinases, including Ca^{2+}/calmodulin-dependent protein kinase II (CaMKII), ERK1/2, PKA, and mitogen-activated protein kinase-activating protein kinase II (MAPKAPK-2). Phosphorylation at Ser40 has the most powerful effect on TH activity increase compared to other serine residues. The primary outcome of phosphorylation at Ser40 in TH protein is to relieve the feedback inhibition by catecholamines (Le Bourdelles et al., 1991). TH activity increased by 20-fold after the Ser40 of the dopamine-bound TH is phosphorylated by PKA (Daubner et al., 1992), while phosphorylation of Ser31 mediated by ERK1/2 *in vitro* only leads to a less than two-fold increase (Haycock et al., 1992). However, the prior phosphorylation of Ser31 in rat TH can elevate the rate of Ser40 phosphorylation by up to 9-fold *in vitro* (Lehmann et al., 2006). Unlike Ser40 and Ser31, the phosphorylation of Ser8 and Ser19 cannot directly regulate TH activity. However, phosphorylation of Ser19 by CaMKII can enhance the binding of 14-3-3 protein to TH and further lead to a 2-fold increase of TH activity. And the Ser19 phosphorylation also results in the elevated phosphorylation level of Ser40 (Haycock et al., 1998). ERK1/2 can phosphorylate the Ser8 site of

TH, but there is no strong evidence showing that it is related to the TH activity regulation (Kansy et al., 2004).

Dephosphorylation at these four serine residues in the regulatory domain of TH protein by phosphatases will reverse the phosphorylation-dependent TH activity. Phosphoprotein phosphatase 2A (PP2A) plays a crucial role in the dephosphorylation regulation of TH activity. Many pieces of evidence have indicated PP2A can dephosphorylate TH at Ser19, Ser31, and Ser40 and subsequent suppression of TH activity both *in vitro* and *in vivo*. For example, PP2A-treated bovine adrenal chromaffin cells exhibit different dephosphorylation levels at Ser19, Ser31, and Ser40 of TH (Leal et al., 2002). The inhibition of TH activity in dopaminergic cells induced by manganese exposure is caused by PKC delta and PP2A activity (Zhang et al., 2011). Lipopolysaccharide (LPS) injection *in vivo* reduces the TH activity due to the inhibitory effect on the phosphorylation of Ser31 and Ser40 caused by PP2 activity (Ong et al., 2017).

1.2.1.2.7 Feedback inhibition by catecholamines

The catecholamine feedback inhibition is a very important regulatory mechanism to provide fine control of catecholamine production. This inhibitory effect is achieved by the binding of the catecholamines to specific sites in TH. It is currently believed that there are two catecholamine binding sites in TH: one is a high-affinity site, another is a low-affinity site (Ong et al., 2017). The interaction of catecholamines to the high-affinity site leads to a decrease of the TH activity by preventing BH4 from interacting with the active site or forming a tight enzyme-iron-catecholamine complex (Tekin et al., 2014). This kind of interaction can only be released by phosphorylation of TH at Ser40. The interaction of catecholamines to the low-affinity site, from which catecholamines are easily dissociable, can be found in both the non-phosphorylated TH and the Ser40 phosphorylated TH. In the non-phosphorylated TH and Ser40-phosphorylated TH, the dissociation of catecholamine from the low-affinity site can respectively increase TH activity by twelve and nine times (Gordon et al., 2008). This flexible TH activity regulation is more likely to be the main mechanism to control the catecholamine production in most instances and to prevent excessive accumulation of cytosolic catecholamines.

1.2.2 Catecholamine secretion and regulation

In the study of the secretion mechanism of neuroendocrine cells, adrenal gland chromaffin cells (AGCCs) are widely used as a model. The research on catecholamine secretion from chromaffin cells can be traced back to the last century. More and more molecules have been found to be involved in the multiple steps of catecholamine secretion regulation, including secretory vesicle recruitment, docking, priming, fusion, and release. Catecholamine secretion processes and regulatory mechanisms are constantly discovered by cell biology researchers.

1.2.2.1 The stimulus-evoked response of chromaffin cells

AGCCs are mainly innervated by the splanchnic nerve and respond to the neurotransmitters released from pre-synaptic sympathetic ganglia, such as acetylcholine (ACh) and pituitary adenylate cyclase-activating polypeptide (PACAP). The classic stimulus-secretion coupling in AGCCs will be initiated once ACh binds to the nicotinic receptors on the AGCCs' membrane. At first, a small amount of Na^+ and Ca^{2+} flows into the cells through activated nicotinic receptors, and causes a mild depolarization of the cell membrane. Next, the voltage-gated Na^+ channels are opened by depolarization, causing more Na^+ influx and enhancing depolarization, which further activates the voltage-gated Ca^{2+} channels (VGCCs) and allows large amounts of Ca^{2+} influx. The increase of intracellular Ca^{2+} concentration further launches the exocytosis of catecholamine vesicles (Aunis, 1998) (Fig.5A). Although the muscarinic receptors are also expressed on the surface of AGCCs, they are not as important as nicotinic receptors for the catecholamine exocytosis. It is worth noting that this stimulus-secretion coupling can be amplified by the gap junction-mediated cell-to-cell communication to elevate the efficiency of catecholamine secretion (Colomer et al., 2009).

In addition to ACh, another neurotransmitter secreted by splanchnic nerve terminals named PACAP is reported as the major neurotransmitter to activate AGCCs following stress. PACAP stimulation can promote both synthesis and secretion of catecholamines in AGCCs. The binding of PACAP to the AGCCs activates the PACAP-preferring receptor on the cell membrane, which activates phospho-dependent depolarizing cation conductance (PDCC) via the cAMP-Epac-PKC

pathway. The activation of PDCC causes cell depolarization and further opens VGCCs to induce Ca^{2+} influx and results in subsequent catecholamine exocytosis (Eiden et al., 2018) (Fig.5B).

Besides the neurotransmitter stimulation, many other stimuli can also evoke catecholamines secretion from AGCCs (Aunis, 1998). Depolarization by high K^+ concentrations can directly activate VGCCs and secretion. Histamine, angiotensin II, and bradykinin can directly bind to their receptors on the membrane of AGCCs, stimulating the catecholamine exocytosis.

Different from the stimuli above, many other factors play negative regulatory roles on catecholamines secretion. Long-term exposure to ACh will cause a rapid decrease in the release of catecholamines by AGCCs. This phenomenon is called desensitization, which mainly relates to the desensitization of the nicotinic receptors via PKA-mediated phosphorylation (Paradiso and Brehm, 1998). Interaction between dopamine agonists and Dopamine D2 receptors located on the surface of AGCCs shows an inhibitory effect on Ca^{2+} influx and catecholamine secretion (Sontag et al., 1990). Other molecules, such as GABA (Inoue et al., 2010), and neuroactive peptides (Role et al., 1981; Venihaki et al., 1996), are also revealed in many studies negatively regulating the catecholamine exocytosis in AGCCs. Due to the diversity of the membrane receptors, the stimulus-evoked responses of AGCCs are very complex and involve many different mechanisms to secret the right amount of catecholamines.

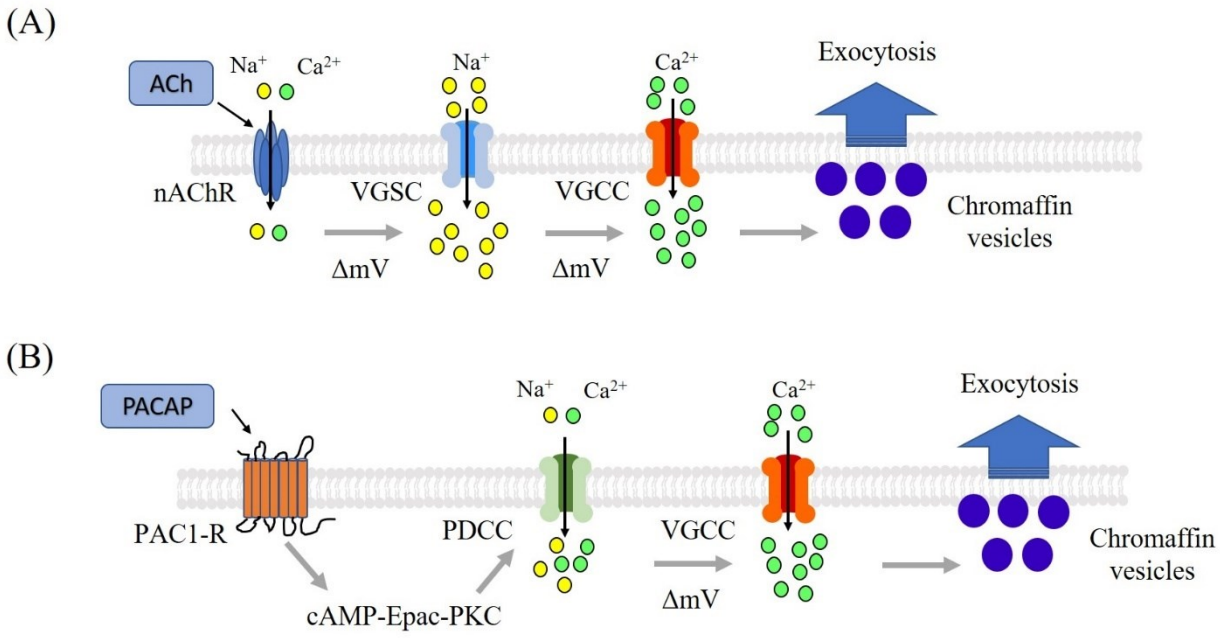

Figure 5. – Schematic illustration of the signaling pathways of catecholamines secretion induced by ACh and PACAP in adrenal gland chromaffin cells. Image modified from Smith, 2012 (Smith and Eiden, 2012).

1.2.2.2 Chromaffin vesicle exocytosis

After catecholamines are synthesized in the AGCCs, they are transported into chromaffin vesicles by vesicular monoamine transporters in an ATP-dependent way (Wimalasena, 2011). These chromaffin vesicles containing dense-core aggregate originate from the Golgi network. During the maturation of vesicles, many molecules, including catecholamines, ATP, enzymes, peptides, and grains, are assembled into the vesicles, and these vesicles are transported along microtubules from their initial site deep in the cytoplasm to the F-actin-rich cell cortex, waiting for further docking, priming, fusion, and exocytosis (Fig.6). These chromaffin vesicles are majorly located at two pools constructed from actin cytoskeleton: the reserve pool and release-ready pool (Rose et al., 2002). Most of the chromaffin vesicles are restricted in the cortical F-actin network of the reserve pool away from the plasma membrane. In contrast, a small amount (1%-4%) of the vesicles stay in the release-ready pool within a 50 nm subplasmalemmal zone in the resting state (Heinemann et al., 1993; Vitale et al., 1995). Myosin VI and Synapsin II may help to anchor chromaffin vesicles to the actin filaments to maintain the reserve pool (Villanueva et al., 2006; Tomatis et al., 2013). The movement of chromaffin vesicles from the reserve pool to the release-ready pool is mainly triggered by the rise of intracellular Ca^{2+} concentration and ATP hydrolysis. This process requires F-actin remodeling and microtubule trails to liberate and guide (Trifaro, 2008). Two molecular motors, myosin II and Va, play important roles on the cortex F-actin dynamics, and drive the vesicles to exocytotic sites through the trails (Neco et al., 2002). In addition to Ca^{2+} influx, the disassembly of F-actin also can be triggered by PKC activation after treatment with phorbol esters (Trifaro et al., 2000).

After the vesicle traffic, there are three more steps (docking, priming, fusion) before the final vesicle exocytosis. Docking is the process by which the vesicles are tethered to the cell membrane in the release-ready pool. It has been proposed that the docking process in chromaffin cells is

controlled by syntaxin, synaptosomal-associated protein 25 (SNAP-25), and synaptotagmin-1 (Borisovska et al., 2005). SNAP-25 binds to membrane protein syntaxin to form SNARE complex and further wraps with the vesicular membrane protein synaptotagmin-1 to anchor the vesicle to the cell membrane. Another molecule, mammalian uncoordinated (Munc)18-1, also contributes to the docking process by facilitating the formation of a more compatible SNARE complex for docking (Dawidowski and Cafiso, 2016).

Once the docking of vesicles is finished, a priming step is required for the vesicles to become fusion competent. According to the newly developed kinetics studies, the priming process is divided into two steps. They are modulated by three Ca^{2+} sensors with distinct Ca^{2+} sensitivities, which are Munc13, Ca^{2+}-activated dependent activator protein for secretion (CAPS), and synaptotagmin-1, in a Ca^{2+} -dependent way. In the first step, the conformation of syntaxin in the SNARE complex is opened by the catalysis of Munc13, allowing synaptobrevin and more SNAP-25 to participate in the assembly of the upgraded SNARE complex (Ma et al., 2011). The population of chromaffin vesicles in this state is classified as a slow releasable pool (SRP). In the second step, CAPSs further bind to “opened” syntaxin, leading to a more stable open state of syntaxin to form a full SNARE complex (Parsaud et al., 2013). The population of chromaffin vesicles in this state is classified as a readily releasable pool (RRP) (Fig.6). The deletion of CAPSs in the chromaffin cells results in a sharp decrease of the chromaffin vesicles in RRP and a sustained release of catecholamines during constant stimulation (Liu et al., 2008). Moreover, the interaction of synaptotagmin-1 with SNAP-25 not only contributes to the docking process but also plays a powerful role in stabilizing the primed chromaffin vesicles. Mutation of the synaptotagmin-1 binding sites in the SNARE complex causes the loss of SRP and RRP (Mohrmann et al., 2013).

After the priming process, the chromaffin vesicles are ready to fuse with the cell membrane. The SNARE complex continues to play a central role in the fusion process. Mutations in multiple different sites of the SNARE complex all result in impaired fusion function of chromaffin vesicles (Wang et al., 2011; Mohrmann et al., 2013). At the resting state, the SNARE complex is restrained in a pre-fusion state due to the binding of small cytosolic protein complexins (Schaub et al., 2006). When intracellular Ca^{2+} concentration is raised after stimulation, Ca^{2+} will bind to synaptotagmin-1, and the bound complexins will be released from the SNARE complex, triggering the next fusion

process. According to electrophysiological recordings in AGCCs, catecholamines flow out through a high conductance channel named “fusion pore”. SNARE complexes are the main components of the fusion pore, and they are involved in regulating the conductance and the diameter of the fusion pore (Fang et al., 2013; Chang et al., 2015). In addition, many works suggest that F-actin and myosin II are also essential to the fusion events (Neco et al., 2004; Miklavc et al., 2015). They may contribute to conducting and maintaining the open state of the fusion pore (Wen et al., 2016) and promote neurotransmitter release by enhanced membrane tension (Miklavc et al., 2015).

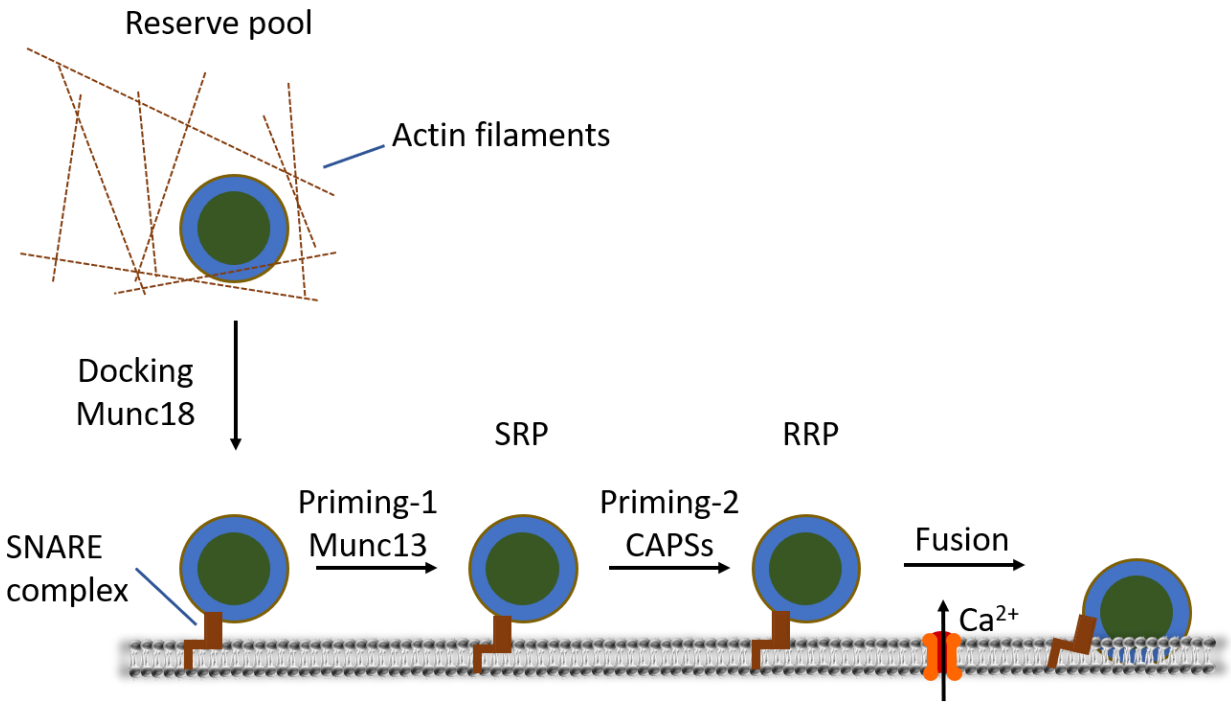

Figure 6. – Model of chromaffin granule exocytosis. Image modified from Marengo and Cardenas, 2018 (Marengo and Cardenas, 2018).

1.2.2.3 Ca^{2+} regulation of catecholamine secretion

The Ca^{2+}-dependent stimulus-secretion coupling is the first revealed mechanism and also is the most important mechanism for the catecholamine secretion from AGCCs (Douglas and Rubin, 1961). The increase of the cytosol Ca^{2+} concentration is essential for the chromaffin vesicles exocytosis. The strength and duration of the cytosolic Ca^{2+} signals contribute to the regulation of

chromaffin vesicles distribution in the different pools and every step of the exocytosis, including recruitment, docking, priming, and fusion.

The intracellular Ca^{2+} concentration is not homogeneously distributed in the AGCCs. The extracellular Ca^{2+} cations flux into AGCCs through the VGCCs activated by stimuli, inducing the Ca^{2+}-induced Ca^{2+} release from the endoplasmic reticulum to amplify the Ca^{2+} signal. The Ca^{2+} is also taken up by mitochondria and promotes the increase of the respiration rate to produce more ATP (Garcia et al., 2006). The Ca^{2+} redistribution in the cell leads to the formation of the sub-membrane Ca^{2+} gradients and Ca^{2+} microdomains. These microdomains, whose sizes are about 0.35 μm, are distributed in the region about 200 nm away from the plasma membrane and are neighboring with the VGCCs, close to the docked chromaffin vesicles. In a buffered Ca^{2+} diffusion model, by stimulating AGCCs with short depolarization, the Ca^{2+} concentration in the microdomains adjacent to the mouse of VGCCs is increased to 30 μM within microseconds, while the Ca^{2+} level only rises to 1.9 μM within milliseconds in the region 300 nm away from the channel pore (Klingauf and Neher, 1997). In resting conditions, the cytosolic Ca^{2+} concentration near the VGCCs only rises very briefly and cannot achieve the accumulation of residual Ca^{2+} under the low-frequency repetitive stimulation. However, high-frequency stimulation can provoke a large Ca^{2+} influx, leading to the Ca^{2+} accumulation in the region further away from the VGCCs (Klingauf and Neher, 1997).

The temporal and spatial characteristics of sub-membrane Ca^{2+} gradients have a close relationship with the chromaffin vesicle burst secretion and sustained secretion. In the resting condition, the low-frequency stimulation only increases the Ca^{2+} concentration of the Ca^{2+} microdomains around VGCCs, which induces a small group of RRR chromaffin vesicles close to the channels, named immediately releasable pool (IRP), to be rapidly released (Alvarez and Marengo, 2011). Many studies demonstrated the P/Q-type VDCCs are mainly responsible for the IRP exocytosis in mouse AGCCs (Alvarez et al., 2008; Alvarez et al., 2013). Due to the small IRP size and the slow speed of IRP replenishment (5-10 s), it is difficult to sustain the chromaffin vesicle secretion (Moya-Diaz et al., 2016). A recent study challengingly suggested that there is another rapid manner of IRP replenishment (0.5-1.5 s) linked to dynamin-dependent fast endocytosis during individual action potentials stimulation (Montenegro et al., 2020). Therefore, there may be different

replenishment mechanisms for regulating the IRP exocytosis by different stimulation. When receiving high-frequency repetitive stimulation, the chromaffin vesicles in the release-ready pool will be quickly released synchronously with stimuli, and the vesicles in the reserve pool will mature and refill the release-ready pool to maintain subsequently sustained exocytosis (Stevens et al., 2011). This process requires sufficient calcium accumulation around the chromaffin vesicles. The F-actin remodeling during the vesicle traffic is basically Ca^{2+}-dependent. High cytosolic Ca^{2+} concentrations can both activate scinderin to cut the actin filaments (Dumitrescu Pene et al., 2005) and activate ERK1/2 and Src kinases, which are involved in actin polymerization (Olivares et al., 2014; Gonzalez-Jamett et al., 2017). In the following docking, priming, and fusion processes, there are many different types of Ca^{2+} sensors involving in the formation of the core component SNARE complex. These Ca^{2+} sensors have distinct Ca^{2+} sensitivity and require different levels of Ca^{2+} signal to be activated. Thus, Ca^{2+} ions drive the whole process of catecholamine secretion.

1.2.2.4 Role of F-actin in catecholamine secretion

The role of F-actin in catecholamine secretion has been studied for about 50 years. The earliest knowledge of F-actin was limited to its peripheral cortical barrier function. It restrains the chromaffin vesicles in the reserve pool and prevents them from accessing the submembrane releasing sites in AGCCs (Gutierrez and Villanueva, 2018). The increased cytosolic Ca^{2+} concentration after stimulation leads to the dense F-actin network fragmentation and subsequent entry of the chromaffin vesicles into the secretory sites. Later studies demonstrated the new role of F-actin in the chromaffin vesicles transport system. The remodeling of F-actin also forms F-actin trails together with microtubules to guide the vesicles moving from the reserve pool to the readily releasable pool with the help of myosin. In recent years, more and more complex roles of F-actin in the chromaffin vesicle exocytosis have been revealed. F-actin participates in the fusion process by adjusting the surface tension of the cell membrane to open the fusion pore and even the duration of the fusion pore. The co-localization of the SNARE complex with VGCCs needs the structural support of F-actin cortical cytoskeletal cages, which also contributes to the construction of the Ca^{2+} microdomain. The dynamics of F-actin are even involved in the transport of many organelles, such as mitochondria and endoplasmic reticulum, which is also related to the

construction of Ca^{2+} microdomain (Gutierrez and Villanueva, 2018). Due to the fundamental roles of F-actin in so many processes of catecholamine secretion, the regulation of F-actin dynamic remodeling is crucial.

1.2.2.5 Regulation of F-actin dynamics

F-actin remodeling is a dynamic process of the transition between monomeric globular actin (G-actin) and F-actin. This particular process of actin filament formation is called "treadmilling." When G-actin binds to ATP, the ATP-actin monomers prefer to join the filament's fast-growing barbed end to assemble the F-actin. As an ATPase, actin hydrolyzes ATP and changes into ADP+P_i-actin, which shows ADP-actin binding with P_i noncovalently, relatively rapidly after ATP-actin adds to the barbed end. The ADP+P_i-actin will remain for some time and then convert to ADP-actin at the pointed end, ready for disassembly (Lee and Dominguez, 2010). The ratio of these three components in F-actin varies according to different states, which is the core mechanism of F-actin remodeling. Many specific actin-binding proteins (ABPs) control each step of the dynamic actin treadmilling, including nucleation, elongation, depolymerization, end-capping, cutting, cross-link, and actin monomer separation (Fig. 7).

The most important ABPs are the G-actin-binding proteins: profilin, Thymosin β4 (T-β4), and ADF/cofilin. Profilin can catalyze the ADP-actin to ATP-actin and binds to the latter, promoting its combination to the barbed end of the F-actin. At the same time, ADF/cofilin functions by binding to ADP-actin and further destabilizes it, accelerating its dissociation from the pointed end (dos Remedios et al., 2003). T-β4 is another ABP with a high affinity to G-actin, and the binding of T-β4 and G-actin not only inhibits the nucleotide exchange on G-actin but also blocks ATP-actin aggregation (Hertzog et al., 2004; Xue et al., 2014). T-β4 binds to ATP-actin competitively with profilin since they have a similar affinity to ATP-actin. However, most ATP-actin monomers bind to T-β4 instead of profilin because the amount of T-β4 is much larger than profilin in the cells (Skruber et al., 2018). Moreover, the binding of profilin with the membrane phospholipid phosphoinositol 4,5-bisphosphate (PIP2) further reduces the probability of forming the profilin-ATP-actin complex (Skruber et al., 2018). Thus, T-β4 helps to hold the ATP-actin in the "reserve

pool" waiting for polymerization. When needed, profilin can replace with T-β4 by converting into profilin-ATP-actin for polymerization (Pantaloni and Carlier, 1993). The phosphorylation of profilin can enhance its binding with actin and subsequent actin polymerization (Fan et al., 2012).

Actin-related protein (Arp) 2/3 complex can mimic the timer/tetramer, which is the critical structure of actin nucleation. Thus it is considered as a key nucleator for actin filaments nucleation. The activity of Arp2/3 complex is limited unless activated by nucleation promoting factors (NPF), such as Wiskott–Aldrich syndrome protein (WASP), WASP family verprolin-homologous protein (WAVE), and WASP and SCAR homologue (WASH) complex (Rotty et al., 2013). The classic nucleation manner of Arp2/3 is to form a nucleus with actin monomers for filament branch generation on a pre-existing filament. The structural studies reveal the branch and the main filament have a characteristic 70° angle (Pollard, 2007).

Formins are another critical group of nucleation/elongation factors, mainly responsible for the assembly of the unbranched actin filament. The dimerization of formins with actin monomers enhances the stabilization of actin dimers, which is used as a nucleus for actin assembly. During filament elongation, actin monomers are added to formins-actin dimer sequentially at the barbed end to assemble the filament (Xu et al., 2004). Formins can also recruit the profilin-actin complexes binding to their proline-rich formin homology (FH) 1 domain to participate in the filament elongation (Breitsprecher and Goode, 2013).

Capping is a crucial step to control the length and amount of the actin filaments by capping in both nonequivalent ends of the filaments. The most common capping protein at the barbed-end is CapZ, while the pointed-end is predominantly capped by tropomodulin protein (dos Remedios et al., 2003). In the cells, capping can be modulated by PIP and PIP2, which promote the capping proteins separating from the ends of filaments, leading to dynamic filament remodeling. Besides, the profilin binds to the barbed ends of actin filaments competing with capping proteins, resulting in the inhibition of the interaction between capping proteins and barbed ends.

Disassembly of the F-actin messy network usually requires two steps: debranching and severing. Arp2/3 complex is the main nucleator for generating the branched actin filaments, thus inhibiting the activity Arp2/3 complex facilitates the dissociation of the branched filaments from the main

filaments. There are many Arp2/3 inhibitors contributing to this debranching process, such as coronin, glia maturation factor, and Arpin. They directly bind to the Arp2/3 complex and induce distinct open conformations of the complex, resulting in the inhibition of the Arp2/3 activity and the detachment of branched filaments (Sokolova et al., 2017). ADF/cofilin family proteins have both debranching and severing effects on the F-actin network. The interaction of ADF/cofilin with the actin filaments promotes the phosphate dissociating from the ADP+P_i-actin and the F-actin helical structure's turnover, which reduces the affinity of Arp2/3 complex for the actin filament causing the debranching at branch junction. The ADF/cofilin and Arp2/3 also competitively bind to the actin filaments. (Chan et al., 2009). These mechanisms explain how the ADF/cofilin proteins play their debranching role in the F-actin turnover. In addition, the turnover of the actin network by ADF/cofilin binding also causes the breakage of the inter-subunit bonds of mother filaments, which cuts the F-actin into several shorter fragments for further disintegration from the pointed ends, and even from barbed ends in the presence of capping proteins (Wioland et al., 2017). A similar severing function also can be found on another powerful severing protein, gelsolin (dos Remedios et al., 2003). Their severing activities are restricted by their interaction with PIP2, so hydrolysis of PIP2 will release them and leads to the acting filaments disassembly. The activity of ADF/cofilin is also regulated by phosphorylation. It is well known that the activity of ADF/cofilin is inhibited due to its phosphorylation by LIM kinases (LIMKs), whose activities are controlled by Rho GTPases (dos Remedios et al., 2003).

The disassembly of F-actin is not only regulated by the ABPs, but also by post-translational modifications. In 2010, a novel F-actin-disassembly factor Mical was found in Drosophila. It can directly bind to F-actin and precisely disassemble the actin filaments by reduction-oxidation (redox) enzymatic reactions (Hung et al., 2010). As a redox enzyme, Mical selectively exerts its oxidation activity on two amino acids, methionines 44 and 47, within the pointed end of F-actin, catalyzing F-actin disassembly and inhibiting actin re-polymerization until the oxidation is relieved (Hung et al., 2011; Grintsevich et al., 2017). Later research further found that the collaborative interaction between Mical and cofilin can magnify their individual roles in F-actin disassembly and results in a more thorough and faster dismantling of the actin network (Grintsevich et al., 2016).

Cross-linking between the cortical actin filament and the cell membrane is important for cortical actin filament stabilization. ERM proteins, including ezrin, radixin, moesin, are such membrane-cytoskeleton linker proteins. The interruption of ERM function in growth cones leads to a lack of increased F-actin beneath the plasma membrane under the stimulation of nerve growth factor (Marsick et al., 2012). Phosphorylation or binding to PIP2 can enhance the activity of ERM and the subsequent actin cross-linking (Bosk et al., 2011). The phosphorylation of ERM can be regulated by several kinases, such as Rho kinase, PKC, and NF-kappa-B-inducing kinase (Fehon et al., 2010).

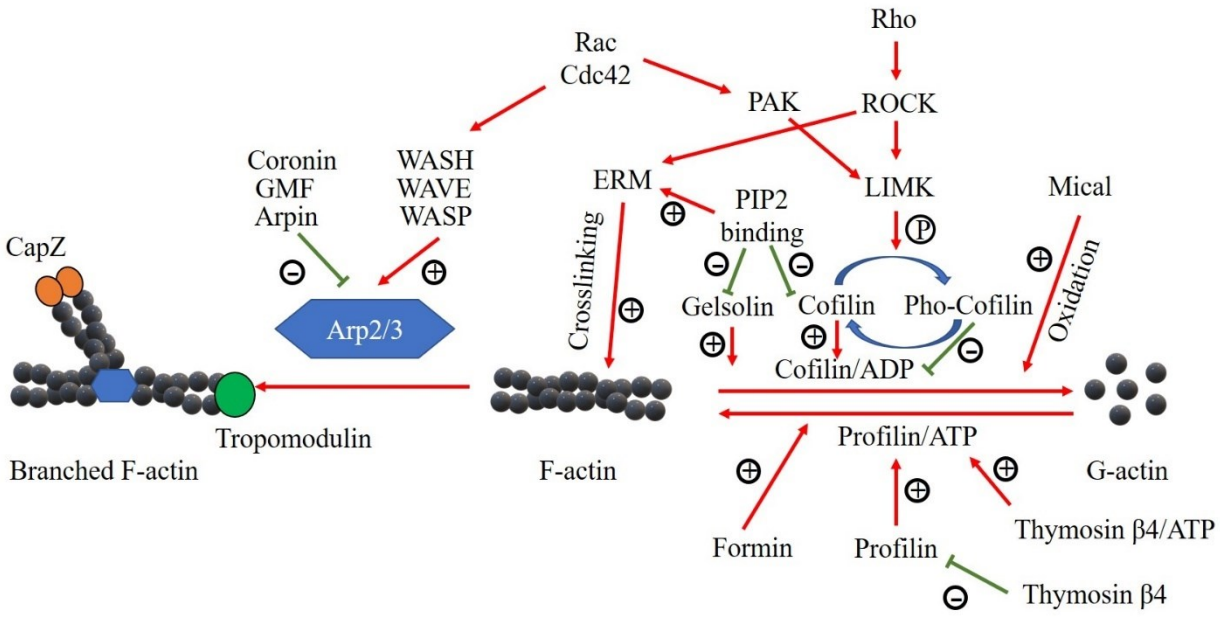

Figure 7. – The regulation of F-actin remodeling. Image modified from Uray, 2020 (Uray et al., 2020).

1.2.3 Catecholamine degradation

The degradation of catecholamines mainly depends on two important enzymes: monoamine oxidases (MAO) and catechol-O-methyltransferases (COMT). There are some differences in the degradation processes of three catecholamine components (DA, NE, Epi). After the deamination by MAO and methylation by COMT, DA is eventually converted to its end-product homovanillic

acid (HVA), while NE and Epi are converted to vanillylmandelic acid (VMA). In addition to exocytosis by vesicles, a small number of catecholamines passively leak from the storage vesicles into the cytoplasm and start to be degraded. In a resting state, more catecholamines are degraded after leakage than after exocytosis (Eisenhofer et al., 2004).

It should be noted that the neurons only contain MAO, while chromaffin cells possess both MAO and COMT. So, the intermediates after deamination in the neurons need to be transported to the extracellular space for further catalysis by COMT. In contrast, catecholamines in the cytoplasm of chromaffin cells can be completely converted to VMA. DA is primarily produced in the dopaminergic neurons in the brain. Part of DA undergoes deamination in the cells, but the degradation of DA mainly happened in the extracellular space before getting to the liver (Anggard et al., 1974). In contrast, NE, Epi, and their intermediate metabolites are sent to the liver through the blood circulation for further degradation. Their end-products, VMA and HVA, are eventually excreted by the kidneys.

1.2.4 Catecholamine function

Catecholamines perform their function by binding to and activating specific receptors located on target effector cells' surface. Epi and NE target the adrenergic receptors, while DA mainly targets the DA receptor. These receptors all belong to G protein-coupled receptors (GPCR), and they can induce either excitation or inhibition of the target cell according to the subtypes of the receptors. We will fully discuss the catecholamines' different physiological effects on the different targets.

1.2.4.1 Epinephrine and norepinephrine

Epi and NE function by binding to the G protein-coupled adrenergic receptors. The adrenergic receptors are composed of two main groups, α and β, with several subtypes. α receptors are further divided into $\alpha1$ and $\alpha2$ subtypes, and the β receptors are further divided into $\beta1$, $\beta2$ and $\beta3$ subtypes. Catecholamines show different affinities to different receptor subtypes. NE has a

high affinity to α receptors, but a much weaker affinity to β receptors, while Epi has a strong affinity to both α and β receptors, but is more effective at β receptors.

1.2.4.1.1 α1 receptor

α1 adrenergic receptors, coupled with the G_q protein, are mainly located on all vascular smooth muscles, including those of the kidney, skin, gastrointestinal (GI) system, urethral sphincters, and bronchioles. The binding of agonists to α1 receptors initiates the Phospholipase C

(PLC) - Diacylglycerol- PKC pathway and raises the cytosolic Ca^{2+} concentration via Ca^{2+} influx from VGCCs and IP3-induced Ca^{2+} release from the endoplasmic reticulum, enhancing the myosin light chain kinase (MLCK) phosphorylation to promote the VSMCs contraction (Graham et al., 1996). Thus, α1 receptors activation causes the constriction of blood vessels, which raises the blood pressure, increases the tone of the GI and urethral sphincters, promotes glycogenolysis and gluconeogenesis from adipose tissue and liver, and causes bronchoconstriction. Furthermore, α1 receptor activities in the renal system also cause sodium retention, which is one of the fundamental causes of essential hypertension (Cotecchia, 2010).

1.2.4.1.2 α2 receptor

α2 adrenergic receptors are more inclined to couple with the $G_{i/o}$ protein. They are abundantly located on vascular prejunctional termini and also can be found in VSMCs of skin arterioles or veins. The activation of α2 adrenergic receptors decreases the production of cAMP and reverses the smooth muscle relaxation caused by cAMP (Traish et al., 1997). α2 adrenergic receptors activation also inhibits Ca^{2+} channel currents but activates the G protein-coupled inwardly-rectifying K^+ channels, causing the inhibition of transmitter release (North, 1989; Hille, 1992; Li and Bayliss, 1998). α2 receptors are characterized as presynaptic receptors, inducing negative feedback on NE release. So, the α2 agonists can be used to control hypertension caused by an overactive sympathetic nervous system (Giovannitti et al., 2015). Moreover, they can also inhibit insulin release but induce glucagon release from the pancreas (Hsu et al., 1991).

All the 3 β adrenergic receptors are coupled with G_s proteins, and their activation increases the activity of intracellular cAMP. The β2 and β3 receptors can also be coupled to G_i proteins to activate other pathways.

1.2.4.1.3 β1 receptor

β1 adrenergic receptors are primarily located in the cardiac pacemaker and myocardium. They have strong effects on regulating contraction and relaxation of the cardiac muscle. Activation of β1 receptors can elevate the cardiac output via increasing the heart conduction, beating rate, and myocardium contractility (Najafi et al., 2016). These effects may depend on the proteins that are phosphorylated by PKA, whose activity is triggered by the increase of cAMP after agonist binding to β receptors. These proteins include L-type calcium channels, the sarcolemma p27 protein, troponin I, phospholamban, and phosphorylase kinases (Walsh and Van Patten, 1994). The stimulation of β1 receptors can also increase renin secretion from the kidney (Osborn et al., 1981) and ghrelin secretion from the stomach (Zhao et al., 2010).

1.2.4.1.4 β2 receptor

β2 adrenergic receptors are located on smooth muscles vasculature, especially the skeletal muscle arteries and some coronary vessels, and in the GI tract, urinary bladder, bronchial tree, liver, and heart. Upon β2 adrenergic receptor activation, although the cardiac myocyte contraction is enhanced resulting in the increase of cAMP, the smooth muscle is relaxed because of the inhibition of MLCK by the increased cAMP (Kotlikoff and Kamm, 1996). Thus, the β2 receptors activation results in vasodilation of blood vessels, relaxation of the smooth muscle in bronchi, urinary bladder, and GI tract, increased insulin (Santulli et al., 2012) and renin (Kim et al., 2007) secretion, and some enhanced metabolic processes such as lipolysis in the adipose tissue (Schiffelers et al., 2001) and glycogenolysis and gluconeogenesis in the liver (Erraji-Benchekroun et al., 2005).

1.2.4.1.5 β3 receptor

β3 adrenergic receptors are primarily distributed in the adipose tissue but are also identified in the smooth muscle of the GI tract and urinary bladder. Their specific roles in increasing the lipolysis and thermogenesis in the adipose tissue have been well-studied (Ferrer-Lorente et al., 2005; Mund and Frishman, 2013). Their activation also results in the relaxation of the GI tract and urinary bladder (Fletcher et al., 1998; Hristov et al., 2008).

Taken together, the activation of α1 and β1 receptors often leads to stimulatory responses, while inhibitory responses are caused by the activation of α2, β2, and β3 receptors.

1.2.4.2 Dopamine

DA mainly functions as a neurotransmitter that delivers stimuli in the brain. DA receptors are all G-protein-coupled receptors and have five subtypes: D1, D2, D3, D4, and D5. Based on the structure homology, these five subtypes of DA receptors can be subdivided into two categories, D1-like family receptors (D1 and D5) and D2-like family receptors (D2, D3, and D4). D1 receptors are the most abundant DA receptors in CNS, while D2 receptors are the second most abundant ones. In contrast, the expression of the other three receptors is very low. The affinity of DA to D2-like family receptors is 10-100 fold greater than to D1-like family receptors. So, the D1-like family receptors are more likely to be activated by high-dose DA, while the D2-like family receptors can respond more sensitively to low-dose of DA stimulation (Grace et al., 2007).

1.2.4.2.1 D1-like family receptor

D1-like family receptors prefer to couple with G_s or G_{olf} proteins. The activity of D1-like family receptors leads to the cAMP production and the activation of PKA. PKA, in turn, phosphorylates DA- and cAMP-regulated phosphoprotein of 32kD, which can enhance the PKA signal conversely and lead to downstream effects, such as the increase of intracellular Ca^{2+} concentration via L-type calcium channel currents and inhibition of voltage potassium channels (Savica and Benarroch, 2014). This pathway leads to the target neuron excitation. However, D1-like receptors can also

result in the stimulation of phospholipid hydrolysis and the opening of the potassium channel to increase K^+ efflux, which leads to the inhibition of the neuron (Beaulieu and Gainetdinov, 2011). The functions of the D1-like receptors involve growth and development regulation, sleep, reward, attention, reproductive behavior, learning, working memory, self-regulated movements, pain, feeding, and movement control (Klein et al., 2019).

1.2.4.2.2 *D2-like family receptor*

The D2-like family receptors mainly couple with G_i proteins. Such an interaction results in the inhibition of the adenylate cyclase activity and reduced intracellular cAMP levels. Subsequently, PKA activity and its downstream effects are inhibited. Moreover, D2-like family receptors can induce the inhibition of the calcium channel and activation of voltage-sensitive potassium channels by interacting with $G_{\beta\gamma}$ subunits. The D2-like activation usually leads to the inhibition of the target neuron. The functions of D2-like receptors involve reward-motivation functions, emotions, motor function regulation, cognitive functions regulation, and endocrine function regulation (Klein et al., 2019).

Based on the various physiological functions exhibited by different dopamine receptors, DA has a dual role in stimulating or inhibiting neurons. This mainly depends on the type of dopamine receptors or other GPCRs, ion channel activation, and second messenger responses in the target cells (Beaulieu and Gainetdinov, 2011).

1.2.4.3 The role of catecholamines in blood pressure regulation

It is well-known that catecholamines play different roles by binding to different receptors distributed throughout the body. Both Epi and NE can exert a positive chronotropic effect, positive dromotropic effect, and positive inotropic effect on the heart. However, they exert different effects on the regulation of vascular tone. α receptors are responsible for vasoconstriction caused by catecholamine stimulation, whereas vasodilation depends on β2 receptors. NE has a high affinity with α receptors but a weak affinity with β2 receptors; in contrast,

Epi has a much stronger affinity with β2 receptors. Thus, NE can induce strong vasoconstriction on all vascular beds by activating the α receptors. When circulating Epi is at a low level, it can produce a vasodilatory effect via the activation of β2 receptors. However, this effect will reverse to vasoconstriction when the concentration of circulating Epi is at a higher level. The effects on α receptors in most vascular beds will overwhelm the effects on β2 receptors. Hence, under the stimulation of Epi, the cardiac output will increase due to the increased stroke volume and heart rate, and systolic pressure will rise, but diastolic pressure will be constant or fall slightly. However, NE has a much stronger effect on α receptors than on β receptors. The direct cardiac stimulation by NE is too weak, so NE stimulation will cause a rise of diastolic pressure due to vasoconstriction of the vascular beds and a reflex decrease in heart rate because of the increased diastolic pressure (Tank and Lee Wong, 2015). In addition, Epi and NE can activate the α1 receptors in the proximal tubule and loop of Henle to increase Na^+ reabsorption. Their effect activates the β1 receptors in the kidney to turn on the Renin-angiotensin-aldosterone system (RAAS), which causes strong vasoconstriction and elevates the blood pressure (Haase et al., 2017).

The effect of DA on the cardiovascular system depends on its concentration. D1-like receptors are present on the vascular smooth muscles of the most important vascular beds. When DA is at a low level, it will directly bind to the D1-like receptors and cause vasodilation in the kidney, mesentery, and coronary blood vessels. When the DA concentration is slightly increased more, DA will activate the β1 receptors in the heart, leading to the increased cardiac output. However, NE release will be reduced because of the feedback inhibition by the activated D2-like receptors on the sympathetic nerve terminals (Missale et al., 1998). Thus, the positive effect of DA on the heart will decline due to the reduced NE level. When the DA reaches a high level, the α receptors in the vascular smooth muscles will be activated, causing increased blood pressure due to general vasoconstriction. When the kidney is under high salt conditions, DA can decrease the reabsorption of Na^+ in tubules and inhibit the RAAS system. This will increase natriuresis in the kidney, resulting in blood pressure regulation (Carey, 2013).

In our EPHB6 KO mice model, impaired catecholamine levels in KO male mice played a compensatory feedback effect on the increased VSMCs contraction induced by EPHB6 KO. Such a

compensatory effect was eliminated after castration and led to higher blood pressure. It is crystal clear that the sex hormones were involved in the blood pressure regulation in EPHB6 KO mice. In the next section, we will review the effects of the sex hormones, especially their association with hypertension.

1.3 Sex hormones and blood pressure regulation

According to the 2020 "Heart Disease and Stroke Statistic" report of the American Heart Association, the incidence and severity of hypertension are typically lower in premenopausal women than in age-matched men, but this situation is quickly reversed after menopause when the incidence of hypertension or the incidence of cardiovascular disease rises sharply in women (Reckelhoff and Roman, 2011; Virani et al., 2020). The sex differences in the incidence of hypertension risk factors, blood pressure regulation, and the response to antihypertensive drugs have been reported in many studies (Gerdts et al., 2008; Rabi et al., 2008; Reckelhoff, 2019; Medina et al., 2020). The roles of sex, especially sex hormones in blood pressure regulation, are worthy of additional in-depth studies.

1.3.1 Sex hormones and sex chromosomes

The role of sex in blood pressure regulation involves two possible aspects: sex hormones or sex chromosomes. The Four Core Genotype (FCG) mouse model creates the SRY transgene expression on an autosome instead of the Y chromosome. When these transgenic mice mate with a female XX, they will produce XX females, XY females, XY males, and XX males. This is a good model to study the role of the sex chromosomes in these sex-dependent phenotypes independent of sex hormones (De Vries et al., 2002). When studying the contribution of sex hormones to sex-dependent phenotypes, castration or ovariectomy is a good choice to verify the hypothesis.

Although a large number of studies have shown that sex hormones are majorly responsible for sex-dependent phenotypes, some research also demonstrates the independent role of sex chromosomes on blood pressure regulation and hypertension risk factors. Hong *et al.* used the

FCG mouse model to explore the effect of sex chromosomes on blood pressure and reported the mean arterial pressure in the XX group is higher than in the XY group in the gonadectomized state after the treatment with angiotensin II, which hints a possible effect of the XX sex chromosome on hypertension in women with ovarian hormone deficiency (Ji et al., 2010). Another study also reported that as a hypertension risk factor, increased adiposity has a closer relationship with the copy number of the X chromosome than the Y chromosome, independently of the gonadal sex (Chen et al., 2012). In addition to the X chromosome, the Y chromosome also has a direct genetic influence on hypertension in spontaneously hypertensive rats (Ely and Turner, 1990). Overexpression of the SRY3 gene in normotensive male rats leads to increased RAAS activity and enhanced sodium reabsorption and raises systolic blood pressure by 10-20 mmHg compared with controls (Ely et al., 2011). This evidence suggests the contribution of sex chromosomes to hypertension. These effects may depend on the activation of some blood pressure-regulating genes in the sex chromosomes.

1.3.2 Androgens

Androgens are the male sex hormones promoting the formation of male reproductive organs and the development of secondary sexual characteristics. Testosterone is the major androgen in males, and it can be further converted to dihydrotestosterone (DHT), whose activity is greater than testosterone. Androgens can be found in both males and females since they are produced in many organs, including testes, ovaries, and adrenal glands. They exert their functions by binding to the androgen receptors, which are the ligand-dependent nuclear transcription factors (Chang et al., 1995).

1.3.2.1 Androgen receptor

The androgen receptor (AR) is a member of the steroid hormone nuclear receptor family, which includes estrogen receptor (ER), mineralocorticoid receptor, progesterone receptor, and glucocorticoid receptor (Mangelsdorf et al., 1995). The structure of AR mainly comprises three

parts: the N-terminal transcriptional regulation domain (NTD), the DNA binding domain (DBD), and the C-terminal ligand-binding domain (LBD) (Davey and Grossmann, 2016). ARs are widely distributed in multiple tissues throughout the body, including bone, adipose tissue, cardiovascular system, muscle, brain, and prostate, so AR signaling is deeply involved in the regulation of various physiological functions (Rana et al., 2014). AR is activated by binding to androgens and regulates cell activity mainly through two different mechanisms: the genomic effect (DNA binding-dependent) or the non-genomic effect (non-DNA binding-dependent) (Fig.8).

1.3.2.1.1 Genomic effect of androgen receptor

The genomic effect is the primary mechanism of AR action, which regulates the cell function by directly binding to the target DNA to regulate gene transcription. Before binding with androgens, AR is in an inactive conformation in the cytoplasm in association with molecular chaperones, including heat shock proteins and other co-chaperones. Upon androgens binding, AR dissociates from chaperones and undergoes a conformational change. With the help of cytoskeletal protein filamin A, this androgen/AR complex is translocated to the nucleus and dimerizes. The dimers then bind to androgen response elements (AREs) within the genomic DNA, resulting in target gene transcription (Davey and Grossmann, 2016). For example, the level of transmembrane serine protease 2 (TMPRSS2) is increased in prostate cancer cells upon the treatment with androgens. It is induced by the interaction of androgen and the putative ARE site in the *TMPRSS2* promoter region (Lin et al., 1999). Many studies also show that AR can regulate the expression of prostate-specific antigen (*PSA*) in the prostate cancer cells by binding to three ARE sites located in the proximal 6kb of the *PSA* promoter (Cleutjens et al., 1996; Cleutjens et al., 1997). There are many other such examples, e.g., c-FLIP (Gao et al., 2005), caspase‐2 (Rokhlin et al., 2005), insulin-like growth factor 1 receptor (Pandini et al., 2005), and kallikrein 2 (Dehm and Tindall, 2006). The activation of these genes by androgens contributes to the progression of prostate cancer.

1.3.2.1.2 Non-genomic effect of androgen receptor

In addition to the genomic effect, AR has the second manner of action by the non-genomic effect. In this case, AR transmits signals through second messenger pathways instead of direct DNA binding to regulate cell function. Although by this pathway, AR cannot mediate gene transcription directly, the non-genomic AR signaling can influence the target gene expression indirectly by activating the downstream transcription factors, such as AP-1 (Kallio et al., 1995) and CREB (Unni et al., 2004). Many downstream second messenger pathways after the activation of AR have been revealed in various target cells. For instance, the cell membrane-impermeable BSA-conjugated testosterone can only bind to AR on the cell membrane rather than enter into the cytoplasm. Such binding induces the IP3-mediated intracellular Ca^{2+} release and Ras/MEK/ERK pathway activation in skeletal muscle cells (Estrada et al., 2003). A similar Ras/Raf/MAPK/ERK cascade is also reported in the non-genomic AR signaling-mediated prostate cancer cell proliferation (Liao et al., 2013). Furthermore, the activated AR can also interact with other signal molecules, such as SRC and AKT, to trigger the MAPK/ERK cascade to achieve the same effect. In prostate cancer cells, the non-genomic AR signaling induces actin polymerization through Rho/ROCK/actin signaling pathway.

AR can also have a ligand-independent effect. The activity of AR can be induced by the interaction with cytokines, growth factors, and osteoblast-derived factors independent of androgen. For example, interleukin-6 (IL-6) can activate AR NTD via the Ras/Raf/MAPK and STAT3 signaling pathway in human prostate cancer cells, leading to the upregulation of PSA expression upon the binding of activated AR to its ARE site (Ueda et al., 2002). During the progression of prostate cancer, AR activity also can be promoted by epidermal growth factor (EGF) and Insulin-like growth factor (IGF) via GEF VAV3/Rac1 signaling (Lyons et al., 2008).

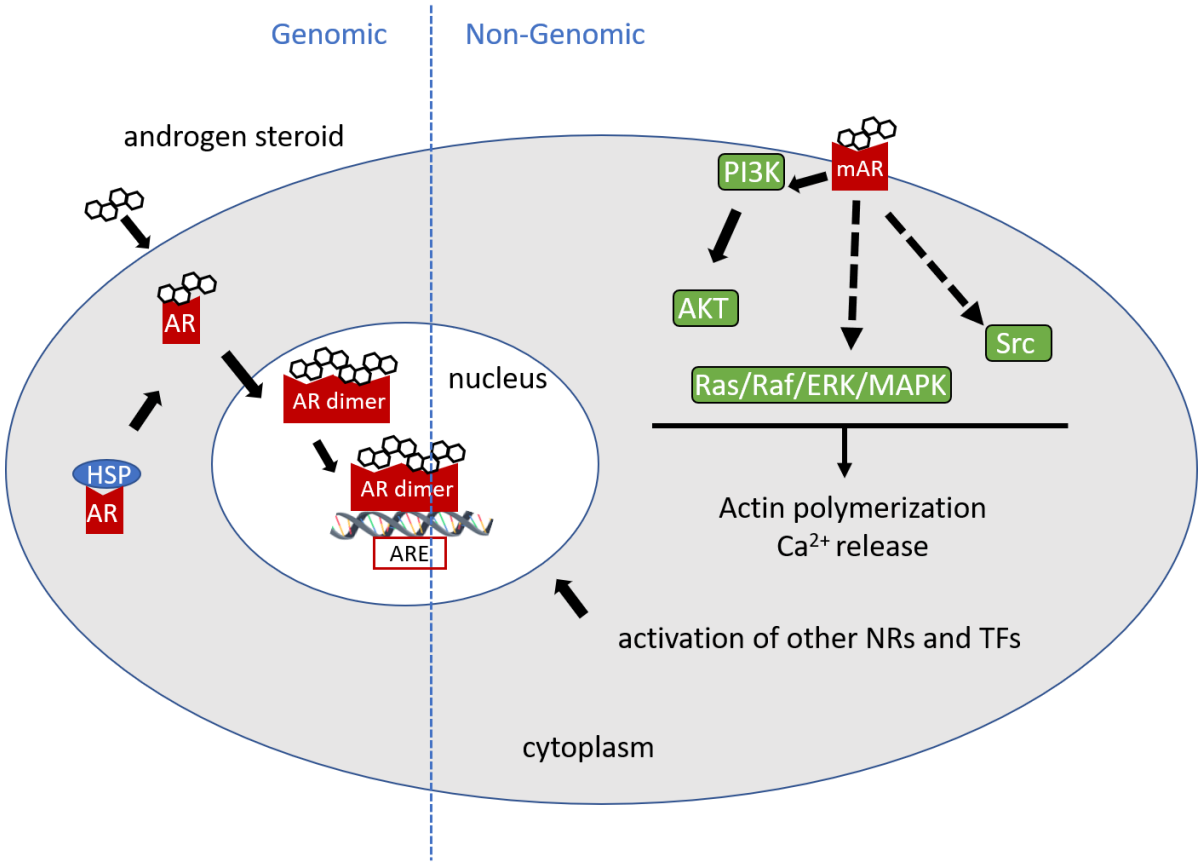

Figure 8. – Genomic and Non-Genomic effect of androgen. Image modified from Lorin et al. 2015 (Lorin et al., 2015).

1.3.2.2 Androgen and hypertension

Ever-increasing evidence confirms that androgens play an important role in hypertension and cardiovascular disease, but the specific mechanism is not fully clear. Interestingly, androgens have both protective and promoting effects on hypertension, which suggests androgens may function on both vasoconstriction and vasodilation pathways.

The promoting effect of androgens on hypertension and cardiovascular disease has been reported in many animal studies. In Dahl salt-sensitive rats model, treatment with testosterone enhanced the severity of hypertension, whereas castration on neonatal males postponed the onset of salt-induced hypertension (Rowland and Fregly, 1992). In the spontaneously hypertensive rats model, the systolic blood pressure in males was 20-30 mmHg higher than in

females or in castrated males, and the testosterone treatment on ovariectomized females raised the blood pressure by 11% compared to untreated ones (Reckelhoff et al., 1998). The pro-hypertensive effect of androgens is also found in humans. Premenopausal women with high androgen levels tend to have a higher risk of hypertension (Moretti et al., 2017). Hyperandrogenemia caused by polycystic ovary syndrome (PCOS) in reproductive-age women leads to a high prevalence of obesity, metabolic syndrome, and hypertension (Azziz et al., 2006). This effect of androgens is further proved in a PCOS female rats model induced by long-term treatment of DHT. DHT treatment causes a sustained extra increase in food intake, body weight, and fat in the female rats, and the rats eventually develop hypertension, hypercholesterolemia, hyperinsulinemia, and hyperleptinemia (Yanes et al., 2011).

The mechanism of the pro-hypertensive effect of androgens is widely studied. Many mechanisms have been demonstrated in animal studies. AR activation can activate the sympathetic nervous system by upregulating the TH expression. The treatment of testosterone on castrated spontaneously hypertensive rats causes increased *TH* mRNA levels in the adrenal medulla and the subsequent elevation of catecholamine levels and blood pressure (Kumai et al., 1995). The increase of TH expression is induced by the binding of activated AR to the ARE site in the *TH* promoter region (Jeong et al., 2006). The stimulation of androgens on ovariectomized spontaneously hypertensive rats enhances the renal sodium reabsorption and increases glomerulosclerosis, resulting in hypertension (Liu and Ely, 2011). The activity of RAAS, which is critical in blood pressure regulation, is also regulated by androgens. The renin level and angiotensinogen mRNA level in ovariectomized spontaneously hypertensive female rats are increased after administration of testosterone, which was responsible for the raised blood pressure (Chen et al., 1992). Furthermore, androgens also contribute to other RAAS component regulations. The deficiency of androgens causes decreased angiotensin-converting enzyme (ACE) levels (Freshour et al., 2002), while the presence of androgens promotes the expression of angiotensin II type 1 (AT1) receptors in abdominal aortas (Henriques et al., 2008) but inhibits the angiotensin II type 2 (AT2) receptors expression levels in the aorta (Mishra et al., 2016). The release and actions of another strong vasoconstrictor, Neuropeptide Y (NPY), is also reported to be up-regulated by androgens (Zukowska-Grojec, 1995). In addition, AR signaling involves in

vascular remodeling associated with hypertension. Androgens promoted the reactive oxygen species (ROS) generation in VSMCs by both genomic and non-genomic effects, which further mediated the VSMCs migration and VSMCs apoptosis during vascular remodeling (Chignalia et al., 2012; Lopes et al., 2014). Many other studies also show that androgens can upregulate the production of endothelin-1 (ET-1), thromboxane A2, and 20-hydroxyeicosatetraenoic acid to induce vasoconstriction and increase of blood pressure (Maturana et al., 2008;Wong et al., 2009;Wu and Schwartzman, 2011).

Although androgens show pro-hypertensive effects in many studies, the deficiency in androgens is also thought to contribute to the development of hypertension. The odds ratios of having hypogonadism are much higher in hypertensive patients (Mulligan et al., 2006). A famous prospective cohort study, the Fourth Tromsø Study, analyzed the testosterone level, the incidence of myocardial infarction, and the mortality of various causes of 1568 men dwelling in randomly selected communities. It demonstrates that the risk of all-cause mortality due to cardiac vascular diseases increases 24% in men with free testosterone levels in the lowest quartile (Vikan et al., 2009). The androgens levels in obese men tend to be lower than normal-weight men (Buvat et al., 2013). The androgen deficiency has also been reported in metabolic syndrome, type II diabetes, and insulin resistance (Jones and Saad, 2009), and it can cause an imbalance in lipid composition resulting in hypertension and increased incidence of atherosclerosis (Traish et al., 2009; Fahed et al., 2012). In these studies, it is not clear whether androgen deficiency is a cause or consequence of these chronic diseases, but many investigators believe its contribution to disease progression (Moretti et al., 2017).

The mechanism of androgen deficiency-induced hypertension is still unclear. Since androgen deficiency aggravates adiposity and insulin resistance induced by a high-fat diet (Dubois et al., 2016), a low androgen level should be closely associated with fat accumulation. Excessive lipid accumulation may lead to cellular apoptosis, which activates macrophages and many inflammatory factors. The increased inflammatory cytokine levels, together with adipocyte dysfunction, promote endothelial dysfunction, increasing the prevalence of hypertension. The adipocyte and endothelial dysfunction may be regulated by the nuclear factor κB (NF-kB) signaling, whose activity is significantly increased when androgen level is insufficient (Moretti et al., 2017).

In addition, in obese men, the reduced androgen level may associate with increased inflammation because androgen supplements treatment can reduce the inflammatory cytokine levels in hypogonadal men (Malkin et al., 2004). Some studies also found that androgens supported the growth and proliferation of endothelial cells (via vascular endothelial growth factor) and endothelial progenitor cells (via PI3K/Akt signaling), which help to repair the endothelial dysfunction (Cai et al., 2011; Liu et al., 2014b). Many androgen replacement therapies in obese men or hypogonadal men can effectively reduce blood pressure, further supporting the close relationship between androgen deficiency and hypertension (Marin et al., 1993; Zitzmann, 2007).

Noteworthy, androgens may directly relax the blood vessels to reduce blood pressure. The androgen-induced vasodilation mainly relies on the non-genomic effect on the blood vessels. Lower concentration of testosterone (100pM–10μM) prefers to trigger vasodilation via an endothelium-dependent mechanism, which involves the release and activation of nitric oxide (NO) (Chou et al., 1996; Molinari et al., 2002), while a higher concentration of testosterone (>10 μM) facilitates blood vessels relaxation through an endothelium-independent mechanism (Perusquia and Stallone, 2010). For example, the vasodilation effect of androgens on blood vessels depends on potassium efflux through large-conductance, calcium-activated potassium channel independent of the endothelium (Deenadayalu et al., 2001), or decreased external Ca^{2+} influx by inactivating VGCCs (Perusquia et al., 2007). A similar endothelium-independent vasodilation effect of androgens is also reported on rabbit coronary arteries and aorta (Yue et al., 1995) and isolated human radial arteries (Seyrek et al., 2007). According to the above researches, androgen deficiency may lose the beneficial effects of androgen on cardiovascular function, resulting in hypertension.

1.3.3 Estrogens

Estrogens are a group of sex hormones responsible for developing female secondary sexual characteristics and regulating the female reproductive system. There are four members of the endogenous estrogens: estrone, estradiol, estriol, and estetrol. Among them, estradiol is the most effective and prevalent circulating estrogen in humans. Estrogens are present in both males and

females, and they are predominantly produced in the ovary in females or Sertoli cells in males. However, some extragonadal tissues, including the adrenal cortex, adipose tissue, and liver, also contribute to estrogen production, vital for maintaining estrogen levels after menopause in women (Miller, 2017).

1.3.3.1 Estrogen receptors

Like androgens, estrogens function by binding to their estrogen receptors (ERs), which have three members: two nuclear estrogen receptors (ERα and ERβ) and a G protein-coupled membrane estrogen receptor (GPER-1). They are widely distributed throughout the body, and their location in the kidneys, brain, vasculature, or heart is particularly critical for blood pressure regulation (Maranon and Reckelhoff, 2013). ERα and ERβ share a similar structure, including three functional domains (NTD, DBD, and LBD), while the GPER-1 has a classic structure of G protein-coupled receptor (seven-transmembrane α-helical regions, four extracellular segments, and four cytosolic segments) (Barton et al., 2018). The binding affinity to estrogens is higher for ERα and ERβ than for GPER-1 (Prossnitz and Barton, 2014). Estrogens regulate the target cell function primarily through the genomic effect and non-genomic effect, whereas the ligand-independent effect and ER-independent effect also contribute to estrogen-mediated signaling mechanisms.

1.3.3.1.1 Genomic effect of estrogen receptor

The genomic effect of ERs is the classical mechanism to regulate the target cell function by estrogens. ERα and ERβ play the role of ligand-activated transcription factors in this process. ERs are activated by estrogen binding in the cytosol. This is followed by a series of subsequent processes, including their translocation to the nucleus, dimerization, interaction with EREs or binding to other elements by transcriptional cross-talk in the target gene promoter region, and regulating the transcription of the downstream DNA (Fuentes and Silveyra, 2019). The EREs sites are widely distributed in many promoter regions. In the mouse and human genomes, about 70,000 high-affinity EREs have been identified by a genome-wide screening study, and a quarter of them are located near the transcriptional start sites (Bourdeau et al., 2004). Besides directly

binding to EREs, ERs can also interact with other transcription factors, such as Ap-1, NF-κB, and Sp-1, or other transcriptional modulators to either activate or block the corresponding components in the regulatory region of the target gene, eventually up-regulating or down-regulating gene expression (Fuentes and Silveyra, 2019).

1.3.3.1.2 Non-genomic effect of estrogen receptor

The non-genomic effect is the main way for the cell surface receptor GPER-1 to perform its function. The activation of GPER-1 by the binding of estrogens rapidly transmits the signals into the cell via different intracellular signaling cascades triggered by second messengers, indirectly regulating the production or function of the downstream proteins. The nuclear receptors ERα and ERβ can also exert the non-genomic effect by interacting with scaffold proteins (e.g., caveolin-1), membrane receptors (e.g., tyrosine kinase receptors), G proteins, and some submembrane signaling molecules (e.g., Src family kinase, Ras GTPase, and PI3Ks) (Chambliss et al., 2000; Li et al., 2007; Zabransky and Park, 2014; Hong and Choi, 2018; du Rusquec et al., 2020). So far, many ER signaling transduction cascades have been identified. GPER activation triggers the PLC/IP3/PKC signaling cascade in breast cancer cells (Boyan et al., 2003). Inhibiting ERs activity by tamoxifen suppresses the Ras/Raf-1/MAPK pathway-mediated development and progression of breast cancer (McGlynn et al., 2009). Betulinic acid-induced endothelial NO synthase activity is regulated by the ERs via the PI3K/Akt pathway (Hohmann et al., 2016). The vasodilation of porcine coronary arteries induced by GPER is controlled by the activity of myosin light chain phosphatase (MLCP) via the cAMP/PKA signaling pathway (Yu et al., 2014).

In addition to the above-described two primary estrogen-mediated signaling mechanisms, ER activity can also be triggered in a ligand-independent way. The ligand-independent activity of ERs depends on the signaling cross-talk. Many factors, such as EGF, IGF, dopamine, and cytokines, bind to their respective receptors on the cell membrane and trigger the cAMP, PKA, PKC, or MAPK cascades to induce the phosphorylation of ERs, leading to the activity of ligand-independent ERs signaling (Bennesch and Picard, 2015). In addition, estrogens exert their antioxidant and

neuroprotective effect in an ER-independent manner. These findings have enriched our understanding of the mechanisms of estrogen signal transduction (Moosmann and Behl, 1999).

1.3.3.2 Estrogen and hypertension

The benefits of estrogens in preventing hypertension have been demonstrated extensively. The systolic blood pressure in postmenopausal women raises by 3-5 mmHg compared to that in perimenopausal women, and this difference is still significant after adjustment for age, body mass index (BMI), and other mixed factors (Zanchetti et al., 2005;Li et al., 2012). Many animal studies also gave strong support to the beneficial effect of estrogen on hypertension. The baseline blood pressure of rats increased about 10 mmHg after ovariectomy, but chronic estrogen replacement treatment reversed the raised blood pressure (Hernandez et al., 2000). A similar protection role of estrogens is also reported in the Dahl hypertension rat model, in which hypertension is induced by sodium intake (Hinojosa-Laborde et al., 2000) and in the angiotensin II-induced hypertension mouse model (Xue et al., 2008). However, the effect of hormone replacement treatment on hypertension in postmenopausal females remains controversial. The blood pressure after exogenous estrogen treatment might decrease, increase, or have no change. This different outcome might be due to the dose of estrogen, the type of exogenous estrogen, and the initiation time of the therapy (Rosano et al., 2006; Colafella and Denton, 2018). Here, we will explore the possible mechanisms of estrogen in blood pressure regulation.

Estrogens have always been considered as a vasodilator since their vasorelaxant effects on blood vessels have been well established. Estrogen-induced vasodilation is closely associated with NO. The stimulation of estrogens increases the NO production by up-regulating the expression of endothelial nitric oxide synthase (eNOS) in endothelial cells via an ER-mediated genomic effect or by increasing eNOS activity via the non-genomic effect on the PI3K/cAMP signaling cascades or PI3K/Akt pathway (Han et al., 2012; Fardoun et al., 2020). Furthermore, NO production in VSMCs can be triggered by a long-term administration of estrogens (Salhab et al., 2000). Many studies also report that ERs activity inhibits the Ca^{2+} influx and enhances Ca^{2+} efflux in the VSMCs, leading to a reduced intracellular Ca^{2+} concentration and subsequent vasodilation (Ruehlmann et al., 1998;

Prakash et al., 1999; Cairrao et al., 2012). ERs activity in the VSMCs also triggers the current through large-conductance Ca^{2+} and voltage-activated K+ channels, further enhancing the intracellular Ca^{2+} deficiency and the vascular relaxation (White et al., 2002).

Noteworthy, estrogens wildly act on various blood pressure-regulating systems, including the RAAS system, sympathetic nervous system, and kidney. In an ovariectomized rat model, the aorta ACE activity is significantly increased, and the treatment with estrogens reverses the elevated ACE activity (Tanaka et al., 1997). In contrast, estrogen treatment upregulates the renal ACE2 activity, speeding up the conversion of angiotensin II to angiotensin (1-7) (Ji et al., 2008), which reduces the vasoconstriction effect of angiotensin II and enhances the latter's vasodilation effect. Furthermore, estrogens are able to downregulate the AT1 receptor (Nickenig et al., 1998) and upregulate the AT2 receptor (Armando et al., 2002), both of which bring benefits of lowering blood pressure. Estrogens also play an essential role in sodium and water balance. A recent study found that estrogens downregulated the expression of the epithelial sodium channel in the distal kidney nephron, which is responsible for sodium reabsorption by promoting Derlin-1 expression and AMP-activated protein kinase activation (Zhang et al., 2019a). The role of estrogens on the sympathetic nervous system is worth noting when studying the anti-hypertensive effect of estrogens. They can restrict the sympathetic nervous activity in the brain by upregulating the AT2 receptor expression and NO levels and by suppressing the AT1 receptor expression and ROS levels (Fardoun et al., 2020). Estrogen treatment in ovariectomized female Wistar rats improves the redox status by decreasing the ROS production and enhancing NO bioavailability, eventually significantly reducing the arterial pressure and sympathetic vascular drive (Campos et al., 2014).

Although the antihypertensive effect of estrogens has been generally acknowledged, the benefit of estrogen on the protection against primary or secondary cardiovascular events is still controversial (Grady et al., 2002). More and more studies focusing on the vasoconstriction effect of estrogens question the benefits of estrogen. There is still a long way to clarify the role of estrogen in blood pressure regulation completely.

So far, the roles of sex hormones in chromaffin cell biological function and hypertension have not been fully clarified yet. In this study, we will try to investigate the joint effect of sex hormones and EPH/EFN molecules in chromaffin cell biology and its potential impact on blood pressure regulation.

Chapitre 2 – HYPOTHESIS AND OBJECTIVES

We have reported that EPHB6 KO mice with hypogonadism (caused by castration) become hypertensive. EPHB6 has at least two target tissues: vascular smooth muscle cells and adrenal gland chromaffin cells. The roles of EPHs/EFN signaling in VSMCs have been elucidated in our previous studies, but AGCCs have not been investigated. We have found that EphB6 in concert with testosterone regulated ambient catecholamine levels in mice. In this study, we will further explore whether the EPHB6 receptor and EFNB ligands, together with sex hormones, are involved in regulating catecholamine synthesis and secretion in AGCCs, and what underlying molecular mechanisms are involved. We believe that this regulation may contribute to hypertension observed in EPHB6 KO castrated male mice.

Hypothesis

1. EPHB6 has an effect on AGCCs catecholamine synthesis and secretion via reverse signaling through EFNBs;

2. EPHB6/EFNBs interact with cholinergic receptors and/or cell surface ion channels, impacting their function in a testosterone-dependent fashion;

3. EPHB6/EFNBs reverse signaling regulates catecholamine secretion in AGCCs by controlling F-actin disassembly in a testosterone-dependent way;

4. Testosterone, in concert with EPHB6/EFNB reverse signaling, influences the transcription of molecules that regulate catecholamine synthesis in AGCCs.

Objectives

1. To investigate the mechanisms by which EPHB6 and testosterone, in concert, control catecholamine biosynthesis and secretion in AGCCs.

2. To dissect the genetic association between compromised EphB6 signaling and hypertension in ageing male hypogonadic patients based on human genetic studies.

Chapitre 3 – ARTICLE-1

TITLE: EPHB6 and testosterone in concert regulate epinephrine release by adrenal gland chromaffin cells

[a,d*]Yujia Wang, [a*]Wei Shi, [b]Alexandre Blanchette, [a]Junzheng Peng, [a]Shijie Qi, [a]Hongyu Luo, [b]Jonathan Ledoux, and [a,c]Jiangping Wu

Running title: *EPHB6 and catecholamine release*

[a]Research Centre, Centre hospitalier de l'Université de Montréal (CRCHUM), Montreal, Quebec,Canada H2X 0A9; [b]Montreal Heart Institute, Montreal, Quebec, Canada H1T 1C8; [c]Nephrology Department, CHUM, Montreal, Quebec, Canada H2L 4M1; [d]The Children's Hospital, Zhejiang University School of Medicine, Hangzhou, Zhejiang, China 310003.

To whom correspondence should be addressed: Dr. Jiangping Wu, CRCHUM, 900 rue St-Denis, R12-428, Montreal, Quebec, Canada H2X 0A9, Telephone: (514) 890-8000 Extension 25164, E-mail: jianping.wu@umontreal.ca, Dr. Jonathan Ledoux, Montreal Heart Institute, Montreal, Quebec, Canada H1T 1C8, Telephone (514) 376-3330 Extension 2476, E-mail: jonathan.ledoux@umontreal.ca, or Dr. Hongyu Luo, CRCHUM, 900 rue St-Denis, R12-426, Montreal, Quebec, Canada H2X 0A9, Telephone: (514) 890-8000 Extension 25319, E-mail: hongyu.luo@umontreal.ca

Keywords: EPHB6, chromaffin cells, catecholamine secretion, calcium influx, testosterone, BK channel

Footnote: *Y.W. and W.S. contributed equally to this work.

Published in Scientific Reports 2018 Jan; 8(1):842.

Candidate's Contribution

W.S. was involved in generating the concept and initiating this project. W.S. conducted experiments in the cellular level and molecular level and generated the research outcomes in the Fig. 1(C,D), Fig. 2, Fig. 3, Fig. 6, and supplementary Figure 1,2. W.S. was involved in drafted the manuscript. W.S. contribution to this publication was about 50%.

Abstract

Erythropoietin-producing human hepatocellular receptor (EPH) B6 (EPHB6) is a member of the receptor tyrosine kinase family. We previously demonstrated that EPHB6 knockout reduces catecholamine secretion in male but not female mice, and castration reverses this phenotype. We showed here that male EPHB6 knockout adrenal gland chromaffin cells presented reduced acetylcholine-triggered Ca^{2+} influx. Such reduction depended on the non-genomic effect of testosterone. Increased large conductance calcium-activated potassium channel current densities were recorded in adrenal gland chromaffin cells from male EPHB6 knockout mice but not from castrated knockout or female knockout mice. Blocking of the large conductance calcium-activated potassium channel in adrenal gland chromaffin cells from male knockout mice corrected their reduced Ca^{2+} influx. We conclude that the absence of EPHB6 and the presence of testosterone would lead to augmented large conductance calcium-activated potassium channel currents, which limit voltage-gated calcium channel opening in adrenal gland chromaffin cells. Consequently, acetylcholine-triggered Ca^{2+} influx is reduced, leading to lower catecholamine release in adrenal gland chromaffin cells from male knockout mice. This explains the reduced resting-state blood catecholamine levels, and hence the blood pressure, in male but not female EPHB6 knock mice. These findings have certain clinical implications.

Introduction

Erythropoietin-producing hepatocellular receptors (EPHs), the largest family of receptor tyrosine kinases, comprise about 25 percent of known receptor tyrosine kinases (Committee, 1997). They are divided into A and B subfamilies (EPHAs and EPHBs), based on sequence homology. The EPHA subfamily has nine members, and EPHB has five members. Their ligand ephrins (EFNs) are also cell surface molecules (Committee, 1997;Pasquale, 2008), which are also classified into A and B subfamilies (EFNAs and EFNBs) based on the way they anchor on the cell surface. EFNAs bind to the cell surface via glycosylphosphatidylinositol, while EFNBs are transmembrane proteins. The signaling from their ligand EFNs to EPHs is called forward signaling. EFNs, although ligands, can also transduce signals into cells (Pasquale, 2008), and signaling from EPHs to EFNs is called reverse

signaling. Interactions among EPHs and EFNs are promiscuous: a given EPH can interact with multiple EFNs and *vice versa*. In general, EPHA members bind preferentially to EFNA members, as EPHB members do to EFNB members (Pasquale, 2008).

EPHs/EFNs function in many organs and systems (Pasquale, 2008). Our laboratory was the first to report the critical roles of EPHs and EFNs in the immune system (Luo et al., 2001;Luo et al., 2002;Yu et al., 2003a;b;Luo et al., 2004;Yu et al., 2004;Wu and Luo, 2005;Yu et al., 2006;Luo et al., 2011a;Luo et al., 2011b;Jin et al., 2014;Hu et al., 2015;Luo et al., 2016). In the past five years, we have discovered novel functions of EPHs/EFNs in regulating blood pressure (Luo et al., 2012;Wu et al., 2012;Wang et al., 2015;Wang et al., 2016a;Wang et al., 2016b;Wang et al., 2016c). We reported that while EPHB6, EFNB1 and EFNB3 deletion results in blood pressure elevation, EPHB4 and EFNB2 deletion reduces it. Thus, EPHBs and EFNBs are a novel yin and yang system that finely tunes blood pressure homeostasis. In all such cases, sex hormones act in concert with these EPHs/EFNs for blood pressure regulation. We have established that vascular smooth muscle cells are target tissues for the blood pressure-regulating effect of these molecules. EPHB6, however, also targets cells responsible for catecholamine secretion. Male EPHB6 knockout (KO) mice have reduced blood catecholamine levels in a resting state (Luo et al., 2012), which counteracts the outcome of increased vascular smooth muscle cell contractility, resulting in normal blood pressure. Castration of male KO mice leads to blood catecholamines returning to the normal level (Luo et al., 2012). This, concomitantly with enhanced vascular smooth muscle cell contractility, results in blood pressure elevation in these castrated KO mice. This body of evidence indicates that EPHB6 and male sex hormones are acting in concert to regulate catecholamine secretion and blood pressure.

In the present study, we investigated the mechanism by which EPHB6 regulates adrenal gland chromaffin cell catecholamine secretion. We found that adrenal gland chromaffin cells from male KO mice were characterized by a reduced acetylcholine-dependent Ca^{2+} influx, involving non-genomic effects of testosterone. We further demonstrated that Ca^{2+} influx decrease was the consequence of enhanced large conductance calcium-activated potassium (BK) currents in these cells.

Materials and methods

EPHB6 gene KO mice

EPHB6 KO mice were generated in our laboratory, as described previously(Luo et al., 2004). They were backcrossed to the C57BL/6 background for more than 15 generations. Age- and sex-matched wild type (WT) littermates were used as controls. All experiments involving castrated mice were conducted at least three weeks post-operation.

Reverse transcription-quantitative polymerase chain reaction (RT-qPCR)

mRNA levels of *EPHBS*, *EFNBS* and *BK* channel subunits were measured by RT-qPCR. Total RNA from the adrenal glands, adrenal gland medullae and spleen was extracted with TRIzol® (Invitrogen, Burlington, Ontario, Canada) and reverse-transcribed with iScript™cDNA Synthesis Kit (Bio-Rad Laboratories (Canada) Ltd., Mississauga, Ontario, Canada). The primers used for PCR are listed in Supplementary Table 1. Conditions for the qPCR reactions were as follows: two minutes at 50°C, two minutes at 95°C, followed by 40 cycles of 10 seconds at 94°C, 20 seconds at 58°C, and 20 seconds at 72°C. β-actin mRNA levels were considered as internal controls. qPCR signals between 22 and 30 cycles were analyzed. Samples were tested in triplicate, and the data were expressed as signal ratios of target RNA/ β-actin mRNA.

Primary adrenal gland chromaffin cell culture

Mouse adrenal gland chromaffin cells were isolated, as described by Kolski-Andreaco *et al*., (Kolski-Andreaco et al., 2007) with modifications. Briefly, we obtained adrenal glands from 8- to 10-week-old mice, and fat and cortex were removed from these glands. Papain (P4762, Sigma-Aldrich, Oakville, Ontario, Canada) was activated with 5 mmol/L L-cysteine. Adrenal gland medullae were digested by activated papain in Hank's buffer (2 medullae/100 µl Hank's buffer containing four units of activated papain) at 37°C for 25 min. They were washed twice with Hank's

buffer and then triturated by pipetting in 300 µl Hank's buffer until they became feather-like. Cells were pelleted at 3,700 *g* for three minutes and re-suspended in Dulbecco's modified Eagle's medium (DMEM) containing 15 % (v/v) fetal calf serum (FCS) for culture.

Epinephrine measurements

Adrenal glands were resected from EPHB6 KO and WT mice, and cut in half to expose the medulla. They were then stimulated with 5 mmol/L acetylcholine chloride (A2661, Sigma-Aldrich) in 300 µl Hank's buffer at room temperature for one minute. Epinephrine levels in the supernatants were measured with Epinephrine Research ELISA kit (BAE-5100, Rocky Mountain Diagnostics, Colorado Springs, CO, USA), according to the manufacturer's instructions. Samples were tested in duplicate by ELISA.

Immunofluorescence microscopy

Adrenal gland chromaffin cells were cultured in 6-well plates with cover glass placed at the bottom of the wells. After one day, the cells were washed once with phosphate-buffered saline (PBS) and fixed with 4% (w/v) paraformaldehyde for 20 minutes. They were then blocked with 10% (v/v) FCS in PBS for 20 minutes and incubated overnight at 4°C with goat anti-mouse EPHB6 antibody (Ab; 2 µg/ml, R&D Systems, Minneapolis, MN, USA). They were then reacted with Alexa-488-conjugated donkey anti-goat Ab (2 µg/ml, Molecular Probes, Eugene, OR, USA) for two hours at room temperature, and imbedded with ProLong® Gold anti-fade reagent (Molecular Probes). Cell staining was examined with a Zeiss microscope.

Ca^{2+} influx measurements

Acetylcholine-stimulated Ca^{2+} influx in adrenal gland chromaffin cells was measured by microfluorescence technique (Grynkiewicz et al., 1985;Luo et al., 2012). Briefly, isolated adrenal gland chromaffin cells were incubated for 24 hours in DMEM containing 15% (v/v) FCS. The cells

were loaded with Fura-2-AM (5 μmol/L) for 60 minutes at 37℃. They were rinsed once in warm DMEM containing 15% (v/v) FCS without dye and placed in Hank's balanced salt solution containing 1.26 mmol/L Ca^{2+} at 37℃. They were stimulated with acetylcholine (5 mmol/L) at 37℃ and imaged for 120 seconds at a rate of approximately one measurement per two seconds for the two excitation wave lengths (the exposure time of a particular experiment varied slightly) with a Zeiss fluorescence microscope. Excitation wavelengths were recorded alternatively at 340 nm and 380 nm, and emission was registered at 510 nm. Signals from more than 15 randomly selected cells were recorded, and the results expressed as ratios of fluorescence intensity at 510 nm excited by 340 nm versus 380 nm.

Whole-cell patch clamping

Adrenal gland chromaffin cells were isolated and cultured for 24-48 hours. They were voltage-clamped to measure calcium and potassium current densities at 20-22℃, with the perforated whole-cell (amphotericin B; 200μg/mL) configuration of the patch clamp technique as described in detail elsewhere.(Ledoux et al., 2003;Ledoux et al., 2008) For calcium current density monitoring, adrenal gland chromaffin cells were voltage-clamped at -70 mV, and 200-ms depolarizing pulses were applied at 5-mV steps from -50 to +45 mV, to construct I-V curves. For potassium current density measurement, adrenal gland chromaffin cells were voltage-clamped at -70 mV, and 750-ms depolarizing pulses were applied at 10-mV steps from -70 to +100 mV, in the absence or presence of paxilline, a BK channel blocker. Membrane currents were recorded and normalized to cell capacitance (I(pA/pF)) and current density-voltage curves were generated.

Ethics statement

All animal studies were approved by the Animal Protection Committee (Comité institutionnel d'intégration de la protection des animaux) of the CRCHUM. All experiments were conducted in accordance with relevant guidelines and regulations of the local government.

Statistical analysis

All results are presented as means ± S.E. The data were analyzed statistically by 2-tailed Student's *t*-test, or a linear mixed-effect model (with genotype, individual cell, sex, sex hormone and time as qualitative factors). *P*-values of <0.05 are considered to be statistically significant.

Results

Reduced epinephrine secretion by adrenal glands from male but not female EPHB6 KO mice

We previously reported that male EPHB6 KO mice present decreased 24-hour urine catecholamine levels (Luo et al., 2012). To establish causality of this phenotype to the adrenal glands, we measured the KO adrenal gland catecholamine secretion by RT-PCR. As anticipated, RT-qPCR showed that the adrenal gland from KO mice did not express EPHB6 at the mRNA level (Fig. 1A). No compensatory mRNA up-regulation of other EPHB members, such as EPHB1, EPHB2, EPHB3 or EPHB4, was evident in adrenal glands (Supplementary Figure 1 (S. Fig.1) from male, female or castrated KO mice. Nor was there abnormal expression of mRNA levels of EPHB6 ligands (EFNB1, EFNB2 and EFNB3) in these KO adrenal gland chromaffin cells (S. Fig. 2). EPHB6 protein expression was undetectable by immunofluorescence in KO adrenal gland chromaffin cells (Fig. 1B). KO adrenal glands were of similar size as WT counterparts and showed no histological abnormalities (Fig. 1C). No significant difference in the size of adrenal gland chromaffin cells isolated from KO versus WT adrenal glands was observed (Fig. 1D). Acetylcholine-stimulated catecholamine secretion by KO adrenal glands was then assessed with epinephrine as a representative catecholamine. Adrenal glands from male but not female KO mice presented reduced epinephrine secretion, but castration reversed this KO phenotype by augmenting epinephrine secretion to normal levels (Fig. 1E). This observation is consistent with catecholamine levels in the *in vivo* KO mice, and supports the hypothesis that EPHB6 and male sex hormones jointly regulate catecholamine secretion from adrenal gland chromaffin cells.

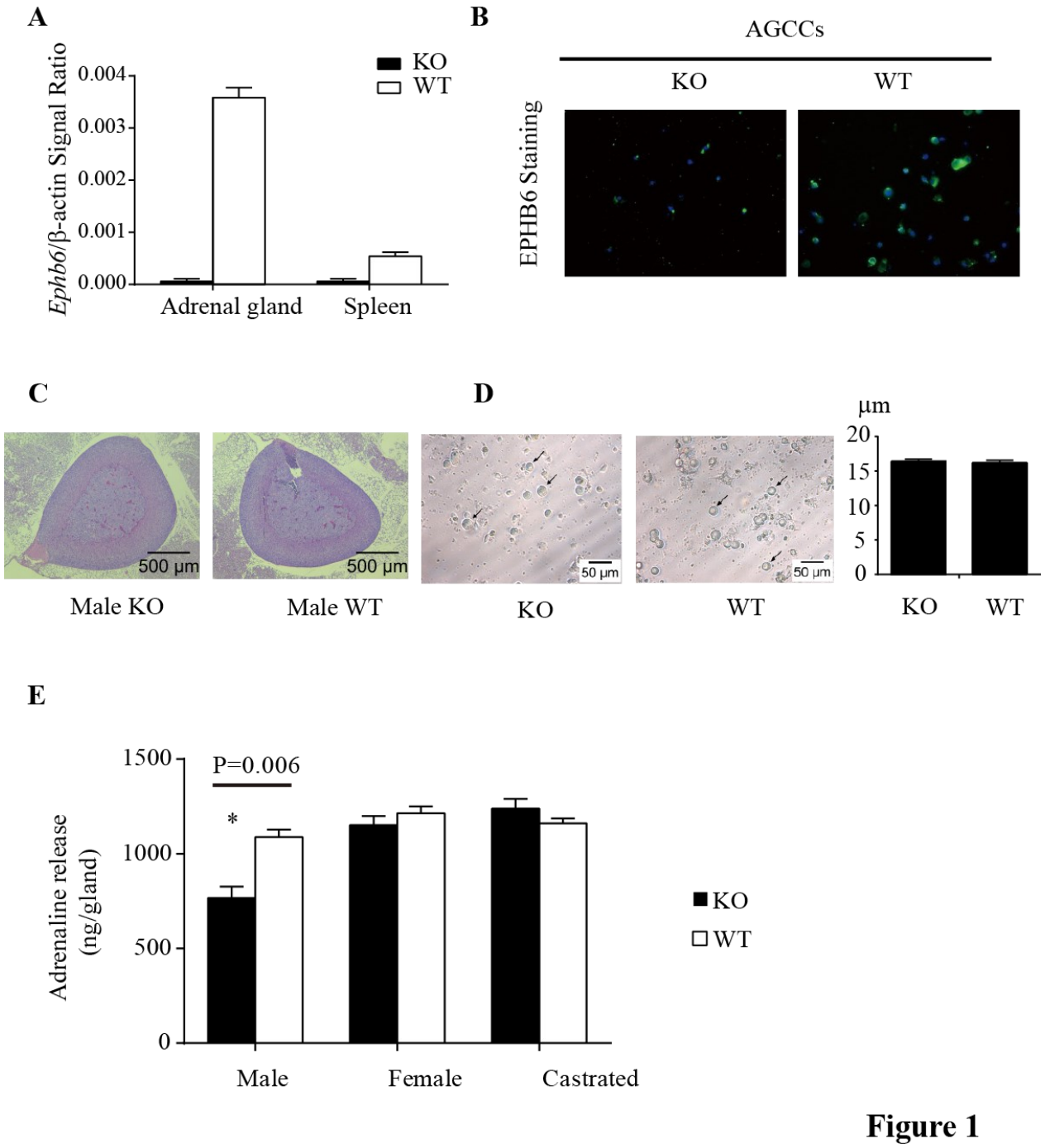

Figure 1

Figure 1. Characterization of adrenal glands and adrenal gland chromaffin cells of EPHB6 KO mice

For A, B and C, experiments were conducted three times and representative data are presented. AGCCs: adrenal gland chromaffin cells.

A. EPHB6 mRNA deletion in the adrenal glands and spleen of EPHB6 KO mice

Total RNA was extracted from the adrenal glands and spleen of male WT and EPHB6 KO mice and analyzed by RT-qPCR for EPHB6 mRNA levels. β-actin levels were used as internal controls. Samples in RT-qPCR were in triplicate, and EPHB6/ β-actin signal ratios are shown as means ± S.E.

B. EPHB6 deletion in adrenal gland chromaffin cells from EPHB6 KO mice according to immunofluorescence

Adrenal gland chromaffin cells isolated from adrenal glands of male WT and EPHB6 KO mice were cultured for one day, and then stained with goat anti-mouse EPHB6 Ab followed by Alexa-488-conjugated donkey anti-goat Ab (green). Nuclei were stained with DAPI (blue).

C. Normal histology of EPHB6 KO adrenal glands

Sections of adrenal glands from 8- to 10-week-old male WT and EPHB6 KO mice were stained with hematoxylin/eosin.

D. Adrenal gland chromaffin cells from male WT and EPHB6 KO and WT mice are similar in size

Left panel: phase-contrast micrographs of adrenal gland chromaffin cells from WT and KO mice after 24-hour culture. Right panel: diameters of adrenal gland chromaffin cells from WT and KO mice after 24-hour culture. Means $\pm$ S.E. of the diameters of more than 30 adrenal gland chromaffin cells (more than 10 cells/mouse and three mice/group) from male WT and KO mice are shown. No significant difference is observed (2-way Student's *t* test).

E. Epinephrine release from the adrenal glands of WT and KO mice

Adrenal glands, isolated from male, female and castrated male KO and WT mice, were cut in half, and were stimulated with acetylcholine (5 mmol/L) in 300 µl Hank's buffer for one minute at room temperature. The supernatants were analyzed for epinephrine levels by ELISA. Data from three independent experiments (each using one KO mouse and one WT control) were pooled, analyzed by two-way Student's *t* test, and reported as means ± S.E. *: $p<0.05$.

EPHB6 and testosterone jointly regulate adrenal gland chromaffin cell Ca^{2+} influx

Ca^{2+} influx is the main trigger for catecholamine release in adrenal gland chromaffin cells. Defective catecholamine release in adrenal gland chromaffin cells from male KO mice prompted the examination of Ca^{2+} influx in these cells. Acetylcholine-stimulated Ca^{2+} influx was significantly reduced in adrenal gland chromaffin cells from male but not female KO mice (Fig. 2A), corroborating the catecholamine phenotype *in vivo*. Castration rescued Ca^{2+} influx in KO adrenal gland chromaffin cells to a level similar to that of their WT counterparts, while it had no impact on that of adrenal gland chromaffin cells from WT males (Fig. 2B). To disentangle the effects between sex hormones and sex, we treated adrenal gland chromaffin cells from castrated males with testosterone. While Ca^{2+} influx in adrenal gland chromaffin cells from castrated WT mice was not affected by 15-minute testosterone treatment, it was augmented in adrenal gland chromaffin cells from castrated KO mice to the level of their WT counterparts (Fig. 3A), indicating that testosterone rather than sex influenced Ca^{2+} influx. The rapid response of adrenal gland chromaffin cells to testosterone treatment (15 minutes) also suggests that the effect is non-genomic. To confirm this finding, adrenal gland chromaffin cells were treated with bovine serum albumin (BSA)-conjugated testosterone, which cannot penetrate the cell membrane and can only exert non-genomic effects. Again, similarly to regular testosterone, 15-minute treatment with this membrane-impermeable testosterone augmented Ca^{2+} influx in adrenal gland chromaffin cells from castrated KO mice, but not in adrenal gland chromaffin cells from castrated WT mice (Fig. 3B), indicating that the effect is indeed non-genomic.

Based on these findings, testosterone-induced Ca^{2+} influx suppression in the absence of EPHB6 is expected in adrenal gland chromaffin cells from female KO mice. Indeed, 15-minute testosterone treatment reduced Ca^{2+} influx in adrenal gland chromaffin cells from female KO but not in WT mice (Fig. 3C). Moreover, BSA-conjugated cell membrane-impermeable testosterone was equally effective in these adrenal gland chromaffin cells from female KO mice (Fig. 3D), supporting non-genomic effects of the testosterone on adrenal gland chromaffin cells Ca^{2+} influx.

The lack of estrogen as a potential cause for the observed reduced Ca^{2+} influx in adrenal gland chromaffin cells from male KO mice was then explored. Adrenal gland chromaffin cells from male KO mice were exposed to estrogen for 15 minutes (Fig. 3E) or 24 hours (Fig. 3F). Regardless of the exposure time, estrogen had no effect on adrenal gland chromaffin cells from male KO or WT

mice in terms of acetylcholine-stimulated Ca^{2+} influx. This strongly suggests that testosterone alone, but not estrogen, in concert with EPHB6, regulates adrenal gland chromaffin cell Ca^{2+} influx.

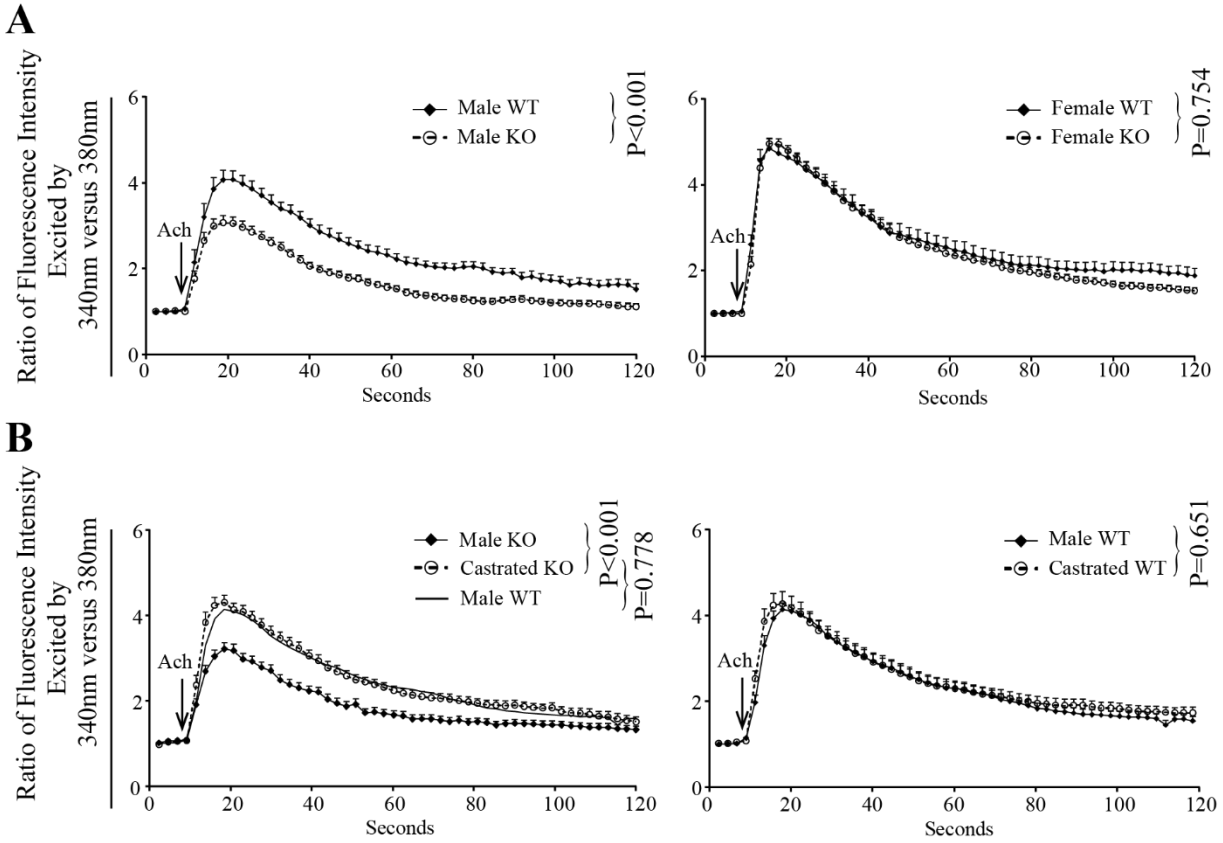

Figure 2

Figure 2. Ca^{2+} influx in adrenal gland chromaffin cells from EPHB6 KO and WT mice

Adrenal gland chromaffin cells were loaded with Fura2-AM, and stimulated with acetylcholine (5 mmol/L) at 37℃. The cells were imaged for 120 seconds at a rate of one measurement per two seconds. Arrows indicate the time points where acetylcholine was added. Signals from more than 15 randomly selected cells per group were recorded, and the results expressed as means ± S.E. of ratios of fluorescence intensity at 510 nm excited by 340 nm versus 380 nm. The data were analyzed in a linear mixed-effect model, with genotype, individual cells, sex and time as qualitative factors. *P*-values are indicated. The experiments were repeated at least three times. Data from representative experiments are shown.

A. Male but not female KO adrenal gland chromaffin cells present reduced Ca^{2+} influx compared to their WT counterparts

B. Castration reverses low Ca^{2+} influx in KO adrenal gland chromaffin cells to normal but has no effect on WT adrenal gland chromaffin cells

The S.E. of the solid line curve representing male WT adrenal gland chromaffin cell Ca^{2+}-influx in the left panel is omitted for better visualization.

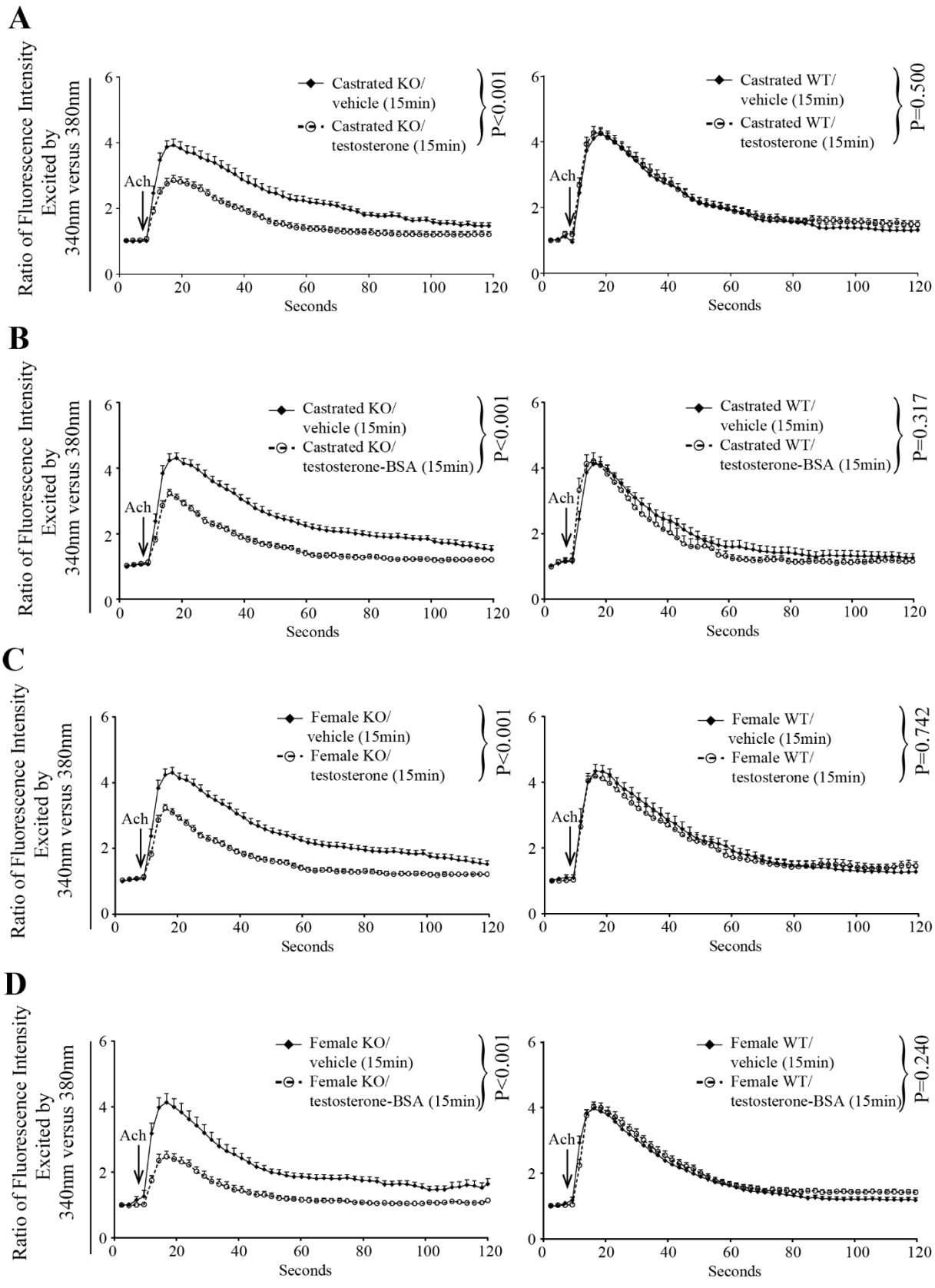
A
Ratio of Fluorescence Intensity Excited by 340nm versus 380nm
Castrated KO/ vehicle (15min)
Castrated KO/ testosterone (15min)
P<0.001
Castrated WT/ vehicle (15min)
Castrated WT/ testosterone (15min)
P=0.500
Ach
Seconds
B
Castrated KO/ vehicle (15min)
Castrated KO/ testosterone-BSA (15min)
P<0.001
Castrated WT/ vehicle (15min)
Castrated WT/ testosterone-BSA (15min)
P=0.317
C
Female KO/ vehicle (15min)
Female KO/ testosterone (15min)
P<0.001
Female WT/ vehicle (15min)
Female WT/ testosterone (15min)
P=0.742
D
Female KO/ vehicle (15min)
Female KO/ testosterone-BSA (15min)
P<0.001
Female WT/ vehicle (15min)
Female WT/ testosterone-BSA (15min)
P=0.240

Figure 3

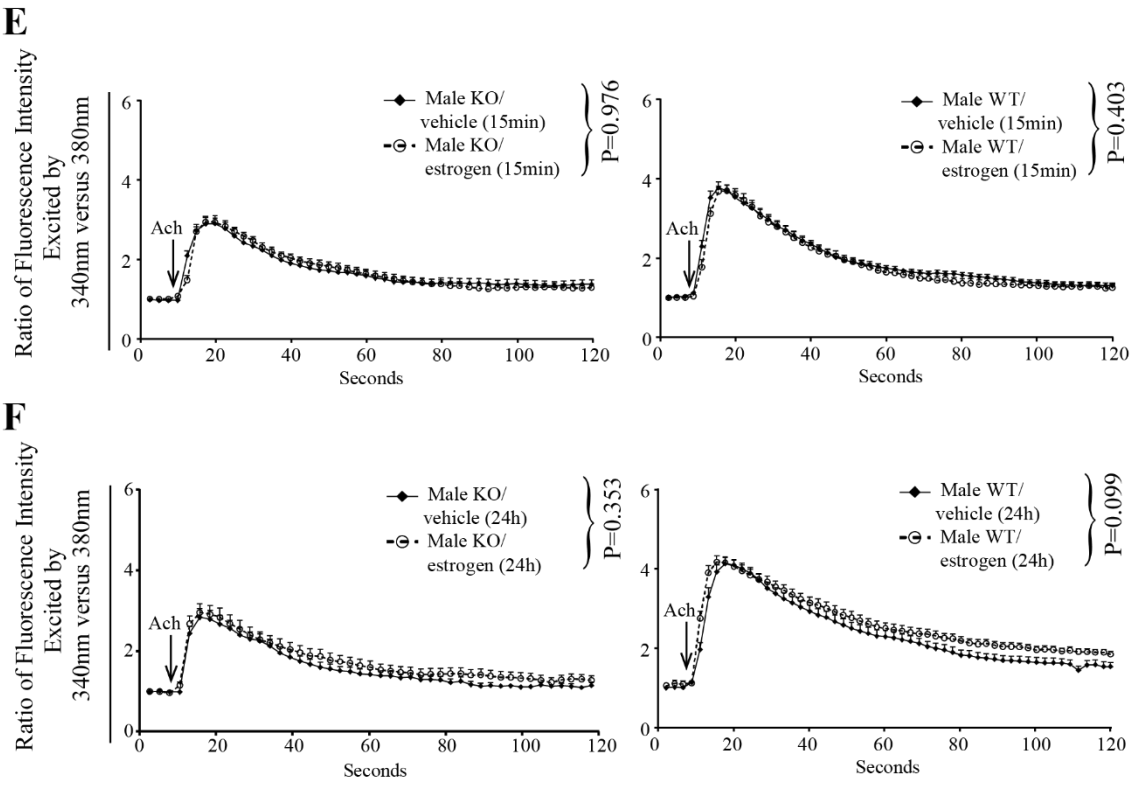

Figure 3 Continued

Figure 3. Effects of sex hormones on Ca^{2+} flux in adrenal gland chromaffin cells from EPHB6 KO and WT mice

The experiment procedures and data presentation are the same as described in Figure 2. The data were analyzed in a linear mixed-effect model, with genotype, individual cells, sex, sex hormone and time as qualitative factors.

A. Fifteen-minute testosterone treatment rapidly lowers Ca^{2+} influx in castrated KO but not in WT adrenal gland chromaffin cells

B. Cell membrane-impermeable, BSA-conjugated testosterone rapidly (within 15 minutes) lowers Ca^{2+} influx in castrated KO but not WT adrenal gland chromaffin cells

C. Fifteen-minute testosterone treatment rapidly lowers Ca^{2+} influx in female KO but not WT adrenal gland chromaffin cells

D. Cell membrane-impermeable, BSA-conjugated testosterone rapidly (within 15 minutes) lowers Ca^{2+} influx in female KO but not WT adrenal gland chromaffin cells

E. Short-term (15-minute) estrogen treatment does not affect male KO and WT adrenal gland chromaffin cell Ca^{2+} influx

F. Long-term (24-hour) estrogen treatment does not affect male KO and WT adrenal gland chromaffin cell Ca^{2+} influx

Effects of EPHB6 and male sex hormone on adrenal gland chromaffin cell electrophysiological properties

Voltage-gated calcium channel function in adrenal gland chromaffin cells from KO mice was electrophysiologically assessed using the perforated patch clamp technique (Fig. 4). According to the calcium influx data, smaller calcium current densities were expected. Unexpectedly, calcium current densities were significantly higher in male KO adrenal gland chromaffin cells (Fig. 4A). Whilst castration increased Ca^{2+} current densities in WT adrenal gland chromaffin cells (Fig. 4B), no significant changes were observed in male KO adrenal gland chromaffin cells (Fig. 4C). As a consequence, castration abolished the difference in calcium current-voltage relationships between WT and KO adrenal gland chromaffin cells (Fig. 4D). It should be noted that although the deletion of EPHB6 and the presence of testosterone could potentially increase voltage-gated calcium channels current densities during patch clamping, such increase might not happen in an intact cell under a physiological condition (otherwise, the Ca^{2+} influx would have increased in male KO adrenal gland chromaffin cells), and hence the alternation of voltage-gated calcium channel function is not the direct cause for the EPHB6-associated decrease in Ca^{2+} influx of male KO adrenal gland chromaffin cells.

Indirect modulation of voltage-gated calcium channels activity, and subsequent calcium influx, can occur through the regulation of membrane potential. Opening of BK channels strongly hyperpolarizes cell membrane and thus leads to the closure of voltage-gated calcium channels in adrenal gland chromaffin cells. The impact of EPHB6 and testosterone on BK channel function

was investigated. Outward K^+ currents were significantly larger in adrenal gland chromaffin cells from male KO mice compared to their WT counterparts (Fig. 5A). Paxilline, a BK channel blocker, almost completely abolished the currents in both groups (Fig. 5B). This indicates that the outward K^+ currents in WT and KO adrenal gland chromaffin cells occur mainly via BK channels. The paxilline-sensitive BK channel currents were significantly higher in male KO adrenal gland chromaffin cells than that in WT adrenal gland chromaffin cells (Fig. 5C), and castration significantly decreased BK currents in KO but not WT adrenal gland chromaffin cells (Figs. 5D and 5E). Therefore, BK currents became similar in WT and KO adrenal gland chromaffin cells after castration (Fig. 5F).

We identified BK function as a critical link in response to testosterone with regard to Ca^{2+} influx in the EPHB6 KO adrenal gland chromaffin cells. *In vitro* (or rather, *ex vivo*), the Ca^{2+} current density of adrenal gland chromaffin cells of the KO mice was rapidly augmented within 15 minutes by testosterone, suggesting non-genomic effect of the androgen. However, this cannot exclude the possibility that *in vivo*, testosterone and EPHB6 also affect BK channel expression through genomic effects via classical nuclear androgen receptors (Lubahn et al., 1988), which would increase BK current densities *in vivo* or *ex vivo*. Besides, *in vivo*, the longer time frame will allow the rapid non-genomic signaling of testosterone via Src kinases (Yu et al., 2012) or cell surface androgen receptors (Thomas et al., 2017) to travel to the nuclei, converting non-genomic effects to genomic effects. Therefore, it is necessary to evaluate the BK expression *ex vivo* from WT and KO chromaffin cells. BK channels are composed of four pore-forming alpha subunits and a regulatory beta-subunit isoform (Yuan et al., 2010). We probed for their expression in mouse adrenal gland chromaffin cells, and found that the beta 2 subunit (KCNMB2) was the dominant beta subunit isoform in these cells (S. Fig. 3). However, no difference in the expression of either the alpha or beta subunit mRNA was detected in adrenal gland chromaffin cells from KO males WT in males or from castrated KO and WT males. This suggests that the regulation of BK channels by EPHB6 and testosterone do not occur at the expression level.

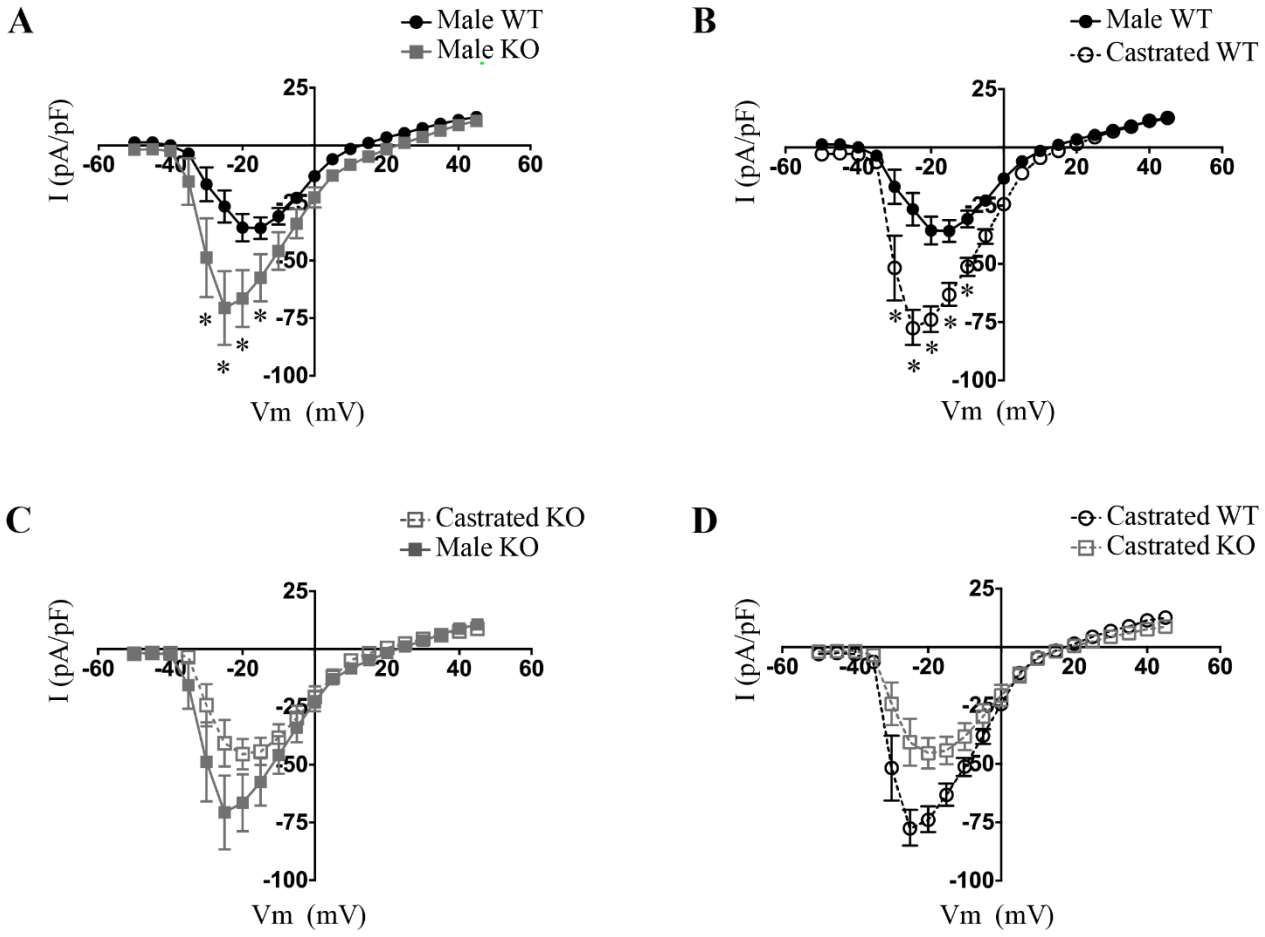

Figure 4

Figure 4. Voltage-dependent calcium current densities in adrenal gland chromaffin cells from WT and EPHB6 KO mice, with or without castration

Total calcium current densities recorded in adrenal gland chromaffin cells with the perforated patch technique. Current-voltage curves are presented as means ± S.E. of I(pA/pF). Curves are generated from pooled data from 8-10 cells from 2-3 mice: WT (n=11 cells from 3 mice), KO (n=8 cells from 2 mice), castrated WT (n=10 cells from 3 mice), castrated KO (n=8 cells from 3 mice). *: $p < 0.05$ (2-tailed Student's *t* test).

A. Male KO adrenal gland chromaffin cells *showed higher Ca^{2+}current densities compared to their WT counterparts*

B. Castration significantly increased voltage-gated Ca^{2+} current densities in WT adrenal gland chromaffin cells

C. Castration did not significantly increase voltage-gated Ca^{2+} current densities in KO adrenal gland chromaffin cells

D. Voltage-gated Ca^{2+} current densities became similar in adrenal gland chromaffin cells from castrated WT and KO adrenal gland chromaffin cells

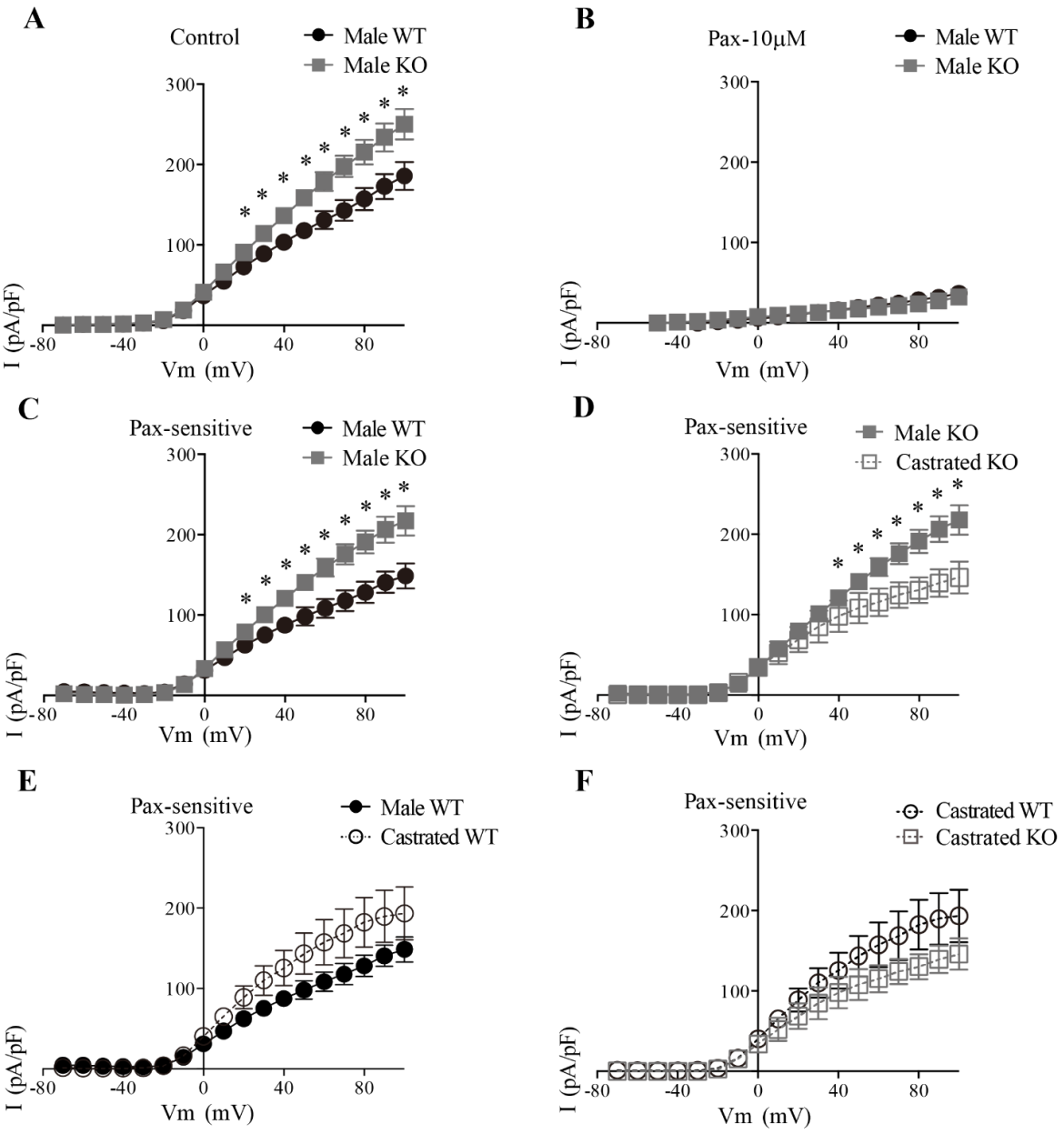

Figure 5

Figure 5. BK channel current densities in adrenal gland chromaffin cells from WT and KO mice, with or without castration

Outward potassium current densities were recorded with the perforated patch clamp technique in the absence or presence of paxilline (Pax; 10 μM), a BK channel blocker. Current-voltage curves are presented as means ± S.E. of I(pA/pF). Curves are generated from pooled data from 4-12 cells from 2-5 different mice: WT (n=7 cells from 4 mice), KO (n=12 cells from 3 mice), castrated WT (n=8 cells from 5 mice), castrated KO (n=4 cells from 2 mice). *: $p < 0.05$ (2-tailed Student's *t* test).

A. KO adrenal gland chromaffin cells showed higher voltage-gated K^+ current densities

B. Voltage-gated K^+ current densities were almost abolished by the BK channel blocker paxilline

C. KO adrenal gland chromaffin cells showed higher voltage-gated, paxilline-sensitive K^+ current densities

D. Castration significantly decrease voltage-gated paxilline-sensitive K^+ current densities in KO adrenal gland chromaffin cells

E. Castration did not significantly change voltage-gated, paxilline-sensitive K^+ current densities in WT adrenal gland chromaffin cells

F. Paxilline-sensitive BK current densities from WT and KO adrenal gland chromaffin cells become similar after castration

Our data indicate that enhanced BK currents in male KO adrenal gland chromaffin cells might lead to decreased open probability of voltage-gated calcium channels, reducing Ca^{2+} influx in these cells. If so, blocking BK channels would prevent voltage-gated calcium channel inhibition and increase Ca^{2+} influx in male KO adrenal gland chromaffin cells. To test this hypothesis, adrenal gland chromaffin cells were treated with a BK channel inhibitor, penitrem A. Ca^{2+} influx was unaltered by penitrem A in male WT adrenal gland chromaffin cells (Fig. 6A), but it was significantly increased in KO adrenal gland chromaffin cells, reverting to WT control levels (Fig. 6B).

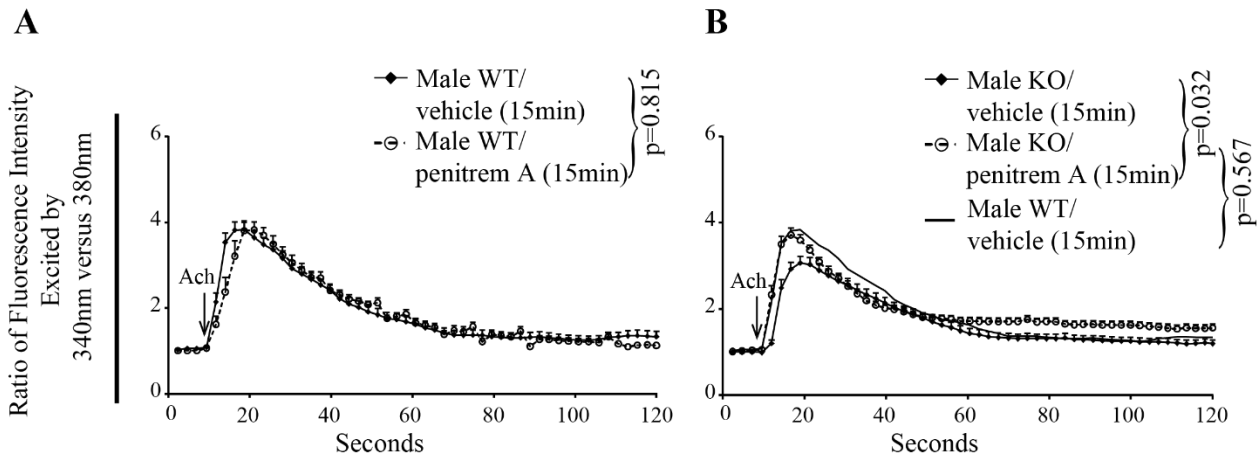

Figure 6

Figure 6. The BK channel blocker penitrem A augments acetylcholine-triggered Ca^{2+}influx in KO adrenal gland chromaffin cells to a normal level

WT (A) and KO (B) adrenal gland chromaffin cells from male mice were loaded with Fura2-AM for one hour, and then treated with a BK channel blocker penitrem A (10 μmol/L) for 15 minutes. The cells were then washed and stimulated with acetylcholine at 37℃. Their Ca^{2+} flux was recorded for 120 seconds at a rate of measurement per two seconds. Arrows indicate time points where acetylcholine was added. Signals from more than 15 or more randomly-selected cells per group were recorded, and the results expressed as means ± S.E. of ratios of fluorescence intensity at 510 nm excited by 340 nm versus 380 nm. In B, the means of WT adrenal gland chromaffin cell signals were presented as a thin line without S.E. for better viewing. The data were analyzed by linear mixed-effect model, with genotype, individual cells, penitrem A and time as qualitative factors. *P*-values are indicated. Experiments were conducted at least three times. Data from representative ones are shown.

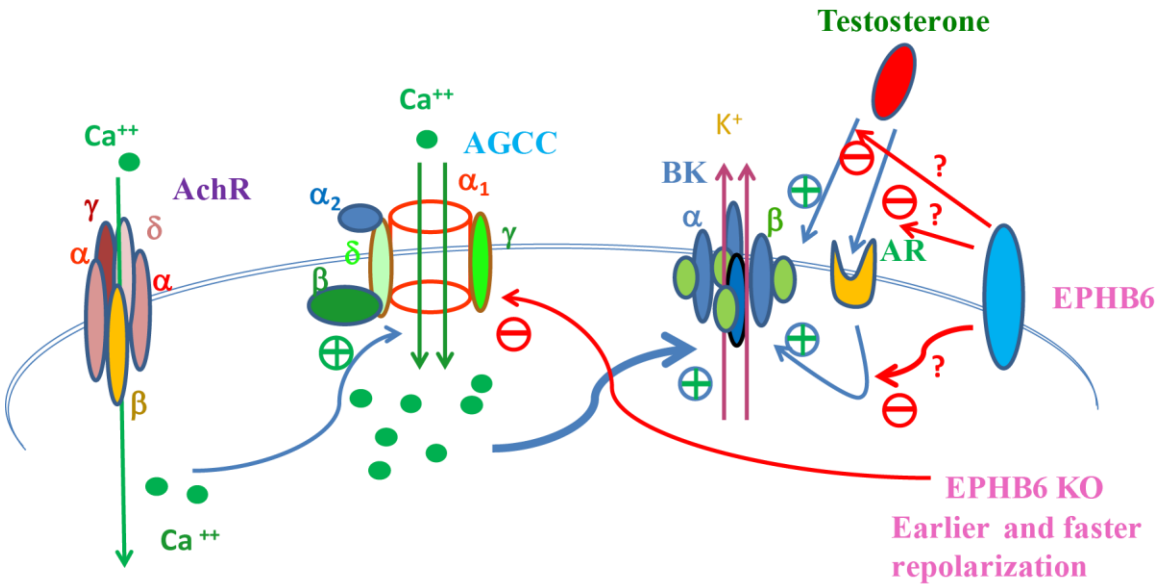

Figure 7

Figure 7. A model illustrating the concerted effect of EPHB6 and testosterone in regulating Ca^{2+} influx in adrenal gland chromaffin cells

In adrenal gland chromaffin cells, acetylcholine (ACh) stimulation of acetylcholine receptors (AChR) causes initial depolarization by allowing a small amount of Ca^{2+} influx plus a large amount of Na^{+} influx. The combined effect of both inward cation fluxes opens voltage-gated calcium channels for larger Ca^{2+} influx. BK channels are then activated by depolarization as well as by increased Ca^{2+} concentration, allowing K^{+} ions efflux, therein repolarizing the cells. As a consequence, voltage-gated calcium channels (VGCC) are shut down, terminating Ca^{2+} influx. Testosterone promotes the BK currents by direct binding with the BK channel, or by non-genomic signaling via its cell surface androgen receptors (AR) or via intracellular Src kinases. EPHB6 might interfere with the testosterone-BK association, or block the interaction between testosterone and AR, or suppress Src signaling. These 3 possible mechanisms are to be tested, and hence marked with question marks. As a consequence, the presence of EPHB6 suppresses the positive effect of testosterone on the BK currents. EPHB6 KO liberates this positive impact, leading to a larger K^{+} outflow. This results in earlier and faster repolarization, an earlier closure of voltage-gated calcium channels, and the subsequently reduced Ca^{2+} influx.

Discussion

The present study revealed that EPHB6 deletion decreased male but not female adrenal gland chromaffin cell Ca^{2+} influx and catecholamine secretion. Testosterone was required for this phenotype, as the absence of both EPHB6 and testosterone reversed the KO adrenal gland chromaffin cell phenotype to that of their WT controls. The functional mechanism involves BK channels.

Ca^{2+} influx is an essential signal triggering catecholamine release from adrenal gland chromaffin cells. Our data shows that this Ca^{2+} influx is compromised in male EPHB6 KO adrenal gland chromaffin cells. The electrophysiology of adrenal gland chromaffin cells related to Ca^{2+} influx is depicted in Figure 7. In adrenal gland chromaffin cells, acetylcholine stimulation of acetylcholine receptors evokes a small Ca^{2+} influx plus a large Na^{+} influx. The combined effect of these inward cations causes depolarization, which increases voltage-gated calcium channels open probability and leads to a larger Ca^{2+} influx (Fenwick et al., 1982). Ensuing BK channel activation re-hyperpolarizes adrenal gland chromaffin cell membrane(Martinez-Espinosa et al., 2014). This re-hyperpolarization reduces voltage-gated calcium channels' opening and thus terminates Ca^{2+} influx (Solaro et al., 1995). The decreased calcium influx and catecholamine release observed in male EPHB6 KO mice could have resulted from a decrease in calcium channels' function. However, perforated patch recordings show voltage-gated calcium channels' current densities were rather larger in adrenal gland chromaffin cells from KO compared to that of their WT littermates. These results strongly suggest that EPHB6 modulation of calcium influx is not due to direct suppression of voltage-gated calcium channel function.

Alternatively, EPHB6's control of Ca^{2+} influx could be indirect through stabilizing (or repolarizing) the membrane potential of adrenal gland chromaffin cells. Given the high input resistance of adrenal gland chromaffin cells, a small modification of membrane conductance would be sufficient to abolish or substantially limit membrane depolarization. K^{+} currents thus play a major role in controlling membrane potential of adrenal gland chromaffin cells and catecholamine release. Indeed, K^{+} currents appear to be modified in male KO adrenal gland chromaffin cells. BK channels were the main K^{+} conductance altered by EPHB6 expression, as their current densities were in accordance with the adrenal gland chromaffin cell phenotype observed. In male KO

adrenal gland chromaffin cells, BK current densities were substantially increased (Fig. 5C), and castration abolished such increase (Figs. 5D and 5F). We thus propose the model illustrated in Figure 7 to portray the mechanism by which EPHB6 and testosterone act in concert to modulate adrenal gland chromaffin cell Ca^{2+} influx. Testosterone enhances BK currents either through direct binding with the ion channel (Suárez et al., 2015), by non-genomic signaling through Src kinases (Yu et al., 2012) or its cell surface androgen receptors (Thomas et al., 2017). On the other hand, EPHB6 might interfere with the testosterone-BK channel, testosterone-androgen receptor, or testosterone-Src interactions (to be confirmed, and hence marked with question marks). As a consequence, the presence of EPHB6 suppresses the positive effect of testosterone on BK channel activity. Abolished expression of EPHB6 in KO mice alleviates the inhibitory influence of testosterone over BK channels, leading to a larger K^+ efflux. This evokes an earlier and faster repolarization, decreases sustained voltage-gated calcium channels' probability to open, and subsequently reduces Ca^{2+} influx.

This proposed model (Fig. 7) is validated by our experimental data. Indeed, a BK channel blocker, penitrem A, effectively augmented Ca^{2+} influx in male KO adrenal gland chromaffin cells, corroborating the critical role of BK channel activity in decreasing Ca^{2+} influx in these cells. The current literature also supports our model. Testosterone has been shown to increase the BK current (Han et al., 2008). A recent report indicated that testosterone can interact directly with BK channel subunits in rat anterior pituitary tumor cells and modulate their function in patch-clamp assays (Suárez et al., 2015). Therefore, direct testosterone binding to BK channels in adrenal gland chromaffin cells might enhance BK channel activity. BK channel function would not be altered in male WT adrenal gland chromaffin cells by testosterone, because EPHB6 blocks BK channel's association with the latter. BK currents are not altered in female KO adrenal gland chromaffin cells either, despite the absence of EPHB6, because of low testosterone levels. Moreover, BK channel currents are normal in female WT adrenal gland chromaffin cells, due to both the absence of testosterone and the presence of EPHB6. To test these hypotheses, we conducted immunoprecipitation and fluorescence resonance energy transfer to assess physical interactions between EPHB6 and KCNMB2, the major regulatory β subunit, but to no avail. Limitations of the approaches, such as assay sensitivity and affinity between EPHB6 and BK β-

subunit, could account for such negative results. Further investigation in this regard would thus be required.

Androgens have two major forms: testosterone and 5α-dihydrotestosterone. The latter is a metabolite of the former, and binds with higher affinity to androgen receptors (Toth and Zakar, 1982). Classical androgen receptors are intracellular proteins, and upon binding to testosterone or 5 α-dihydrotestosterone, they translocate into nuclei and serve as DNA-binding transcription factors that regulate genes with androgen-responsive elements (Heemers and Tindall, 2007). This is called genomic action. Androgen receptors can also interact directly with Src kinases and trigger their activation (Yu et al., 2012). Cell membrane androgen receptors exist too, and they may be G protein–associated but are poorly characterized (Benten et al., 1999a;Benten et al., 1999b;Nakhla et al., 1999;Thomas et al., 2017). The latter two actions are non-genomic.

Our study *in vitro* reveals that the non-genomic effect of testosterone appears to be sufficient to cause increased Ca^{2+} influx in male KO adrenal gland chromaffin cells. It is likely that this observed androgen effect is not unique for testosterone; other testosterone derivatives, such as the more potent 5 α-dihydrotestosterone, might also be effective. This will need to be confirmed. Such *in vitro* non-genomic effect does not exclude the existence of possible *in vivo* genomic effect of androgens, as they are not mutually exclusive. The possible *in vivo* genomic effect of androgen on Ca^{2+} influx could be confirmed or refuted by using mice with adrenal gland-specific null mutation of the classical intracellular androgen receptor. To the best of our knowledge, such a study has not been conducted and would be interesting to perform.

It is conceivable that males with EPHB6 loss-of-function mutations might become hypertensive later in life because of decreased testosterone levels, which may cause them to lose the blood pressure-lowering beneficial effect of EPHB6 mutation by increasing their resting-state catecholamine levels. Consequently, their blood pressure might increase due to other genetic and environmental factors, as hypertension is a polygenic and multifactorial disease. For these patients, testosterone replacement therapy might restore the protective influence of EPHB6 mutation in lowering catecholamine secretion and hence, blood pressure.

The effect of testosterone on blood pressure is often controversial. In animal studies, castration often results in lower blood pressure (Masubuchi et al., 1982;Chen and Meng, 1991;Reckelhoff et al., 1998). In humans, different studies reported mixed results, probably due to the heterogeneity of the human population. Male hypogonadism is known to associate with hypertension (Hughes et al., 1989;Phillips et al., 1993;Jaffe et al., 1996;Liu et al., 2003;Zitzmann, 2009;Garcia-Cruz et al., 2012). There are multiple articles showing blood pressure reduction after testosterone replacement therapy (Bhattacharya et al., 2011;Haider et al., 2014;Traish et al., 2014;Yassin et al., 2014). These and additional favorable results with regard to testosterone replacement therapy in reducing cardiovascular risks including blood pressure are discussed in two recent review papers (Miner et al., 2014;Anaissie et al., 2017). It is true that a couple of large retrospective studies have revealed that testosterone replacement therapy is associated with increased cardiovascular risks (Vigen et al., 2013;Finkle et al., 2014). However, the conclusions from these studies are disputed as “retrospective, highly statistical and only with a minor effect size” and “are unlikely reproducible or accurate” (Miner et al., 2014). It is safe to say that the effects of testosterone replacement therapy on cardiovascular risks are not conclusive.

The results of clinical studies are rarely black and white (*i.e.,* with 100% penetrance). Rather, the conclusions depend heavily on statistical analysis, which has the limitation of discounting the responses of a subpopulation within the case group. For example, in a drug efficacy study, if we assume a placebo effect occurs in 20% of a control group, and a positive therapeutic effect of 35 % in a drug-treated group, which represents a very moderate efficacy, we will only need 138 individuals each in the control and treated group to achieve 80% power to arrive at a conclusion that the treatment is statistically effective. In this case, the fate of 65% of treated but non-responsive patients is practically ignored. In a real example of using diuretics in treating acute failure, more than 50% of the treated patients are not responding to 40 mg/furosemide in terms of body weight reduction (Valente et al., 2014), and yet furosemide is still used to treat this condition. For the same reason but in a reverse way, the statistically significant side-effect of testosterone replacement therapy does not mean that the side-effect occurs in all the individuals. It is totally possible that for a subpopulation of hypogonadic patients with EPHB6 loss-of-function mutations, testosterone replacement therapy does not cause increased cardiovascular risks, but

reduces resting state catecholamine secretion, and hence their blood pressure. For these individuals, testosterone might be a causative rather than symptomatic treatment for their hypertension. After all, testosterone administered in a proper dosage and format will restore what they used to have in sufficient quantity in their adult life.

The potential risk of testosterone in promoting prostate cancer is a concern. However, this is mitigated because patients with prostate cancer or elevated prostates-specific antigen levels are routinely excluded from testosterone replacement therapy. Also, multiple short- and long-term (five years) testosterone replacement therapy studies have found no evidence of prostate-specific antigen level increases (English et al., 2000;Haider et al., 2014;Yassin et al., 2014), further alleviating the concern.

The current anti-hypertensive drugs are highly effective with minimal side-effects. This has made the entry threshold of testosterone as a new therapeutic agent much higher. However, in the age of personalized medicine, for those whose hypertension is caused by EPHB6 mutations and subsequent hypogonadism, if testosterone could address the cause rather than symptoms, its therapeutic application should be considered.

The present study reveals a novel mechanism by which EPHB6 and testosterone jointly regulate catecholamine release from adrenal gland chromaffin cells. The results might explain some controversial findings with regard to cardiovascular benefits or risks after testosterone replacement therapy. Further, this study has raised a possibility of using testosterone as a personalized medicine to lower resting-state catecholamine secretion and hence, blood pressure.

Funding

This work was supported by the Fonds de recherche du Québec – Santé (Ag-06) and the J.-Louis Lévesque Foundation to J.W. It was also financed in part by grants from the Canadian Institutes of Health Research to J.W. (MOP69089 and MOP 123389), H.L. (MOP97829), and J.L. (MOP123395), the Natural Sciences and Engineering Research Council of Canada (RGPIN-2017-

04790) and the Juvenile Diabetes Research Foundation (17-2013-440) to J.W., and a grant from the National Sciences Foundation of China to Y.W. (#81700363).

Author contributions

Y.W., W.S., H.L., J. L. and J.W. generated the concept and initiated this project. Y.W. and W.S conducted experiments in the cellular level and molecular level. A.B. and J. L. performed patch clamping experiments. J.P. was responsible for animal husbandry. S.Q. performed castration. Y.W., W.S., H.L., J. L. and J.W. drafted the manuscript.

References

Anaissie, J., Roberts, N.H., Wang, P., and Yafi, F.A. (2017). Testosterone Replacement Therapy and Components of the Metabolic Syndrome. *Sex Med Rev* 5**,** 200-210.

Benten, W.P., Lieberherr, M., Giese, G., Wrehlke, C., Stamm, O., Sekeris, C.E., Mossmann, H., and Wunderlich, F. (1999a). Functional testosterone receptors in plasma membranes of T cells. *FASEB J* 13**,** 123-133.

Benten, W.P., Lieberherr, M., Stamm, O., Wrehlke, C., Guo, Z., and Wunderlich, F. (1999b). Testosterone signaling through internalizable surface receptors in androgen receptor-free macrophages. *Mol Biol Cell* 10**,** 3113-3123.

Bhattacharya, R.K., Khera, M., Blick, G., Kushner, H., Nguyen, D., and Miner, M.M. (2011). Effect of 12 months of testosterone replacement therapy on metabolic syndrome components in hypogonadal men: data from the Testim Registry in the US (TRiUS). *BMC Endocr Disord* 11**,** 18.

Chen, Y.F., and Meng, Q.C. (1991). Sexual dimorphism of blood pressure in spontaneously hypertensive rats is androgen dependent. *Life Sci* 48**,** 85-96.

English, K.M., Steeds, R.P., Jones, T.H., Diver, M.J., and Channer, K.S. (2000). Low-dose transdermal testosterone therapy improves angina threshold in men with chronic stable

angina: A randomized, double-blind, placebo-controlled study. *Circulation* 102**,** 1906-1911.

Eph Nomenclature Committee (1997). Unified nomenclature for Eph family receptors and their ligands, the ephrins. *Cell* 90**,** 403-404.

Fenwick, E.M., Marty, A., and Neher, E. (1982). Sodium and calcium channels in bovine chromaffin cells. *J Physiol* 331**,** 599-635.

Finkle, W.D., Greenland, S., Ridgeway, G.K., Adams, J.L., Frasco, M.A., Cook, M.B., Fraumeni, J.F., Jr., and Hoover, R.N. (2014). Increased risk of non-fatal myocardial infarction following testosterone therapy prescription in men. *PLoS One* 9**,** e85805.

Garcia-Cruz, E., Piqueras, M., Huguet, J., Perez-Marquez, M., Gosalbez, D., Peri, L., Izquierdo, L., Luque, P., Ribal, M.J., and Alcaraz, A. (2012). Hypertension, dyslipidemia and overweight are related to lower testosterone levels in a cohort of men undergoing prostate biopsy. *Int J Impot Res* 24**,** 110-113.

Grynkiewicz, G., Poenie, M., and Tsien, R.Y. (1985). A new generation of Ca2+ indicators with greatly improved fluorescence properties. *J Biol Chem* 260**,** 3440-3450.

Haider, A., Saad, F., Doros, G., and Gooren, L. (2014). Hypogonadal obese men with and without diabetes mellitus type 2 lose weight and show improvement in cardiovascular risk factors when treated with testosterone: an observational study. *Obes Res Clin Pract* 8**,** e339-349.

Han, D.H., Chae, M.R., Jung, J.H., So, I., Park, J.K., and Lee, S.W. (2008). Effect of testosterone on potassium channel opening in human corporal smooth muscle cells. *The journal of sexual medicine* 5**,** 822-832.

Heemers, H.V., and Tindall, D.J. (2007). Androgen receptor (AR) coregulators: a diversity of functions converging on and regulating the AR transcriptional complex. *Endocr Rev* 28**,** 778-808.

Hu, Y., Wang, X., Wu, Y., Jin, W., Cheng, B., Fang, X., Martel‐Pelletier, J., Kapoor, M., Peng, J., and Qi, S. (2015). Role of EFNB1 and EFNB2 in Mouse Collagen‐Induced Arthritis and Human Rheumatoid Arthritis. *Arthritis & Rheumatology* 67**,** 1778-1788.

Hughes, G.S., Mathur, R.S., and Margolius, H.S. (1989). Sex steroid hormones are altered in essential hypertension. *J Hypertens* 7**,** 181-187.

Jaffe, A., Chen, Y., Kisch, E.S., Fischel, B., Alon, M., and Stern, N. (1996). Erectile dysfunction in hypertensive subjects. Assessment of potential determinants. *Hypertension* 28**,** 859-862.

Jin, W., Luo, H., and Wu, J. (2014). Effect of reduced EPHB4 expression in thymic epithelial cells on thymocyte development and peripheral T cell function. *Molecular immunology* 58**,** 1-9.

Kolski-Andreaco, A., Cai, H., Currle, D.S., Chandy, K.G., and Chow, R.H. (2007). Mouse adrenal chromaffin cell isolation. *J Vis Exp***,** 129.

Ledoux, J., Bonev, A.D., and Nelson, M.T. (2008). Ca2+-activated K+ channels in murine endothelial cells: block by intracellular calcium and magnesium. *The Journal of general physiology* 131**,** 125-135.

Ledoux, J., Greenwood, I., Villeneuve, L.R., and Leblanc, N. (2003). Modulation of Ca2+ ‐dependent Cl− channels by calcineurin in rabbit coronary arterial myocytes. *The Journal of physiology* 552**,** 701-714.

Liu, P.Y., Death, A.K., and Handelsman, D.J. (2003). Androgens and cardiovascular disease. *Endocr Rev* 24**,** 313-340.

Lubahn, D.B., Joseph, D.R., Sar, M., Tan, J., Higgs, H.N., Larson, R.E., French, F.S., and Wilson, E.M. (1988). The human androgen receptor: complementary deoxyribonucleic acid cloning, sequence analysis and gene expression in prostate. *Mol Endocrinol* 2**,** 1265-1275.

Luo, H., Broux, B., Wang, X., Hu, Y., Ghannam, S., Jin, W., Larochelle, C., Prat, A., and Wu, J. (2016). EphrinB1 and EphrinB2 regulate T cell chemotaxis and migration in experimental autoimmune encephalomyelitis and multiple sclerosis. *Neurobiology of disease* 91**,** 292-306.

Luo, H., Charpentier, T., Wang, X., Qi, S., Han, B., Wu, T., Terra, R., Lamarre, A., and Wu, J. (2011a). Efnb1 and Efnb2 proteins regulate thymocyte development, peripheral T cell differentiation, and antiviral immune responses and are essential for interleukin-6 (IL-6) signaling. *Journal of Biological Chemistry* 286**,** 41135-41152.

Luo, H., Qi, S., Wu, Z., Han, B., Wang, X., and Wu, J. (2011b). EFNB1 and EFNB2 physically bind to IL-7R-alpha and retard its internalization from the cell surface (57.2). *The Journal of Immunology* 186**,** 57.52-57.52.

Luo, H., Wan, X., Wu, Y., and Wu, J. (2001). Cross-linking of EphB6 resulting in signal transduction and apoptosis in Jurkat cells. *The Journal of Immunology* 167**,** 1362-1370.

Luo, H., Wu, Z., Tremblay, J., Thorin, E., Peng, J., Lavoie, J.L., Hu, B., Stoyanova, E., Cloutier, G., and Qi, S. (2012). Receptor tyrosine kinase Ephb6 regulates vascular smooth muscle contractility and modulates blood pressure in concert with sex hormones. *Journal of Biological Chemistry* 287**,** 6819-6829.

Luo, H., Yu, G., Tremblay, J., and Wu, J. (2004). EphB6-null mutation results in compromised T cell function. *The Journal of clinical investigation* 114**,** 1762-1773.

Luo, H., Yu, G., Wu, Y., and Wu, J. (2002). EphB6 crosslinking results in costimulation of T cells. *The Journal of clinical investigation* 110**,** 1141-1150.

Martinez-Espinosa, P.L., Yang, C., Gonzalez-Perez, V., Xia, X.M., and Lingle, C.J. (2014). Knockout of the BK beta2 subunit abolishes inactivation of BK currents in mouse adrenal chromaffin cells and results in slow-wave burst activity. *J Gen Physiol* 144**,** 275-295.

Masubuchi, Y., Kumai, T., Uematsu, A., Komoriyama, K., and Hirai, M. (1982). Gonadectomy-induced reduction of blood pressure in adult spontaneously hypertensive rats. *Acta Endocrinol (Copenh)* 101**,** 154-160.

Miner, M., Barkin, J., and Rosenberg, M.T. (2014). Testosterone deficiency: myth, facts, and controversy. *Can J Urol* 21 Suppl 2**,** 39-54.

Nakhla, A.M., Leonard, J., Hryb, D.J., and Rosner, W. (1999). Sex hormone-binding globulin receptor signal transduction proceeds via a G protein. *Steroids* 64**,** 213-216.

Pasquale, E.B. (2008). Eph-ephrin bidirectional signaling in physiology and disease. *Cell* 133**,** 38-52.

Phillips, G.B., Jing, T.Y., Resnick, L.M., Barbagallo, M., Laragh, J.H., and Sealey, J.E. (1993). Sex hormones and hemostatic risk factors for coronary heart disease in men with hypertension. *J Hypertens* 11**,** 699-702.

Reckelhoff, J.F., Zhang, H., and Granger, J.P. (1998). Testosterone exacerbates hypertension and reduces pressure-natriuresis in male spontaneously hypertensive rats. *Hypertension* 31**,** 435-439.

Solaro, C.R., Prakriya, M., Ding, J.P., and Lingle, C.J. (1995). Inactivating and noninactivating Ca(2+)- and voltage-dependent K+ current in rat adrenal chromaffin cells. *J Neurosci* 15**,** 6110-6123.

Suárez, L., Bilal, U., Bordallo, J., Cantabrana, B., and Sánchez, M. (2015). Androgens block outward potassium currents and decrease spontaneous action potentials in GH3 cells. *Naunyn-Schmiedeberg's archives of pharmacology* 388**,** 67-78.

Thomas, P., Converse, A., and Berg, H.A. (2017). ZIP9, a novel membrane androgen receptor and zinc transporter protein. *Gen Comp Endocrinol*.

Toth, M., and Zakar, T. (1982). Relative binding affinities of testosterone, 19-nortestosterone and their 5 alpha-reduced derivatives to the androgen receptor and to other androgen-binding proteins: a suggested role of 5 alpha-reductive steroid metabolism in the dissociation of "myotropic" and "androgenic" activities of 19-nortestosterone. *J Steroid Biochem* 17**,** 653-660.

Traish, A.M., Haider, A., Doros, G., and Saad, F. (2014). Long-term testosterone therapy in hypogonadal men ameliorates elements of the metabolic syndrome: an observational, long-term registry study. *Int J Clin Pract* 68**,** 314-329.

Valente, M.A., Voors, A.A., Damman, K., Van Veldhuisen, D.J., Massie, B.M., O'connor, C.M., Metra, M., Ponikowski, P., Teerlink, J.R., Cotter, G., Davison, B., Cleland, J.G., Givertz, M.M., Bloomfield, D.M., Fiuzat, M., Dittrich, H.C., and Hillege, H.L. (2014). Diuretic response in acute heart failure: clinical characteristics and prognostic significance. *Eur Heart J* 35**,** 1284-1293.

Vigen, R., O'donnell, C.I., Baron, A.E., Grunwald, G.K., Maddox, T.M., Bradley, S.M., Barqawi, A., Woning, G., Wierman, M.E., Plomondon, M.E., Rumsfeld, J.S., and Ho, P.M. (2013). Association of testosterone therapy with mortality, myocardial infarction, and stroke in men with low testosterone levels. *JAMA* 310**,** 1829-1836.

Wang, Y., Hamet, P., Thorin, E., Tremblay, J., Raelson, J., Wu, Z., Luo, H., Jin, W., Lavoie, J.L., and Peng, J. (2016a). Reduced blood pressure after smooth muscle EFNB2 deletion and the potential association of EFNB2 mutation with human hypertension risk. *European Journal of Human Genetics 24, 1817-1825.*

Wang, Y., Thorin, E., Luo, H., Tremblay, J., Lavoie, J.L., Wu, Z., Peng, J., Qi, S., and Wu, J. (2015). EPHB4 protein expression in vascular smooth muscle cells regulates their contractility, and EPHB4 deletion leads to hypotension in mice. *Journal of Biological Chemistry* 290**,** 14235-14244.

Wang, Y., Wu, Z., Luo, H., Peng, J., Raelson, J., Ehret, G.B., Munroe, P.B., Stoyanova, E., Qin, Z., Cloutier, G., Bradley, W.E., Wu, T., Shen, J.Z., Hu, S., and Wu, J. (2016b). The role of GRIP1 and ephrin B3 in blood pressure control and vascular smooth muscle cell contractility. *Sci Rep* 6**,** 38976.

Wang, Y., Wu, Z., Thorin, E., Tremblay, J., Lavoie, J.L., Luo, H., Peng, J., Qi, S., Wu, T., and Chen, F. (2016c). Estrogen and testosterone in concert with EFNB3 regulate vascular smooth muscle cell contractility and blood pressure. *American Journal of Physiology-Heart and Circulatory Physiology* 310**,** H861-H872.

Wu, J., and Luo, H. (2005). Recent advances on T-cell regulation by receptor tyrosine kinases. *Current opinion in hematology* 12**,** 292-297.

Wu, Z., Luo, H., Thorin, E., Tremblay, J., Peng, J., Lavoie, J.L., Wang, Y., Qi, S., Wu, T., and Wu, J. (2012). Possible role of Efnb1 protein, a ligand of Eph receptor tyrosine kinases, in modulating blood pressure. *Journal of Biological Chemistry* 287**,** 15557-15569.

Yassin, D.J., Doros, G., Hammerer, P.G., and Yassin, A.A. (2014). Long-term testosterone treatment in elderly men with hypogonadism and erectile dysfunction reduces obesity parameters and improves metabolic syndrome and health-related quality of life. *J Sex Med* 11**,** 1567-1576.

Yu, G., Luo, H., Wu, Y., and Wu, J. (2003a). Ephrin B2 induces T cell costimulation. *The Journal of Immunology* 171**,** 106-114.

Yu, G., Luo, H., Wu, Y., and Wu, J. (2003b). Mouse ephrinB3 augments T-cell signaling and responses to T-cell receptor ligation. *Journal of Biological Chemistry* 278**,** 47209-47216.

Yu, G., Luo, H., Wu, Y., and Wu, J. (2004). EphrinB1 is essential in T-cell-T-cell co-operation during T-cell activation. *Journal of Biological Chemistry* 279**,** 55531-55539.

Yu, G., Mao, J., Wu, Y., Luo, H., and Wu, J. (2006). Ephrin-B1 is critical in T-cell development. *Journal of Biological Chemistry* 281**,** 10222-10229.

Yu, J., Akishita, M., Eto, M., Koizumi, H., Hashimoto, R., Ogawa, S., Tanaka, K., Ouchi, Y., and Okabe, T. (2012). Src kinase-mediates androgen receptor-dependent non-genomic activation of signaling cascade leading to endothelial nitric oxide synthase. *Biochem Biophys Res Commun* 424**,** 538-543.

Yuan, P., Leonetti, M.D., Pico, A.R., Hsiung, Y., and Mackinnon, R. (2010). Structure of the human BK channel Ca2+-activation apparatus at 3.0 A resolution. *Science* 329**,** 182-186.

Zitzmann, M. (2009). Testosterone deficiency, insulin resistance and the metabolic syndrome. *Nat Rev Endocrinol* 5**,** 673-681.

Supplementary information

RT-qPCR primer sequences		
Gene	sense sequences	antisense sequences
β-actin	5’-TCGTACCACAGGCATTGTGATGGA-3’	5’-TGATGTCACGCACGATTTCCCTCT-3’
EPHB1	5’-ACCATGAGGAGCATCACCTTGTCA-3’	5’-TAGCCCATCGATACGTGCTGTGTT-3’
EPHB2	5’-CCAGTGATGTGTGGAGCTATG-3’	5’-GGAGGTAGTCTGTAGTCCTGTT-3’
EPHB3	5’-AGTTCGCCAAGGAGATCGATGTGT-3’	5’-TCAGCGTCTTGATAGCCACGAACA-3’
EPHB4	5’-CTACGTCTCTAACCTCCCATCT-3’	5’-GCTGGTCACCCTTTCTCTTT-3’
EPHB6	5’-CTTTGCCTTTGTTCACCGAGCACT-3’	5’-AGCAAGGAACTTGAACCCTGAGGA-3’
EFNB1	5’-ACCAGGAAATCCGCTTCACCATCA-3’	5’-ACAGCATTTGGATCTTGCCCAACC-3’
EFNB2	5’-TTCTGCTGGATCAGCCAGGAATCA-3’	5’-TCCTGATGCGATCCCTGCGAATAA-3’
EFNB3	5’-AGTTCCGATCCCACCACGATTACT-3	5’-AGAAGCACCTTCATGCCTCTGGTT-3
Kcnma1	5’-CAACGTGTTCTTCCTCCTCTAC-3’	5’-CAGGAGGGACTGTGAAGAAATC-3’
Kcnmb1	5’-CCCTGACTTCAGTTGGTTCATA-3’	5’-AGAGAGAGCACGTAGGGATAG-3’
Kenmb2	5’-CCAGGTCTCTGTTCTGAGTTTC-3’	5’-CACTTGCTACAGGGCTCAATA-3’
Kcnmb3	5’-GGAGTTGTTCTGAGGAAGTCTG-3’	5’-GCCTCCCAGCAAAGTCAATA-3’
Kcnmb4	5’-TCCTATATCCCGCCCTGTAA-3’	5’-CTGGGAACCGATCTCATCTTT-3’
Cacna1g	5’-GGGAGCAGGAGTATTTCAGTAG-3’	5’-GATGTTTCTGCCTGGGTATCT-3’
Cacna1h	5’-TCCTTCTGCTGTGCTTCTTC-3’	5’-CAGGAAGGTCAGGTTGTTGT-3’
Cacna1i	5’-GCCCTACTATGCCACCTATTG-3’	5’-AGGCAGATGATGAAGGTGATG-3’

Supplementary Table 1. RT-qPCR primer sequences

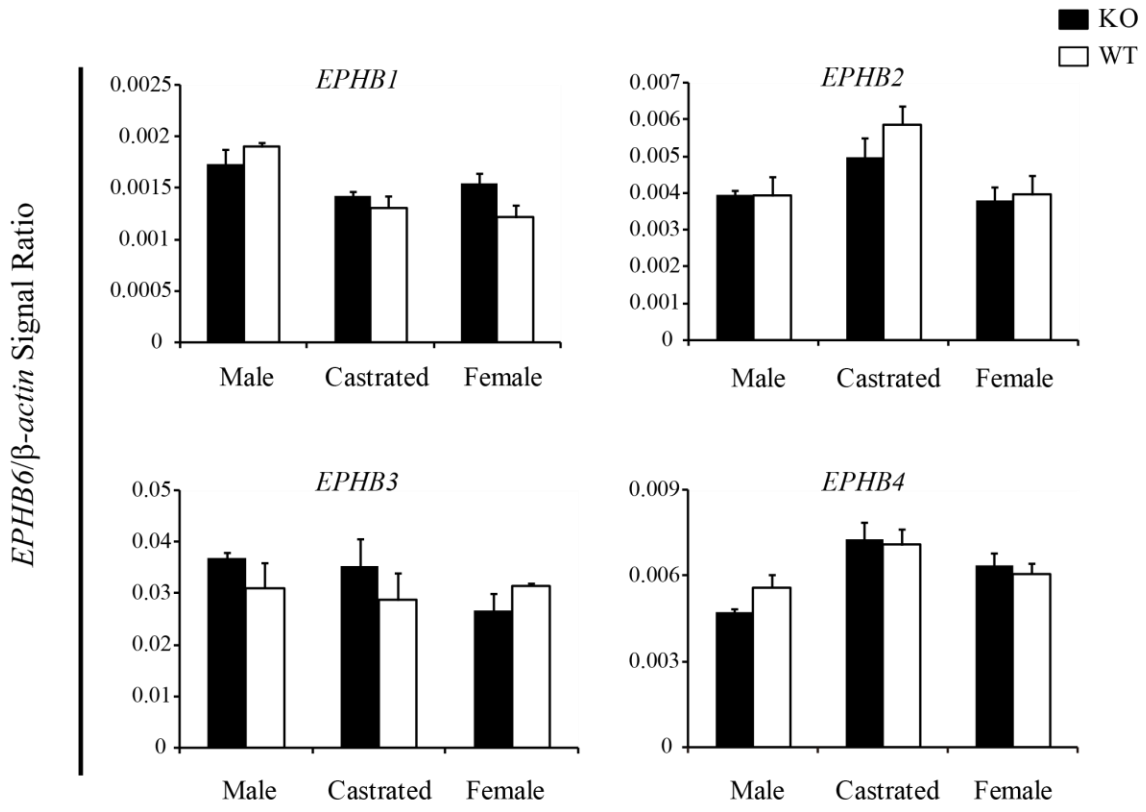

Supplementary Figure 1

Supplementary Figure 1. Normal expression of EPHB1, EPHB2, EPHB3 and EPHB4 mRNA in adrenal gland medullae from male, female and castrated male WT and EPHB6 KO mice

Total RNA was extracted from adrenal gland medullae of male and female WT and *EPHB6* KO mice and from castrated WT and KO mice. *EPHB1*, *EPHB2*, *EPHB3* and *EPHB4* mRNA levels were analyzed by RT-qPCR. β-actin levels were used as internal controls. RT-qPCR samples were in triplicate. The experiments were conducted three times, and means ± SEM of *EPHB*/*β-actin* signal ratios of pooled data from the three experiments are shown. Student's *t* tests were used for statistical analysis, and no significant difference was found among different test groups.

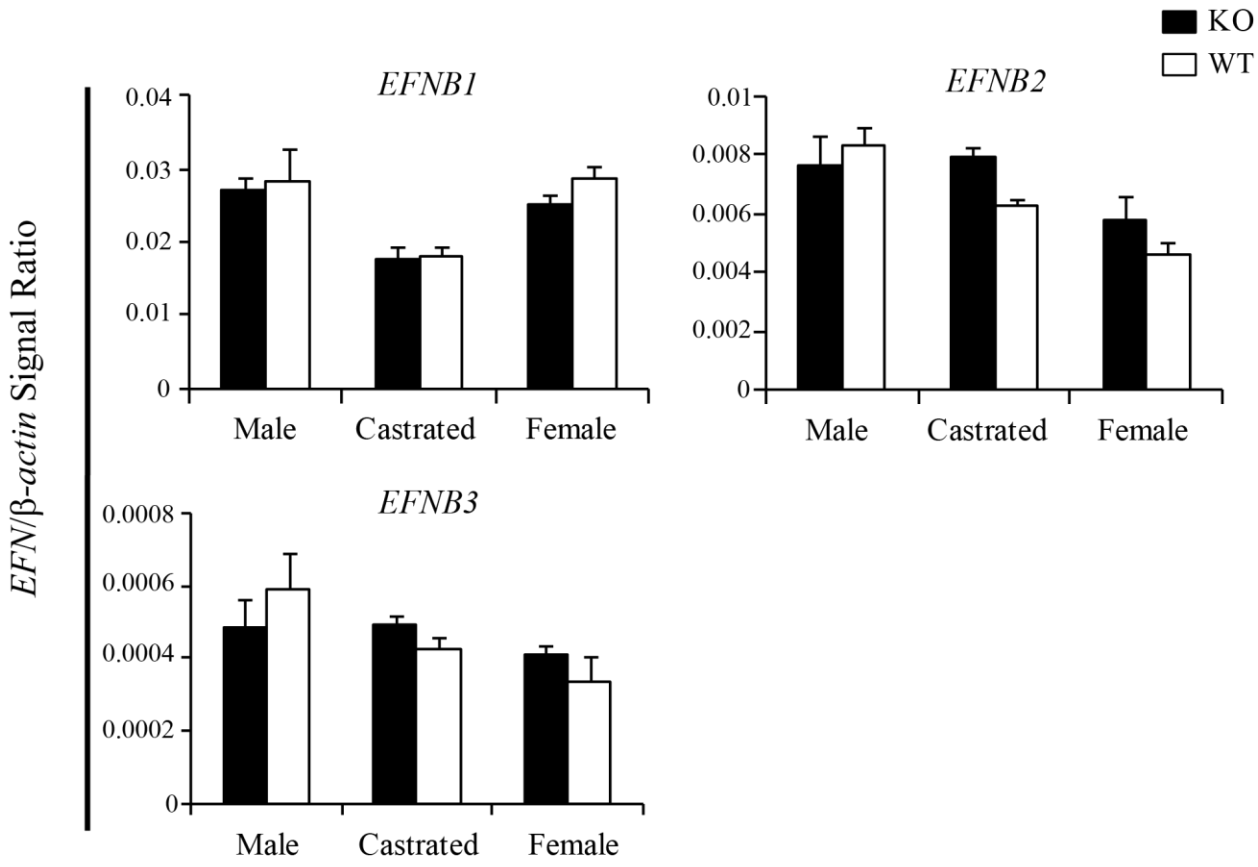

Supplementary Figure 2

Supplementary Figure 2. Normal EFNB1, EFNB2 and EFNB3 mRNA expression in adrenal gland medullae from male, female and castrated male EPHB6 KO mice

Total RNA was extracted from adrenal gland medullae of male, female and castrated male WT and *EFNB6* KO mice. *EFNB1, EFNB2 and EFNB3* mRNA levels the medullae were measured by RT-qPCR. Experiments and data analysis were conducted as described in Supplementary Figure 1.

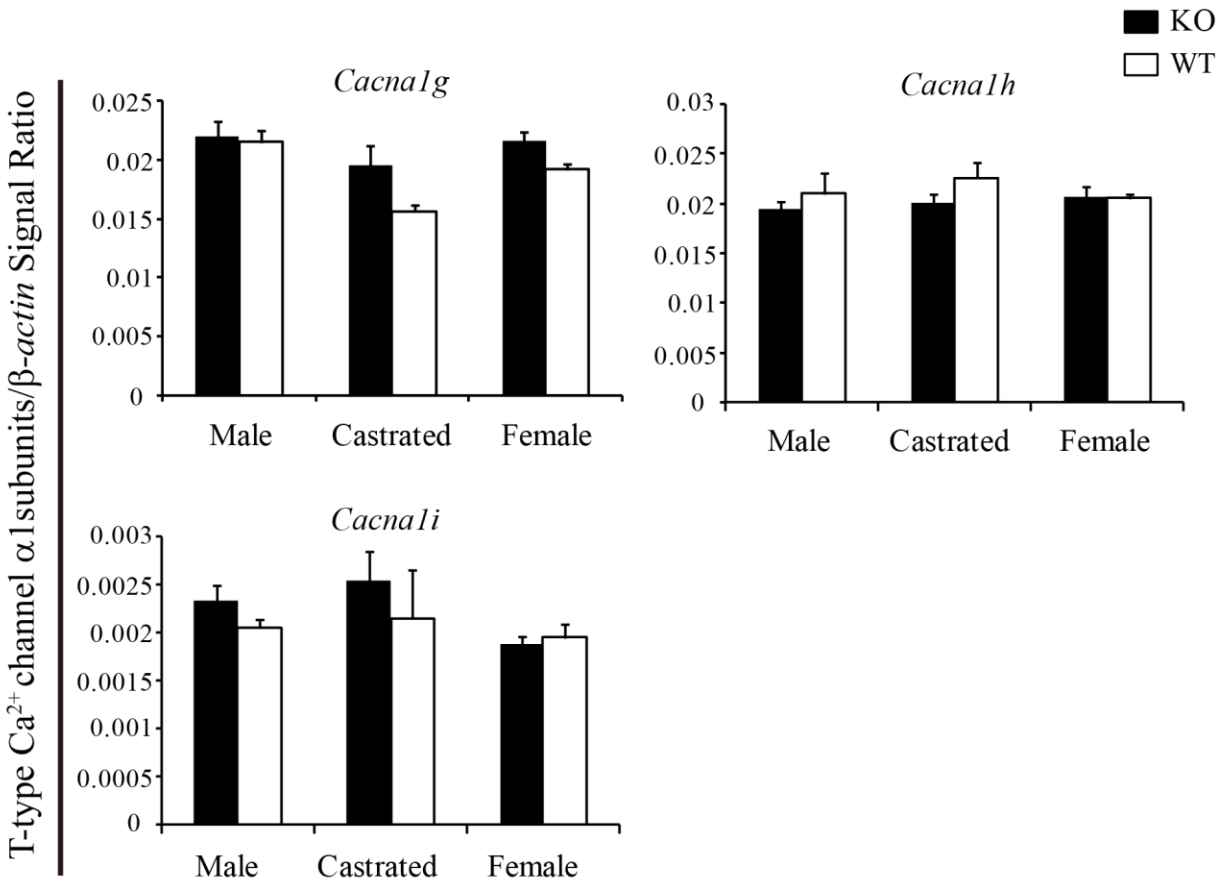

Supplementary Figure 3

Supplementary Figure 3. Normal mRNA expression of T-type Ca^{2+} channel α1 subunits in the adrenal gland medullae of male, female and castrated male EPHB6 KO mice

Total RNA was extracted from adrenal gland medullae of male, female and castrated male WT and *EPHB6* KO mice. T-type Ca^{2+} channel α1 subunit *Cacna1g*, *Cacna1h* and *Cacna1i*mRNA levels in the tissues were measured by RT-qPCR. Experiments and data analysis were conducted as described in Supplementary Figure 1.

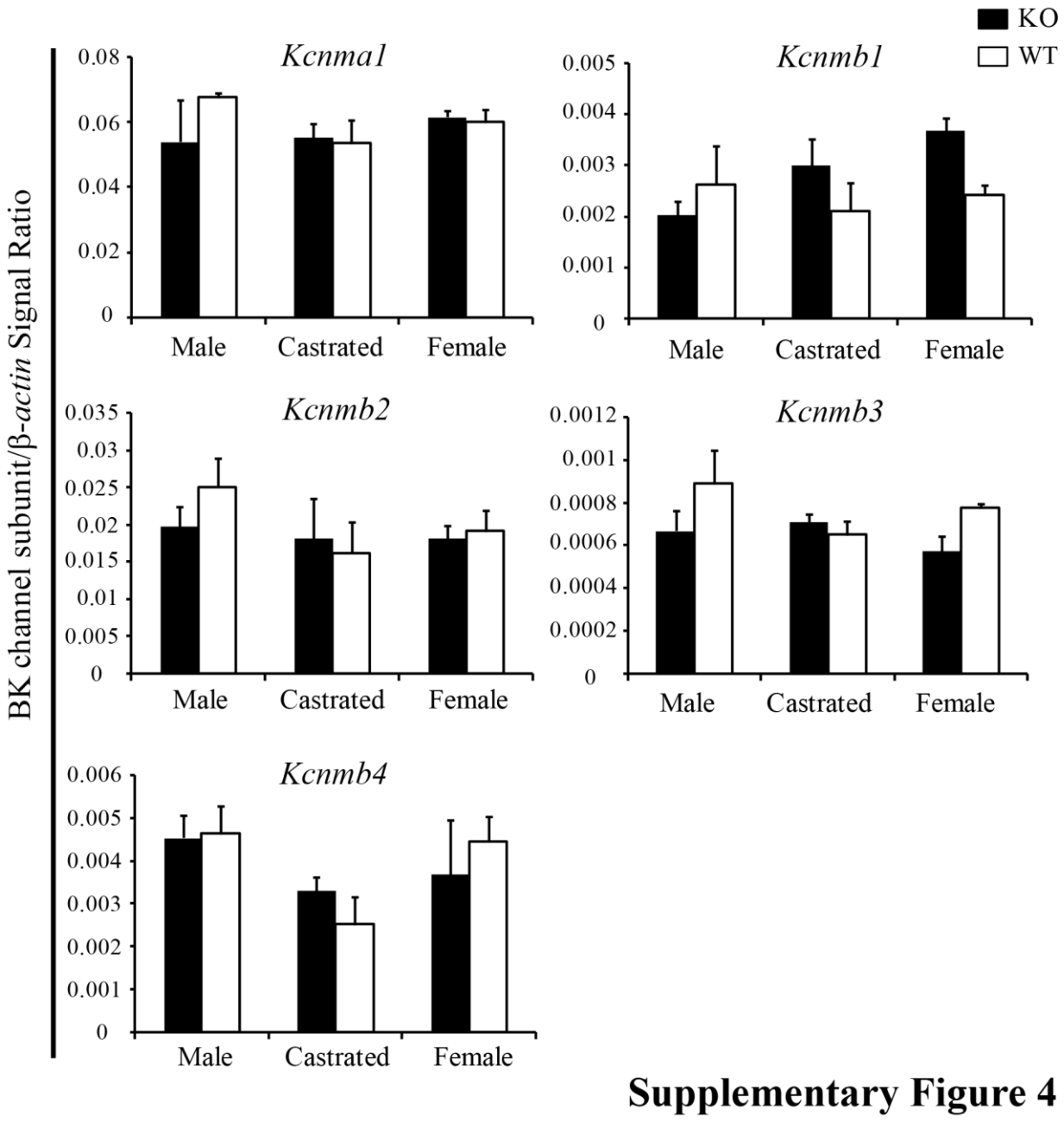

Supplementary Figure 4. Normal mRNA expression of BK channel subunits in adrenal gland medullae of male, female and castrated male KO and WT mice

Total RNA was extracted from adrenal gland medullae of WT and *EPHB6* KO male, female and castrated male mice. mRNA levels of the BK channel α subunit *Kcnma1* or the β-subunits *Kcnmb1, Kcnmb2, Kcnmb3 and Kcnmb4* in the medullae were measured by RT-qPCR. Experiments and data analysis were conducted as described in Supplementary Figure1.

Chapitre 4 – ARTICLE-2

TITLE: EPHB6 controls catecholamine biosynthesis by up-regulating tyrosine hydroxylase transcription in adrenal gland chromaffin cells

Wei Shi[1], Yujia Wang[1,2], Junzheng Peng[1], Shijie Qi[1], Nicolas Vitale[3], Norio Kaneda[4], Tomiyasu Murata[4], Hongyu Luo[1*], and Jiangping Wu[1,5*]

Running title: *EPHB6 controls catecholamine biosynthesis*

From [1]Research Centre, Centre hospitalier de l'Université de Montréal (CRCHUM), Montreal, Quebec, Canada H2X 0A9; [2]Children's Hospital, Zhejiang University School of Medicine, Hangzhou, Zhejiang, China 310003; [3]Institut des Neurosciences Cellulaires et Intégratives, UPR-3212 CNRS-Université de Strasbourg, 5 rue Blaise Pascal Strasbourg, France 67000, [4]Department of Analytical Neurobiology, Faculty of Pharmacy, Meijo University, Tempaku, Nagoya, Japan 4688503; [5]Nephrology Department, CHUM, Montreal, Quebec, Canada H2X 0A9

[*]To whom correspondence should be addressed: Dr. Jiangping Wu, CRCHUM, 900 rue St-Denis, R12-428, Montreal, Quebec, Canada H2X 0A9, telephone: (514) 890-8000 Extension 25164, e-mail: jianping.wu@umontreal.ca, or Dr. Hongyu Luo, CRCHUM, 900 rue St-Denis, R12-426, Montreal, Quebec, Canada H2X 0A9, telephone: (514) 890-8000 Extension 25319, e-mail: hongyu.luo@umontreal.ca

Key words: EPHB6, adrenal gland chromaffin cells, catecholamine, tyrosine hydroxylase, early growth response 1 (EGR1), c-JUN, cell signaling, androgen receptor, ion channel

Published in Journal of Biological Chemistry 2019 Apr; 294(17):6871-6887.

Candidate's Contribution

W.S. was involved in generating the concept and initiating this project. W.S. conducted experiments in the cellular level and molecular level and generated the research outcomes in the Fig. 1 (B,C,D), Fig. 2 (B,C), Fig. 3, Fig. 4, Fig. 5, Fig. 6, Fig. 7, Fig. 8, and all supplementary data. W.S. was involved in drafted the manuscript. W.S. contribution to this publication was about 90%.

Abstract

EPHB6 is a member of the erythropoietin-producing hepatocellular kinase (EPH) family and a receptor tyrosine kinase with a dead kinase domain. It is involved in blood pressure regulation and adrenal gland catecholamine (CAT) secretion, but several facets of EPHB6-mediated CAT regulation are unclear. In this study, using biochemical, RT-qPCR, immunoblotting, and gene microarray assays, we found that EPHB6 up-regulates CAT biosynthesis in adrenal gland chromaffin cells (AGCCs). We observed that epinephrine content is reduced in the AGCCs from male EPHB6-KO mice, caused by decreased expression of tyrosine hydroxylase (TH), the rate-limiting enzyme in CAT biosynthesis. We demonstrate that the signaling pathway from EPHB6 to TH expression in AGCCs involves Rac family small GTPase 1 (RAC1), MAP kinase kinase 7 (MKK7), C-Jun N-terminal kinase (JNK), proto-oncogene C-Jun (c-JUN), activator protein 1 (AP1), and early growth response 1 (EGR1). On the other hand, signaling via extracellular signal–regulated kinase (ERK1/2), p38 mitogen-activated protein kinase, and ELK1, ETS transcription factor (ELK1) was not affected by the EPHB6 deletion. We further report that EPHB6's effect on AGCCs was via reverse signaling through ephrin B1, and EPHB6 acted in concert with the non-genomic effect of testosterone to control CAT biosynthesis. Our findings elucidate the mechanisms by which EPHB6 modulates CAT biosynthesis and identify potential therapeutic targets for diseases such as hypertension caused by dysfunctional CAT biosynthesis.

Introduction

EPHB6 is a member of erythropoietin-producing hepatocellular kinases (EPH), the largest family of receptor tyrosine kinases (Committee, 1997;Pasquale, 2008). The ligands of EPH are called ephrins (EFNs), which are also membrane proteins. EFNs can trigger EPH signaling by canonic forward signaling, *i.e,* from ligand EFNs to receptor EPHs. However, EFNs can also receive signaling from EPHs and transduce signals into cells, and such noncanonical action (*i.e.,* from EPHs to EFNs) is called reverse (Pasquale, 2008). The interaction between EPHs and EFNs are promiscuous: one EPH can bind to multiple EFNs, and one EFN, to multiple EPHs. In general, the EPHA family members bind to EFNAs, and EPHB family members binds to EFNBs (Pasquale, 2008).

EPHs/EFNs function in many organs and systems (Pasquale, 2008). We first reported the critical involvement of EPHs and EFNs in the immune system (Luo et al., 2001;Luo et al., 2002;Yu et al., 2003a;b;Luo et al., 2004;Yu et al., 2004;Wu and Luo, 2005;Yu et al., 2006;Luo et al., 2011a;Luo et al., 2011b;Jin et al., 2014;Hu et al., 2015;Luo et al., 2016). In the past 5 years, we have demonstrated that EPHs/EFNs are involved in regulating blood pressure (BP), which was previously unknown, in a series of publications (Kolski-Andreaco et al., 2007;Luo et al., 2012;Wu et al., 2012;Wang et al., 2015;Wang et al., 2016a;Wang et al., 2016b;Wang et al., 2016c). We reported, using gene knockout mouse models, that while EPHB6, EFNB1, EFNB3 and EPHA4 deletion results in BP elevation (Luo et al., 2012;Wu et al., 2012;Wang et al., 2016c), EPHB4 and EFNB2 deletion lowers it (Wang et al., 2015;Luo et al., 2016;Wang et al., 2016a). Thus, members of EPHBs/EFNBs are a novel yin and yang system that fine-tunes BP homeostasis. In all such cases, sex hormones act in concert with these EPHs/EFNs for controlling BP. Some of these findings from the mouse model have been corroborated by human genetic studies, in which we revealed that some variants in the EFNB2, EFNB3 and EPHA4 genes or a related signaling molecule gene are significantly associated with hypertension in a sex-specific way (Kolski-Andreaco et al., 2007;Wang et al., 2016a).

EPHB6 is highly expressed in the medullae of adrenal glands, which are the major source of catecholamine (CAT) in the circulation. The ambient blood CAT level reflects this hormone's effect on the homeostasis of BP (Gale et al., 2001;Ledoux et al., 2008). We showed that male EPHB6 gene knockout (KO) mice produce reduced amounts of 24-h urinary CAT (Luo et al., 2012), but such phenotype disappears after castration (Luo et al., 2012). We further demonstrated that CAT release in male KO adrenal gland chromaffin cells (AGCCs) is decreased as a consequence of compromised Ca^{2+} influx triggered by acetylcholine (ACh) (Ledoux et al., 2003). This decrease was caused by EPHB6 deletion in combination with the non-genomic effect of testosterone, and hence after castration or in females, the CAT secretion by KO AGCCs is normal (Luo et al., 2012). We further demonstrated that reduced Ca^{2+} influx in male KO AGCCs is the result of augmented Big Potassium channel (BK) current, which causes an earlier closure of voltage-gated calcium channels, leading to decreased Ca^{2+} influx (Ledoux et al., 2003).

In the present study, we report that EPHB6 also plays a critical role in regulating CAT biosynthesis. The signaling pathway from EPHB6 to CAT biosynthesis was investigated.

Materials and methods

EPHB6 *gene KO mice*

EPHB6 KO mice were generated in our laboratory, as described previously (Luo et al., 2004). They were backcrossed to the C57BL/6 genetic background for more than 15 generations. Age- and gender-matched wild type (WT) littermates served as controls. Experiments using castrated mice were conducted at least 3 weeks post-operation.

Epinephrine and norepinephrine assays

The adrenal glands were resected from EPHB6 KO and WT mice, or castrated KO mice, and were homogenized in 300 μl 0.01 N HCL in the presence of 0.15 mM EDTA. Epinephrine levels in the cleared supernatants were determined by Epinephrine Research ELISA Kits (Rocky Mountain Diagnostics, Colorado Springs, CO, USA, BAE-5100) according to the manufacturer's instructions. For cultured primary AGCCs, they were pretreated with a cell membrane-impermeable BSA-conjugated testosterone [1.1 μg/ml, testosterone-3-(O-carboxymethyl)-oxime-BSA; testosterone-BSA; Aviva Systems Biology] or BSA for 15 min, and then washed and stimulated with Nicotine (20 μmol/L) for 16 h at 37°C. The cells were washed once with Hank's buffer and were lysed in 400 μl 0.01 N HCL in the presence of 0.15 mM EDTA. Norepinephrine levels in the cleared supernatants were determined by Norepinephrine Research ELISA Kits (Rocky Mountain Diagnostics). For nonmalignant AGCC line tsAM5NE cells, they were lysed with repeated (3 times) freeze-thaw after being transfected with *siRNA*s. Norepinephrine levels in the cleared supernatants were determined by noradrenaline ELISA kits (LifeSpan BioScernces, Seattle, USA, LS-F10598) according to the manufacturer's instructions. Samples were assayed in duplicate.

Reverse transcription-quantitative polymerase chain reaction (RT-qPCR)

mRNA levels of TH*,* and *Egr1* were measured by RT-qPCR. Total RNA from the adrenal glands medullar cells or tsAM5NE cells was extracted with TRIzol® (Invitrogen, Burlington, Ontario, Canada) and reverse-transcribed with iScript™ cDNA Synthesis Kit (Bio-Rad Laboratories (Canada) Ltd., Mississauga, Ontario, Canada). Supporting Information Table 1 (SI-Table 1) lists the qPCR primers used. qPCR conditions were as follows: 2 min at 50°C, 2 min at 95°C, followed by 40 cycles of 10 s at 94°C, 20 s at 58°C, and 20 s at 72°C. β-actin mRNA levels were considered as internal controls. qPCR signals between 22 and 30 cycles were analyzed. Samples were tested in triplicate, and the data were expressed as signal ratios of target RNA/β-actin mRNA.

Immunoblotting

Adrenal gland medullae were isolated from 8- to 10-week old male mice, and cultured in Opti-MEM™ Reduced Serum Media (ThermoFisher scientific, Burlington, Ontario, Canada, Cat. #31985070) at 37°C for 2 hours. In some experiments, nicotine (20 μM) (Sigma-Aldrich, Winston, Ontario, N3876) was used to stimulate the medullae for 2.5 and 5 minutes post the 2-hour culture period. The tissues were then lysed by immunoprecipitation assay buffer (RIPA), which contained PhosSTOP and protease inhibitor mixtures (Roche Applied Science, MeylanCedex, France). For tsAM5NE cells, they were lysed with RIPA buffer 72 hours after being transfected with *Egr1* siRNA or 4 hours after nicotine (40 μM) stimulation in the coated plates. Forty μg of lysate protein per sample was resolved on 10% SDS-PAGE. Proteins were transferred from the gel to PVDF membranes (Invitrogen), which were then incubated in blocking buffer containing 5% (w/v) skim milk or 5% BSA for 1 hour at room temperature. The membranes were incubated overnight at 4°C with rabbit anti-TH Ab (2792; Cell Signaling Technology, Danvers, US), rabbit anti-EGR1 Ab (ab182624; Abcam), rabbit anti-MKK7 (phospho S277+T275) Ab (ab78148; Abcam), rabbit anti-MKK7 Ab (4172; Cell Signaling Technology), rabbit anti-phospho-c-JUN (Ser63) Ab (9261; Cell Signaling Technology), rabbit anti-c-JUN monoclonal Ab (9165; Cell Signaling Technology), rabbit anti-phospho-JNK (Thr183/Tyr185) Ab (9251; Cell Signaling Technology, Danvers, US), rabbit anti-

JNK Ab (9252; Cell Signaling Technology), mouse anti-phospho-ERK1/2 (Thr202/Tyr204) Ab (9106; Cell Signaling Technology), rabbit anti-ERK1/2 Ab (9102; Cell Signaling Technology), rabbit anti-phospho-p38MAPK (Thy180/Tyr182) Ab (9211; Cell Signaling Technology), rabbit anti-p38MAPK Ab (9212; Cell Signaling Technology), rabbit anti-phospho-ELK1 (S383) Ab (ab218133; Abcam), rabbit anti-ELK1 Ab (9182; Cell Signaling Technology), or rabbit anti-β-actin Ab (4967; Cell Signaling Technology). Blots were washed and then incubated with horseradish peroxidase-conjugated secondary Abs for 2 hours. All the antibodies were used at the manufacturers' recommended dilutions. Signals were visualized by SuperSignal West Pico Chemiluminescent Substrate (ThermoFisher Scientific).

Adrenal gland medulla organ culture

Adrenal gland medullae were isolated from 8- 10-week old EPHB6 KO and WT mice, and cultured in DMEM medium with 15% FCS at 37°C for 0, 2.5 and 5 minutes after nicotine (20 μM) stimulation. The medullae were harvested for the subsequent EMSA or immunoblotting. In some experiments, they were cultured for 4 h in the presence of RAC1 inhibitor (50 μM; 53502, Sigma-Aldrich, Winston, Ontario), MKK7 inhibitor (50 μM; 335140001, Sigma-Aldrich, Winston, Ontario), JNK inhibitor SP600125 (20 μM; S5567, Sigma-Aldrich, Winston, Ontario) or vehicle. The medullae were then harvested for the measurement of *Egr1* mRNA levels by RT-qPCR.

DNA microarray

Total RNA was extracted using RNeasy Mini Kit (74104, Qiagen, Toronto, Ontario, Canada) from adrenal glands of male, female and castrated male EPHB6 KO mice and their WT counterparts. Three biological replicates using different mice for each group were employed. The RNA was quantified using NanoDrop Spectrophotometer ND-1000 (NanoDrop Technologies, Inc.) and its integrity was assessed using a 2100 Bioanalyzer (Agilent Technologies). Double stranded cDNA was synthetized from 250 ng of total RNA, and *in vitro* transcription was performed to produce biotin-labeled cRNA using Illumina® TotalPrep RNA Amplification Kit, according to manufacturer's

instructions (Life Technologies). The labeled cRNA was normalized at 1,500 ng and hybridized on MouseWG-6_V2 array according to Illumina's Whole-Genome Gene Expression Direct Hybridization Assay Guide. The BeadChips were incubated in an Illumina Hybridization oven at 58°C for 16 hours at a standard rocking speed of 5 according to the oven speedometer. Beadchips were washed according to Illumina's protocol mentioned previously and scanned on an Illumina iScan Reader.

Mean expression signal levels of all the genes of 3 replicates in each group were first obtained. Using the mean expression signal level of each gene of the male WT group for comparison, genes with more than 2-fold changes in their expression in the male KO groups were selected. The fold changes of these selected genes in the female KO group with respect to the female WT group, and the fold changes of these genes in the castrated male KO group with respect to the castrated WT group were calculated and presented.

GTPase activation assay for RAC1

Activated RAC1 G-protein within samples (25μg/sample) was determined by the G-LISA assay (Cytoskeleton, Inc.), performed according to the manufacturer's instructions. Briefly, adrenal gland medullae were isolated from 8-10-week old EPHB6 KO and WT mice, and cultured in Opti-MEMTM Reduced Serum Media at 37°C for 2 hours. Nicotine (20 μM) was used to stimulate the adrenal medulla for 2.5 minutes, which in pilot studies we determined was the peak activation time. Proteins were extracted from the tissues on ice for 5 minutes in G-LISA cell lysis buffers containing protease inhibitor cocktails (Cytoskeleton, Inc, Denver, Colorado; BK128). The cleared supernatants were snap frozen in liquid nitrogen and stored at -80°C until the assay. Samples were assayed in duplicate. Three independent experiments were conducted and the results were normalized according to the values of WT samples at time 0. The relative RAC1 activity was calculated as follows:

The relative RAC1 activity = RAC1 activity of a given sample/RAC1 activity of WT cells at time 0.

Chromaffin cell line culture

AGCC line tsAM5NE cells were cultured in collagen IV-coated 24-well flat bottom plates (Corning, New York, USA, 354430) in DMEM medium with 15% FCS and G5 supplement (ThermoFisher scientific, Burlington, Ontario, Canada, 17503012) in an environment of 5% CO_2 at 33°C. In some experiments, these cells were cultured in wells coated with goat anti-EPHB6 Ab (AF611, R&D systems, Oakville, Ontario, Canada), normal goat IgG (sc-2028, Santa Cruz Biotechnology, Mississauga, Ontario, Canada), recombinant EPHB6-Fc (E9777, Sigma-Aldrich, Oakville, Ontario, Canada), normal human IgG (0150-01, Southern Biotech, Birmingham, USA), rabbit anti-EFNB1 Ab (sc-1011, Santa Cruz Biotechnology), normal rabbit IgG (sc-2027, Santa Cruz Biotechnology), or goat anti-EFNB2 Ab (AF496, R&D systems) (2 μg/ml during overnight coating at 4°C) for 24 hours. Nicotine (40 μM) was used to stimulate these cells for 4 hours.

Small interfering RNA (siRNA) transfection

SMARTpool *Egr1 siRNA* (M-040286-01-0005), which contained 4 pairs of *siRNA* targeting different regions of *Egr1* mRNA, as well as negative control *siRNA* (D-001206-13-05) were synthesized by Dharmacon (Lafayette, Colorado, USA). The *siRNA* sequences are listed in SI-Table 2. tsAM5NE cells at a density of 2 x 10^5 cells/well in 24-well plates were transfected with *siRNAs* (30 nM) with DharmaFECT 1 Transfection Reagent (Dharmacon; T-2001-02) immediately after passage. The transfected cells were cultured for additional 24 to 72 hours before further manipulation.

EMSA and EMSA-immunoblotting

The EPHB6 KO and WT male mice were subcutaneously injected with nicotine in PBS (2 mg/kg body weight) or an equal volume of PBS as a control. The mice were placed in an incubator to prevent hypothermia. After 2 hours, their adrenal medullae were isolated and nuclear proteins were extracted with NE-PER™ Nuclear and Cytoplasmic Extraction Reagents (ThermoFisher scientific, Burlington, Ontario, Canada, 78833). EMSA were performed according to the manufacturer's protocols (Odyssey infrared EMSA kit; LI-COR Biosciences, Lincoln, Nebraska,

USA). Duplexed oligonucleotides (5′ -GGACTTAGGACTGACCTAGAACAATCA-3′) containing the AP-1-binding sequence (positions +383 to +393) in the 5' untranslated region of mouse *Egr1* gene were labeled at 5′ -end with IRDye 800 infrared dye (Integrated DNA Technologies, Skokie, Illinois, USA), and used as probes. The extracted nuclear protein (10 μg) was incubated with 5 nM of the IRdye800-labeled probes for 30 minutes. For background control, 200-fold molar excess of unlabeled probes was added to a sample containing WT nuclear extracts to determine the background association of the probes with the nuclear proteins. DNA-protein mixtures were separated by 5% non-denaturing polyacrylamide gel electrophoresis in 0.5 × TBE buffer. Gels were imaged by a LI-COR Odyssey imaging system. The specific AP-1 binding activity was calculated as follows.

The AP-1 binding activity = AP-1 signal of testing samples – signal of the background control

For each experiment, the AP-1 binding activity of WT cells without nicotine stimulation (*i.e.,* treated with PBS) was used to normalize the values of all other samples to calculate their respective normalized relative AP-1 binding activity, using the formula below.

The normalized relative AP-1 binding activity = the specific AP-1 binding activity of a given sample / the specific AP-1 binding activity of WT samples treated with PBS.

To identify c-JUN and c-FOS proteins in the shifted bands, proteins in non-denaturing polyacrylamide gels of EMSA were transferred to PVDF membranes. The membranes were blocked with PBS containing 5% (w/v) skim milk for 1 hour at room temperature. They were then reacted overnight at 4°C with rabbit anti-c-JUN mAb (9165; Cell Signaling Technology), or rabbit anti-c-FOS Ab (ab190289, Abcam). The membranes were washed and then incubated with horseradish peroxidase- conjugated secondary Ab for 2 hours. All the Abs were used at the manufacturers' recommended dilutions. Signals were visualized by SuperSignal West Pico Chemiluminescent Substrate (ThermoFisher Scientific).

Primary AGCC culture

Primary mouse AGCCs were isolated as previously described (Wang et al., 2018). Briefly, adrenal gland medullae were obtained from 8- to 10-week-old mice. Papain (P4762, Sigma-Aldrich, Oakville, Ontario, Canada) was activated with 5 mM L-cysteine. The medullae were digested by the activated papain in Hank's buffer at 37°C for 25 min. They were washed twice with Hank's buffer and then triturated by pipetting in 300 μl Hank's buffer until they became feather-like. Cells were pelleted at 3,700 *g* for 3 min and re-suspended in DMEM containing 15 % (v/v) FCS for culture. BSA-conjugated testosterone (1.1 μg/ml, testosterone-3-(O-carboxymethyl)-oxime-BSA; Aviva Systems Biology, San Diego, USA) or BSA was added to the culture 15 min prior to the addition of nicotine (20 μM), and the cells were cultured for 16 h at 37°C before being harvested for their norepinephrine content measurement.

Ethics statement

All animal studies were approved by the Animal Protection Committee (Comité institutionnel d'intégration de la protection des animaux) of the CRCHUM.

Results

Adrenal glands from male EPHB6 KO mice showed reduced epinephrine content

Our previous study demonstrated that male but not female EPHB6 KO mice have reduced CAT secretion (Luo et al., 2012). Secretion and biosynthesis of CAT are distinct but yet interrelated events. To assess whether the KO adrenal glands were also compromised in CAT biosynthesis, we measured their CAT content, using epinephrine as a representative CAT, as our previous study showed that the levels of three major types of CAT (epinephrine, norepinephrine and dopamine) in the 24-h urine were similarly reduced in the male KO mice. As shown in Figure 1A, the epinephrine content in male KO but not female KO adrenal glands was significantly reduced, but castration brought the level of male KO AGCCs to that seen in uncastrated WT counterparts. This

pattern is consistent with that of 24-hour urine CAT levels in the KO mice before and after castration (Luo et al., 2012). The size of adrenal gland medullae from male, female and castrated male KO mice was similar to their WT counterparts (Fig. 1B), suggesting that the change in the epinephrine content in the male KO mouse adrenal glands is not due to altered size of the gland medullae.

We then investigated whether the reduced epinephrine content in the male KO adrenal glands was due to the decreased levels of TH, the rate-limiting enzyme in CAT biosynthesis. As shown in Figure 1C, the TH mRNA levels were decreased in the male but not female KO glands, compared to their WT counterparts. Such a decrease was abolished after castration. This pattern of TH expression was also confirmed at the protein level (Fig. 1D). Therefore, EPHB6 deletion correlated to reduced TH expression in a male sex hormone-dependent fashion, TH being the rate-limiting enzyme of CAT biosynthesis.

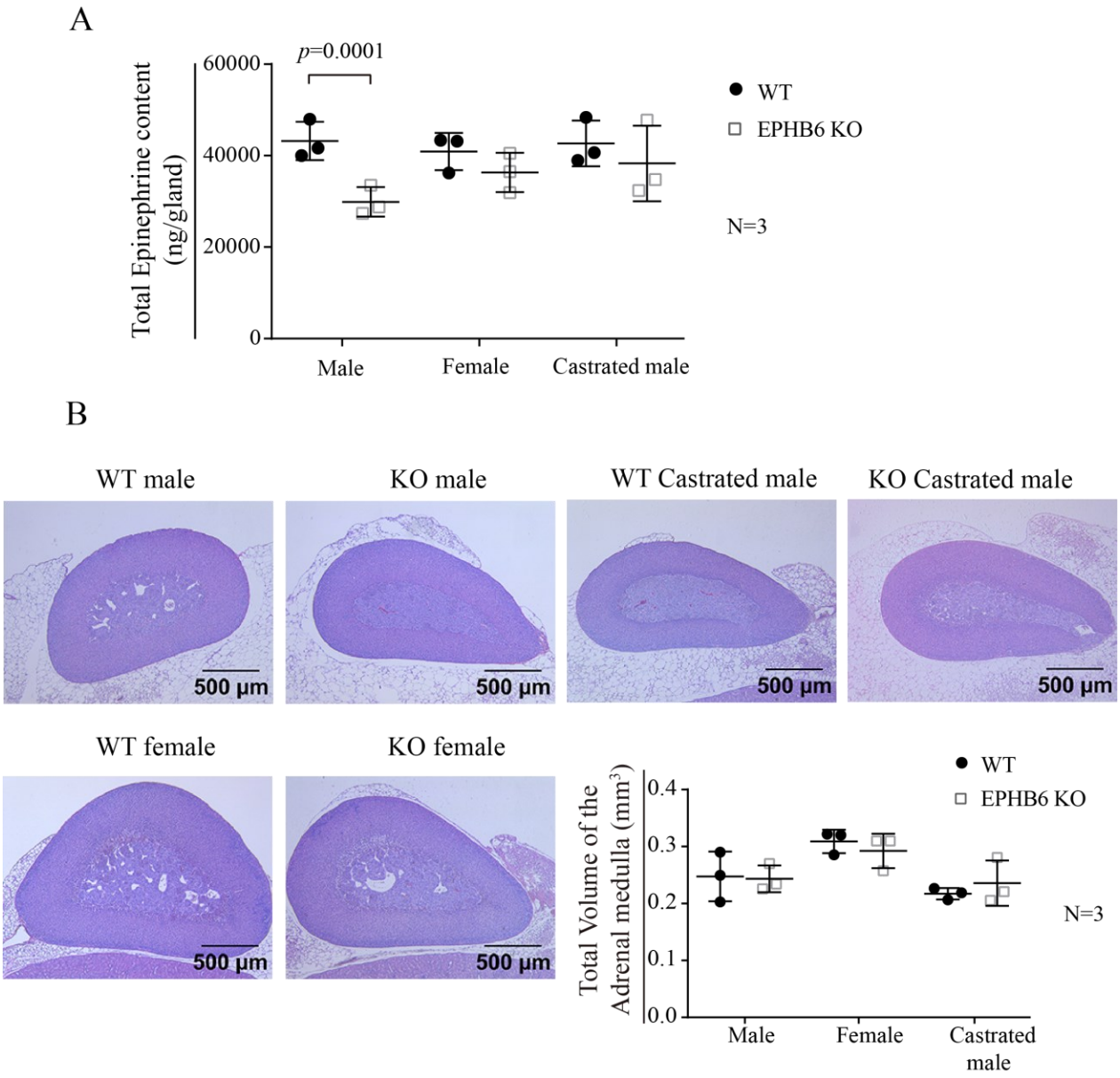
A
p=0.0001
60000
40000
20000
0
Total Epinephrine content (ng/gland)
Male
Female
Castrated male
WT
EPHB6 KO
N=3
B
WT male
KO male
WT Castrated male
KO Castrated male
500 µm
WT female
KO female
Total Volume of the Adrenal medulla (mm3)
0.4
0.3
0.2
0.1
0.0
Male
Female
Castrated male
WT
EPHB6 KO
N=3

Figure 1

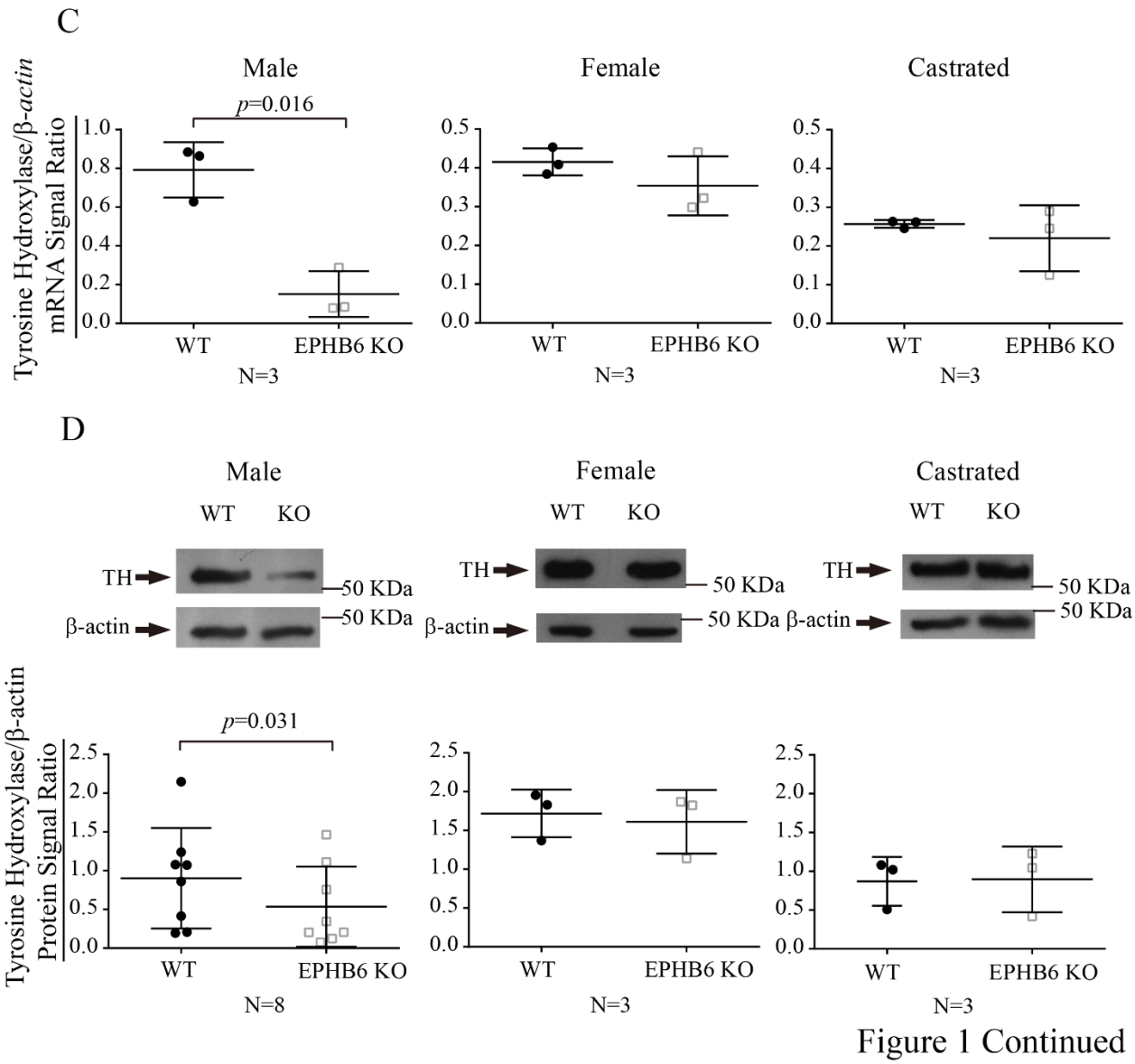

Figure 1. Epinephrine content and TH expression in the adrenal glands of WT and KO mice

A. Total epinephrine content in the adrenal glands of WT and KO mice

The results from three independent experiments using different mice were pooled, and the results are shown as means ± SD with data points. The data were analyzed by 2-way paired Student's *t* test, and the significant *p*-value is indicated.

B. Similar sizes of KO and WT adrenal glands

Adrenal glands were serially sectioned at an interval of 50 μm at 5 μm thickness. Representative micrographs of the largest HE-stained transection of the gland from each group is presented.

The total volume of the adrenal gland medullae was determined by following formula:

Size of the medulla= mean area of all the sections that contains the medulla $\times$ length of the medulla

The results from three individual medullae from different mice of each group were pooled, and the results are shown as means ± SD with data points. No significant difference between KO and their WT counterparts is found (2-way paired Student's *t* test).

C. TH mRNA expression in adrenal gland medullae of KO and WT mice

Total RNA was extracted from adrenal medullae. TH mRNA level was analyzed by RT-qPCR. β-actin levels were used as internal controls. Samples were measured in triplicate, and the data from three independent experiments using different mice were pooled and expressed as graphs of TH signal/ β-actin signal ratios (means ± SD with data points). The significant *p*-value (2-way paired Student's *t* tests) is indicated.

D. TH protein expression in the adrenal medullae of KO and WT mice

TH protein levels in the adrenal gland medullae were analyzed by immunoblotting. The representative immunoblotting images are illustrated. The signal ratios of TH versus β-actin were quantified by densitometry. Densitometry data from three or more (as indicated) independent experiments using different mice were pooled and are presented as graphs (means ± SD with data points). The significant *p*-value (2-way paired Student's *t* tests) is indicated.

EPHB6 KO decreased the transcription factor Egr1 expression in adrenal gland medullae

To elucidate molecular mechanisms underlying the defective TH expression in the adrenal gland medullae, we subjected the WT and KO medullae to transcriptome microarray analysis.

The array data were deposited to the Gene Expression Omnibus with accession number GSE120400.

Since the TH expression was decreased in male but not female KO medullae, and such a change disappeared after castration, we sought out for genes whose expression pattern fitted to this pattern, *i.e.,* they were altered in male but not female KO medullae, and such alteration in males would disappear after castration. We first compared the gene expression profile of the male WT versus KO adrenal gland medullae. Twenty genes had more than 2-fold higher expression in the WT medullae than in the KO medullae, but none had more than 2-fold lower expression in such comparison, as shown in the heat map of Figure 2A (left column). The expression of these 20 genes in female WT versus KO medullae and in castrated WT versus castrated KO medullae was then compared (Fig. 2, middle and right column). Only 2 genes (*LOC666403 and CFD*) still showed more than 2-fold higher expression in the female WT and castrated WT medullae, compared to their KO counterparts. The remaining 18 genes resembled the expression pattern which we were looking, and could potentially be involved in regulating TH expression.

We selected the top 4 hits from the 18 genes for further investigation. The selection criterion was that they had more than 3-fold higher expression in the male WT medullae compared to KO ones *(i.e*., *Egr1*, 11.1 fold; *JunB*, 5.8 fold; *Fos*, 3.8 fold; and *Dusp1*, 3.2 fold). The first 3 are transcription factors and the last one is a phosphatase. Although *Hspa1a* had a similar high level change (3.5 fold), due to the ubiquitous presence of this heat shock protein and its being neither a transcription factor nor an enzyme, it was excluded from further study.

Even though we could confirm by RT-qPCR that the mRNA expression of *JUNB, FOS* and *DUSP1* was significantly reduced in the male KO medullae, their protein levels showed no change (Supporting Information Fig. 2). Therefore, no further investigation was carried out on these 3 genes.

We confirmed by RT-qPCR that *Egr1* mRNA expression was significantly lower in male but not in female KO medullae, compared to their WT counterparts (Fig. 2B). This decrease was ameliorated after castration. This was verified at the protein level by immunoblotting (Fig. 2C), *i.e.,* the male

but not female KO medullae had lower EGR1 protein level, and this was reversed to normal levels after castration.

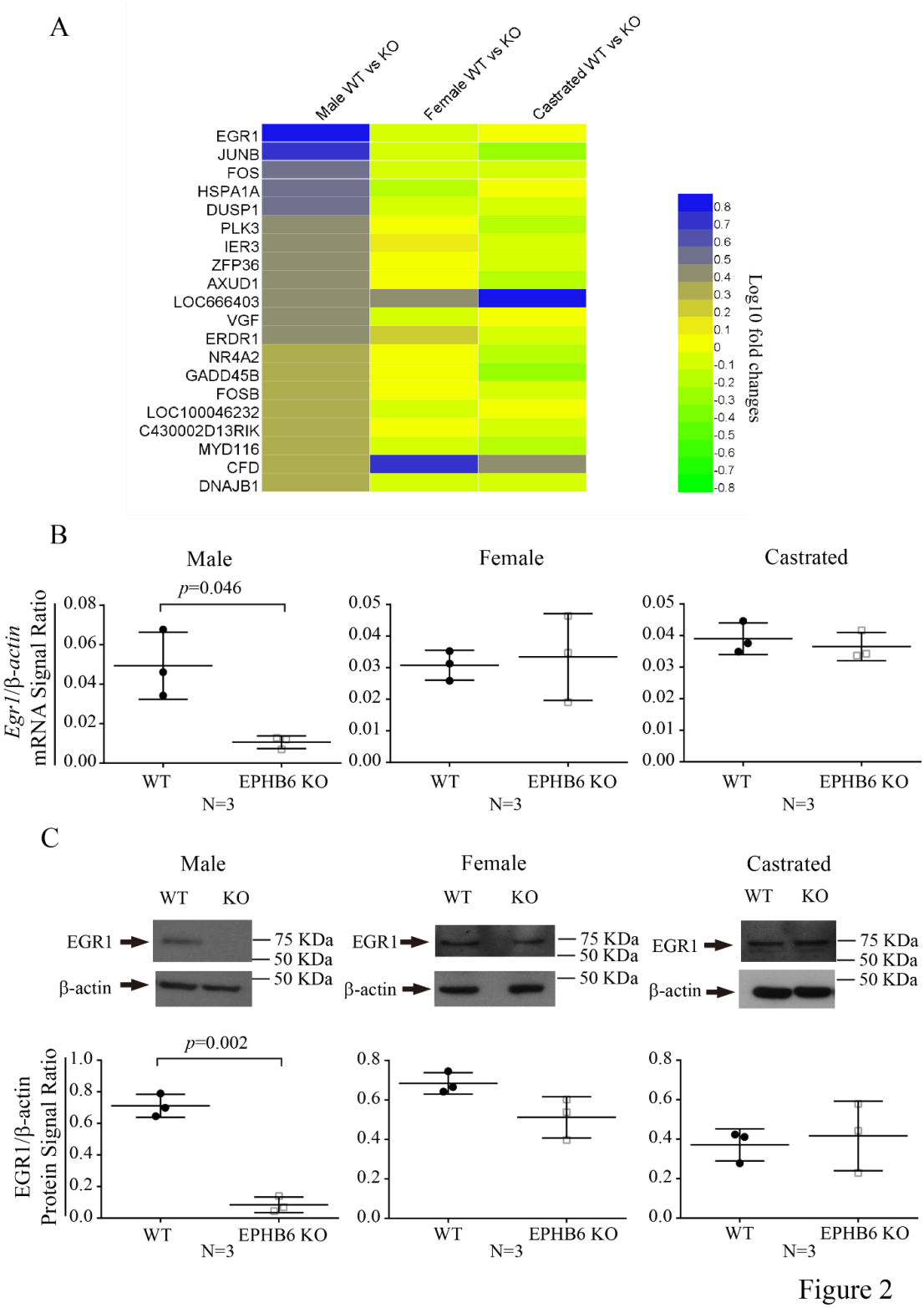

Figure 2

Figure 2. Identification of reduced Egr1 expression in the adrenal glands of male KO mice

A. Significantly altered expression of genes in the cRNA microarray analysis of adrenal gland medullae from KO mice and WT

Total RNA was extracted from adrenal glands and subjected to cRNA microarray analysis. Three biological replicates using difference mice for each group were employed and mean signal levels of each gene in each group were calculated. The genes with their mean signal levels differed above 2-folds between male WT and KO male groups were selected, and the ratios of their mean signal levels were presented in the left column of a $\log_{10}$-scaled heat map. The ratios of the mean signal levels of these selected genes for the female WT versus female KO groups are presented in the middle column, while those between the castrated WT males versus castrated KO males are presented in the right column.

B. Reduced expression of Egr1 mRNA in adrenal medullae from male KO mice

Egr1 mRNA levels in the adrenal gland medullae were analyzed by RT-qPCR. β-actin levels were used as internal controls. Samples in RT-qPCR were in triplicate, and *Egr1*/ β-actin signal ratios from three independent experiments using different mice were pooled and expressed as means ± SD with data points. The significant *p*-value (2-way paired Student's *t* tests) is indicated.

C. Reduced Egr1 protein expression in the adrenal medullae of male EPHB6 KO mice

EGR1 protein levels of adrenal gland medullae were analyzed by immunoblotting, and representative images are shown. The intensity of the EGR1 and β-actin bands was measured by densitometry. The results of three independent experiments using different mice were pooled and the signal ratios of EGR1 versus β-actin are presented as graphs (means ± SD with data points). The significant *p*-value (2-way paired Student's *t* tests) is indicated.

Reduced EGR1 expression in KO chromaffin cells was correlated to decreased TH expression

EGR1 is a transcription factor. To prove that reduced EGR1 level was responsible for the decreased TH expression and hence reduced CAT biosynthesis, we knocked down EGR1 expression by *siRNA*

in a non-malignant mouse AGCC cell line (tsAM5NE cells) (Kohno et al., 2011). The efficiency of *Egr1/*EGR1 knockdown at the mRNA and protein levels was confirmed by RT-qPCR and immunoblotting (Fig. 3A). As a consequence of EGR1 knockdown, TH expression at the mRNA and protein level was reduced (Fig. 3B), indicating the EGR1 transcription factor is indeed responsible for enhancing TH mRNA transcription. It is to be noted that tsAM5NE cells, although being normal AGCCs, only produce norepinephrine but not epinephrine (Kohno et al., 2011), and therefore, the former was used as a surrogate representative of CAT in our assay. The norepinephrine content in the tsAM5NE cells was decreased, as expected (Fig. 3C), after EGR1 knockdown, as a consequence of reduced TH level. Thus, these results showed that reduced EGR1 expression is correlated to reduced CAT synthesis in AGCCs from EPHB6 KO-mice.

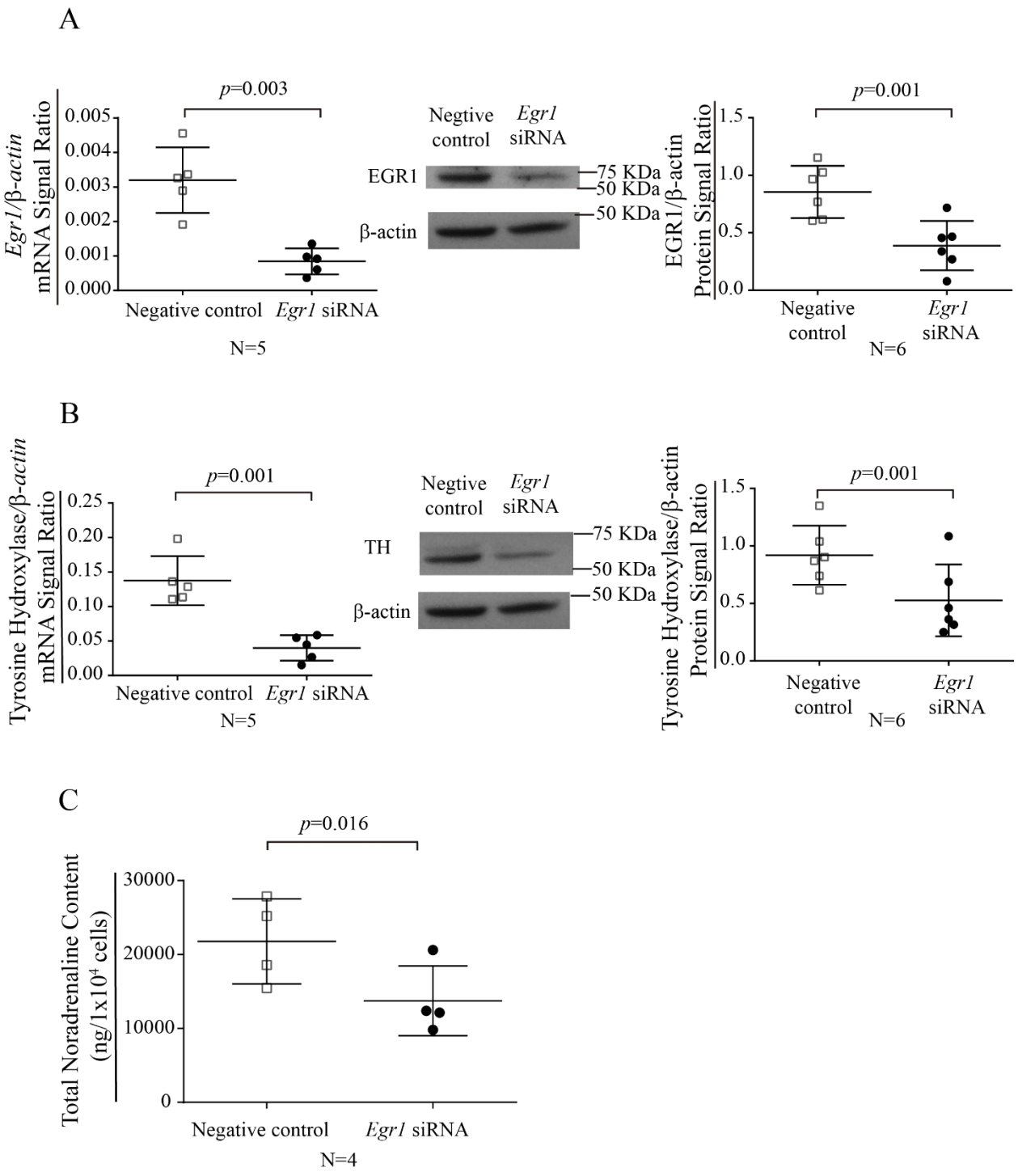

Figure 3

Figure 3. Egr1 knockdown by siRNA reduces TH expression and epinephrine content of chromaffin cell line tsAM5NE

Egr1 siRNA and negative control *siRNA* were transfected into adrenal gland chromaffin cell line tsAM5NE cells.

A. Reduced expression of Egr1 in tsAM5NE cells after Egr1 knockdown

The cells were harvested 24 hours after the *Egr1* and control siRNA transfection, and the *Egr1* mRNA (left panel) and protein (right panel) levels were determined by RT-qPCR and immunblotting, respectively. Data from five or more (as indicated) independent experiments were pooled and presented as means ± SD with data points of the ratios of *Egr1* mRNA signal versus β-*actin* mRNA signal, and ratios of EGR1 protein signal versus β-actin protein signal. *P*-values are indicated (2-way paired Student's *t* tests).

B. TH expression was reduced in tsAM5NE cells after Egr1 knockdown

tsAM5NE cells were harvested 72 hours after *Egr1* siRNA transfection, the TH mRNA (left panel) and protein (right panel) levels were determined by RT-qPCR and immunblotting, respectively. Data from five or more (as indicated) independent experiments were pooled and are presented as means ± SD with data points of the ratios of TH mRNA signal versus β-actin mRNA signal, and ratios of TH protein signal versus β-actin protein signal. P-values are indicated (2-way paired Student's *t* tests).

C. Reduced noradrenaline content in tsAM5NE chromaffin cells after Egr1 knockdown

tsAM5NE cells were harvested and then lysed 72 hours after *Egr1* siRNA transfection. Noradrenaline levels in the cleared supernatants were determined by noradrenaline ELISA, in which samples were measured in duplicate. Results from four independent experiments were pooled and presented as means ± SD with data points *p*-value is indicated (2-way paired Student's *t* tests).

EPHB6 KO leads to reduced AP-1 association with its binding site in the Egr1 gene enhancer

One possible mechanism by which EPHB6 may control *Egr1* expression is that it acts through transcription factors, which associate with *Egr1* gene enhancers. There is an AP-1 binding site

between positions +383 and +393 in the 5' untranslated region of the *Egr1* gene. AP-1 promotes gene transcription when bound to enhancers, *i.e*., AP-1 binding sites, of many genes (Hess et al., 2004). ACh and nicotine are known to increase TH expression and consequently CAT synthesis in AGCCs. These two molecules similarly bind to nicotinic and muscarinic acetylcholine receptors (nAChR and mAChR, respectively). We used nicotine *in lieu* of ACh in this and the rest of the experiments to stimulate AGCCs as nicotine is more stable for storage and in the culture medium. According to electrophoretic mobility shift assays (EMSA), AP-1 binding to the AP-1-binding sequence in the 5' upstream region of the *Egr1* gene was reduced with the nuclear extracts of AGCCs from male EPHB6 KO mice, compared to those from WT counterparts (Fig. 4A). We confirmed that the shifted AP-1 bands in EMSA contained both c-JUN and c-FOS (Supporting Information Figs. 1A and 1B). AP-1 is a dimer of JUN and FOS family members, and c-JUN is the major subtype of JUN proteins. Nicotine-triggered c-JUN phosphorylation was compromised in male EPHB6 KO AGCCs, compared to that in the WT counterparts (Fig. 4B).

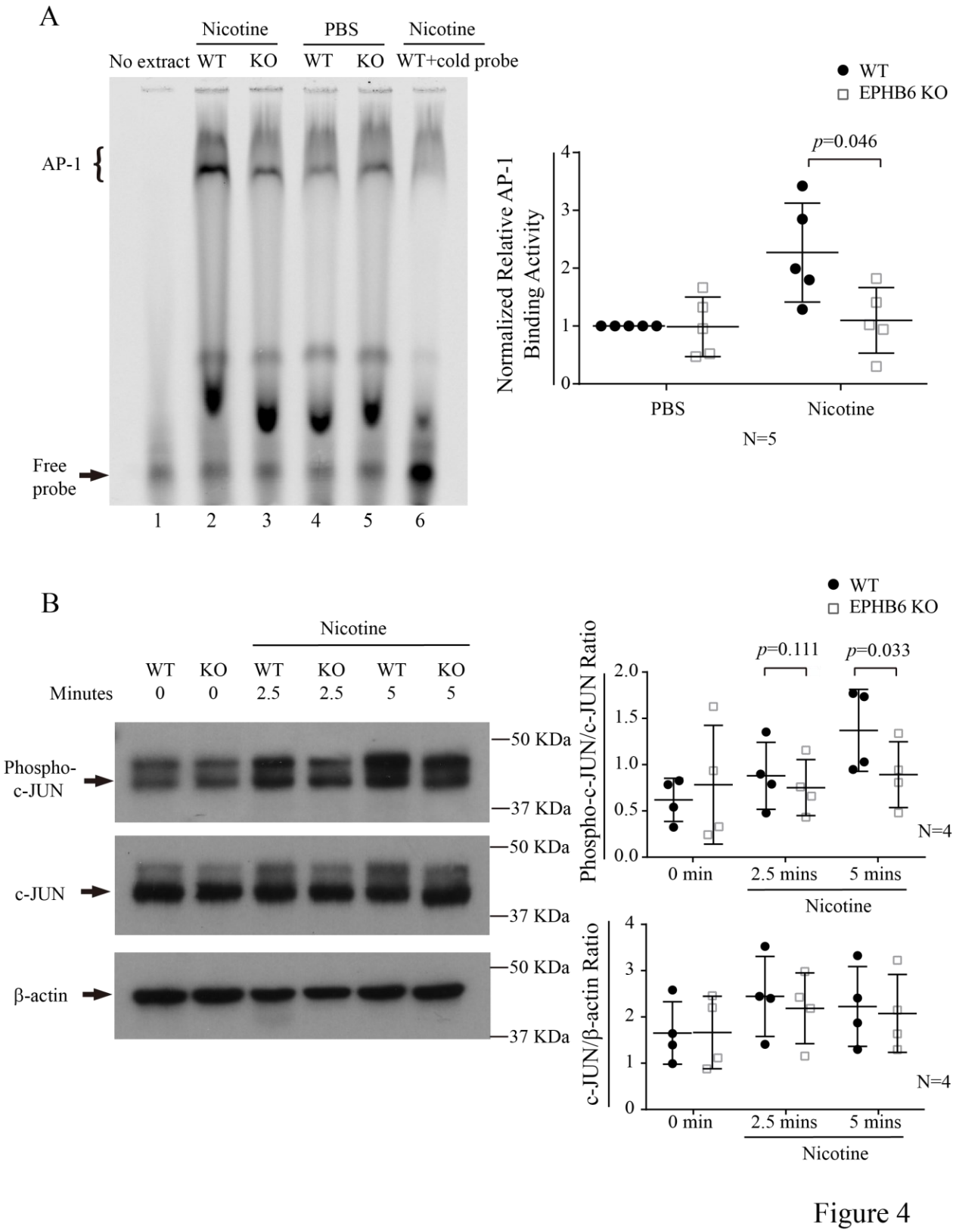

Figure 4. AP-1 level and c-JUN activation in KO and WT adrenal gland medullae

A. Decreased AP-1 association with its binding site in the Egr1 gene in AGCCs of male Ephb6 KO mice

The binding of AP-1 of AGCCs with the AP-1-binding site in the *Egr-1* gene enhancer was analyzed by EMSA. A representative image is shown at left. The shifted AP-1 bands in the assay are indicated by the bracket. Lane 1: no nuclear protein was added. All other lanes: 10-μg nuclear protein from WT or KO adrenal gland medullae was added to the reaction. Last lane: 200-fold molar excess of unlabeled probe as competitor was added to the reaction to determine the background of the AP-1 binding.

The signals of the shifted AP-1 bands were quantified by densitometry. Specific AP-1 binding signal of each sample was determined by the intensity of the shifted AP-1 band minus the background signal of that region in lane 6. The results were normalized to determine normalized relative AP-1 binding activity (specific AP-1 binding signal of a test sample / specific AP-1 binding signal of WT AGCCs stimulated with PBS). Results of five independent experiments using different mice were pooled, and the normalized relative AP-1 binding signals (means ± SD with data points) are presented in a graph at right. The significant *p*-value is shown (2-way paired Student's *t* test).

B. Decreased c-JUN phosphorylation in adrenal medullae from male EPHB6 KO mice

Adrenal medullae from male KO and WT mice were isolated and cultured for 2 hours. They were then lysed at 0, 2.5 and 5 minutes after nicotine (20 μM) stimulation. Nuclear proteins from the medullae were extracted. Total and phosphorylated c-JUN levels in the nuclear proteins were determined by immunoblotting. Four independent experiments were conducted. Representative immunoblotting images are shown at left. The signals were quantified by densitometry. The signal ratios of phosphorylated versus total c-JUN, and total c-JUN versus β-actin of four independent experiments using different mice were pooled and are presented as graphs (means ± SD with data points) in the right panels. Significant *p*-values are indicated (2-way paired Student's t tests).

Compromised signaling pathways upstream of c-JUN in male EPHB6 KO AGCCs

We assessed the activation status of signaling molecules upstream of c-JUN. Results indicated reduced JNK phosphorylation at T173/Y185 (Fig. 5A) and also MKK7 phosphorylation at S227/T275 (Fig. 5B) in male KO AGCCs stimulated by nicotine. In these cells, G-LISA assay revealed reduced activation of the further upstream signaling molecule, RAC1 (Fig. 5C).

Using inhibitors for JNK, MKK7 and RAC1, and employing *Egr1* mRNA expression as a readout, we revealed that the suppression of these signaling molecules could indeed repress *Egr1* expression in AGCCs from WT male mice (Fig. 5D-F, left panels), demonstrating the relevance of the reduced activity of these molecules in male KO AGCCs to decreased *Egr1* expression. On the other hand, these inhibitors had no effect on mRNA expression of an unrelated molecule *Cbl* (Fig. 5D-F, right panels), indicating that the effect of these inhibitors on *Egr1* expression was not due general toxicity.

On the other hand, the activation of ELK1, ERK1/2 and p38MAPK, which could theoretically promote *Egr1* expression, was not changed in male KO AGCCs, compared to their WT counterparts (Fig. 6A-C).

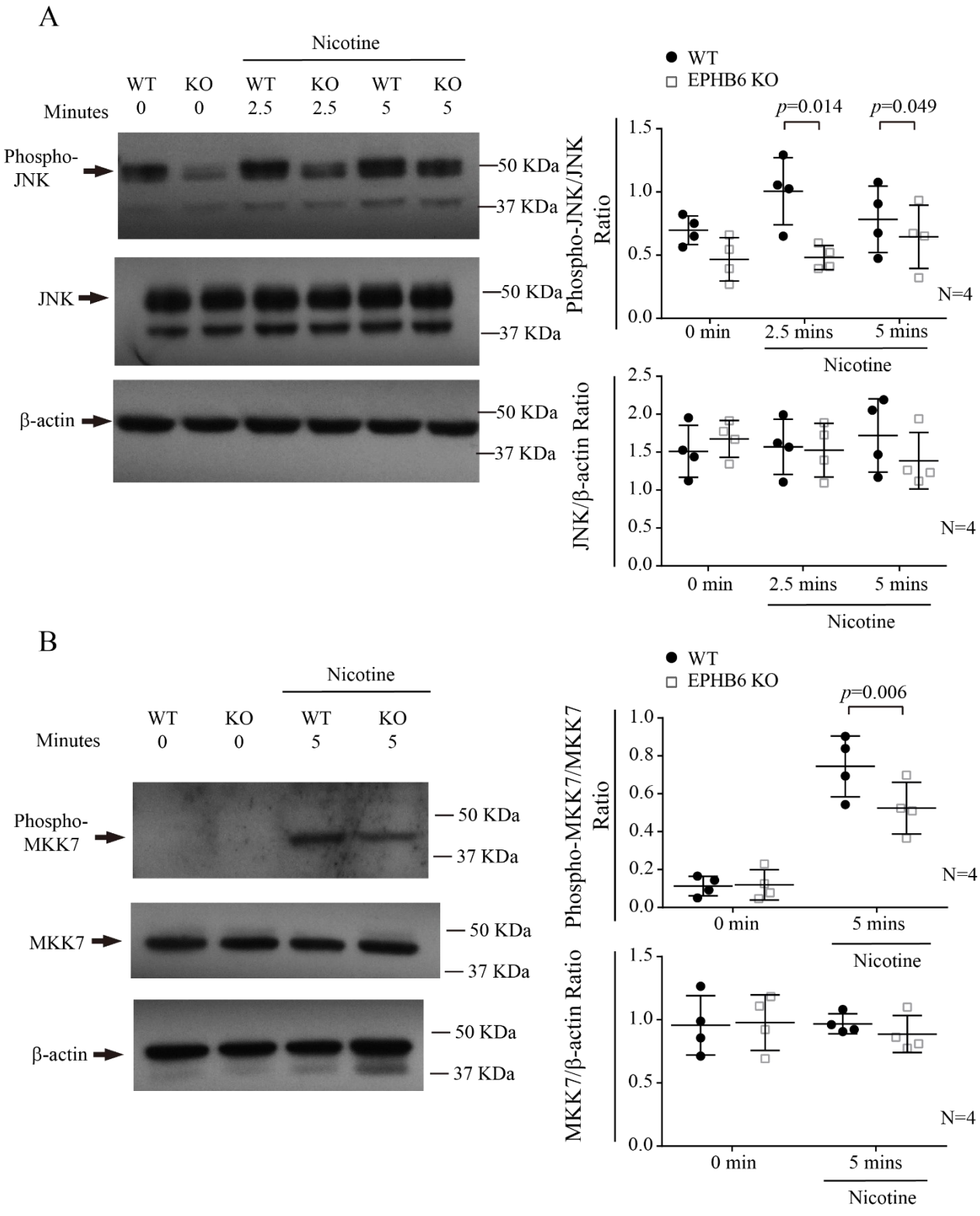
A
Nicotine
WT KO WT KO WT KO
Minutes 0 0 2.5 2.5 5 5
Phospho-JNK
JNK
β-actin
50 KDa
37 KDa
WT
EPHB6 KO
p=0.014
p=0.049
Phospho-JNK/JNK Ratio
JNK/β-actin Ratio
N=4
0 min
2.5 mins
5 mins
Nicotine
B
Nicotine
WT KO WT KO
Minutes 0 0 5 5
Phospho-MKK7
MKK7
β-actin
50 KDa
37 KDa
WT
EPHB6 KO
p=0.006
Phospho-MKK7/MKK7 Ratio
MKK7/β-actin Ratio
N=4
0 min
5 mins
Nicotine

Figure 5

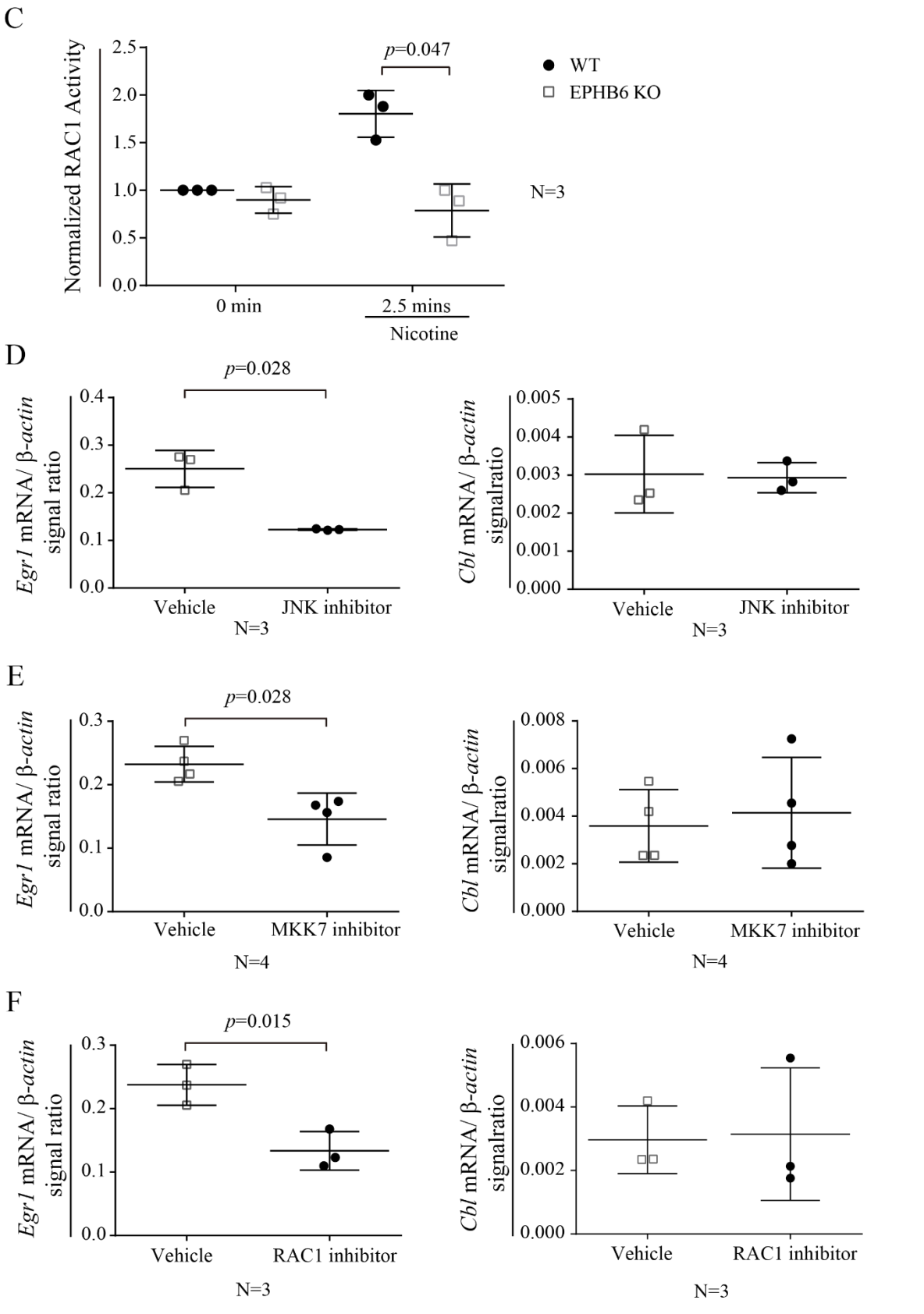

Figure 5 Continued

Figure 5. EPHB6 signaling pathway upstream of c-JUN

A. Decreased MKK7 phosphorylation in adrenal medullae from male EPHB6 KO mice after nicotine stimulation

B. Decreased JNK phosphorylation in adrenal medullae from male EPHB6 KO mice after nicotine stimulation

For A and B, adrenal medullae from male KO and WT mice were prepared as described in Figure 4B. They were then lysed at 0, 2.5 and 5 minutes after nicotine (20 μM) stimulation. Total and phosphorylated MKK7 and JNK in the lysates were analyzed by immunoblotting. Representative immunoblotting images are shown at left. The signals were quantified by densitometry and the signal ratios of phospho-MKK7 versus total MKK7, total MKK7 versus β-actin, phospho-JNK versus total JNK, and total JNK versus β-actin from four independent experiments using difference mice were pooled and are presented as graphs (means ± SD with data points) in the right panels. Significant *p*-values are indicated (2-way paired Student's *t* tests).

C. Male KO adrenal gland medullae presented reduced RAC1 activity

The adrenal gland medullae were stimulated by nicotine (20 μM) at 37°C for 0 and 2.5 minutes. Activated RAC1 in the tissue was extracted and quantified by a RAC1 G-LISA kit. Samples were assayed in duplicate. Three independent experiments using different mice were performed and the results were normalized according to the formula below.

Normalized RAC1 activity = RAC1 activity of a sample / RAC1 activity of WT medulla at 0 minute

Means ± SD with data points of the normalized RAC1 activity of the three independent experiments are shown. The significant *p*-value is indicated (2-way paired Student's *t* test).

D-F. JNK, MKK7 and RAC1 inhibitors repressed Egr1 mRNA expression in WT adrenal gland medullae

The adrenal gland medullae were isolated from WT male mice. They were cultured in the presence of JNK inhibitor (25 μM), MKK7 inhibitor (50 μM), or RAC1 inhibitor (50 μM) for 4 hours at 37°C. Total RNA from the adrenal gland medullae were isolated and *Egr1*, *β-actin*, and *Cbl*

mRNA transcripts were amplified by RT-PCR. Three or more (as indicated) independent experiments using different mice were conducted. The pooled data from these experiments were expressed as means ± SD with data points of signal ratios of target RNA/ *β-actin* mRNA. The significant *p*-values are indicated (2-way paired Student's *t* test).

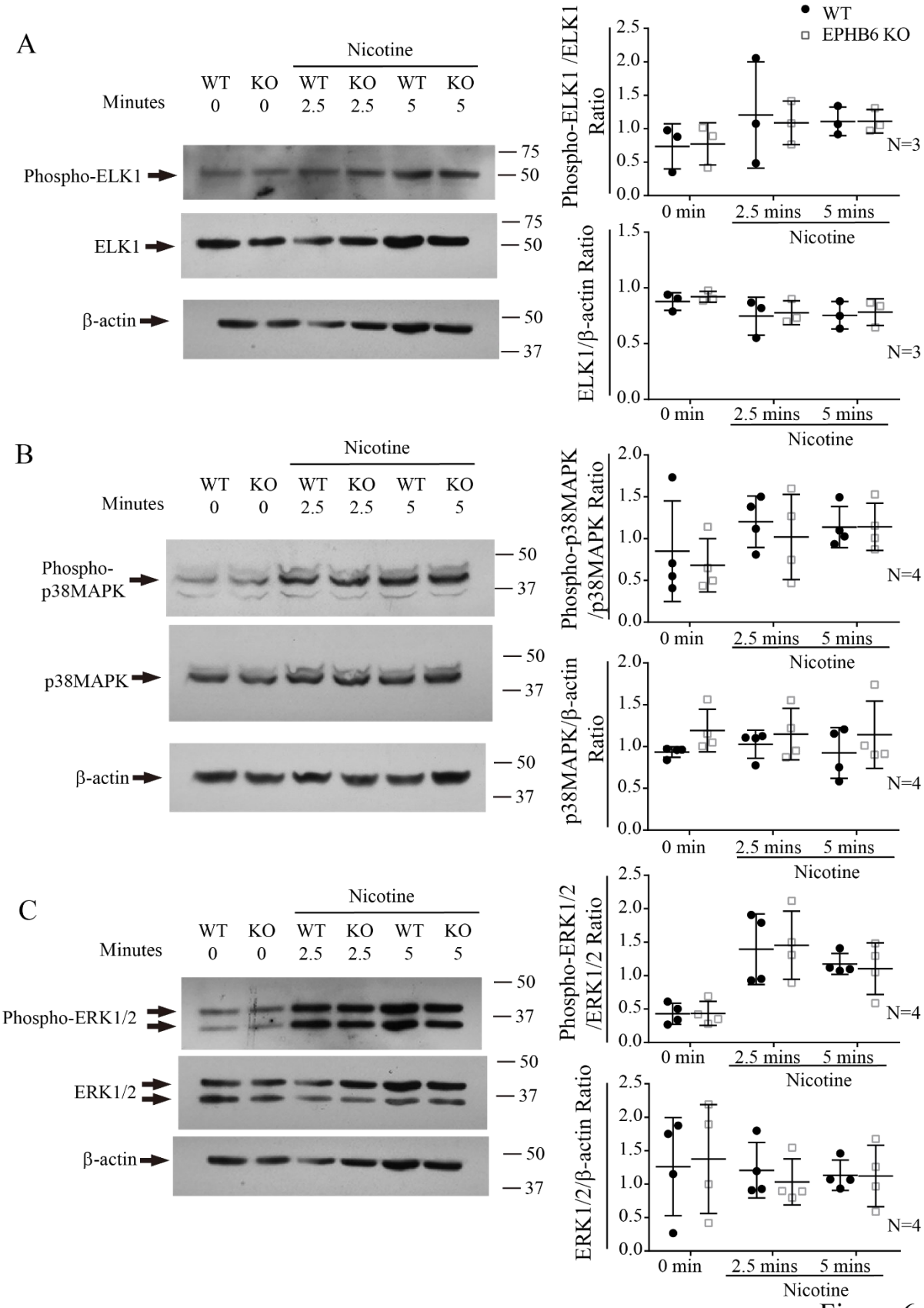
A
Nicotine
Minutes
WT KO WT KO WT KO
0 0 2.5 2.5 5 5
Phospho-ELK1
ELK1
β-actin
75
50
37
WT
EPHB6 KO
Phospho-ELK1 /ELK1 Ratio
N=3
0 min
2.5 mins
5 mins
Nicotine
ELK1/β-actin Ratio
B
Phospho-p38MAPK
p38MAPK
Phospho-p38MAPK /p38MAPK Ratio
N=4
p38MAPK/β-actin Ratio
C
Phospho-ERK1/2
ERK1/2
Phospho-ERK1/2 /ERK1/2 Ratio
ERK1/2/β-actin Ratio

Figure 6

Figure 6. ERK1/2, p38MAPK and ELK1 were not in the EPHB6 signaling pathway leading to CAT synthesis

Nicotine-stimulated ERK1/2 (**A**), p38MAPK (**B**) and ELK1 (**C**) phosphorylation in adrenal medullae from male KO and WT mice were determined as described in Figure 4B. Representative immunoblotting images are shown at left of each panel. The intensity of the bands was measured by densitometry. The results of three or more (as indicated) independent experiments using different mice were pooled and the signal ratios of phospho-ERK1/2 versus total ERK1/2, total ERK1/2 versus β-actin, phospho-p38MAPK versus total p38MAPK, total p38MAPK versus β-actin, phospho-ELK1 versus total ELK1, and total ELK1 versus β-actin of the KO and WT medullae are presented as graphs (means ± SD with data points). No significant differences between the KO and WT medullae were found (2-way paired Student's *t* tests).

EPH/EFN signaling direction and the role of testosterone

We assessed the signaling direction between EPHB6 and EFNBs, by using solid phase anti-EPHB6-Ab (for forward signaling) and EPHB6-Fc (for reverse signaling). As shown in Fig. 7A, when tsAM5NE chromaffin cells were cultured on EPHB6-Fc- but not anti-EPHB6 Ab-coated wells, their nicotine-stimulated TH level was augmented, suggesting that reverse signaling from EPHB6 to EFNBs enhances TH synthesis.

EPHB6 can interact with EFNB1, EFNB2 and EFNB3. We investigated which one(s) was essential for the reverse signaling. Since EFNB3 KO in mice manifested no CAT secretion phenotype (Wang et al., 2016c), we focused on EFNB1 and EFNB2. As shown in Fig. 7B, solid phase anti-EFNB1 Ab but not anti-EFNB2 Ab augmented nicotine-stimulated TH expression in tsAM5NE chromaffin cells (Fig. 7B), suggesting EPHB6's effect on CAT synthesis is mainly via EFNB1 reverse signaling.

To clarify the role of testosterone in reducing CAT synthesis in AGCCs from male KO mice, we cultured AGCCs from female KO mice in the presence or absence of testosterone. As shown in Fig. 7C, cell membrane impenetrable BSA-conjugated testosterone caused lower CAT content in AGCCs from KO but not WT female mice. This indicates that the non-genomic effect of

testosterone, but not the simple presence of testicles in the adult life or during fetal development is responsible for the observed diminished AGCC CAT biosynthesis in male KO mice.

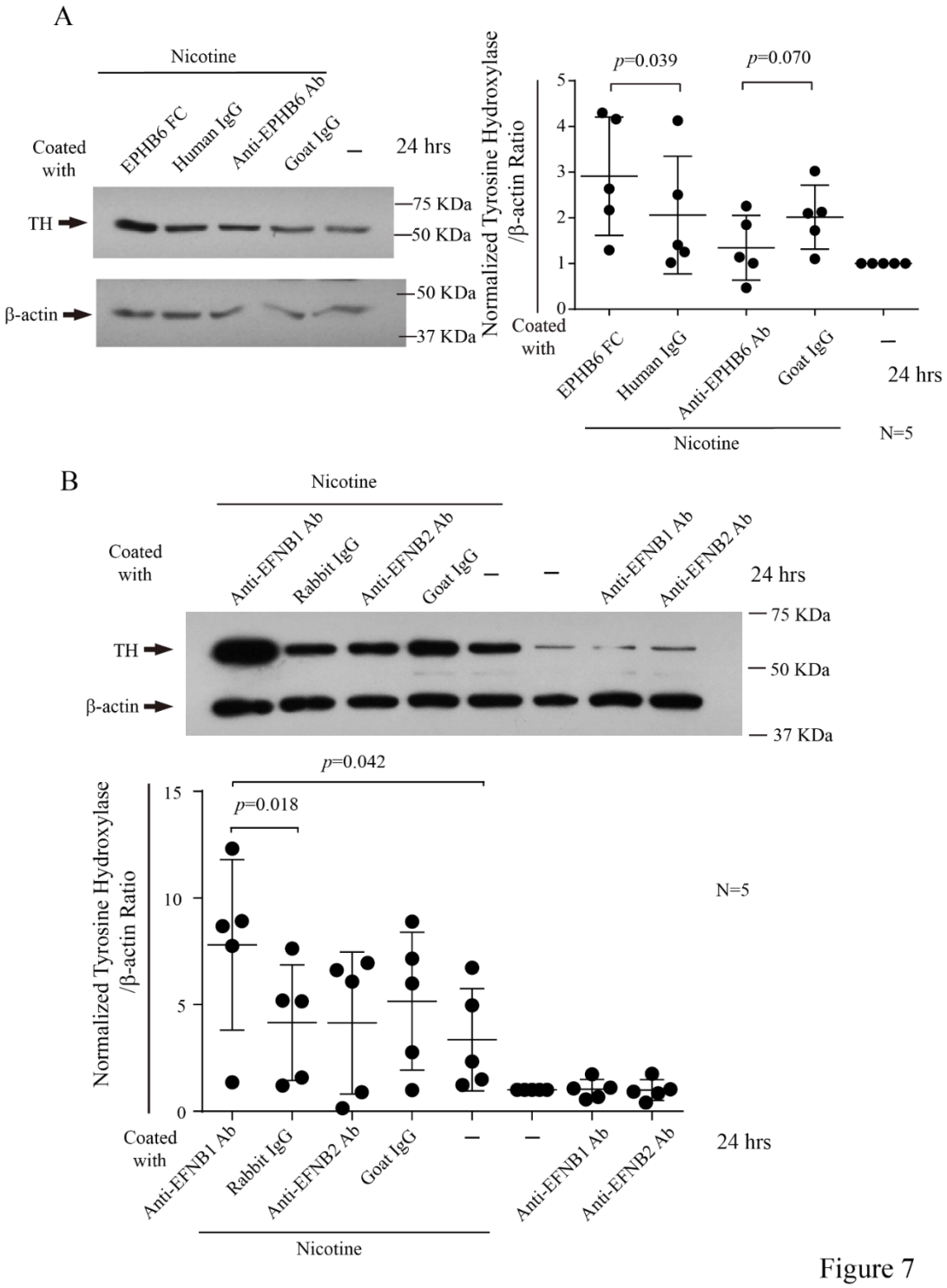

Figure 7

C

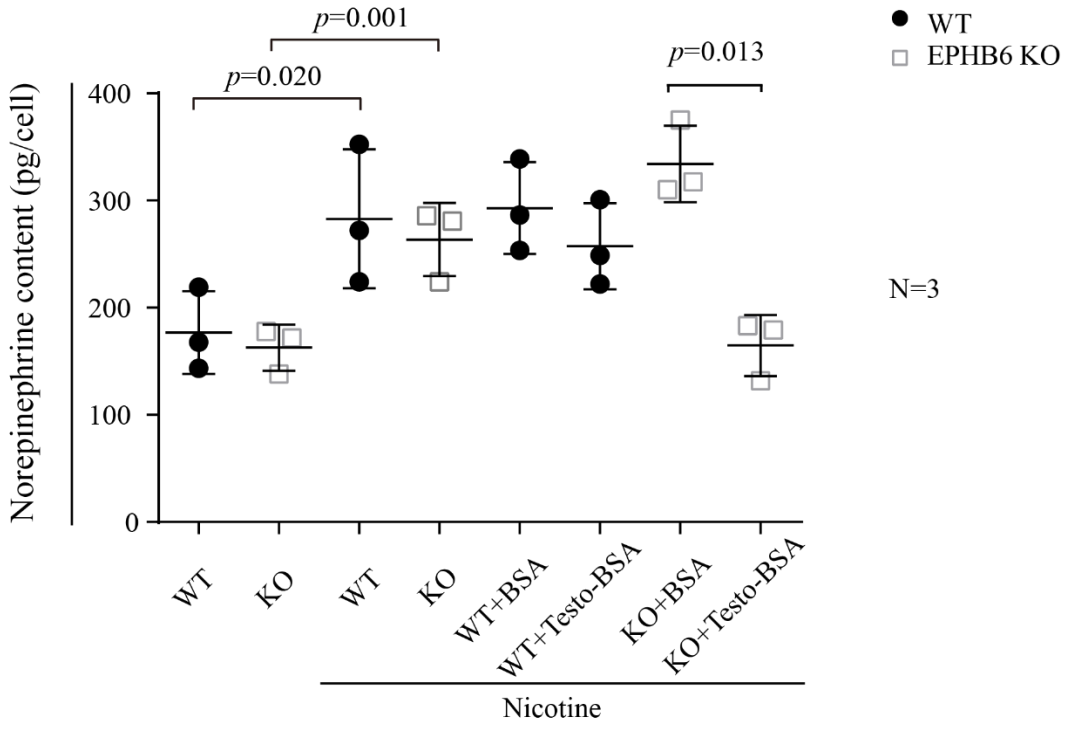

Figure 7 Continued

Figure 7 EPH/EFN signaling direction and the role of testosterone

A. *Reverse but not forward signaling between EPHB6 and EFNBs promotes TH protein expression upon nicotine stimulation*

tsAM5NE chromaffin cells were cultured in the 24-well plates coated with anti-EPHB6 Ab, normal goat IgG, recombinant EPHB6-Fc or normal human IgG (2 μg/ml for coating) for 24 hours. They were lysed 4 hours after nicotine (40 μM) stimulation at 33°C. TH protein levels of the cells were determined by immunoblotting. β-actin was used as loading control. Five independent experiments were performed and a representative immunoblot is shown in the upper panel. The signals of the immunoblots were determined by densitometry. The results were normalized by the formula below.

Normalized TH protein expression = ratio of TH/ β-actin of cells cultured in different coated wells / ratio of TH/ β-actin of cells cultured in wells without any coating

Normalized TH protein expression levels of the five experiments were pooled and their means ± SD with data points are presented as a graph in the lower panel. Significant *p*-values are indicated (2-way paired Student's *t* tests),

B. EFNB1 but not EFNB2 promotes TH protein expression in tsAM5NE chromaffin cells upon nicotine stimulation.

The experiments were carried out and the results are presented as described in (A), except that the wells were coated with anti-EFNB1 Ab, normal rabbit IgG, goat anti-EFNB2 Ab or normal goat IgG (2 μg/ml for coating) for 24 hours. Normalized TH protein expression levels of five experiments were pooled and their means ± SD with data points are presented as a graph in the lower panel. Significant *p*-values are indicated (1-way paired Student's *t* tests).

C. Non-genomic effect of testosterone on norepinephrine synthesis in AGCCs from female EPHB6 KO and WT mice

Mouse AGCCs were isolated from female EPHB6 KO and WT mice and were cultured in DMEM containing 15 % (v/v) FCS (10,000 cells per well). The cells were pretreated with a cell membrane-impermeable BSA-conjugated testosterone (1.1 μg/ml; Testo-BSA) or BSA for 15 min. Nicotine (20 μM) was then added to the culture. The cells were cultured for 16 h at 37°C, and harvested. They were lysed and norepinephrine levels in the cleared lysates were measured by ELISA. Samples were assayed in duplicate. Norepinephrine content per cell were calculated based on the cell number per well and amount of norepinephrine detected in the lysate of all the cells in a well. The means ± SD with data points of norepinephrine levels per cells of three independent experiments are pooled and are presented. Significant *p*-values are indicated (2-way Student's *t* test).

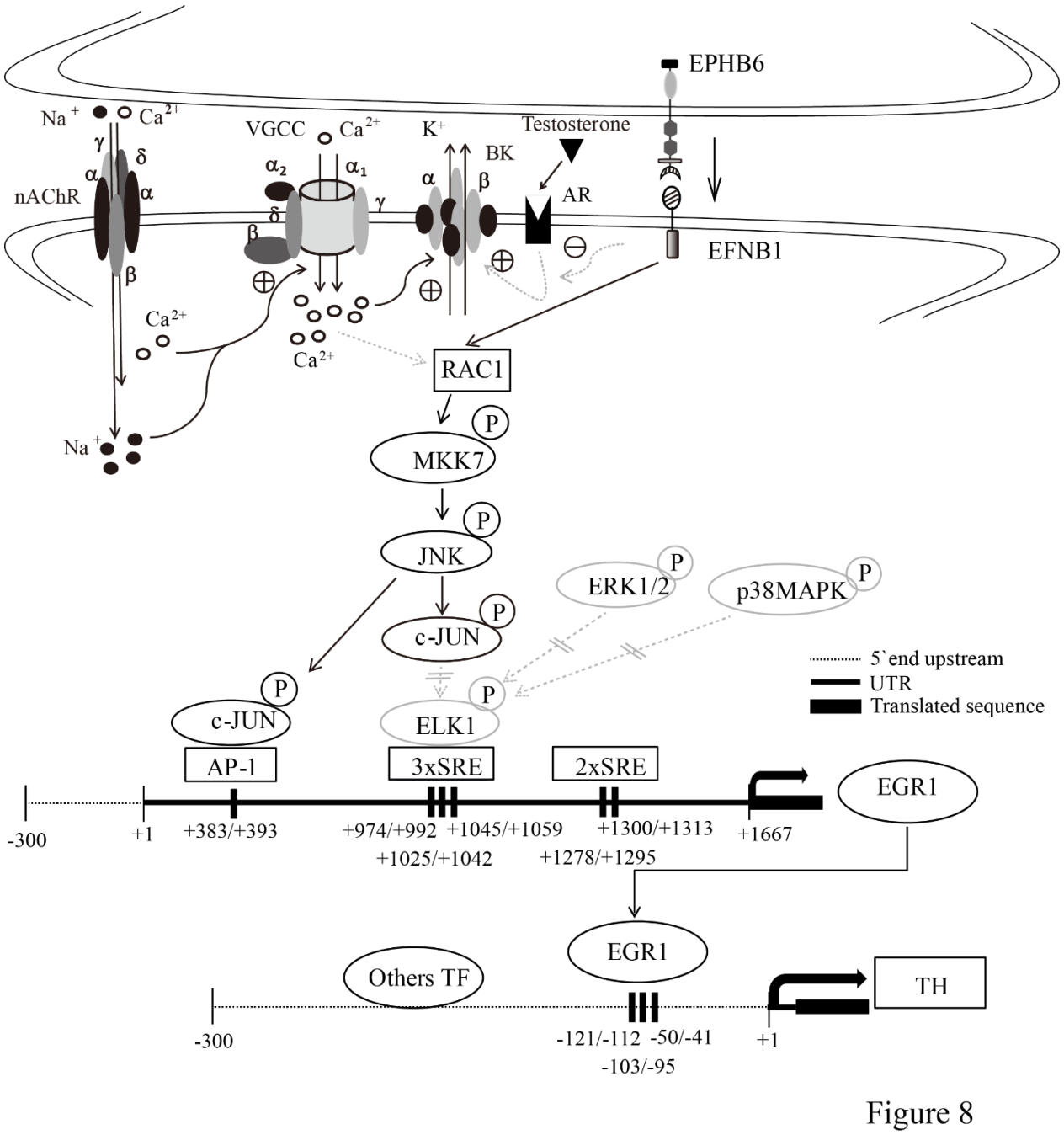

Figure 8

Figure 8. A model of the signaling pathway from EPHB6 to catecholamine biosynthesis in AGCC

This diagram illustrates a hypothetic pathway from cell surface EPHB6 to CAT biosynthesis in AGCCs. EPHB6 exerts reverse signaling through EFNB1, which transduces signals into AGCCs and activates RAC1. RAC1 in turn activates MKK7. MKK7 phosphorylates and activates JNK, which further phosphorylates c-JUN. c-JUN phosphorylation leads to increased nuclear AP-1 association

with the AP-1 site in the 5' untranslated region (+ 383/+393) of the *Egr1* gene. This augments *Egr1* expression at both the mRNA and protein levels. EGR1 binds to 3 EGR1-binding sites in the 5' upstream sequence of the *TH* gene at -121/-112, -103/-96 and -50/-41, and augments transcription and translation of TH, the rate-limiting enzyme in CAT biosynthesis. This pathway merges with the signaling pathway of AChR > Ca^{2+} > RAC1 > MKK7 > JNK > JUN/AP1 > EGR1 > TH > CAT starting from RAC1, and is necessary for the optimal function of the latter. Deletion of EPHB6 (hence diminished reverse signaling via EFNB1) compromises this signaling pathway, resulting decreased CAT biosynthesis. The default non-genomic effect of testosterone is to augment K^+ outflow via the BK channel, leading to a faster closure of VGCC, hence lower total Ca^{2+} influx triggered by ACh. EFNB1 reverse signaling negatively regulates such testosterone effect. In the absence of EPHB6 (hence reduced EFNB1 reverse signaling), the suppressive effect of testosterone on K^+ efflux is abolished, leading to faster VGCC closure and resulting a negative impact on the Ca^{2+} > RAC1 > MKK7 > JNK > JUN/AP1 > EGR1 > TH > CAT pathway.

On the other hand, although in the 5' untranslated region of *Egr1* gene, there are 5 SREs, they are not involved in the EPHB6 signaling pathway to TH biosynthesis, because the activation of *ELK1*, which forms a complex with SRF to become a transcription factor binding to SRE, and the activation of *ELK1* upstream kinases *ERK2* and *p38MAPK*, are not affected by EPHB6 deletion. Dark lines with arrows: signaling proven in this study. Blocked grey lines with arrows: theoretically possible signaling based on other studies, but not functional in AGCCs according to our study. TF: transcription factor

Solid dark lines with arrows: signaling proven in this study. Dashed grey lines with arrows: theoretically possible signaling based on other studies or hypothetical signaling pathways suggested by this study. Dashed grey lines with blockage signs: theoretically possible signaling based on other studies, but not functional according to our study. TF: transcription factor; nAChR: nicotinic acetylcholine receptor; VGCC: voltage-gated calcium channel; AR: androgen receptor; small solid circle: Na^+; small solid circle: Ca^{2+}; large empty triangle: testosterone.

Discussion

Our previous study shows that EPHB6 is highly expressed in the medullae of adrenal gland, and EPHB6 KO leads to reduced 24-urine CAT levels (Luo et al., 2012). We further demonstrated that EPHB6 is critical in regulating AGCC ion channel opening and consequently in controlling acute CAT secretion (Ledoux et al., 2003). The acute secretion of CAT from AGCCs is from stored immediately-releasable pool of CAT-containing vesicles docked near the cell membrane (Gasman et al., 2003). Long-term secretion of CAT, caused by repeated stimulation of AGCCs acetylcholine, involves recruitment of vesicles from the reserve pool (Wong and Tank, 2007). The 24-h urine CAT levels reflect the sum of both acute and long-term CAT secretion. CAT biosynthesis might affect both of these processes by controlling their respective pool sizes. In order to assess this, we examined the CAT content of adrenal glands from the KO mice. Even though the size of the glands and their medullae from male and female KO mice was similar to their WT and the castrated male KO counterparts, the epinephrine content of the adrenal gland medullae from male KO mice was significantly lower compared to the WT counterparts. This suggests that CAT biosynthesis and/or degradation in the male KO adrenal gland is abnormal.

TH is the rate-limiting enzyme in CAT biosynthesis (Dunkley et al., 2004). The reduced TH levels in KO AGCCs likely led to the lowered CAT biosynthesis in these KO cells. TH activity in AGCCs is regulated by phosphorylation of its serine residues and by its protein level. Its S31 phosphorylation augments its activity, while S40 and S19 phosphorylation alleviates feedback inhibition (Daubner et al., 2011). Examination of TH phosphorylation at S31, S40 and S19 in the adrenal glands from male KO mice without or with nicotine stimulation, revealed no consistent differences from the WT counterparts (data not elaborated). However, the TH protein and mRNA levels were reduced in the male KO adrenal glands, indicating reduced transcription from TH gene.

To elucidate the mechanisms by which EPHB6 regulates TH gene transcription, we profiled transcriptome of adrenal glands from male, female and castrated KO and WT mice. We have confirmed by RT-qPCR and immunoblotting that the expression of the top hit *Egr1*/EGR1 was decreased in the adrenal gland medullae of male KO mice and such a change disappeared after

castration, agreeing well with the phenotype of TH expression and CAT content of the KO adrenal glands. EGR1 is a zinc-finger protein belonging to the EGR family transcription factors (Shimizu et al., 1992). It activates the genes containing EGR1-binding sites. We searched a 300-bp 5' upstream sequence of the mouse (C57BL/6) TH gene with a transcription factor-finding program AliBaba2.1, and found 2 EGR1-binding sites at -41/-50, -112/-121 (the first nucleotide before the TH gene is designated as position -1) (Fig. 8). siRNA knockdown of EGR1 in AGCCs led to reduced TH expression at both mRNA and protein levels, with concurrent reduction of norepinephrine content in the AGCCs, proving that EGR1 indeed positively regulates TH expression. In support of our conclusion, Papanikolaou et al. reported that in the 5' upstream sequence of rat TH gene from positions -122 to -114, there is an EGR1-binding site CACCCCCGC, which is proven to positively regulate TH transcription in a reporter assay (Papanikolaou and Sabban, 2000). This rat EGR1-binding sequence is identical to another EGR1-binding site in the mouse TH gene between positions -103 and -95 (CACCCCCGC). Our current *Egr1* expression and knockdown results established the correlation between *Egr1* expression levels and CAT biosynthesis.

The reduced *Egr1* mRNA levels in KO AGCCs suggested that EPHB6 deletion decreased *Egr1* transcription. In the 5' untranslated region of the first exon of mouse *Egr1* gene, there is an AP-1 binding site (ACTGACCTAGA) between positions +383 and +393 (the first nucleotide in exon 1 is designated as position +1; the start codon is at position +1667) (Fig. 8). This site has been proven to be functional in enhancing *Egr1* transcription in a reporter gene assay in human HEK293 cells (Hoffmann et al., 2008). Using EMSA, we found that in the EPHB6 KO AGCCs, AP-1-binding site in the *Egr1* gene had less association with AP-1 transcription factor, compared to WT AGCCs. Our data established the correlation between active AP-1 binding and *Egr1* expression. Earlier literature showed that the reduced association of nuclear AP-1 with its binding of its target genes is correlated to the level of its target gene transcription (Weiss et al., 2003;Nateri et al., 2004). There are other AP-1 binding sites in the mouse *Egr1* gene 5' sequence (positions -153 to -144) and TH gene 5' sequence (positions -285 to -276). Conceivably, enhancer activity of all these AP-1-binding sites might be similarly affected by the reduced AP-1 association in the KO AGCCs, leading to diminished expression of *Egr1* and *TH* transcription sequentially or simultaneously.

AP-1 is a dimeric transcription factor composed of JUN and FOS family members. JUN proteins can form homodimers or form heterodimers with FOS proteins, both of which can associate with AP-1-binding sites, but FOS proteins can only bind to the AP-1 site via JUN proteins (Kouzarides and Ziff, 1988;Nakabeppu et al., 1988). Heterodimeric c-JUN and c-FOS have high affinity to the AP-1-binding sites in many genes (Kouzarides and Ziff, 1988). c-JUN S63 and S73 phosphorylation increases transcription of AP-1 target genes (Nateri et al., 2005), although is not necessary for AP-1 nuclear import (Schreck et al., 2011). We have shown that c-JUN S63 phosphorylation was reduced in male KO AGCCs.

JUN N-terminal kinase (JNK) is responsible for c-JUN S63 and S73 phosphorylation (Ip and Davis, 1998). JNK is activated by dual phosphorylation at its T183/Y185 in the kinase domain (Ip and Davis, 1998). MKK7 is the specific upstream kinase for such phosphorylation (Foltz et al., 1998;Wang et al., 2007) (Fig. 7). MKK7 itself is activated by phosphorylation at S271, T275 and S277 (Holtmann et al., 1999). Further upstream, GTPase RAC1 controls MKK7 activation (Holland et al., 1997), although molecular details of how RAC1 affects MKK7 phosphorylation remain to be elucidated. We have demonstrated, as illustrated in Figure 5A-C, that activation of all the key molecules in this signaling pathway, *i.e*., JNK, MKK7 and RAC1, was compromised in the male KO AGCCs. Further, inhibitors of these signaling molecules repressed *Egr1* expression (Figure 5D-F), as expected, demonstrating the relevance of these molecules to *Egr1* expression. As *Egr1* knockdown led to decreased TH expression, the relevance of these molecules to the final CAT synthesis is also suggested.

We investigated the signaling events further upstream, where EPHB6 on the surface interacts with its cell surface ligands EFNs. As reviewed in the introduction, multiple EFN ligands can bind an EPH, and trigger forward signaling. In the case of EPHB6, it has three potential ligands: EFNB1, EFNB2 and EFNB3. These ligands can also function as receptors, receive stimulation from EPHB6 and conduct reverse signaling into the cells. To mimic forward signaling from cell surface EFNBs to cell surface EPHB6, we coated anti-EPHB6 Ab on the wells. The use of the anti-EPHB6 Ab provides specific stimulation to EPHB6 but not to other EPHs, which EFNBs could also interact with. Such treatment did not augment nicotine-stimulated TH expression (Fig. 7A), suggesting that the forward signaling is not relevant. To mimic the reverse signaling from cell surface EPHB6

to cell surface EFNBs, we coated recombinant human IgG Fc-conjugated EPHB6 (EPHB-Fc) on the wells, and such solid phase EPHB6 could enhance the elevated TH expression stimulated by nicotine. This indicates that the reverse signaling from EPHB6 to EFNBs is responsible for the observed AGCC phenotype. To further dissect the reverse signaling pathway, we coated anti-EFNB1 and anti-EFNB2 Abs on the wells to initiate specific reverse signaling through these molecules, and identified EFNB1 as the essential one (Fig. 7B). As our early study has already determined that EFNB3 KO does not cause any AGCC phenotype, we concluded that the EPHB6 to EFNB reverse signaling in AGCCs is via EFNB1. It is well known that EFNBs co-localize with and activate RHO family GTPases, including RAC1 in many different types of cells (Nakada et al., 2006;Nakayama et al., 2013;O'Neill et al., 2016). Thus, a putative signaling pathway starting from EPHB6 to EFNB1/RAC1/MKK7/JNK/JUN/AP-1/EGR1/TH/CAT is suggested.

The above postulated pathway was active when the AGCCs were stimulated with AChR agonist nicotine, which binds to nAChR and mAChR, similar to acetylcholine. The major consequence of nAChR and mAChR activation by nicotine or ACh is the change of cytosolic cation concentration. This leads to larger Ca^{2+} influx through voltage-gated calcium channels (VGCCs). The increased Ca^{2+} concentration induces a cascade of downstream signaling events. These events include the activation RAC1/MKK7/JNK/JUN-AP1, as demonstrated in our experiments using WT AGCCs (Figs. 4 and 5). The details of the signaling between Ca^{2+} and RAC1 remain to be further elucidated. Obviously, the EFNB1 reverse signaling pathway overlaps with the AChR signaling pathway starting from RAC1 in the RAC1/MKK7/JNK/JUN-AP1 cascade (Fig 8), and is needed for the optimal function or the latter as the deletion of EPHB6 (the stimulator of EFNB1) caused compromised strength of this RAC1/MKK7/JNK/JUN-AP1 pathway, leading to decreased CAT synthesis.

We conducted an additional experiment to show that the non-genomic effect of testosterone was responsible for the suppressed CAT synthesis in KO AGCCs. In this experiment, AGCCs from female KO mice were treated with testosterone. The use of female mice guaranteed a lack of exposure of AGCCs to high levels of testosterone *in vivo*. While AGCCs from female KO mice in the absence of exogenous testosterone had no phenotype with regard to *Egr1* expression, the testosterone treatment rendered them a phenotype similar to that seen in male KO AGCCs. This suggests that the presence of testosterone in the adult life but not during fetal development is responsible for

its action in concert with EPHB6 in leading to the *Egr1* phenotype, and consequently the CAT phenotype.

Our previous publication (Wang et al., 2018) suggests that such the non-genomic effect of testosterone is responsible for promoting outward K^+ efflux, hence earlier closure of VGCCs. We hypothesize that under a normal circumstance, EFNB1 has a suppressive impact on testosterone's K^+ efflux-promoting effect, as illustrated in Figure 8. In the absence of EFNB1, such suppressive effect is released. This results in a larger K^+ efflux, and earlier termination of the Ca^{2+} surge, leading to a lower strength of the RAC1/MKK7/JNK/JUN/AP-1 signaling pathway. In such a way, EFNB1, nAChR, and cell surface testosterone receptor signaling pathways interact among themselves. The sum of their effect determines the outcome of CAT synthesis (Fig. 8).

In the 5' upstream region of *Egr1* gene, there are two groups of serum responsive elements (SRE). The proximal group has 2 SREs at positions +1278/+1295 and +1300/+1313, and the distal group has 3 SREs at positions +974/+992, +1025/+1042, and +1045/+1059 . Depending on the cell type, either of the SRE groups has been shown to enhance *Egr1* transcription (Hoffmann et al., 2008;Gregg and Fraizer, 2011). ELK1 associates with serum responsive factors (SRF) and the complex binds to SREs of target genes to enhance their transcription (Dalton and Treisman, 1992). ELK1 phosphorylation at S383 and S389 leads to its de-SUMOylation and allows its nuclear translocation and activation (Rao et al., 1989;Yang et al., 2003). ERK2 and p38MAPK are the upstream kinases responsible for such phosphorylation (Cruzalegui et al., 1999). We found no difference in the activation of ELK1, ERK2 and p38MAPK, based on their phosphorylation, suggesting that the pathway ERK2 > p38MAPK > ELK1 > SRE in *Egr1* transcriptional regulation is not involved in EPHB6-mediated phenotype in AGCCs with regard to catecholamine biosynthesis (Fig. 8).

In summary, with the results of this study, we could construct a hypothetic pathway of EPHB6 > EFNB1 > RAC1 > MKK7 > JNK > JUN/AP1 > EGR1 > TH > CAT, delineating the regulation CAT biosynthesis by EPHB6, as shown in Figure 8. This pathway merges with the signaling pathway of AChR > Ca^{2+} > RAC1 > MKK7 > JNK > JUN/AP1 > EGR1 > TH > CAT starting from RAC1, and is necessary for the optimal function of the latter. Deletion of EPHB6 (hence diminished reverse

signaling via EFNB1) compromises this signaling pathway, resulting decreased CAT biosynthesis. The default non-genomic effect of testosterone is to augment K^+ outflow via the BK channel, leading to a faster closure of VGCC, hence lower total Ca^{2+} influx triggered by ACh. EFNB1 reverse signaling negatively regulates such testosterone effect. In the absence of EPHB6 (hence reduced EFNB1 reverse signaling), the suppressive effect of testosterone on K^+ efflux is abolished, leading to faster VGCC closure and resulting a negative impact on the Ca^{2+} > RAC1 > MKK7 > JNK > JUN/AP1 > EGR1 > TH > CAT pathway.

In addition to enhancing our knowledge in the area of chromaffin cell biology, the elucidation of this signaling pathway from EPHB6 to CAT and the interactions among EPHB6, AChR and testosterone in the present study could provide us with potential drug targets in regulating catecholamine biosynthesis, which is implicated in normal and pathological conditions such as blood pressure regulation and Parkinson's disease. In future studies, gaps in the signaling pathways between EFNB1 and RAC1, between RAC1 and MKK7, and between EFNB1 and cell surface androgen receptors need to be further investigated.

Acknowledgements

This work was supported by the Fonds de recherche du Québec – Santé to J.W. and H.L. and the J.-Louis Lévesque Foundation to J.W. It was also funded in part by grants from the Canadian Institutes of Health Research to J.W. (MOP272014), the Natural Sciences and Engineering Research Council of Canada (RGPIN-2017-04790) and the Juvenile Diabetes Research Foundation (17-2013-440) to J.W.

References

Cruzalegui, F.H., Cano, E., and Treisman, R. (1999). ERK activation induces phosphorylation of Elk-1 at multiple S/T-P motifs to high stoichiometry. Oncogene 18, 7948-7957.

Dalton, S., and Treisman, R. (1992). Characterization of SAP-1, a protein recruited by serum response factor to the c-fos serum response element. Cell 68, 597-612.

Daubner, S.C., Le, T., and Wang, S. (2011). Tyrosine hydroxylase and regulation of dopamine synthesis. Arch Biochem Biophys 508, 1-12.

Dunkley, P.R., Bobrovskaya, L., Graham, M.E., Von Nagy-Felsobuki, E.I., and Dickson, P.W. (2004). Tyrosine hydroxylase phosphorylation: regulation and consequences. J Neurochem 91, 1025-1043.

Eph Nomenclature Committee, E.N. (1997). Unified nomenclature for Eph family receptors and their ligands, the ephrins. Cell 90, 403-404.

Foltz, I.N., Gerl, R.E., Wieler, J.S., Luckach, M., Salmon, R.A., and Schrader, J.W. (1998). Human mitogen-activated protein kinase kinase 7 (MKK7) is a highly conserved c-Jun N-terminal kinase/stress-activated protein kinase (JNK/SAPK) activated by environmental stresses and physiological stimuli. J Biol Chem 273, 9344-9351.

Gale, N.W., Baluk, P., Pan, L., Kwan, M., Holash, J., Dechiara, T.M., Mcdonald, D.M., and Yancopoulos, G.D. (2001). Ephrin-B2 selectively marks arterial vessels and neovascularization sites in the adult, with expression in both endothelial and smooth-muscle cells. Developmental biology 230, 151-160.

Gasman, S., Chasserot-Golaz, S., Bader, M.F., and Vitale, N. (2003). Regulation of exocytosis in adrenal chromaffin cells: focus on ARF and Rho GTPases. Cell Signal 15, 893-899.

Gregg, J., and Fraizer, G. (2011). Transcriptional Regulation of EGR1 by EGF and the ERK Signaling Pathway in Prostate Cancer Cells. Genes Cancer 2, 900-909.

Hess, J., Angel, P., and Schorpp-Kistner, M. (2004). AP-1 subunits: quarrel and harmony among siblings. J Cell Sci 117, 5965-5973.

Hoffmann, E., Ashouri, J., Wolter, S., Doerrie, A., Dittrich-Breiholz, O., Schneider, H., Wagner, E.F., Troppmair, J., Mackman, N., and Kracht, M. (2008). Transcriptional regulation of EGR-1 by the interleukin-1-JNK-MKK7-c-Jun pathway. J Biol Chem 283, 12120-12128.

Holland, P.M., Suzanne, M., Campbell, J.S., Noselli, S., and Cooper, J.A. (1997). MKK7 is a stress-activated mitogen-activated protein kinase kinase functionally related to hemipterous. J Biol Chem 272, 24994-24998.

Holtmann, H., Winzen, R., Holland, P., Eickemeier, S., Hoffmann, E., Wallach, D., Malinin, N.L., Cooper, J.A., Resch, K., and Kracht, M. (1999). Induction of interleukin-8 synthesis integrates effects on transcription and mRNA degradation from at least three different cytokine- or stress-activated signal transduction pathways. Mol Cell Biol 19, 6742-6753.

Hu, Y., Wang, X., Wu, Y., Jin, W., Cheng, B., Fang, X., Martel‐Pelletier, J., Kapoor, M., Peng, J., and Qi, S. (2015). Role of EFNB1 and EFNB2 in Mouse Collagen‐Induced Arthritis and Human Rheumatoid Arthritis. Arthritis & Rheumatology 67, 1778-1788.

Ip, Y.T., and Davis, R.J. (1998). Signal transduction by the c-Jun N-terminal kinase (JNK)--from inflammation to development. Curr Opin Cell Biol 10, 205-219.

Jin, W., Luo, H., and Wu, J. (2014). Effect of reduced EPHB4 expression in thymic epithelial cells on thymocyte development and peripheral T cell function. Molecular immunology 58, 1-9.

Kohno, S., Murata, T., Koide, N., Hikita, K., and Kaneda, N. (2011). Establishment and characterization of a noradrenergic adrenal chromaffin cell line, tsAM5NE, immortalized with the temperature-sensitive SV40 T-antigen. Cell Biol Int 35, 325-334.

Kolski-Andreaco, A., Cai, H., Currle, D.S., Chandy, K.G., and Chow, R.H. (2007). Mouse adrenal chromaffin cell isolation. J Vis Exp, 129.

Kouzarides, T., and Ziff, E. (1988). The role of the leucine zipper in the fos-jun interaction. Nature 336, 646-651.

Ledoux, J., Bonev, A.D., and Nelson, M.T. (2008). Ca2+-activated K+ channels in murine endothelial cells: block by intracellular calcium and magnesium. The Journal of general physiology 131, 125-135.

Ledoux, J., Greenwood, I., Villeneuve, L.R., and Leblanc, N. (2003). Modulation of Ca2+‐dependent Cl− channels by calcineurin in rabbit coronary arterial myocytes. The Journal of physiology 552, 701-714.

Luo, H., Broux, B., Wang, X., Hu, Y., Ghannam, S., Jin, W., Larochelle, C., Prat, A., and Wu, J. (2016). EphrinB1 and EphrinB2 regulate T cell chemotaxis and migration in experimental autoimmune encephalomyelitis and multiple sclerosis. Neurobiology of disease 91, 292-306.

Luo, H., Charpentier, T., Wang, X., Qi, S., Han, B., Wu, T., Terra, R., Lamarre, A., and Wu, J. (2011a). Efnb1 and Efnb2 proteins regulate thymocyte development, peripheral T cell differentiation, and antiviral immune responses and are essential for interleukin-6 (IL-6) signaling. Journal of Biological Chemistry 286, 41135-41152.

Luo, H., Qi, S., Wu, Z., Han, B., Wang, X., and Wu, J. (2011b). EFNB1 and EFNB2 physically bind to IL-7R-alpha and retard its internalization from the cell surface (57.2). The Journal of Immunology 186, 57.52-57.52.

Luo, H., Wan, X., Wu, Y., and Wu, J. (2001). Cross-linking of EphB6 resulting in signal transduction and apoptosis in Jurkat cells. The Journal of Immunology 167, 1362-1370.

Luo, H., Wu, Z., Tremblay, J., Thorin, E., Peng, J., Lavoie, J.L., Hu, B., Stoyanova, E., Cloutier, G., and Qi, S. (2012). Receptor tyrosine kinase Ephb6 regulates vascular smooth muscle contractility and modulates blood pressure in concert with sex hormones. Journal of Biological Chemistry 287, 6819-6829.

Luo, H., Yu, G., Tremblay, J., and Wu, J. (2004). EphB6-null mutation results in compromised T cell function. The Journal of clinical investigation 114, 1762-1773.

Luo, H., Yu, G., Wu, Y., and Wu, J. (2002). EphB6 crosslinking results in costimulation of T cells. The Journal of clinical investigation 110, 1141-1150.

Nakabeppu, Y., Ryder, K., and Nathans, D. (1988). DNA binding activities of three murine Jun proteins: stimulation by Fos. Cell 55, 907-915.

Nakada, M., Drake, K.L., Nakada, S., Niska, J.A., and Berens, M.E. (2006). Ephrin-B3 ligand promotes glioma invasion through activation of Rac1. Cancer Res 66, 8492-8500.

Nakayama, A., Nakayama, M., Turner, C.J., Hoing, S., Lepore, J.J., and Adams, R.H. (2013). Ephrin-B2 controls PDGFRbeta internalization and signaling. Genes Dev 27, 2576-2589.

Nateri, A.S., Riera-Sans, L., Da Costa, C., and Behrens, A. (2004). The ubiquitin ligase SCFFbw7 antagonizes apoptotic JNK signaling. Science 303, 1374-1378.

Nateri, A.S., Spencer-Dene, B., and Behrens, A. (2005). Interaction of phosphorylated c-Jun with TCF4 regulates intestinal cancer development. Nature 437, 281-285.

Niels Grabe [Online]. Available: http://gene-regulation.com/pub/programs/alibaba2/index.html [Accessed].

O'neill, A.K., Kindberg, A.A., Niethamer, T.K., Larson, A.R., Ho, H.H., Greenberg, M.E., and Bush, J.O. (2016). Unidirectional Eph/ephrin signaling creates a cortical actomyosin differential to drive cell segregation. J Cell Biol 215, 217-229.

Papanikolaou, N.A., and Sabban, E.L. (2000). Ability of Egr1 to activate tyrosine hydroxylase transcription in PC12 cells. Cross-talk with AP-1 factors. J Biol Chem 275, 26683-26689.

Pasquale, E.B. (2008). Eph-ephrin bidirectional signaling in physiology and disease. Cell 133, 38-52.

Rao, V.N., Huebner, K., Isobe, M., Ar-Rushdi, A., Croce, C.M., and Reddy, E.S. (1989). elk, tissue-specific ets-related genes on chromosomes X and 14 near translocation breakpoints. Science 244, 66-70.

Schreck, I., Al-Rawi, M., Mingot, J.M., Scholl, C., Diefenbacher, M.E., O'donnell, P., Bohmann, D., and Weiss, C. (2011). c-Jun localizes to the nucleus independent of its phosphorylation by and interaction with JNK and vice versa promotes nuclear accumulation of JNK. Biochem Biophys Res Commun 407, 735-740.

Shimizu, N., Ohta, M., Fujiwara, C., Sagara, J., Mochizuki, N., Oda, T., and Utiyama, H. (1992). A gene coding for a zinc finger protein is induced during 12-O-tetradecanoylphorbol-13-acetate-stimulated HL-60 cell differentiation. J Biochem 111, 272-277.

Wang, X., Destrument, A., and Tournier, C. (2007). Physiological roles of MKK4 and MKK7: insights from animal models. Biochim Biophys Acta 1773, 1349-1357.

Wang, Y., Hamet, P., Thorin, E., Tremblay, J., Raelson, J., Wu, Z., Luo, H., Jin, W., Lavoie, J.L., and Peng, J. (2016a). Reduced blood pressure after smooth muscle EFNB2 deletion and the potential association of EFNB2 mutation with human hypertension risk. European Journal of Human Genetics 24**,** 1817-1825.

Wang, Y., Shi, W., Blanchette, A., Peng, J., Qi, S., Luo, H., Ledoux, J., and Wu, J. (2018). EPHB6 and testosterone in concert regulate epinephrine release by adrenal gland chromaffin cells. Sci Rep 8, 842.

Wang, Y., Thorin, E., Luo, H., Tremblay, J., Lavoie, J.L., Wu, Z., Peng, J., Qi, S., and Wu, J. (2015). EPHB4 protein expression in vascular smooth muscle cells regulates their contractility,

and EPHB4 deletion leads to hypotension in mice. Journal of Biological Chemistry 290, 14235-14244.

Wang, Y., Wu, Z., Luo, H., Peng, J., Raelson, J., Ehret, G.B., Munroe, P.B., Stoyanova, E., Qin, Z., Cloutier, G., Bradley, W.E., Wu, T., Shen, J.Z., Hu, S., and Wu, J. (2016b). The role of GRIP1 and ephrin B3 in blood pressure control and vascular smooth muscle cell contractility. Sci Rep 6, 38976.

Wang, Y., Wu, Z., Thorin, E., Tremblay, J., Lavoie, J.L., Luo, H., Peng, J., Qi, S., Wu, T., and Chen, F. (2016c). Estrogen and testosterone in concert with EFNB3 regulate vascular smooth muscle cell contractility and blood pressure. American Journal of Physiology-Heart and Circulatory Physiology 310, H861-H872.

Weiss, C., Schneider, S., Wagner, E.F., Zhang, X., Seto, E., and Bohmann, D. (2003). JNK phosphorylation relieves HDAC3-dependent suppression of the transcriptional activity of c-Jun. EMBO J 22, 3686-3695.

Wong, D.L., and Tank, A.W. (2007). Stress-induced catecholaminergic function: transcriptional and post-transcriptional control. Stress 10, 121-130.

Wu, J., and Luo, H. (2005). Recent advances on T-cell regulation by receptor tyrosine kinases. Current opinion in hematology 12, 292-297.

Wu, Z., Luo, H., Thorin, E., Tremblay, J., Peng, J., Lavoie, J.L., Wang, Y., Qi, S., Wu, T., and Wu, J. (2012). Possible role of Efnb1 protein, a ligand of Eph receptor tyrosine kinases, in modulating blood pressure. Journal of Biological Chemistry 287, 15557-15569.

Yang, S.H., Jaffray, E., Hay, R.T., and Sharrocks, A.D. (2003). Dynamic interplay of the SUMO and ERK pathways in regulating Elk-1 transcriptional activity. Mol Cell 12, 63-74.

Yu, G., Luo, H., Wu, Y., and Wu, J. (2003a). Ephrin B2 induces T cell costimulation. The Journal of Immunology 171, 106-114.

Yu, G., Luo, H., Wu, Y., and Wu, J. (2003b). Mouse ephrinB3 augments T-cell signaling and responses to T-cell receptor ligation. Journal of Biological Chemistry 278, 47209-47216.

Yu, G., Luo, H., Wu, Y., and Wu, J. (2004). EphrinB1 is essential in T-cell-T-cell co-operation during T-cell activation. Journal of Biological Chemistry 279, 55531-55539.

Yu, G., Mao, J., Wu, Y., Luo, H., and Wu, J. (2006). Ephrin-B1 is critical in T-cell development. Journal of Biological Chemistry 281, 10222-10229.

Supporting Information

RT-qPCR primer sequences		
Gene	sense sequences	antisense sequences
β-actin	5’-TCGTACCACAGGCATTGTGATGGA-3’	5’-TGATGTCACGCACGATTTCCCTCT-3’
EPHB6	5’-CTTTGCCTTTGTTCACCGAGCACT-3’	5’-AGCAAGGAACTTGAACCCTGAGGA-3’
TH	5’-AAGATCAAACCTACCAGCCG-3’	5’-TACGGGTCAAACTTCACAGAG -3’
Egr1	5’-AGCGCCTTCAATCCTCAAG-3’	5’-CCACCATCGCCTTCTCATTAT-3’
Cbl	5’-CTGCACGGTGGACAAGAAGA -3’	5’-GTCTCCTTGGAAGAGTCCGC -3’
JunB	5’-TTAAAGAGGAACCGCAGACC -3’	5’-CTCCTGGTCTTCCATGTTGAT-3’
c-Fos	5’-ATTGTCGAGGTGGTCTGAATG -3’	5’-TCGAAAGACCTCAGGGTAGAA -3’
Dusp-1	5’-CATGGGAGCTGGTCCTTATTT-3’	5’-CTTGCGGTCAAGTCATTGTTG -3’

Supporting Information Table 1. RT-qPCR primer sequences

Gene	Target sequences	Antisense sequences
SMART pool *Egr1* siRNA	5’-UGACAUCGCUCUGAAUAAU-3’	5’-AUUAUUCAGAGCGAUGUCA -3’
	5’-ACUCCACUAUCCACUAUUA-3’	5’-UAAUAGUGGAUAGUGGAGU -3’
	5’-AUGCGUAACUUCAGUCGUA-3’	5’-UACGACUGAAGUUACGCAU -3’
	5’-CGACAGCAGUCCCAUCUAC-3’	5’-GUAGAUGGGACUGCUGUCG -3’
Non-Targeting siRNA pool	5’-UAGCGACUAAACACAUCAA-3’	5’-UUGAUGUGUUUAGUCGCUA -3’
	5’-UAAGGCUAUGAAGAGAUAC -3’	5’-GUAUCUCUUCAUAGCCUUA -3’
	5’-AUGUAUUGGCCUGUAUUAG -3’	5’-CUAAUACAGGCCAAUACAU -3’
	5’-AUGAACGUGAAUUGCUCAA -3’	5’-UUGAGCAAUUCACGUUCAU -3’

Supporting Information Table 2. siRNA sequences

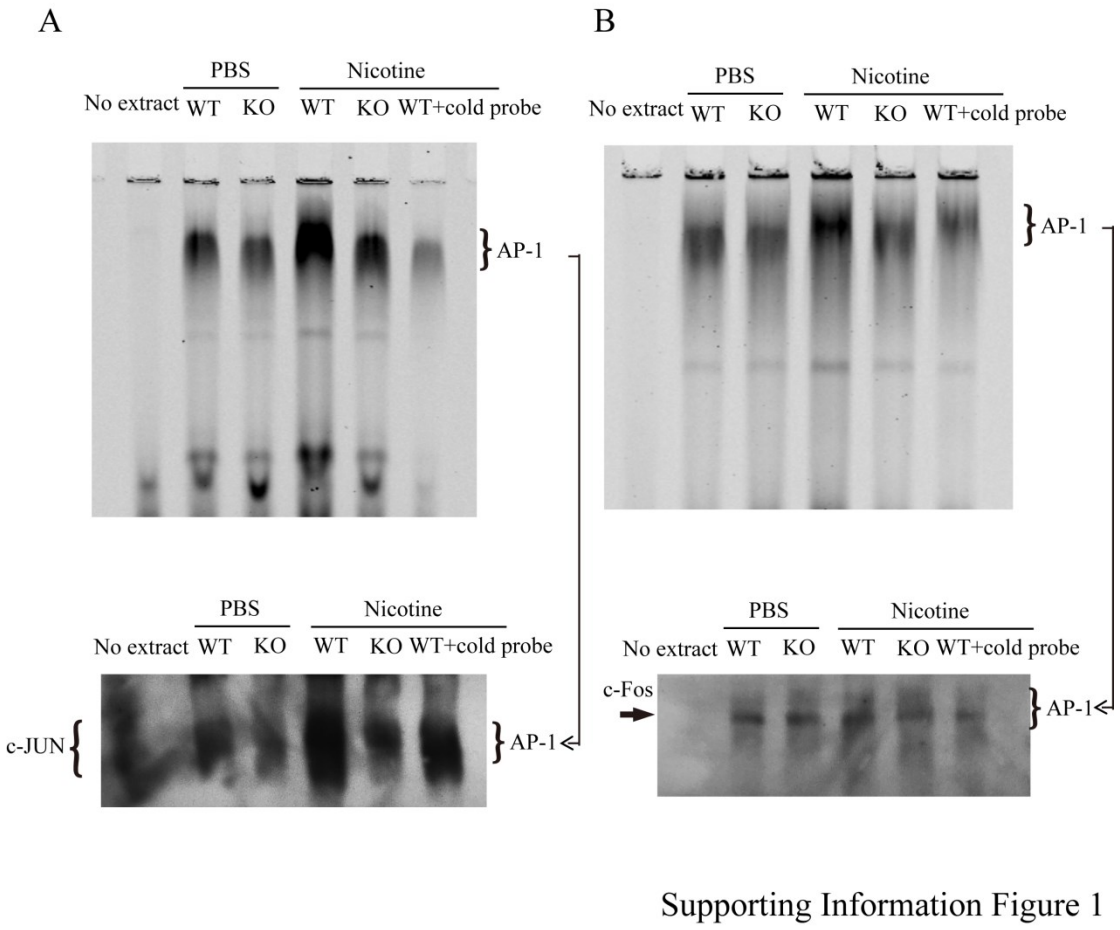

Supporting Information Figure 1

Supporting Information Figure 1. Presence of c-JUN and c-FOS in the shifted bands of EMSA

EMSA was conducted as described in Figure 4. The proteins in the 5% non-denaturing EMSA gel were transferred to PVDF membrane. The presence of c-JUN and c-FOS proteins in the shifted bands were detected by immunoblotting. The upper panels of A and B are EMSA before immunoblotting. The lower panels are immunoblotting for c-JUN (A) and c-FOS (B). The positions of the shifted AP-1 bands in EMSA and the positions of c-JUN and c-FOS are indicated.

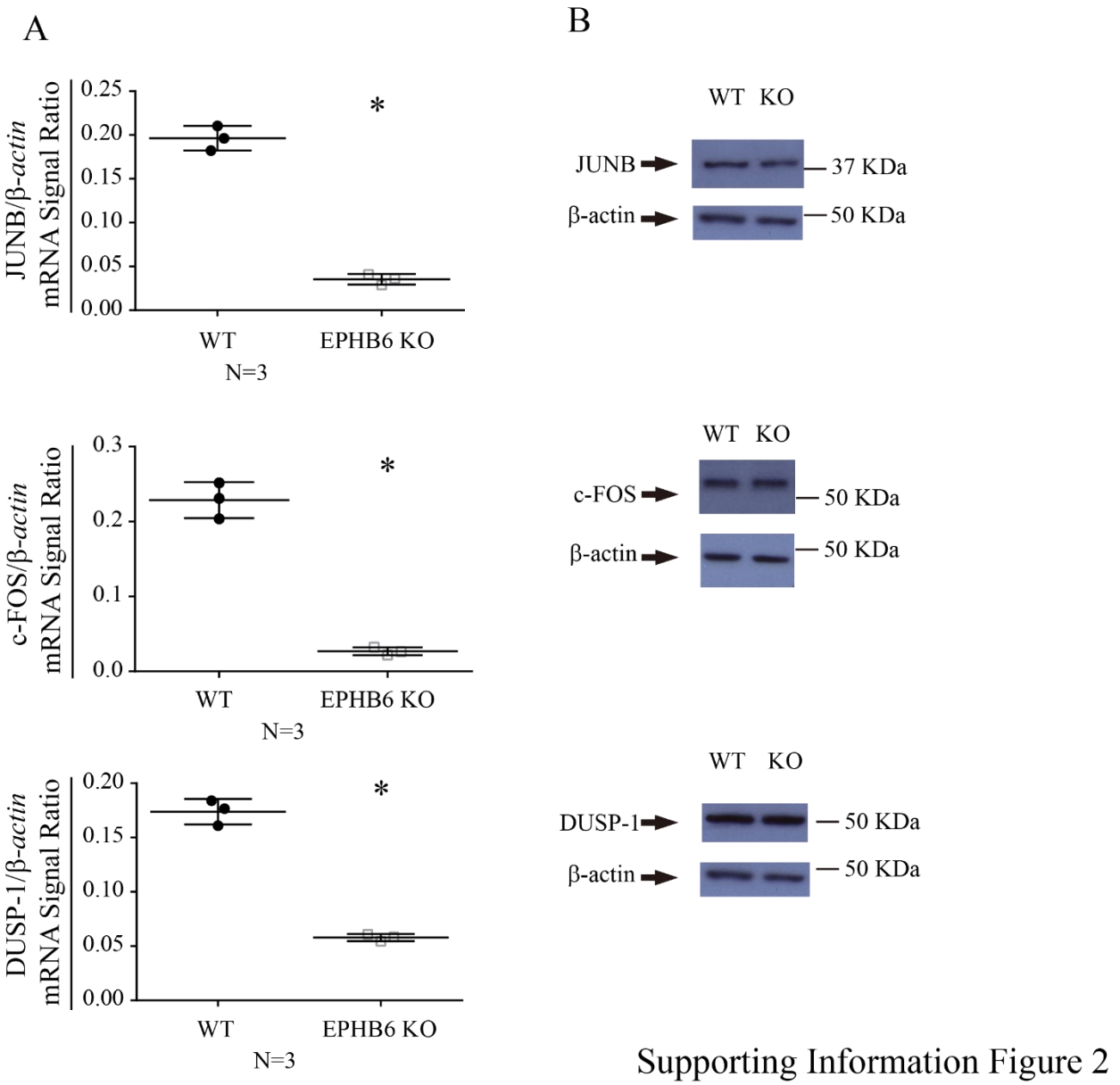

Supporting Information Figure 2

Supporting Information Figure 2. JUNB, c-FOS, DUSP-1 levels in KO and WT adrenal gland medullae

A. Reduced expression of JUNB, c-FOS, DUSP-1 mRNA in adrenal medullae from male KO mice

JUNB, c-FOS, DUSP-1 mRNA levels in the adrenal gland medullae were analyzed by RT-qPCR. β-actin levels were used as internal controls. Samples in RT-qPCR were in triplicate, and *JUNB, c-FOS, DUSP-1* / β-actin signal ratios from three independent experiments using different mice were pooled and expressed as means ± SD with data points. *: $p < 0.05$ (2-tailed Student's *t* test).

B. Normal JUNB, c-FOS, DUSP-1 protein expression in the adrenal medullae of male EPHB6 KO mice

JUNB, c-FOS, DUSP-1 protein levels of adrenal gland medullae were analyzed by immunoblotting, and representative images are shown.

Chapitre 5 – ARTICLE-3

TITLE: The receptor tyrosine kinase EPHB6 regulates catecholamine exocytosis in adrenal gland chromaffin cells

Wei Shi[1#], Bei Ye[1,2#], Marion Rame[3], Yujia Wang[2], Dominique Cioca[4], Sophie Reibel[4], Junzheng Peng[1], Shijie Qi[1], Nicolas Vitale[3], Hongyu Luo[1*], and Jiangping Wu[1,5*]

Running title: *EPHB6 controls catecholamine exocytosis*

From [1]Research Centre, Centre hospitalier de l'Université de Montréal (CRCHUM), Montreal, Quebec, Canada H2X 0A9; [2]Children's Hospital, Zhejiang University School of Medicine, Hangzhou, Zhejiang, China 310003; [3]Institut des Neurosciences Cellulaires et Intégratives, UPR-3212 Centre National de la Recherche Scientifique and Université de Strasbourg, 8 Allée du Général Rouvillois, 67000 Strasbourg, France, [4] Chronobiotron UMS 3415, 8 Allée du Général Rouvillois, 67000 Strasbourg, France; [5]Nephrology Department, CHUM, Montreal, Quebec, Canada H2X 0A9

[*]To whom correspondence should be addressed: Dr. Jiangping Wu, CRCHUM, 900 rue St-Denis, R12-428, Montreal, Quebec, Canada H2X 0A9, telephone: (514) 890-8000 Extension 25164, e-mail: jianping.wu@umontreal.ca; or Dr. Hongyu Luo, CRCHUM, 900 rue St-Denis, R12-426, Montreal, Quebec, Canada H2X 0A9, telephone: (514) 890-8000 Extension 25319, e-mail: hongyu.luo@umontreal.ca; or Dr. Nicolas Vitale, CNRS UPR-3212, 8 allée du Général Rouvillois, 67000 Strasbourg, France, telephone: (33) 388-45-67-12, vitalen@inci-cnrs.unistra.fr

[#]W.S. and B.Y contributed equally to this work.

Key words: : EPH receptor B6 (EPHB6), catecholamine exocytosis, adrenal gland chromaffin cells, F-actin, receptor tyrosine kinase, blood pressure regulation, calcium signaling, ephrin, catecholamine

Published in Journal of Biological Chemistry 2020 May; 295(22):7653-7668.

Candidate's Contribution

W.S. was involved in generating the concept and initiating this project. W.S. conducted experiments in the cellular level and molecular level and generated the research outcomes in the Fig. 2, Fig. 3 (C,D,E,F), Fig. 3, Fig. 4, Fig. 5 (B,C), Fig. 6, Fig. 7, Fig. 8, and all supplementary data. W.S. was involved in drafted the manuscript. W.S. contribution to this publication was about 70%.

Abstract

The erythropoietin-producing human hepatocellular receptor EPH receptor B6 (EPHB6) is a receptor tyrosine kinase that has been shown previously to control catecholamine synthesis in the adrenal gland chromaffin cells (AGCCs) in a testosterone-dependent fashion. EPHB6 also has a role in regulating blood pressure, but several facets of this regulation remain unclear. Using amperometry recordings, we now found that catecholamine secretion by AGCCs is compromised in the absence of EPHB6. AGCCs from male KO mice displayed reduced cortical F-actin disassembly, accompanied by decreased catecholamine secretion through exocytosis. This phenotype was not observed in AGCCs from female KO mice, suggesting that testosterone, but not estrogen, contributes to this phenotype. Of note, reverse signaling from EPHB6 to ephrin B1 (EFNB1) and a seven-amino-acid–long segment in the EFNB1 intracellular tail were essential for the regulation of catecholamine secretion. Further downstream, the Ras homolog family member A (RHOA) and FYN proto-oncogene Src family tyrosine kinase (FYN)–proto-oncogene c-ABL–microtubule-associated monooxygenase calponin and LIM domain containing 1 (MICAL-1) pathways mediated the signaling from EFNB1 to the defective F-actin disassembly. We discuss the implications of EPHB6's effect on catecholamine exocytosis and secretion for blood pressure regulation.

Introduction

Erythropoietin-producing human hepatocellular receptors (EPH) are the largest family of receptor tyrosine kinases. Their ligands are ephrins (EFN), which are also cell membrane molecules (Committee, 1997). EPHs are classified into A and B subfamilies based on their sequence homology. EFNs are also categorized into A and B subfamilies, based on the way they anchor on the cell membrane. EFNAs attach to the cell membrane by a glycosylphosphatidylinositol linkage, and they are without intracellular tails. EFNBs are transmembrane molecules. EPH and EFN interact promiscuously, but generally speaking, EPHAs preferably interact with EFNAs, and EFNBs, with EFNBs (Pasquale, 2008). EPHB6 is an inactive receptor tyrosine kinase due to a mutation in its kinase domain. EPH kinases and EFNs have profound and diverse functions in physiology and

pathophysiology in almost all the systems in our bodies. Their functions were first reported in the nervous system (Flanagan and Vanderhaeghen, 1998;Pasquale, 2008). Subsequently, EPHs and EFNs were found to be essential in intestinal epithelial cell maturation (Holmberg et al., 2006), bone metabolism (Zhao et al., 2006), angiogenesis (Brantley-Sieders and Chen, 2004), immune responses (Wu and Luo, 2005), insulin secretion (Konstantinova et al., 2007), kidney glomerular filtration (Hashimoto et al., 2007), chemotaxis (Salvucci et al., 2006), homeostasis of vestibular endolymph fluid in the inner ear (Dravis et al., 2007), etc.

Our recent work revealed that EPHs/EFNs are critical in controlling blood pressure, according to mouse models and human genetic studies (Luo et al., 2012;Wu et al., 2012;Wang et al., 2015;Wang et al., 2016a;Wang et al., 2016b;Wang et al., 2016c;Tremblay et al., 2017;Wang et al., 2018;Wu et al., 2018;Zhang et al., 2019b). The target tissues of such EPHs/EFN functions are vascular smooth muscles and adrenal gland chromaffin cells (AGCCs). In male but not female EPHB6 gene knockout (KO) mice, their 24-hour urine catecholamine (CAT) levels are reduced, but castration reverts the levels to a normal range(Zhang et al., 2019b). Using isolated AGCCs, we have shown that in the absence of EPHB6, the acetylcholine (ACh)-triggered Ca^{2+} influx of the KO AGCCs is compromised. This is in part caused by an increase in big potassium channel (BK) current, causing premature closure of voltage-gated calcium channels, leading to decreased Ca^{2+} influx(Wang et al., 2018).

Ca^{2+} flux is a secondary messenger in excitable cells and influences multiple downstream events. In AGCCs, it controls long-term CAT synthesis as well as CAT exocytosis(Douglas and Rubin, 1961;Haycock et al., 1982). Accordingly, AGCCs from male EPHB6 KO mice have a lower CAT content, caused by a reduced level of tyrosine hydroxylase(Shi et al., 2019), the rate-limiting enzyme of CAT synthesis. In this study, we assessed whether EPHB6 KO affected CAT exocytosis and studied underlying mechanisms.

Materials and methods

EPHB6 gene KO mice

EPHB6 KO mice were generated in our laboratory, as described previously (Luo et al., 2004). They were backcrossed to the C57BL/6J genetic background for more than 15 generations. Age- and gender-matched WT littermates served as controls. Some male mice underwent castration, and they were used three weeks after the surgery.

Primary AGCC culture for amperometry recording

Mouse AGCCs were isolated, as described earlier (Ory et al., 2013), with modifications. Adrenal glands were obtained from 8- to 12-week old mice. Medullae were separated from fat and cortex in cold Locke's solution then digested with 5U of papain activated in DMEM containing 0.2 mg/ml L-cysteine, 1mM $CaCl_2$, 0.5 mM EDTA, 0.0067 µM beta-mercaptoethanol (200 µl for 2 medullae) at 37°C for 20 minutes. Papain digestion was stopped with 100 µl of an inactivating solution (DMEM, 10% deactivated FCS, 1.25 mg/ml albumin, 1.25 mg/ml trypsin-inhibitor) and incubated for 5 minutes at 37°C. The digested medullae were triturated by pipetting in 300 µl of complete culture medium (DMEM, 1/500 primocin, 1/100 ITSX). Cells were seeded in collagen-coated glass coverslips, then complete culture medium was added 1 hour later. Cells were maintained at 37°C, 5% CO_2 for 24-48h before amperometry recording.

Amperometry

Chromaffin cells from *Ephb6* WT and KO mice were washed with Locke's solution and processed for CAT release measurements by amperometry, which was conducted at room temperature. A carbon fiber electrode of 5-µm diameter (ALA Scientific, New York, USA) was held at a potential of 650 mV compared with the reference electrode (Ag/AgCl) and was approached closely to the cells. The secretion of CAT was induced by 10-s pressure ejection of 100 µM nicotine in Locke's solution from a micropipette positioned at 10 µm from the cell and recorded over 60 s. Amperometric recordings were performed with an AMU130 amplifier (Radiometer Analytical, Loveland, Colorado, USA), sampled at 5 kHz, and digitally low-pass filtered at 1 kHz. The analysis

of amperometric recordings was carried out as previously described (Poea-Guyon et al., 2013) with a Macro software (obtained from the laboratory of Dr. R. Borges; http://webpages.ull.es/users/rborges/) written for Igor Software (Wavemetrics, Portland, USA), allowing automatic spike detection and extraction of spike parameters. The number of amperometric spikes with an amplitude > 5 pA within 60 s after nicotine stimulation was registered. The spike parameter analysis was restricted to these spikes with amplitudes of >5 pA. The quantal size of individual spikes was measured by calculating the spike area above the baseline (Mosharov and Sulzer, 2005). For PSF signals, the analysis was restricted to spikes with foot amplitudes of > 2 pA. Cells responding by fewer than 5 spikes during the 60 seconds were excluded from the analysis, and so were spikes that partially overlapped with another spike. The number of spikes and PSFs were averaged per cell for 2 or 60 seconds after nicotine stimulation. All the other amperometric parameters were calculated according to all the events in all the cells tested during the 60-second recording period.

Primary AGCC culture for biochemical and for confocal microscopic analyses

Mouse AGCCs were isolated, as described by Kolski-Andreaco et al. (Kolski-Andreaco et al., 2007), with modifications. The adrenal glands were obtained from 8- to 10-week old mice. The fat and cortex were removed from the medullae, which were then digested with activated papain (P4762, Sigma-Aldrich, Oakville, Ontario, Canada) in Hank's buffer (2 medullae/100 µl Hank's buffer containing four units of activated papain) at 37°C for 25 minutes. The digested medullae were washed twice with Hank's buffer and triturated by pipetting in 300 µl Hank's buffer until they became feather-like. Cells were pelleted at 3,700*g* for 3 minutes and re-suspended in Dulbecco's modified Eagle's medium (DMEM) containing 15% fetal calf serum (FCS) for culture.

Confocal microscopy of F-actin

AGCCs were cultured in 6-well plates with cover glass placed at the bottom of the wells. After one day, the cells were washed once with pre-warmed PBS and stimulated with nicotine (50 µm) for

0, 20, 40, and 60 seconds. The cells were then washed once with PBS and fixed with paraformaldehyde (4%) in PBS for 10 minutes at room temperature. They were permeabilized with 0.1% Triton X-100 in PBS for 3 minutes. The cells were labeled with rhodamine-conjugated phalloidin (1 unit/ml; R415, ThermoFisher Scientific, Burlington, Ontario, Canada) at room temperature for 20 minutes and imbedded with ProLong® Gold anti-fade reagent (Invitrogen, Burlington, Ontario, Canada). All labeled cells were viewed under a confocal microscope (Leica TCS SP5 MP, Allendale, New Jersey, USA). The integrity of the cortical polymerized F-actin ring of each cell was assessed. At least 60 randomly selected AGCCs per treatment per mouse were examined. If gaps in the cortical F-actin rings were more than 5% the length of the circumference, the rings were considered disassembled.

Chromaffin cell line culture

AGCC line tsAM5NE cells were cultured in collagen IV-coated 24-well flat-bottom wells (Corning, New York, USA, 354430) in DMEM medium containing 15% FCS and G5 supplement (ThermoFisher Scientific, Burlington, Ontario, Canada, 17503012) in an environment of 5% CO_2 at 33°C. In some experiments, these cells were cultured in wells coated with goat anti-EPHB6 Ab (AF611, R&D systems, Oakville, Ontario, Canada), normal goat IgG (sc-2028, Santa Cruz Biotechnology, Mississauga, Ontario, Canada), recombinant EPHB6-Fc (E9777, Sigma-Aldrich, Oakville, Ontario, Canada) or normal human IgG (0150-01, Southern Biotech, Birmingham, USA) (2 μg/ml during overnight coating at 4°C) for 24 hours. Nicotine (40 μM) was used to stimulate these cells.

G-LISA assays for activated RHOA

Adrenal medullae were isolated from *Ephb6* KO and WT male mice, and cultured in Opti-MEM™ Reduced Serum Media at 37 °C for 2 hours. Nicotine (20 μM) was used to stimulate the adrenal medulla for 2.5 minutes, which was determined as the peak activation time according to pilot studies. Proteins were extracted from the tissues on ice for 5 minutes in G-LISA's cell lysis buffers

containing protease inhibitor cocktails (Cytoskeleton, Inc, Denver, Colorado; BK128). The cleared supernatants were snap-frozen in liquid nitrogen and stored at -80°C until the assay. Activated RHOA G-protein within samples (25 μg/sample) was determined by the G-LISA assay (Cytoskeleton, Inc) according to the manufacturer's instructions. Samples were assayed in duplicate.

NE measurements

tsAM5NE AGCCs were cultured for 24 hours. The cells were washed once by pre-warmed Hank's buffer and placed in Hank's buffer at 37℃ for 15 minutes. Then these cells were stimulated with 5 mM ACh chloride (A2661, Sigma-Aldrich) in Hank's buffer for 1 minute. NE levels in the supernatants were measured with the NE Research ELISA kit (BA E-5200, Rocky Mountain Diagnostics, Colorado Springs, CO, USA) according to the manufacturer's instructions. Each sample was tested in duplicate. In some experiments, 10,000 AGCCs from WT or *Ephb6* KO female mice were cultured in collagen IV-coated 24-well plates in DMEM medium with 15% FCS for 16 h at 37℃. These cells were treated with BSA-conjugated testosterone (1.1 μg/ml, testosterone-3-(O-carboxymethyl)-oxime-BSA; Aviva Systems Biology, San Diego, USA) or BSA in Hank's buffer at 37℃ for 15 min after washed once by pre-warmed Hank's buffer. The cells were then stimulated with ACh (5 mM) for 1 minute. The supernatants were harvested and tested for NE levels by ELISA.

Lentivirus preparation and infection

Polymerase chain reaction (PCR)-based deletion mutations of EFNB1 intracellular tails were generated and cloned into the pLentiviral CMV/TO PGK GFP Destination vector (Addgene) as previously described (Hu et al., 2015). The expression plasmid, control plasmid, and packaging constructs plp1, plp2, and plpSV were transfected into HEK 293T cells. The viruses were harvested by collecting the supernatant 72 hours later and concentrated by ultracentrifugation. tsAM5NE cells (1.2 x 10^5 cells/well in 24-well plates) were transfected with lentiviruses in the presence of 10 μg/ml Polybrene (sc-134220, Santa Cruz Biotechnology) immediately after passage. After 72

hours, the transfected cells were re-plated (1.2 x 10^5 cells/well) in 24-well plates coated with collagen IV plus goat anti-EFNB1 Ab (AF473, R&D systems), or normal goat IgG (sc-2028, Santa Cruz Biotechnology) for 24 hours before the measurement of ACh-stimulated NE secretion.

Immunoprecipitation and immunoblotting

Adrenal gland medullae were collected from 8- to 10-week old WT and *Ephb6* KO male mice, and rested in DMEM at 37℃ for 2 hours. They were stimulated with nicotine (20 μm) for 5 or 10 minutes at 37℃ and then lysed by immunoprecipitation assay buffer (RIPA), which contained PhosSTOP and a protease inhibitor mixture (Roche Applied Science, Meylan Cedex, France). Sixty μg of lysate protein per sample was resolved on 7.5% SDS-PAGE and transferred to PVDF membranes (Invitrogen). In some experiments, the lysates were pre-cleared with protein G magnetic beads (1614023, Bio-Rad Laboratories, Mississauga, Ontario, Canada), and then precipitated with anti-phosphotyrosine Ab 4G10 (05321, Sigma) plus protein G magnetic beads at 4℃overnight with gentle rotation. The precipitated proteins were resolved in 7.5% SDS-PAGE and transferred to PVDF membranes. The membranes were blotted with mouse anti-phospho-FYN (Y420) Ab (STJ110851, St John's laboratory, London, UK), mouse anti-FYN-59 Ab (626502, Biolegend, San Diego, CA, USA), rabbit anti-c-ABL Ab (2862, Cell Signaling Technology, Danvers, US), rabbit anti-MICAL1 Ab (ab181145, Abcam), rabbit anti-ELK1 Ab (9182; Cell Signaling Technology), or rabbit anti-β-actin Ab (4967; Cell Signaling Technology). All the Abs were used at the manufacturers' recommended dilutions. Signals were visualized by SuperSignal West Pico Chemiluminescent Substrate (ThermoFisher Scientific).

Ethics statement

All the animal studies were approved by the Animal Protection Committee (Comité institutionnel d'intégration de la protection des animaux) of the CRCHUM or conducted according to the European Council Directive 86/609/EEC.

Data availability

All the data supporting our conclusions are presented in this article.

Results

Reduced CAT exocytosis in male KO AGCCs

Our previous study has shown a reduction of 24-hour urine CAT levels in EPHB6 KO male but not female mice. To prove that such reduction was due to decreased CAT secretion by AGCCs, we conducted amperometry to assess CAT release by individual AGCCs. Typical amperometry traces of AGCCs from male KO and wild-type (WT) mice are shown in Figure 1A. Compared to WT counterparts, KO AGCCs from male mice presented a significantly reduced spike number per cell within the first 2 seconds of nicotine stimulation (Fig. 1B) and within 60 seconds (Fig. 1C). The maximal spike height (Imax, Fig. 1D) and charge per peak (Q, Fig. 1E) of the KO AGCCs were also reduced, although the spike width at the half its height ($T_{1/2}$, Fig. 1F) and the time to reach the peak (T_{peak}, Fig. 1G) were not significantly different from their WT counterparts.

Analysis of the pre-spike feet (PSF) showed that the number of PSF per cell (Fig. 1H), the PSF amplitude (Fig. 1I), and the percentage of spikes with PSF (Fig. 1K) were all significantly reduced in AGCCs from male KO mice, compared to their WT counterparts. However, the PSF charge (Fig. 1K) and duration (Fig. 1L) were comparable between KO and WT AGCCs from male mice.

Of note, all these amperometry parameters, including the number of spikes per cell were not significantly different in AGCCs from female KO and WT mice (Supplementary Figure 1 (S-Fig. 1)).

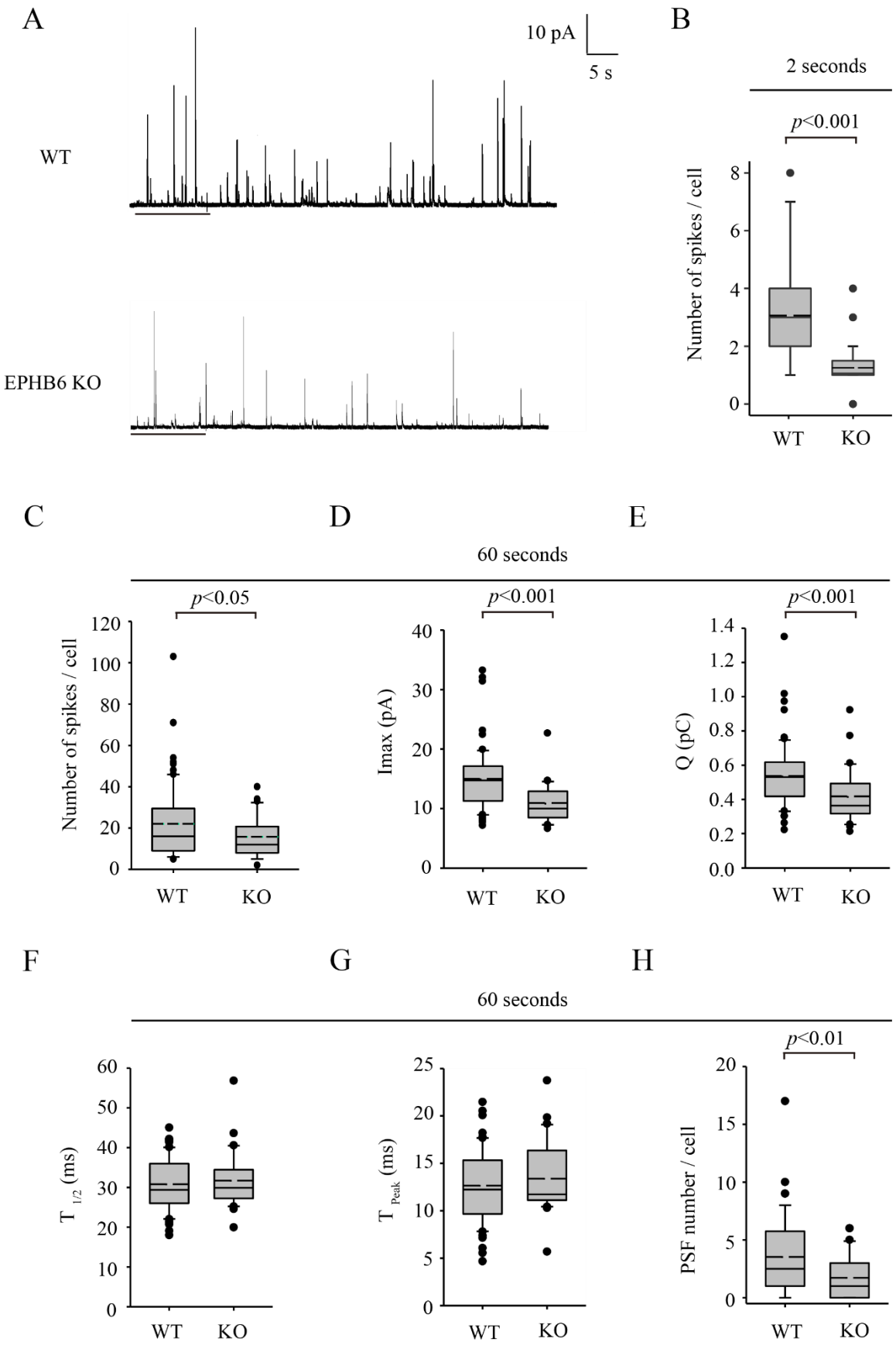
A
10 pA
5 s
WT
EPHB6 KO
B
2 seconds
p<0.001
Number of spikes / cell
WT
KO
C
D
E
60 seconds
p<0.05
Number of spikes / cell
p<0.001
Imax (pA)
p<0.001
Q (pC)
F
G
H
60 seconds
T 1/2 (ms)
T Peak (ms)
p<0.01
PSF number / cell

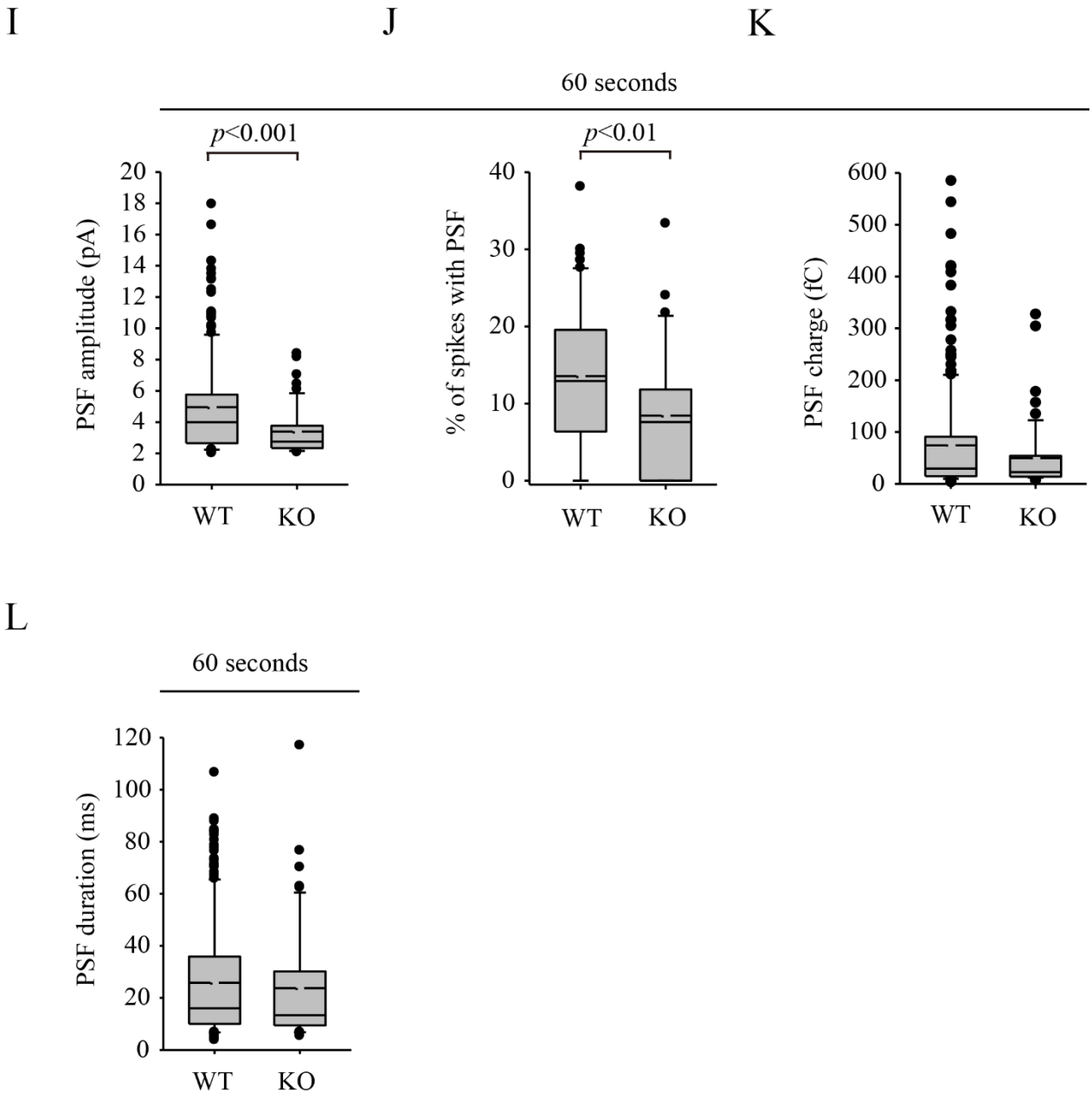

Figure 1

Figure 1. Reduced CAT release from KO AGCCs from KO and WT male mice according to amperometry recording.

AGCCs were isolated from three KO and three WT male mice, and their nicotine-stimulated CAT release was registered by amperometry. Typical traces of amperometry are shown in **A.** Box bar graphs (**B**-**L**) show the medium (solid horizontal line in the box), mean (dashed horizontal line in the box), the 75th percentile (upper part of the box), 25th percentile (lower part of the box), 95th

percentile (upper whisker), 5th percentile (lower whisker), and outliners (dots beyond the 95th and 5th percentile) of each parameter. The Mann-Whitney Rank Sum tests were conducted for statistical analysis due to failed normality tests of the data. Significant *p*-values are shown. The number of spikes per cell observed in the 2- (**B**) or 60-second (**C**) period after nicotine stimulation, the spike peak height (Imax) (**D**), the charge of the spikes (Q) (**E**), the half time to reach the spike peak ($T_{½}$) (**F**), the time to reach the peak (T_{peak})(**G**), the number of PSF observed per cell (**H**), the PSF amplitude (**I**), the percentage of spikes with PSF (**J**), the PSF charge (fC) (**K**), and the PSF duration (**L**) are illustrated. For **B**-**G**, 89 WT cells and 35 KO cells were analyzed; for **H** and **J**, 60 WT cells and 30 KO cells; **I** and **K**, 212 PSF of WT cells, and 52 PSF of KO cells. The values in **B**, **C**, and **H** were averaged per cell for the duration indicated. The values in the rest panels were calculated according to all events that occurred in all the cells tested during the 60-second recording period.

Compromised cortical filamentous actin (F-actin) network disassembly in KO AGCCs upon nicotine stimulation

We next examined the cortical F-actin morphology in AGCCs after nicotine stimulation using confocal microscopy. Typical micrographs of continuous and disassembled cortical F-actin in resting and activated WT AGCCs (40 seconds after nicotine stimulation) are shown in Figure 2A. The percentages of cells with disassembled F-actin ring in the resting KO and WT AGCCs cells are similar (Fig. 2B). When examined between 20 and 60 seconds after nicotine stimulation, KO AGCCs showed a consistently lower percentage of cells with disassembled cortical F-actin (Fig. 2B). However, after castration, the KO AGCCs reverted to the WT morphology as the percentage of cells with disassembled F-actin increased to a level similar to that of WT AGCCs (Fig. 2B). Castration did not affect the F-actin disassembly in WT AGCCs (Fig. 2C). F-actin disassembly in AGCCs from female KO and WT mice was also similar (Fig. 2D). Altogether these results suggest that EPHB6 deletion and testosterone are both indispensable for the compromised F-actin disassembly in AGCCs from male KO mice.

We further elucidated how sex hormones in concert with EPHB6 regulated F-actin disassembly. When AGCCs from female KO mice were treated shortly for 15 min with cell-impermeable BSA-

conjugated testosterone, their F-actin disassembly was compromised (Fig. 2E). BSA-conjugated testosterone had no effect on AGCCs from WT females (Fig. 2F), excluding the possibility that testosterone alone affected the F-actin disassembly. In contrast, when estrogen was added to the culture of AGCCs from male WT (Fig. 2G) or KO (Fig. 2H) mice, it manifested no significant effect on the F-actin disassembly.

To prove that the reduced F-actin disassembly in KO cells due to cell-impermeable testosterone did have functional consequence in terms of CAT secretion, we treated female AGCCs with BSA-conjugated testosterone. Such treatment indeed significantly reduced noradrenaline secretion by KO but not WT AGCCs (Fig. 2I). Altogether, these data indicate that the observed compromised F-actin disassembly in AGCCs from male KO mice is due to EPHB6 deletion in concert with the non-genomic effect of testosterone, while the absence of estrogen does not play a role in this matter. Further, such F-actin disassembly appears functionally associated with CAT secretion.

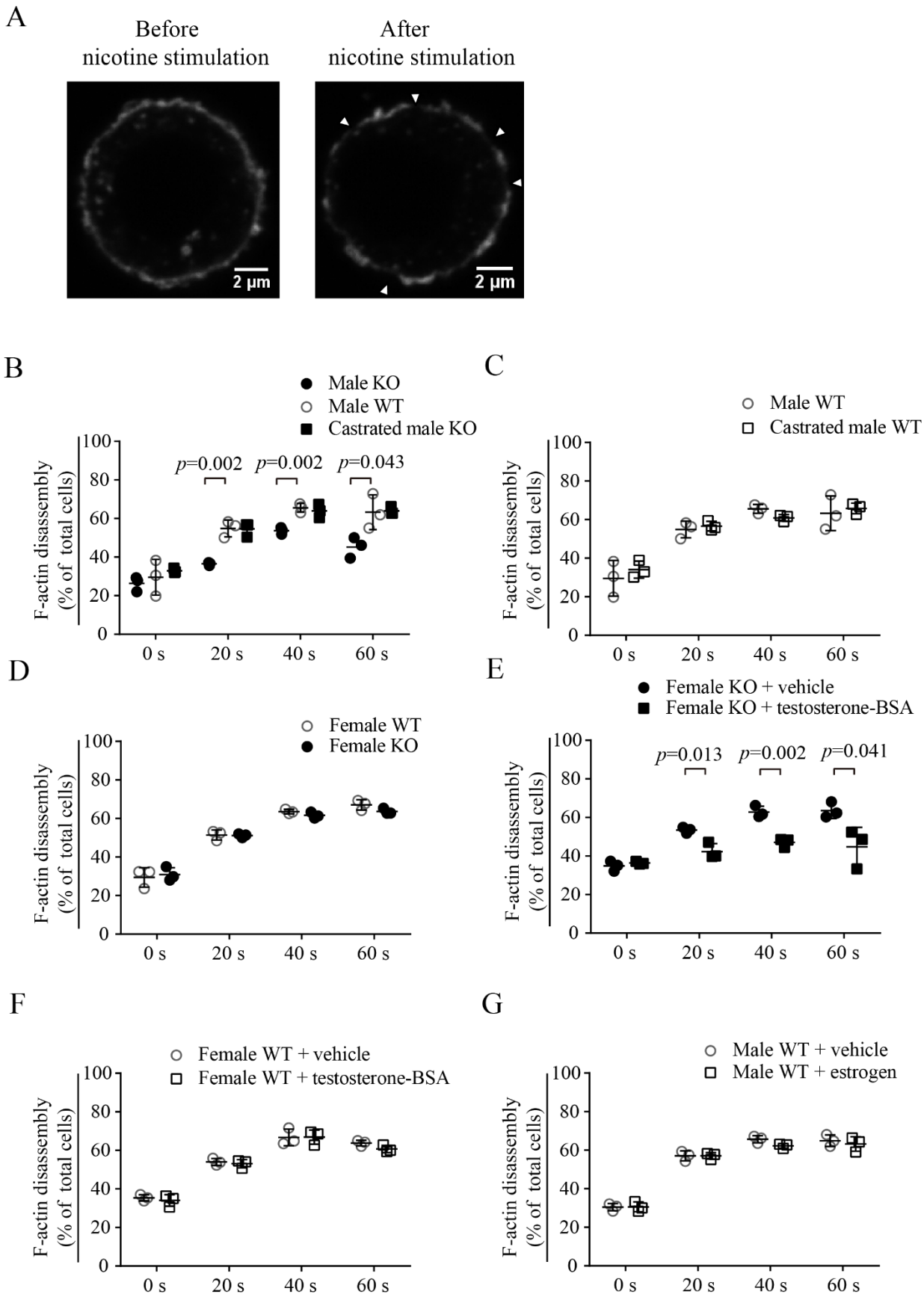
A
Before nicotine stimulation
After nicotine stimulation
2 μm
2 μm
B
Male KO
Male WT
Castrated male KO
p=0.002
p=0.002
p=0.043
F-actin disassembly (% of total cells)
0 s
20 s
40 s
60 s
C
Male WT
Castrated male WT
D
Female WT
Female KO
E
Female KO + vehicle
Female KO + testosterone-BSA
p=0.013
p=0.002
p=0.041
F
Female WT + vehicle
Female WT + testosterone-BSA
G
Male WT + vehicle
Male WT + estrogen

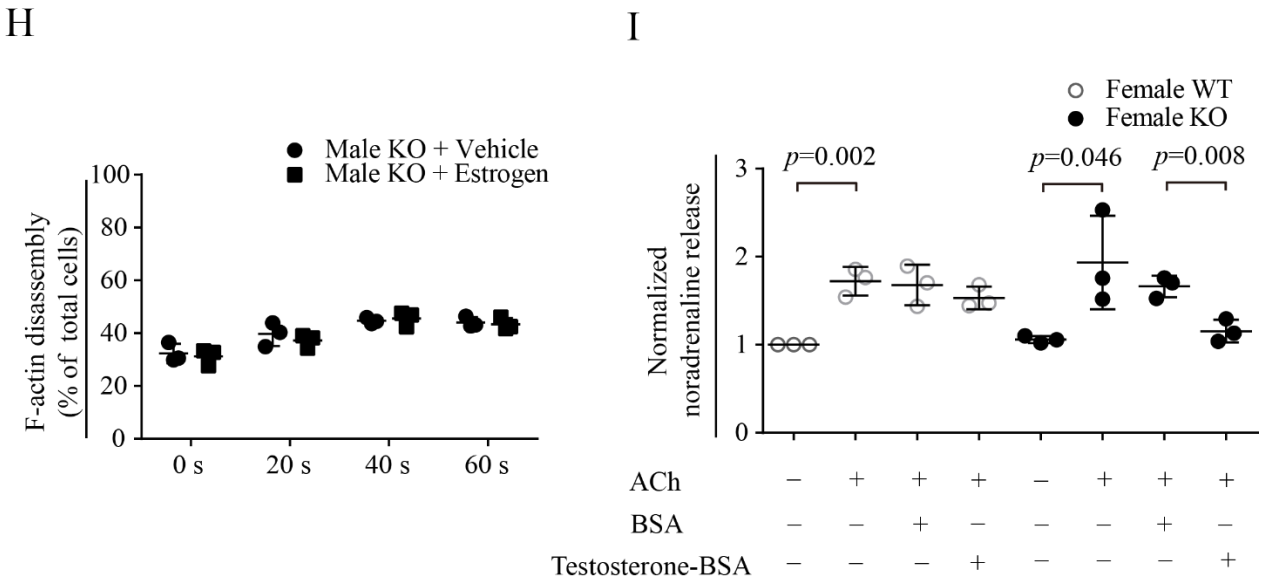

Figure 2

Figure 2. The effect of sex hormones on cortical F-actin disassembly in AGCCs from Ephb6 KO and WT mice.

AGCCs isolated from KO and WT mice were cultured for 24 hours and then stimulated with nicotine (50 μM) for 0, 20, 40, or 60 seconds. The cells were stained with rhodamine-conjugated phalloidin for F-actin and then analyzed according to confocal microscopy. At least 60 AGCCs per adrenal gland per mouse were examined for F-actin disassembly, which was defined as the gaps in the cortical F-actin ring that exceeded more than 5% of the circumference. Three independent experiments, each using one male KO and WT mouse, were performed, and the data of the three experiments were analyzed by two-way paired Means ± SE were presented. Significant *p*-values (Student's *t*-test after arcsine transformation) between the WT and KO AGCCs at a given time point are shown. **A**. Representative micrographs of cortical F-actin rings in WT AGCCs before and after 40-second nicotine stimulation. The arrowheads indicate gaps in the cortical F-actin ring. Scale bar=2 μm. **B**. Male KO AGCCs presented reduced cortical F-actin disassembly, and castration abrogated this phenotype. **C**. Castration did not affect cortical F-actin disassembly in male WT AGCCs. **D**. AGCCs of female KO and WT mice were similar in cortical F-actin disassembly. **E** and **F**. Testosterone rapidly lowered cortical F-actin disassembly in female KO (**E**) but not female WT (**F**)

AGCCs. AGCCs were treated with cell membrane-impermeable BSA-conjugated testosterone (1.1 μg/ml) or vehicle for 15 minutes at 37˚C before nicotine stimulation. **G** and **H**. Estrogen did not affect cortical F-actin disassembly in AGCCs from male WT (**G**) or KO (**H**) mice. AGCCs were treated with 17β-estradiol (100 pg/ml) or vehicle for 15 minutes at 37˚C before nicotine stimulation. **I**. Short-term testosterone treatment lowered NE released from female KO but not from WT AGCCs. Cells obtained for female KO and WT AGCCs (10,000 cells per well) were cultured for 16 hours and then treated with BSA-conjugated testosterone (1.1 μg/ml) or BSA in Hank's buffer at 37℃ for 15 min, and stimulated with 5 mM ACh for 1 minute at room temperature. NE in the supernatants was measured and normalized to base-line NE secretion by female WT AGCCs without testosterone pretreatment or ACh stimulation. Normalized fold changes (means ± SD) of NE secretion of samples with different treatments are shown. Three independent experiments were conducted. Significant *p*-values (2-way paired Student's *t*-test) are indicated. Additional statistical analysis for the changes between different points in time is presented in supplementary Table 1.

EPHB6 reverse signaling through EFNB1 is essential in regulating CAT exocytosis in AGCC

EPHB6 and its ligands (EFNBs) are capable of bidirectional signaling. To discern these two types of signaling related to CAT exocytosis of AGCCs, we employed solid-phase EPHB6 (EPHB6-FC-coated wells) and solid phase anti-EPHB6 Ab (anti-EPHB6 Ab-coated wells) to stimulate tsAM5NE cells, which are derived from normal AGCCs (Kohno et al., 2011). In the adrenal gland medullae, there are two types of chromaffin cells containing either epinephrine (Epi) or norepinephrine (NE) (Tomlinson et al., 1987). They secret Epi or NE, respectively (Vollmer et al., 1992). tsAM5NE cells are NE-secreting AGCCs (Kohno et al., 2011); their NE secretion was used as a readout.

As shown in Figure 3A, solid-phase EPHB6 significantly augmented ACh-triggered NE release by AGCCs, while solid phase anti-EPHB6 Ab had no such effect. Their respective control proteins normal human IgG (the Fc part of EPHB6-Fc was of human IgG origin) or normal mouse IgG did not impact on the NE release. This result indicated that the reverse signaling from EPHB6 to EFNBs was responsible for regulating NE exocytosis in AGCCs.

To identify which EFNB was mediating such reverse signaling, we placed Ab against two major EPHB6 ligands, *i.e*., EFNB1 and EFNB2, on the solid-phase and used them to stimulate tsAM5NE cells. Anti-EFNB1 but not anti-EFNB2 Ab drastically augmented ACh-stimulated NE secretion (Fig. 3B), suggesting that the major reverse signaling was mediated by EFNB1.

EFNBs have no enzymatic activity, and their reverse signaling depends on the association of other signaling molecules with their short intracellular sequences. In the intracellular sequence of EFNB1, there are five tyrosine residues and a PDZ-binding domain at its C-terminus (Fig. 3C). We constructed lentiviruses expressing full-length EFNB1 and various deletion mutants of the EFNB1 intracellular sequence (Fig. 3C). tsAM5NE cells were infected with these viruses. By adjusting virus concentrations, the tsAM5NE cell surface overexpression of different EFNB1 mutants was titrated to a similar level according to flow cytometry (S.-Figure 2). tsAM5NE cells overexpressing the full-length EFNB1 increased NE secretion significantly, compared to the empty virus-infected cells, (both of them were cultured in anti-EFNB1 Ab-coated wells) (Fig. 3D). The cells with full-length EFNB1 overexpression and cultured in anti-EFNB1 Ab-coated wells also had significantly increased NE secretion compared to the same kinds of cells cultured in wells coated with control IgG (*i.e.,* without reverse signaling via EFNB1) (Fig. 3D). These controls validated the assay system as one being able to detect reverse signaling by the overexpressed EFNB1 over the endogenous EFNB1 on the tsMA5NE cell surface. EFNB1-Δ2Y (the deletion of the last 16 aa of the C-terminus including the PDZ-binding domain and two tyrosine residues Y342 and Y343) was equally potent as the full-length EFNB1. The further deletion of seven aa, including tyrosine residues Y323 and Y328 (EFNB1-Δ4Y), significantly reduced the potency of the mutant to stimulate NE secretion. The additional deletion of 11 aa containing the remaining tyrosine residues Y312 and Y316 (EFNB1-Δ6Y) did not result in a further decrease of the potency. These results suggested that the critical sequence mediating EFNB1 reverse signaling in mouse AGCCs in terms of controlling CAT secretion resided within the 7-aa intracellular sequence from aa 322 to aa 328, containing Y323 and Y328.

It has been established that EFNB1 reverse signaling depends on several RHO family G-proteins(Tanaka et al., 2003;Wu et al., 2012;O'Neill et al., 2016;Cho et al., 2018) . We found that RHOA activity after nicotine stimulation in AGCCs from male KO was increased compared to their

WT counterparts (Fig. 3E). This is compatible with prior knowledge that heightened RHOA activity increases actin polymerization (Bader et al., 2004) and hence reduces overall F-actin disassembly as a result. When AGCCs from male WT mice were treated with an RHOA inhibitor Rhosin, no effect on F-actin disassembly was observed (Fig. 3F). However, such inhibition reverted the decreased F-actin disassembly in the KO cells to a level similar to that of the WT counterparts (Fig. 3F). This result indicated that the increased RHOA activity in the KO AGCCs contributed to the diminished F-actin disassembly.

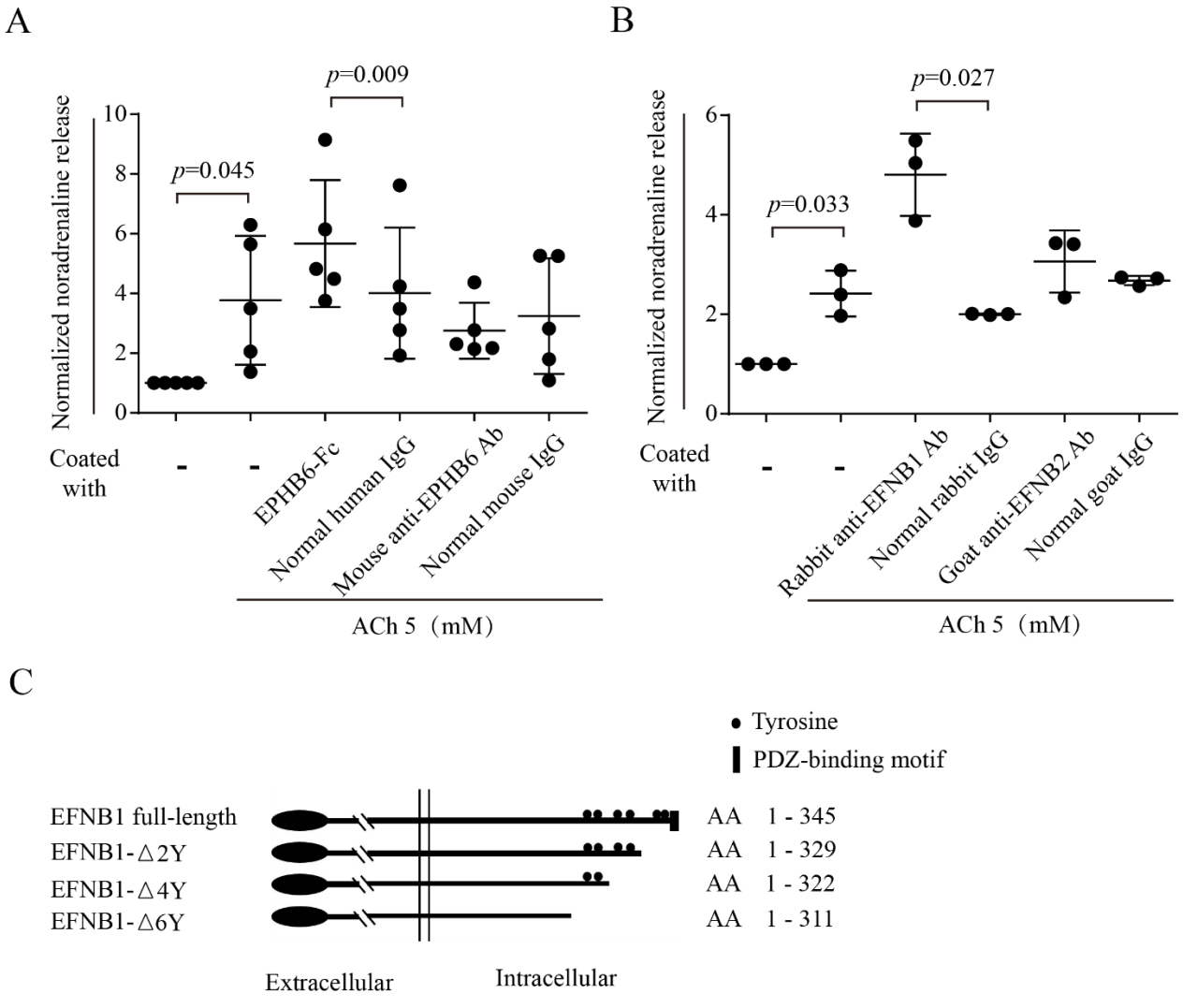

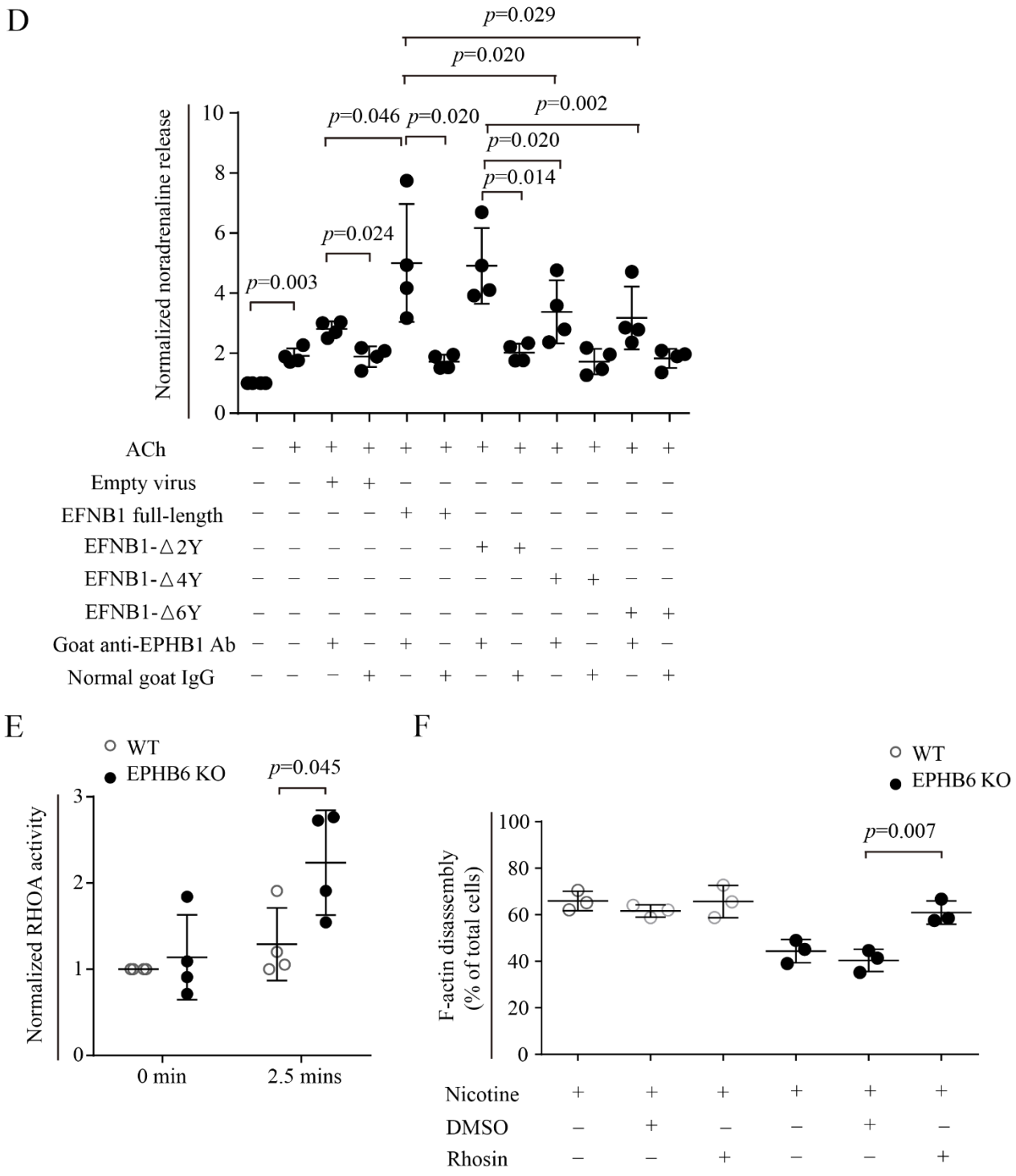

Figure 3

Figure 3. EPHB6 to EFNB1 reverse signaling modulated NE secretion by AGCCs.

tsAM5NE chromaffin cells were cultured in wells coated with anti-EPHB6 Ab, recombinant EPHB6-Fc, anti-EFNB1 Ab, anti-EFNB2 Ab, or their isotype control IgGs for 24 hours, as indicated. The culture medium was replaced with Hank's buffer, and after 15 minutes, cells were stimulated with 5 mM ACh. One minute later, supernatants were harvested for NE measurements. The base-line NE secretion by tsAM5NE cells cultured in uncoated wells without ACh stimulation was considered as 1 fold. The normalized fold changes (means ± SD) of the NE secretion of cells with different treatments are shown. Three to five independent experiments were conducted. Significant *p*-values (2-way paired Student's *t*-test) are indicated. **A**. The ACh-stimulated NE release by tsAM5NE cells was promoted by solid-phase EPHB6-Fc but not by anti-EPHB6 Ab. Data from 5 independent experiments were normalized and presented. **B**. Solid-phase anti-EFNB1 Ab but not anti-EFNB2 Ab augmented ACh-stimulated NE release. The results from 3 independent experiments were normalized and presented. **C**. The structures EFNB1 protein and its deletion mutants. **D**. Identification of the critical intracellular sequence of EFNB1 in mediating the reverse signaling. tsAM5NE cells were infected with lentiviruses encoding full-length and deletion mutants of *EFNB1,* as indicated. The infected cells were seeded in wells coated with anti-EFNB1 Ab or normal goat IgG for 24 hours and then stimulated with ACh for one minute. The ACh-stimulated NE release was measured. Data from 4 independent experiments were normalized and presented. **E**. The activity of RHOA after nicotine stimulation was elevated in adrenal medullae from male KO mice. Adrenal medullae were stimulated with nicotine (20 μM) for 0 and 2.5 minutes. The activated RHOA level in the adrenal medullae was measured by G-LISA. The RHOA activity of WT medulla at 0 minute was considered as one fold for normalization. The results of four independent experiments were normalized, and the fold changes (means ± SD) of different samples are presented. **F**. RHOA inhibitor reverted the low cortical F-actin disassembly in male KO AGCCs to a normal level. AGCCs isolated from male KO or WT mice were cultured for one day and then treated with Rhosin (30 μM) or DMSO in Opti-MEM™ Reduced Serum Media for 4 hours at 37℃. Cells were stimulated with nicotine (50 μM) for 40 seconds, and their cortical F-actin disassembly was assessed by confocal microscopy. The percentages (mean ± SD) of cells with F-actin disassembly from three independent experiments are presented. Significant *p*-value (two-way paired Student's *t*-test after arcsine transformation) is indicated.

The FYN/c-ABL/MICAL-1 pathway conducted signaling from EPHB6 to F-actin disassembly

FYN was previously reported to interact with EFNB1 (Palmer et al., 2002) and therefore is a possible downstream signaling molecule mediating EPHB6 reverse signaling in AGCCs concerning their function in CAT secretion. The SRC-family tyrosine kinase FYN was activated (based on its Y420 phosphorylation) within 5-10 minutes of nicotine stimulation in AGCCs of WT male mice (Fig. 4A). Such phosphorylation was compromised in the KO AGCCs, while the total FYN protein remained unchanged (Fig. 4A). The tyrosine kinase c-ABL is a substrate of FYN kinase (Plattner et al., 1999). Its phosphorylation, which is needed for its activation (Plattner et al., 1999), was diminished, as expected, in AGCCs from male KO mice (Fig. 4B). In this experiment, total phospho-protein was immunoprecipitated, followed by anti-c-ABL Ab blotting. We previously demonstrated that the phosphorylation of ELK1 was not influenced by EPHB6 KO in AGCCs (Shi et al., 2019). Figure 4B showed that ELK1 phosphorylation was similar in all the precipitated samples and was used as a loading and immunoprecipitation efficiency control. Further, the total protein of c-ABL in the KO and WT AGCCs was similar (Fig. 4C).

MICAL-1 is a substrate of the c-ABL kinase (Yoon et al., 2017) and is an F-actin-monooxygenase, which oxidizes methionine residues of actin (Hung et al., 2011). It is essential in promoting the depolymerization of F-actin (Hung et al., 2011), and its phosphorylation is necessary for its activity (Yoon et al., 2017). Although total MICAL-1 protein levels in WT and KO AGCCs were similar in resting and 10-minute nicotine stimulated cells (Fig. 5A), MICAL-1 phosphorylation was significantly increased in stimulated male WT AGCCs (Fig. 5B). This augmentation was compromised in the KO AGCCs (Fig. 5B). FYN inhibitor PP2 suppressed the up-regulation of nicotine-stimulated MICAL-1 phosphorylation in the male WT AGCCs but did not affect the KO counterparts (Fig. 5B), supporting a model in which FYN acted downstream of EPHB6, and this activity appeared upstream of MICAL-1 phosphorylation. When the male WT AGCCs were treated with Imatinib, a c-ABL inhibitor, their MICAL-1 phosphorylation up-regulation upon nicotine stimulation was compromised (Fig. 5C). On the other hand, imatinib had no such effect on KO counterparts, suggesting that c-ABL activity was downstream of EPHB6 and upstream of MICAL-1 phosphorylation in these cells. ELK1 phosphorylation was again employed as an internal control for the efficiency of immunoprecipitation and loading in this experiment.

To assess the functional consequences of FYN and c-ABL inhibition concerning F-actin disassembly, we treated the WT and KO AGCCs with FYN inhibitor PP2 (Fig. 6A) and c-ABL inhibitor imatinib (Fig. 6B). They effectively reduced F-actin disassembly in WT but not KO AGCCs. This finding suggested that reduced FYN and c-ABL activities occurred downstream of EPHB6, and were relevant to the reduced F-actin disassembly seen in the make KO AGCCs.

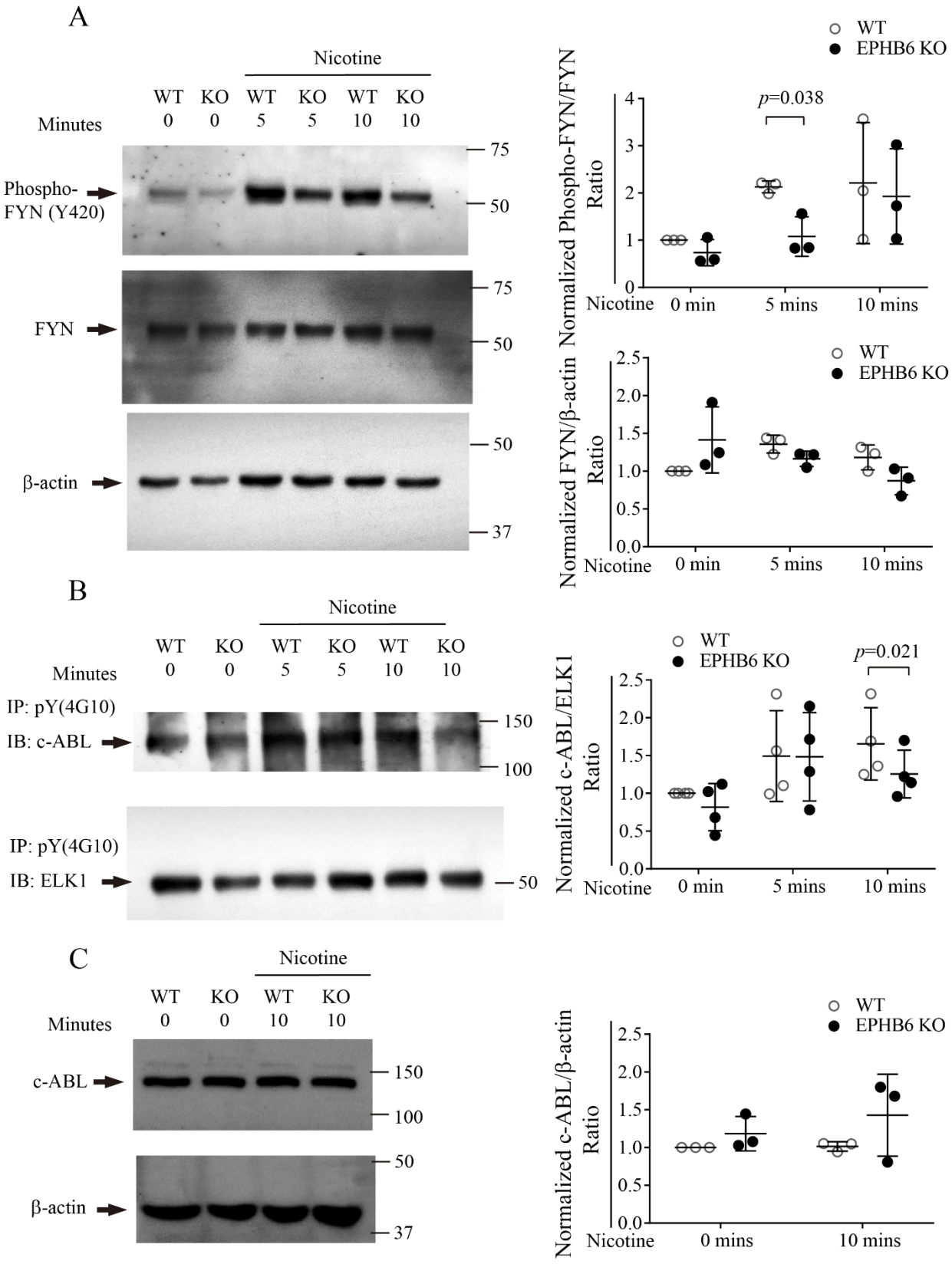
A
Nicotine
WT KO WT KO WT KO
Minutes 0 0 5 5 10 10
Phospho-FYN (Y420)
FYN
β-actin
75
50
75
50
50
37
WT
EPHB6 KO
p=0.038
Normalized Phospho-FYN/FYN Ratio
Nicotine 0 min 5 mins 10 mins
Normalized FYN/β-actin Ratio
B
IP: pY(4G10)
IB: c-ABL
IP: pY(4G10)
IB: ELK1
150
100
50
p=0.021
Normalized c-ABL/ELK1 Ratio
C
c-ABL
β-actin
150
100
50
37
Normalized c-ABL/β-actin Ratio
0 mins 10 mins

Figure 4

Figure 4. Decreased FYN and c-ABL phosphorylation in male KO adrenal medullae upon nicotine stimulation.

Adrenal medullae from male WT and KO mice were stimulated with nicotine (20 μM) for 0 or 10 minutes at 37℃. The phosphorylated FYN, total FYN phosphorylated c-ABL, total ABL, and β-actin levels of the medullae lysates were determined by immunoblotting. **A**. Decreased FYN phosphorylation in medullae obtained from EPHB6 mice. Representative immunoblots of phosphorylated FYN (Y420) (upper panel), total FYN (middle panel), and β-actin (bottom panel) were shown. The densitometry signal ratios of phosphor-FYN versus FYN, and the ratio of total FYN versus β-actin of WT medullae at 0 minute was used to normalize the data from 3 independent experiments. The normalized fold changes (means ± SD) were presented. The significant *p*-values are indicated (2-way paired Student's *t*-test). **B** and **C**. Decreased c-ABL phosphorylation in the KO medullae. Lysate proteins from WT and KO medullae after 0- or 10-minute nicotine stimulation were immunoprecipitated with anti-phospho-protein Ab. The precipitated proteins were immunoblotted with anti-c-ABL or anti-ELK1 Ab. Representative immunoblots on the left show c-ABL and ELK phosphorylation (**B**) and total c-ABL and β-actin (**C**). The densitometry signal ratios of phospho-c-ABL versus phospho-ELK, and total c-ABL versus β-actin of WT medullae at 0 minute were used to normalize the data from four independent experiments. The normalized fold changes (means ± SD) were presented on the right. The significant *p*-values are indicated (2-way paired Student's *t*-test).

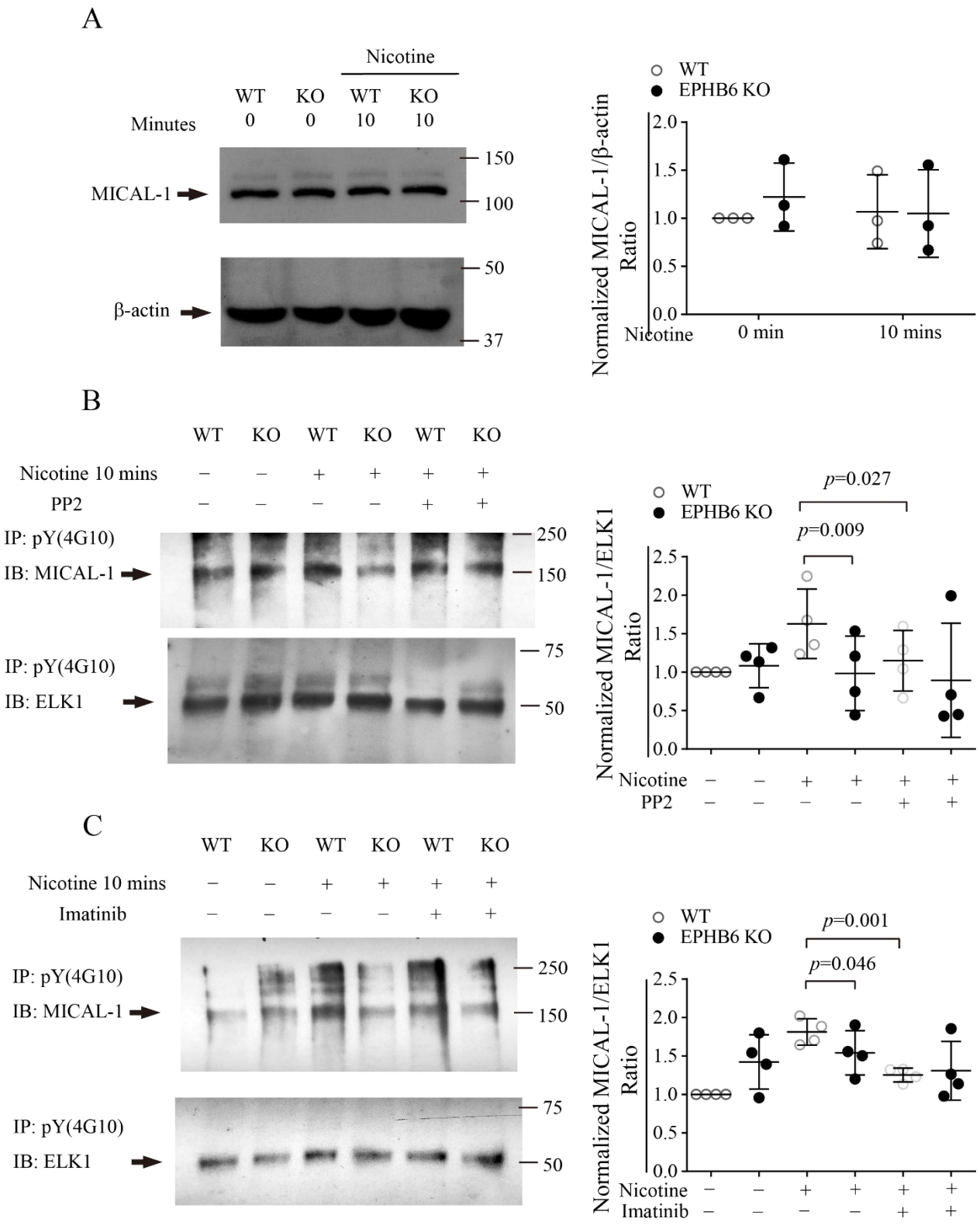
A
Nicotine
WT KO WT KO
Minutes 0 0 10 10
MICAL-1
β-actin
150
100
50
37
WT
EPHB6 KO
Normalized MICAL-1/β-actin Ratio
2.0
1.5
1.0
0.5
0.0
Nicotine
0 min
10 mins
B
WT KO WT KO WT KO
Nicotine 10 mins – – + + + +
PP2 – – – – + +
IP: pY(4G10)
IB: MICAL-1
IP: pY(4G10)
IB: ELK1
250
150
75
50
p=0.027
p=0.009
Normalized MICAL-1/ELK1 Ratio
2.5
2.0
1.5
1.0
0.5
0.0
C
WT KO WT KO WT KO
Nicotine 10 mins – – + + + +
Imatinib – – – – + +
IP: pY(4G10)
IB: MICAL-1
IP: pY(4G10)
IB: ELK1
250
150
75
50
p=0.001
p=0.046
Normalized MICAL-1/ELK1 Ratio
Nicotine – – + + + +
Imatinib – – – – + +

Figure 5

Figure 5. Reduced MICAL-1 phosphorylation in male KO adrenal medullae upon nicotine stimulation.

Adrenal medullae from male WT and KO mice were cultured in the absence or presence of FYN inhibitor PP2 (10 μM) or c-ABL inhibitor Imatinib (20 μM), as indicated, at 37°C for 2 hours, and then stimulated with nicotine (20 μM) for 10 minutes. Their lysates were immunoprecipitated with anti-phospho-protein Ab 4G10 and blotted with anti-MICAL-1 and ELK1 Abs. The densitometry signal ratios of total MICAL-1 versus β-actin and phospho-MICAL-1 versus phospho-ELK in WT male medullae without nicotine stimulation were used to normalize the data from four independent experiments. Representative immunoblots are shown on the left, and normalized fold changes (means ± SD) according to densitometry are shown on the right. The significant *p*-values are indicated (2-way paired Student's *t*-test). **A**. Unchanged total MICAL-1 levels in male KO medullae. **B.** Compromised MICAL-1 phosphorylation in KO medullae after nicotine stimulation, or in WT medullae treated with FYN inhibitor. **C**. Decreased MICAL-1 phosphorylation in WT medullae treated with c-ABL inhibitor.

The same membranes were sequentially blotted with anti-c-ABL (Fig.4C), MICAL-1 and β-actin Abs, with stripping process occurred between these different immunoblottings. The same β-actin immunoblotting was used as loading controls for both Figure 4C and 5A.

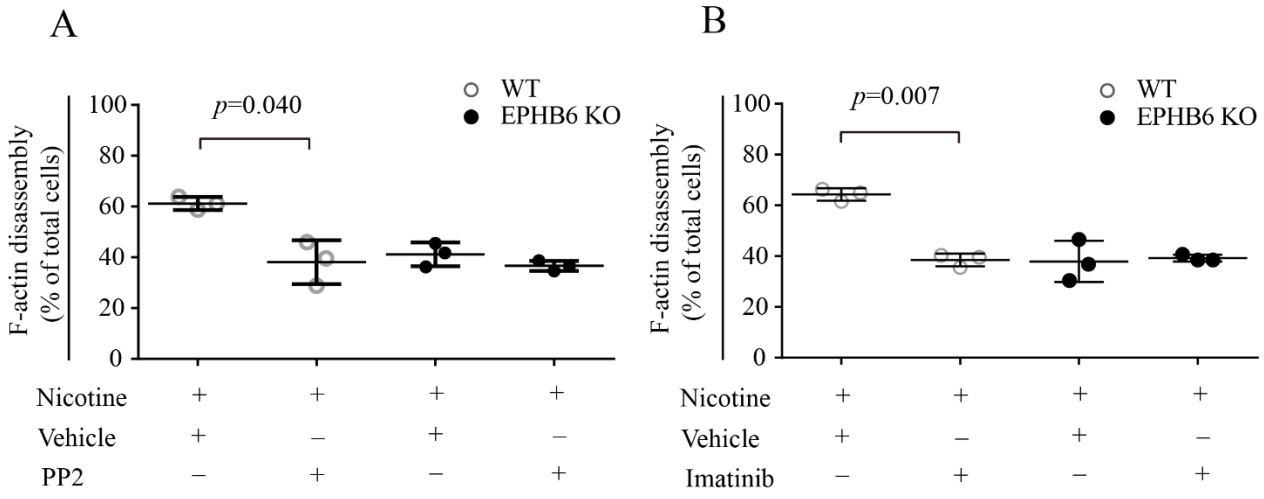

Figure 6

Figure 6. FYN and c-ABL inhibitor repressed cortical F-actin disassembly in male WT but not KO AGCCs.

AGCCs isolated from male KO or WT mice were cultured for 24 hours, and then cultured in the presence of PP2 (10 μM) (**A**) for 1 hour or imatinib (20 μM) (**B**) for 2 hours at 37℃. The cells were stimulated with nicotine (50 μM) for 40 seconds, and their cortical F-actin disassembly was determined according to confocal microscopy. The percentages (means ± SD) of cells with F-actin disassembly from three independent experiments were presented. The significant *p*-values are indicated (2-way paired Student's *t*-test).

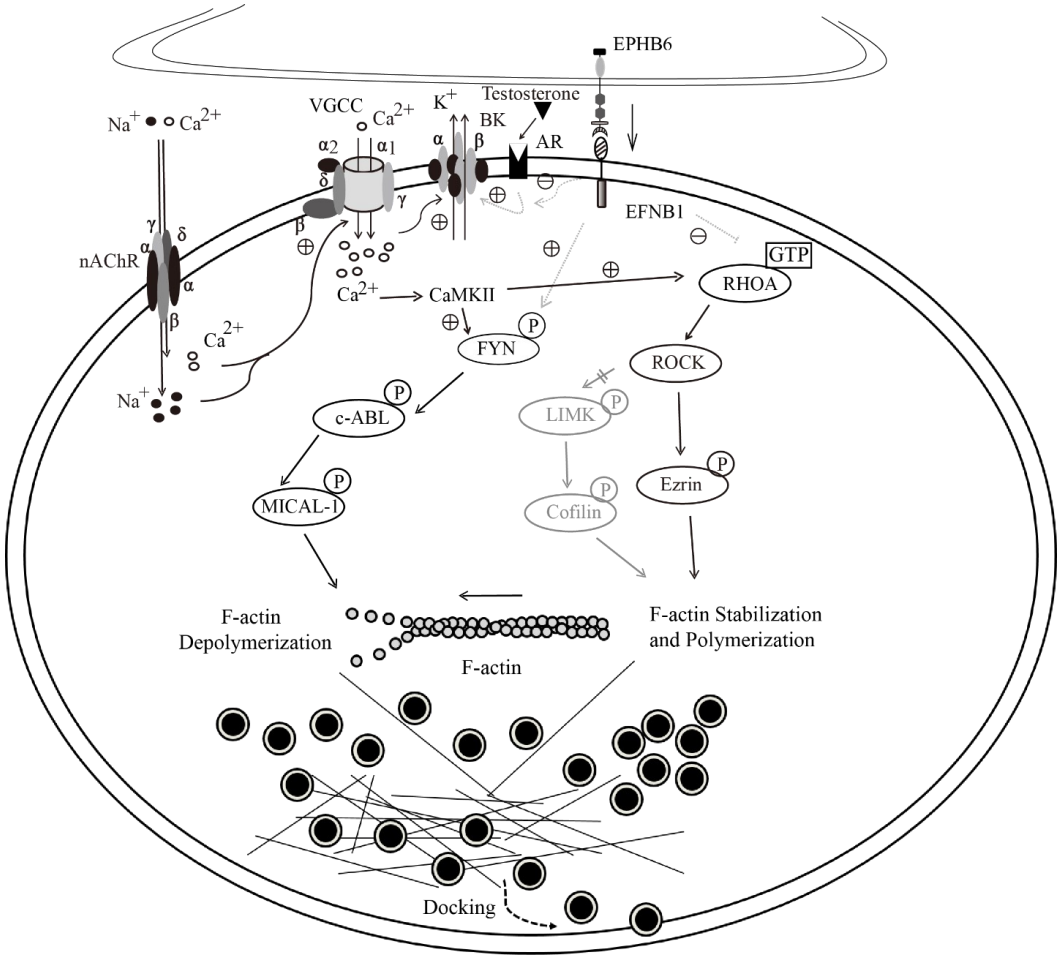

Figure 7

Figure 7. A diagram depicting signaling pathways from EPHB6 to CAT exocytosis in AGCCs.

Solid lines represent pathways verified in this study or already established in the literature, whereas faint dotted lines depict speculated pathways. Circles with black fillings are CAT-containing vesicles. ACh activation of Ach receptor/gated ion channels triggers Na^+ and Ca^{2+} influx (Sala et al., 2008), subsequently amplified by voltage-gated calcium channels (VGCC). The depolarization and the increased Ca^{2+} concentration causes the opening of the big potassium channel (BK), which repolarizes the cells and shuts down VGCC (Solaro et al., 1995;Martinez-Espinosa et al., 2014). The non-genomic effect of testosterone positively regulates BK opening, while EPHB6 to EFNB1 reverse signaling negatively impacts on such an effect of testosterone (Han et al., 2008;Shi et al., 2019). Increased Ca^{2+} levels activate CaMKII (Couchonnal and Anderson, 2008), leading to activation of many downstream signaling events that enhance both CAT biogenesis (Menezes et al., 1996) and exocytosis (this study). The FYN/c-ABL/MICAL-1 pathway that promotes F-actin depolymerization is downstream of and positively regulated by CaMKII (Plattner et al., 1999;Hung et al., 2011;Ginnan et al., 2013;Yoon et al., 2017). The RHOA/ROCK/Ezrin pathway, which promotes F-actin stabilization, is also positively regulated by CaMKII (Niggli and Rossy, 2008;Okamoto et al., 2009). Although the two pathways have opposite effects on F-actin disassembly after the Ca^{2+} influx, under normal circumstances, the balance is in favor of F-actin disassembly. The EPHB6 to EFNB1 reverse signaling by itself has no effect on CAT exocytosis. The effect of the defective reverse signaling on all the downstream events could be due to the initial compromised Ca^{2+} influx. It is also possible that such reverse signaling might modify signaling events directly. The reverse signaling might have a default direct positive effect on the FYN/c-ABL/MICAL-1/F-actin pathway. It might also have a direct default negative effect on RHOA activation, which promotes F-actin stabilization typically. ROCK/Ezrin (Han et al., 2015) and ROCK/LIMK/Cofilin (Geneste et al., 2002) pathways are known to be downstream of RHOA, although the latter is not activated in ACh-stimulated AGCCs. F-actin depolymerization is not only essential in moving the slow-release CAT-containing vesicles to the docking position (Vitale et al., 1995) but is also critical for optimal vesicular fusion and sewage of CAT content from the vesicles in the IRV pool during rapid exocytosis. In the absence of EPHB6/EFNB1 reverse signaling, as is the case in EPHB6 KO, the signaling strength of the FYN/c-ABL/MICAL pathway is compromised,

while the signaling strength of RHOA/ROCK/Ezrin is relatively increased. These changes eventually lead to reduced F-actin disassembly and CAT exocytosis in the male KO AGCCs.

Discussion

In this work, we demonstrated that EPHB6 reverse signaling via a 7-aa intracellular sequence of EFNB1 between aa 322 and 328 was critical for regulating CAT exocytosis in AGCCs. The signaling from EFNB1 traversing through RHOA as well as through the FYN/c-ABL/MICAL-1/F-actin pathways was necessary for EPHB6's effect on CAT secretion.

In our amperometric experiments, CAT vesicles released within 2 and 60 seconds after ACh stimulation were recorded. A reduced number of spikes during the first 2 seconds in KO AGCCs were found (Fig. 1C). Such reduction reflects reduced immediately released CAT. This could be caused by the Ca^{2+} influx decrease in these cells, as we reported previously (Wang et al., 2018), or caused by a smaller pool of immediately-releasable vesicles (IRVs), or both, in the KO AGCCs. Additional experiments will be needed to assess the pool size of IRVs.

Analysis of individual spike parameters is commonly used to quantify the dynamics and size of single vesicular fusion events. We found here that the spike charge Q, reflecting the amount of CAT released per vesicle, was lower in male KO AGCCs, suggesting less catecholamine content in the vesicles in action. This observation is in agreement with our previous report that the male KO AGCCs are compromised in their CAT biogenesis (Shi et al., 2019).

The maximal amplitude (Imax) of the spike is proportional to the rate of catecholamine release and is thus a function of the amount of catecholamine released and the discharge kinetics. $T_{1/2}$ and T_{peak} reflect the discharge kinetics. In the male KO AGCCs, the Imax but not $T_{1/2}$ or T_{peak} was significantly reduced, indicating that the discharge kinetics in the KO AGCCs was normal, and thus the reduced Imax is likely the consequence of a smaller amount of catecholamine released.

The pre-spike feet reflect the fusion pore formation between vesicular and cell membranes, and the small amount of CAT released during this process (Gong et al., 2007). PSFs per cell, PSF

amplitude, and the percentage of PSF present in all spikes were all reduced in the male KO AGCCs, suggesting that EPHB6 was involved in the processes reflected by these parameters. However, the underlying mechanisms and significance of these PSF parameters concerning CAT exocytosis remained to be elucidated.

The cortical F-actin network in resting AGCCs forms a continuous net but is disassembled within seconds after ACh-triggered activation. Such a morphological change does not only allow CAT-containing vesicles in the reserve pool to pass the disrupted F-actin net to replenish the IRV pool but also plays an active role in the fusion of the IRVs with the cell membrane (Gutierrez and Villanueva, 2018). EPHB6 deletion compromised such F-actin disassembly, and this likely also contributes to the decreased CAT exocytosis observed in KO AGCCs. If the role of meshed F-actin in preventing the vesicles in the reserve pool to move to IRV pool overweights its role in the fusion of vesicles to the cell membrane, then the role of EPHB6 is probably more critical in the sustained CAT release by AGCCs.

Our results also showed that the effect of EPHB6 KO in preventing F-actin disassembly depended on the presence of testosterone. This finding was corroborated by the decreased CAT release by female KO AGCCs in the presence of testosterone (Fig. 2I), and our previous in *vivo results* showing that male but not female KO mice presented decreased 24-hour urine CAT levels (Luo et al., 2012).

EPHB6 can trigger signals into cells in two ways. Forward signaling from its ligand EFNs in neighboring cells to EPHB6 on the target cells, occurring through an intracellular sequence of EPHB6. Reverse signaling from EPHB6 on the neighboring cells to the EFNs on the target cells, occurring through the intracellular sequence of EFNBs. Through a series of solid-phase stimulation mimicking the cell surface EPHB6 and EFNs, we determined that reverse signaling through EFNB1 but not forward signaling through EPHB6 was essential for EPHB6's effect on F-actin disassembly. Among the two critical features of the intracellular domain of EFNB1 (*i.e.*, C-terminal PDZ-binding motif and five tyrosine residues potentially associating with SH domain-containing signaling molecules), our results showed that a 7-aa sequence between residues 322 and 328, which contains Y323 and Y328, was critical for CAT release. This region was previously shown to be essential to mediate T cell chemotaxis towards chemokine CXCL12 (Hu et al., 2015). For different

cell types and in responses to various stimuli, different regions of the EFNB1 intracellular domain are implicated, leading to different biological outcomes. For example, in T cells, the 11-aa segment between residues 311 and 321 harboring Y312 and Y316 is indispensable for T cell chemotaxis to chemokine CCL21 (Luo et al., 2016); the 16-aa sequence containing Y342 and Y343 negatively regulates T cell chemotaxis to CXCL12; the 16-aa stretch from residues 331 to 345 is essential for RHOA activation and metalloproteinase secretion in gastric cancer cells (Tanaka et al., 2010). However, these regions did not have a perceptible effect on F-actin disassembly in AGCCs, based on our deletion study.

We tried to decipher the signaling pathways from the EFNB1 intracellular sequence to CAT exocytosis. Possible pathways elucidated in this study or described in the literature from EPHB6/EFNB1 to F-actin disassembly and concerning both CAT exocytosis are illustrated in Figure 7. It seems that EFNB1 has a constitutively suppressive effect on RHOA activation in AGCCs. In its absence in KO AGCCs, such a suppressive effect was released, and hence the level of GTP-bound active RHOA was elevated. Active RHOA favors the maintenance of the cortical F-actin network in AGCCs (Gasman et al., 1997;Gasman et al., 2003;Trifaro et al., 2008) and inhibits AGCC CAT secretion (Bader et al., 2004). Currently, the intermediate molecule linking the EFNB1 peptide sequence aa 323-328 to RHOA remains to be identified. This molecule might be a negative regulator of RHOA activity, such as GTPase activating protein (GAP) or a guanine nucleotide dissociating inhibitor (GDI) (Marjoram et al., 2014). Alternatively, it might be an adaptor protein binding to RHOA regulators (Tanaka et al., 2010). Several paths can lead to RHOA's activity to actin polymerization (Spiering and Hodgson, 2011). We investigated one of them and found that the path RHOA/ROCK/LIMK/COFILIN/F-actin was not implicated. We cannot exclude the possibility that the effect of EPHB6/EFNB1 reverse signaling on regulating RHOA activity is via the initially reduced Ca^{2+} influx (Wang et al., 2018). However, this possibility is incompatible with some literature and our findings. For example, the RHOA/ROCK/Ezrin pathway, which promotes F-actin stabilization, is positively regulated by Ca^{2+} influx and CaMKII (Niggli and Rossy, 2008;Okamoto et al., 2009), as illustrated in Figure 7. This implies that the reduced Ca^{2+} influx caused by EPHB6 KO would reduce RHOA activity, and consequently decreased F-actin stabilization, which favors CAT secretion but not reduced CAT secretion. Additional investigation

is needed to firmly establish if there is Ca^{2+}-independent regulation of RHOA activity by the EPHB6/EFNB1 reverse signaling.

The other pathway from EPHB6/EFNB1 to F-actin involves FYN/c-ABL/MICAL/F-actin. Using FYN inhibitor PP2 and c-ABL inhibitor Imatinib, we showed that these inhibitors affected F-actin disassembly in WT but not in KO AGCCs, indicating that this pathway leading to F-actin is relevant to the EPHB6/EFNB1 reverse signaling and that it is not functional when EPHB6 is absent. FYN is likely immediately downstream of EFNB1, as the SRC family kinases are recruited to the lipid domain where EFNB1 is localized after the reverse signaling is triggered, and FYN is activated (Spiering and Hodgson, 2011), although direct evidence of EFNB1 and FYN co-localization or interaction is still lacking. MICAL-1 is likely to be at the other end of this pathway, and its redox enzymatic activity may specifically destabilize F-actin (Hung et al., 2010). Again, it is possible that the observed effects of EPHB6/EFNB1 reverse signaling on the FYN/c-ABL/MICAL/F-actin pathway are due to its initial impact on the Ca^{2+} influx (Wang et al., 2018). The end results remain the same. In the absence of EPHB6 reverse signaling via EFNB1, MICAL-1 activity was reduced, leading to an increase in F-actin stability.

Although the above-mentioned two pathways have opposite effects on F-actin disassembly after the Ca^{2+} influx, under normal circumstances, the balance is in favor of F-actin disassembly. The EPHB6 to EFNB1 reverse signaling by itself has no effect on CAT exocytosis. The effect of the defective reverse signaling on all the downstream events could be due to the initial compromised Ca^{2+} influx, as mentioned above. It is also possible that such reverse signaling might modify signaling events directly in addition to its effect on Ca^{2+} influx. The reverse signaling might have a default direct positive effect on the FYN/c-ABL/MICAL-1/F-actin pathway. It, on the other hand, might have a direct default negative effect on RHOA activation, which promotes F-actin stabilization typically. ROCK/Ezrin (Han et al., 2015) and ROCK/LIMK/Cofilin (Geneste et al., 2002) pathways are known to be downstream of RHOA, although the latter is not activated in ACh-stimulated AGCCs. F-actin depolymerization is not only essential in moving the slow-release CAT-containing vesicles to the docking position (Vitale et al., 1995) but is also critical for optimal vesicular fusion and sewage of CAT content from the vesicles in the IRV pool during rapid exocytosis. In the absence of EPHB6/EFNB1 reverse signaling, as is the case in EPHB6 KO, the

signaling strength of the FYN/c-ABL/MICAL pathway is compromised, while the signaling strength of RHOA/ROCK/Ezrin is relatively increased. These changes eventually lead to reduced F-actin disassembly and CAT exocytosis in the male KO AGCCs.

We previously demonstrated that the male but not female EPHB6 KO AGCCs presented a lower Ca^{2+} influx after ACh stimulation (Wang et al., 2018). The difference in the Ca^{2+} influx between male and female KO AGCCs was due to the absence of testosterone but not the presence of estrogen in females (Wang et al., 2018). The ACh-triggered Ca^{2+} influx is the first and most important event leading to the activation of many downstream events. It is possible that some abnormal manifestations of these events in the KO cells are the consequence of the initially reduced Ca^{2+} influx. However, it is also possible that EPHB6/EFNB1 has Ca^{2+}-independent regulation of FYN and RHOA activation, as illustrated in Figure 7 by faint dotted lines between EFNB1 and FYN, and between EFNB1 and RHOA. We could induce a maximal Ca^{2+} influx in AGCCs by ionomycin. If under such a circumstance, the activation of the FYN and/or RHOA pathways is still different in the WT and KO AGCCs, then we could conclude that indeed Ca^{2+} influx-independent regulation of FYN and RHOA activation by EPHB6/EFNB1 reverse signaling does exist. Such experiments will be performed shortly.

Although F-actin disassembly became obvious only 20 seconds after nicotine stimulation, it is conceivable that some more subtle actin disassembly, not measurable with our experimental approach, had already occurred in the first several seconds after stimulation. This rapid kinetics is compatible with that of acute CAT secretion, which happens at a similar time scale and is consistent with the more recently described positive role of F-actin disassembly in vesicle fusion (Gasman et al., 2004). Of course, the disassembly is also essential in mobilizing the vesicles from the reserve pool for chronic CAT secretion (Vitale et al., 1995), which is probably more relevant to hypertension caused by chronic stress and chronic sterile inflammation (Sparrenberger et al., 2009;De Miguel et al., 2015;Liu et al., 2017). In our study, the FYN/c-ABL/MICAL-1 pathway activation was demonstrated to occur 5-10 minutes after nicotine stimulation. Such slow kinetics is probably pertinent to the chronic CAT secretion, which requires F-actin disassembly and slow-releasing vesicle mobilization at such a time scale. However, FYN and c-ABL inhibitors effectively suppressed F-actin disassembly in 20 seconds after nicotine stimulation (Figs. 6A and 6B), proving

that this pathway is also essential in acute CAT secretion. Likely, immunoblotting of FYN, c-ABl, and MICAL-1 phosphorylation is not sensitive to detect earlier activation of this pathway within seconds of nicotine stimulation.

The major sources of blood Epi and NE are AGCCs and the nervous system, respectively, while blood dopamine level is very low. Blood pressure increase during acute stress is associated with Epi released from AGCCs. There are different opinions regarding whether the blood Epi level is associated with blood pressure under non-stress conditions. Early publications showed that ambient Epi levels are associated with blood pressure in humans and animals (Axelrod, 1976;Buhler et al., 1982;Dominiak and Grobecker, 1982;Goldstein, 1983;Borkowski and Quinn, 1984;Jablonskis and Howe, 1994). In recent years, chronic stress (Sparrenberger et al., 2009;Liu et al., 2017) and systemic sterile low-level chronic inflammation are found to be significant contributing factors of primary hypertension (De Miguel et al., 2015). These conditions are associated with elevated blood NE levels derived from the nervous system, but increased Epi levels from AGCCs are also often observed (Rivier et al., 1989;Pende et al., 1990;Corssmit et al., 1996;Kannan et al., 1996;Esler et al., 2008;Byrne et al., 2018). In a mouse model, augmented catecholamine release from AGCCs caused by TRPM4 deletion has been shown to cause hypertension (Mathar et al., 2010). These data suggest that the excessive CAT release from the adrenal glands is a contributing factor to hypertension. In the case of EPHB6 mutation, hypogonadism causes an increase of CAT secretion from a depressed to a normal level.

Based on our previous and current findings along with existing literature, it is postulated that EPHB6 acts in concert with testosterone to regulate blood pressure. EPHB6/EFNB1 reverse signaling has a positive constitutive effect on CAT biosynthesis (Shi et al., 2019) and exocytosis, but such effects depend on the presence of testosterone. In the absence of the said reverse signaling due to EPHB6 deletion in individuals with a normal level of testosterone, the ambient CAT biosynthesis and secretion are reduced. Such reduction tends to lower blood pressure, but EPHB6 KO loss-of-function mutations also cause increased resistant artery constriction due to its other function on vascular smooth muscle cells (Luo et al., 2012), inclined toward an increase in blood pressure. These two opposite effects on blood pressure cancel out each other, and the final outcome is that in EPHB6 KO/mutations males with sufficient testosterone, their blood pressure

remains normal. However, if patients with EPHB6 loss-of-function mutations or defective EPHB6-EFNB1 reverse signaling become hypogonadic (castration in the case of mice), their CAT biosynthesis and exocytosis return to the normal level. At the same time, due to the vasoconstrictive effect of EPHB6 KO/mutation, the resistance of blood flow is increased, and hence their blood pressure is augmented. For these patients, testosterone could be a personalized medication for hypertension.

Acknowledgments

This work was supported by the Fonds de recherche du Québec – Santé, and the J.-Louis Lévesque Foundation to J.W. It was also funded in part by grants from the Canadian Institutes of Health Research to J.W. (MOP272014) and the Natural Sciences and Engineering Research Council of Canada (RGPIN-2017-04790) to J.W. and by an ANR grant to N.V. M.R. was supported by an FRM grant to N.V. (DEI20151234424). This study was also made possible by a grant from the National Natural Science Foundation of China (#81700363) to Y.W.

References

Axelrod, J. (1976). Catecholamines and hypertension. *Clin Sci Mol Med Suppl* 3**,** 415s-421s.

Bader, M.F., Doussau, F., Chasserot-Golaz, S., Vitale, N., and Gasman, S. (2004). Coupling actin and membrane dynamics during calcium-regulated exocytosis: a role for Rho and ARF GTPases. *Biochim Biophys Acta* 1742**,** 37-49.

Borkowski, K.R., and Quinn, P. (1984). Adrenaline and the development of genetic hypertension. *J Hypertens Suppl* 2**,** S81-83.

Brantley-Sieders, D.M., and Chen, J. (2004). Eph receptor tyrosine kinases in angiogenesis: from development to disease. *Angiogenesis* 7**,** 17-28.

Buhler, F.R., Amann, F.W., Bolli, P., Hulthen, L., Kiowski, W., Landmann, R., and Burgisser, E. (1982). Elevated adrenaline and increased alpha-adrenoceptor-mediated vasoconstriction in essential hypertension. *J Cardiovasc Pharmacol* 4 Suppl 1**,** S134-138.

Byrne, C.J., Khurana, S., Kumar, A., and Tai, T.C. (2018). Inflammatory Signaling in Hypertension: Regulation of Adrenal Catecholamine Biosynthesis. *Front Endocrinol (Lausanne)* 9**,** 343.

Cho, H.J., Hwang, Y.S., Yoon, J., Lee, M., Lee, H.G., and Daar, I.O. (2018). EphrinB1 promotes cancer cell migration and invasion through the interaction with RhoGDI1. *Oncogene* 37**,** 861-872.

Corssmit, E.P., Heijligenberg, R., Endert, E., Ackermans, M.T., Sauerwein, H.P., and Romijn, J.A. (1996). Endocrine and metabolic effects of interferon-alpha in humans. *J Clin Endocrinol Metab* 81**,** 3265-3269.

Couchonnal, L.F., and Anderson, M.E. (2008). The role of calmodulin kinase II in myocardial physiology and disease. *Physiology (Bethesda)* 23**,** 151-159.

De Miguel, C., Rudemiller, N.P., Abais, J.M., and Mattson, D.L. (2015). Inflammation and hypertension: new understandings and potential therapeutic targets. *Curr Hypertens Rep* 17**,** 507.

Dominiak, P., and Grobecker, H. (1982). Elevated plasma catecholamines in young hypertensive and hyperkinetic patients: effect of pindolol. *Br J Clin Pharmacol* 13**,** 381S-390S.

Douglas, W.W., and Rubin, R.P. (1961). The role of calcium in the secretory response of the adrenal medulla to acetylcholine. *J Physiol* 159**,** 40-57.

Dravis, C., Wu, T., Chumley, M.J., Yokoyama, N., Wei, S., Wu, D.K., Marcus, D.C., and Henkemeyer, M. (2007). EphB2 and ephrin-B2 regulate the ionic homeostasis of vestibular endolymph. *Hear Res* 223**,** 93-104.

Eph Nomenclature Committee (1997). Unified nomenclature for Eph family receptors and their ligands, the ephrins. *Cell* 90**,** 403-404.

Esler, M., Eikelis, N., Schlaich, M., Lambert, G., Alvarenga, M., Kaye, D., El-Osta, A., Guo, L., Barton, D., Pier, C., Brenchley, C., Dawood, T., Jennings, G., and Lambert, E. (2008). Human sympathetic nerve biology: parallel influences of stress and epigenetics in essential hypertension and panic disorder. *Ann N Y Acad Sci* 1148**,** 338-348.

Flanagan, J.G., and Vanderhaeghen, P. (1998). The ephrins and Eph receptors in neural development. *Annu Rev Neurosci* 21**,** 309-345.

Gasman, S., Chasserot-Golaz, S., Bader, M.F., and Vitale, N. (2003). Regulation of exocytosis in adrenal chromaffin cells: focus on ARF and Rho GTPases. *Cell Signal* 15**,** 893-899.

Gasman, S., Chasserot-Golaz, S., Malacombe, M., Way, M., and Bader, M.F. (2004). Regulated exocytosis in neuroendocrine cells: a role for subplasmalemmal Cdc42/N-WASP-induced actin filaments. *Mol Biol Cell* 15**,** 520-531.

Gasman, S., Chasserot-Golaz, S., Popoff, M.R., Aunis, D., and Bader, M.F. (1997). Trimeric G proteins control exocytosis in chromaffin cells. Go regulates the peripheral actin network and catecholamine secretion by a mechanism involving the small GTP-binding protein Rho. *J Biol Chem* 272**,** 20564-20571.

Geneste, O., Copeland, J.W., and Treisman, R. (2002). LIM kinase and Diaphanous cooperate to regulate serum response factor and actin dynamics. *J Cell Biol* 157**,** 831-838.

Ginnan, R., Zou, X., Pfleiderer, P.J., Mercure, M.Z., Barroso, M., and Singer, H.A. (2013). Vascular smooth muscle cell motility is mediated by a physical and functional interaction of Ca2+/calmodulin-dependent protein kinase IIdelta2 and Fyn. *J Biol Chem* 288**,** 29703-29712.

Goldstein, D.S. (1983). Arterial baroreflex sensitivity, plasma catecholamines, and pressor responsiveness in essential hypertension. *Circulation* 68**,** 234-240.

Gong, L.W., De Toledo, G.A., and Lindau, M. (2007). Exocytotic catecholamine release is not associated with cation flux through channels in the vesicle membrane but Na+ influx through the fusion pore. *Nat Cell Biol* 9**,** 915-922.

Gutierrez, L.M., and Villanueva, J. (2018). The role of F-actin in the transport and secretion of chromaffin granules: an historic perspective. *Pflugers Arch* 470**,** 181-186.

Han, D.H., Chae, M.R., Jung, J.H., So, I., Park, J.K., and Lee, S.W. (2008). Effect of testosterone on potassium channel opening in human corporal smooth muscle cells. *The journal of sexual medicine* 5**,** 822-832.

Han, Y., Wang, X., Chen, J., and Sha, S.H. (2015). Noise-induced cochlear F-actin depolymerization is mediated via ROCK2/p-ERM signaling. *J Neurochem* 133**,** 617-628.

Hashimoto, T., Karasawa, T., Saito, A., Miyauchi, N., Han, G.D., Hayasaka, K., Shimizu, F., and Kawachi, H. (2007). Ephrin-B1 localizes at the slit diaphragm of the glomerular podocyte. *Kidney Int* 72**,** 954-964.

Haycock, J.W., Meligeni, J.A., Bennett, W.F., and Waymire, J.C. (1982). Phosphorylation and activation of tyrosine hydroxylase mediate the acetylcholine-induced increase in catecholamine biosynthesis in adrenal chromaffin cells. *J Biol Chem* 257**,** 12641-12648.

Holmberg, J., Genander, M., Halford, M.M., Anneren, C., Sondell, M., Chumley, M.J., Silvany, R.E., Henkemeyer, M., and Frisen, J. (2006). EphB receptors coordinate migration and proliferation in the intestinal stem cell niche. *Cell* 125**,** 1151-1163.

Hu, Y., Wang, X., Wu, Y., Jin, W., Cheng, B., Fang, X., Martel-Pelletier, J., Kapoor, M., Peng, J., and Qi, S. (2015). Role of EFNB1 and EFNB2 in Mouse Collagen-Induced Arthritis and Human Rheumatoid Arthritis. *Arthritis & Rheumatology* 67**,** 1778-1788.

Hung, R.J., Pak, C.W., and Terman, J.R. (2011). Direct redox regulation of F-actin assembly and disassembly by Mical. *Science* 334**,** 1710-1713.

Hung, R.J., Yazdani, U., Yoon, J., Wu, H., Yang, T., Gupta, N., Huang, Z., Van Berkel, W.J., and Terman, J.R. (2010). Mical links semaphorins to F-actin disassembly. *Nature* 463**,** 823-827.

Jablonskis, L.T., and Howe, P.R. (1994). Elevated plasma adrenaline in spontaneously hypertensive rats. *Blood Press* 3**,** 106-111.

Kannan, H., Tanaka, Y., Kunitake, T., Ueta, Y., Hayashida, Y., and Yamashita, H. (1996). Activation of sympathetic outflow by recombinant human interleukin-1 beta in conscious rats. *Am J Physiol* 270**,** R479-485.

Kohno, S., Murata, T., Koide, N., Hikita, K., and Kaneda, N. (2011). Establishment and characterization of a noradrenergic adrenal chromaffin cell line, tsAM5NE, immortalized with the temperature-sensitive SV40 T-antigen. *Cell Biol Int* 35**,** 325-334.

Kolski-Andreaco, A., Cai, H., Currle, D.S., Chandy, K.G., and Chow, R.H. (2007). Mouse adrenal chromaffin cell isolation. *J Vis Exp***,** 129.

Konstantinova, I., Nikolova, G., Ohara-Imaizumi, M., Meda, P., Kucera, T., Zarbalis, K., Wurst, W., Nagamatsu, S., and Lammert, E. (2007). EphA-Ephrin-A-mediated beta cell communication regulates insulin secretion from pancreatic islets. *Cell* 129**,** 359-370.

Liu, Y.Z., Wang, Y.X., and Jiang, C.L. (2017). Inflammation: The Common Pathway of Stress-Related Diseases. *Front Hum Neurosci* 11**,** 316.

Luo, H., Broux, B., Wang, X., Hu, Y., Ghannam, S., Jin, W., Larochelle, C., Prat, A., and Wu, J. (2016). EphrinB1 and EphrinB2 regulate T cell chemotaxis and migration in experimental autoimmune encephalomyelitis and multiple sclerosis. *Neurobiology of disease* 91**,** 292-306.

Luo, H., Wu, Z., Tremblay, J., Thorin, E., Peng, J., Lavoie, J.L., Hu, B., Stoyanova, E., Cloutier, G., and Qi, S. (2012). Receptor tyrosine kinase Ephb6 regulates vascular smooth muscle contractility and modulates blood pressure in concert with sex hormones. *Journal of Biological Chemistry* 287**,** 6819-6829.

Luo, H., Yu, G., Tremblay, J., and Wu, J. (2004). EphB6-null mutation results in compromised T cell function. *The Journal of clinical investigation* 114**,** 1762-1773.

Marjoram, R.J., Lessey, E.C., and Burridge, K. (2014). Regulation of RhoA activity by adhesion molecules and mechanotransduction. *Curr Mol Med* 14**,** 199-208.

Martinez-Espinosa, P.L., Yang, C., Gonzalez-Perez, V., Xia, X.M., and Lingle, C.J. (2014). Knockout of the BK beta2 subunit abolishes inactivation of BK currents in mouse adrenal chromaffin cells and results in slow-wave burst activity. *J Gen Physiol* 144**,** 275-295.

Mathar, I., Vennekens, R., Meissner, M., Kees, F., Van Der Mieren, G., Camacho Londono, J.E., Uhl, S., Voets, T., Hummel, B., Van Den Bergh, A., Herijgers, P., Nilius, B., Flockerzi, V., Schweda, F., and Freichel, M. (2010). Increased catecholamine secretion contributes to hypertension in TRPM4-deficient mice. *J Clin Invest* 120**,** 3267-3279.

Menezes, A., Zeman, R., and Sabban, E. (1996). Involvement of intracellular or extracellular calcium in activation of tyrosine hydroxylase gene expression in PC12 cells. *J Neurochem* 67**,** 2316-2324.

Mosharov, E.V., and Sulzer, D. (2005). Analysis of exocytotic events recorded by amperometry. *Nat Methods* 2**,** 651-658.

Niggli, V., and Rossy, J. (2008). Ezrin/radixin/moesin: versatile controllers of signaling molecules and of the cortical cytoskeleton. *Int J Biochem Cell Biol* 40**,** 344-349.

O'neill, A.K., Kindberg, A.A., Niethamer, T.K., Larson, A.R., Ho, H.H., Greenberg, M.E., and Bush, J.O. (2016). Unidirectional Eph/ephrin signaling creates a cortical actomyosin differential to drive cell segregation. *J Cell Biol* 215**,** 217-229.

Okamoto, K., Bosch, M., and Hayashi, Y. (2009). The roles of CaMKII and F-actin in the structural plasticity of dendritic spines: a potential molecular identity of a synaptic tag? *Physiology (Bethesda)* 24**,** 357-366.

Ory, S., Ceridono, M., Momboisse, F., Houy, S., Chasserot-Golaz, S., Heintz, D., Calco, V., Haeberle, A.M., Espinoza, F.A., Sims, P.J., Bailly, Y., Bader, M.F., and Gasman, S. (2013). Phospholipid scramblase-1-induced lipid reorganization regulates compensatory endocytosis in neuroendocrine cells. *J Neurosci* 33**,** 3545-3556.

Palmer, A., Zimmer, M., Erdmann, K.S., Eulenburg, V., Porthin, A., Heumann, R., Deutsch, U., and Klein, R. (2002). EphrinB phosphorylation and reverse signaling: regulation by Src kinases and PTP-BL phosphatase. *Mol Cell* 9**,** 725-737.

Pasquale, E.B. (2008). Eph-ephrin bidirectional signaling in physiology and disease. *Cell* 133**,** 38-52.

Pende, A., Musso, N.R., Vergassola, C., Puppo, F., Ioverno, A., Criscuolo, D., Indiveri, F., and Lotti, G. (1990). Neuroendocrine effects of interferon alpha 2-a in healthy human subjects. *J Biol Regul Homeost Agents* 4**,** 67-72.

Plattner, R., Kadlec, L., Demali, K.A., Kazlauskas, A., and Pendergast, A.M. (1999). c-Abl is activated by growth factors and Src family kinases and has a role in the cellular response to PDGF. *Genes Dev* 13**,** 2400-2411.

Poea-Guyon, S., Ammar, M.R., Erard, M., Amar, M., Moreau, A.W., Fossier, P., Gleize, V., Vitale, N., and Morel, N. (2013). The V-ATPase membrane domain is a sensor of granular pH that controls the exocytotic machinery. *J Cell Biol* 203**,** 283-298.

Rivier, C., Vale, W., and Brown, M. (1989). In the rat, interleukin-1 alpha and -beta stimulate adrenocorticotropin and catecholamine release. *Endocrinology* 125**,** 3096-3102.

Sala, F., Nistri, A., and Criado, M. (2008). Nicotinic acetylcholine receptors of adrenal chromaffin cells. *Acta Physiol (Oxf)* 192**,** 203-212.

Salvucci, O., De La Luz Sierra, M., Martina, J.A., Mccormick, P.J., and Tosato, G. (2006). EphB2 and EphB4 receptors forward signaling promotes SDF-1-induced endothelial cell chemotaxis and branching remodeling. *Blood* 108**,** 2914-2922.

Shi, W., Wang, Y., Peng, J., Qi, S., Vitale, N., Kaneda, N., Murata, T., Luo, H., and Wu, J. (2019). EPHB6 controls catecholamine biosynthesis by up-regulating tyrosine hydroxylase transcription in adrenal gland chromaffin cells. *J Biol Chem* 294**,** 6871-6887.

Solaro, C.R., Prakriya, M., Ding, J.P., and Lingle, C.J. (1995). Inactivating and noninactivating Ca(2+)- and voltage-dependent K+ current in rat adrenal chromaffin cells. *J Neurosci* 15**,** 6110-6123.

Sparrenberger, F., Cichelero, F.T., Ascoli, A.M., Fonseca, F.P., Weiss, G., Berwanger, O., Fuchs, S.C., Moreira, L.B., and Fuchs, F.D. (2009). Does psychosocial stress cause hypertension? A systematic review of observational studies. *J Hum Hypertens* 23**,** 12-19.

Spiering, D., and Hodgson, L. (2011). Dynamics of the Rho-family small GTPases in actin regulation and motility. *Cell Adh Migr* 5**,** 170-180.

Tanaka, M., Kamata, R., Yanagihara, K., and Sakai, R. (2010). Suppression of gastric cancer dissemination by ephrin-B1-derived peptide. *Cancer Sci* 101**,** 87-93.

Tanaka, M., Kamo, T., Ota, S., and Sugimura, H. (2003). Association of Dishevelled with Eph tyrosine kinase receptor and ephrin mediates cell repulsion. *EMBO J* 22**,** 847-858.

Tomlinson, A., Durbin, J., and Coupland, R.E. (1987). A quantitative analysis of rat adrenal chromaffin tissue: morphometric analysis at tissue and cellular level correlated with catecholamine content. *Neuroscience* 20**,** 895-904.

Tremblay, J., Wang, Y., Raelson, J., Marois-Blanchet, F.C., Wu, Z., Luo, H., Bradley, E., Chalmers, J., Woodward, M., Harrap, S., Hamet, P., and Wu, J. (2017). Evidence from single nucleotide polymorphism analyses of ADVANCE study demonstrates EFNB3 as a hypertension risk gene. *Sci Rep* 7**,** 44114.

Trifaro, J.M., Gasman, S., and Gutierrez, L.M. (2008). Cytoskeletal control of vesicle transport and exocytosis in chromaffin cells. *Acta Physiol (Oxf)* 192**,** 165-172.

Vitale, M.L., Seward, E.P., and Trifaro, J.M. (1995). Chromaffin cell cortical actin network dynamics control the size of the release-ready vesicle pool and the initial rate of exocytosis. *Neuron* 14**,** 353-363.

Vollmer, R.R., Baruchin, A., Kolibal-Pegher, S.S., Corey, S.P., Stricker, E.M., and Kaplan, B.B. (1992). Selective activation of norepinephrine- and epinephrine-secreting chromaffin cells in rat adrenal medulla. *Am J Physiol* 263**,** R716-721.

Wang, Y., Hamet, P., Thorin, E., Tremblay, J., Raelson, J., Wu, Z., Luo, H., Jin, W., Lavoie, J.L., and Peng, J. (2016a). Reduced blood pressure after smooth muscle EFNB2 deletion and the potential association of EFNB2 mutation with human hypertension risk. *European Journal of Human Genetics 24**, 1817-1825***.

Wang, Y., Shi, W., Blanchette, A., Peng, J., Qi, S., Luo, H., Ledoux, J., and Wu, J. (2018). EPHB6 and testosterone in concert regulate epinephrine release by adrenal gland chromaffin cells. *Sci Rep* 8**,** 842.

Wang, Y., Thorin, E., Luo, H., Tremblay, J., Lavoie, J.L., Wu, Z., Peng, J., Qi, S., and Wu, J. (2015). EPHB4 protein expression in vascular smooth muscle cells regulates their contractility, and EPHB4 deletion leads to hypotension in mice. *Journal of Biological Chemistry* 290**,** 14235-14244.

Wang, Y., Wu, Z., Luo, H., Peng, J., Raelson, J., Ehret, G.B., Munroe, P.B., Stoyanova, E., Qin, Z., Cloutier, G., Bradley, W.E., Wu, T., Shen, J.Z., Hu, S., and Wu, J. (2016b). The role of GRIP1 and ephrin B3 in blood pressure control and vascular smooth muscle cell contractility. *Sci Rep* 6**,** 38976.

Wang, Y., Wu, Z., Thorin, E., Tremblay, J., Lavoie, J.L., Luo, H., Peng, J., Qi, S., Wu, T., and Chen, F. (2016c). Estrogen and testosterone in concert with EFNB3 regulate vascular smooth muscle cell contractility and blood pressure. *American Journal of Physiology-Heart and Circulatory Physiology* 310**,** H861-H872.

Wu, J., and Luo, H. (2005). Recent advances on T-cell regulation by receptor tyrosine kinases. *Current opinion in hematology* 12**,** 292-297.

Wu, T., Zhang, B.Q., Raelson, J., Yao, Y.M., Wu, H.D., Xu, Z.X., Marois-Blanchet, F.C., Tahir, M.R., Wang, Y., Bradley, W.E., Luo, H., Wu, J., Sheng, J.Z., and Hu, S.J. (2018). Analysis of the

association of EPHB6, EFNB1 and EFNB3 variants with hypertension risks in males with hypogonadism. *Sci Rep* 8**,** 14497.

Wu, Z., Luo, H., Thorin, E., Tremblay, J., Peng, J., Lavoie, J.L., Wang, Y., Qi, S., Wu, T., and Wu, J. (2012). Possible role of Efnb1 protein, a ligand of Eph receptor tyrosine kinases, in modulating blood pressure. *Journal of Biological Chemistry* 287**,** 15557-15569.

Yoon, J., Kim, S.B., Ahmed, G., Shay, J.W., and Terman, J.R. (2017). Amplification of F-Actin Disassembly and Cellular Repulsion by Growth Factor Signaling. *Dev Cell* 42**,** 117-129 e118.

Zhang, Z., Tremblay, J., Raelson, J., Sofer, T., Du, L., Fang, Q., Argos, M., Marois-Blanchet, F.C., Wang, Y., Yan, L., Chalmers, J., Woodward, M., Harrap, S., Hamet, P., Luo, H., and Wu, J. (2019). EPHA4 regulates vascular smooth muscle cell contractility and is a sex-specific hypertension risk gene in individuals with type 2 diabetes. *J Hypertens* 37**,** 775-789.

Zhao, C., Irie, N., Takada, Y., Shimoda, K., Miyamoto, T., Nishiwaki, T., Suda, T., and Matsuo, K. (2006). Bidirectional ephrinB2-EphB4 signaling controls bone homeostasis. *Cell Metab* 4**,** 111-121.

Supplementary information

Supplementary Methods

Flow cytometry

tsAM5NE AGCCs were harvested after lentivirus infection and washed with PBS once. Cells were blocked with 5% donkey serum in PBS and then reacted with goat anti-EFNB1 Ab (AF473, R&D systems), or normal goat IgG (sc-2028, Santa Cruz Biotechnology) for 1 hour on ice. Cells were then stained with R-phycoerythrin-conjugated donkey anti-goat IgG (705116147, Jackson ImmunoResearch Laboratories, West Grove, PA, USA) for another 1 hour on ice. After wash, samples were analyzed by flow cytometry.

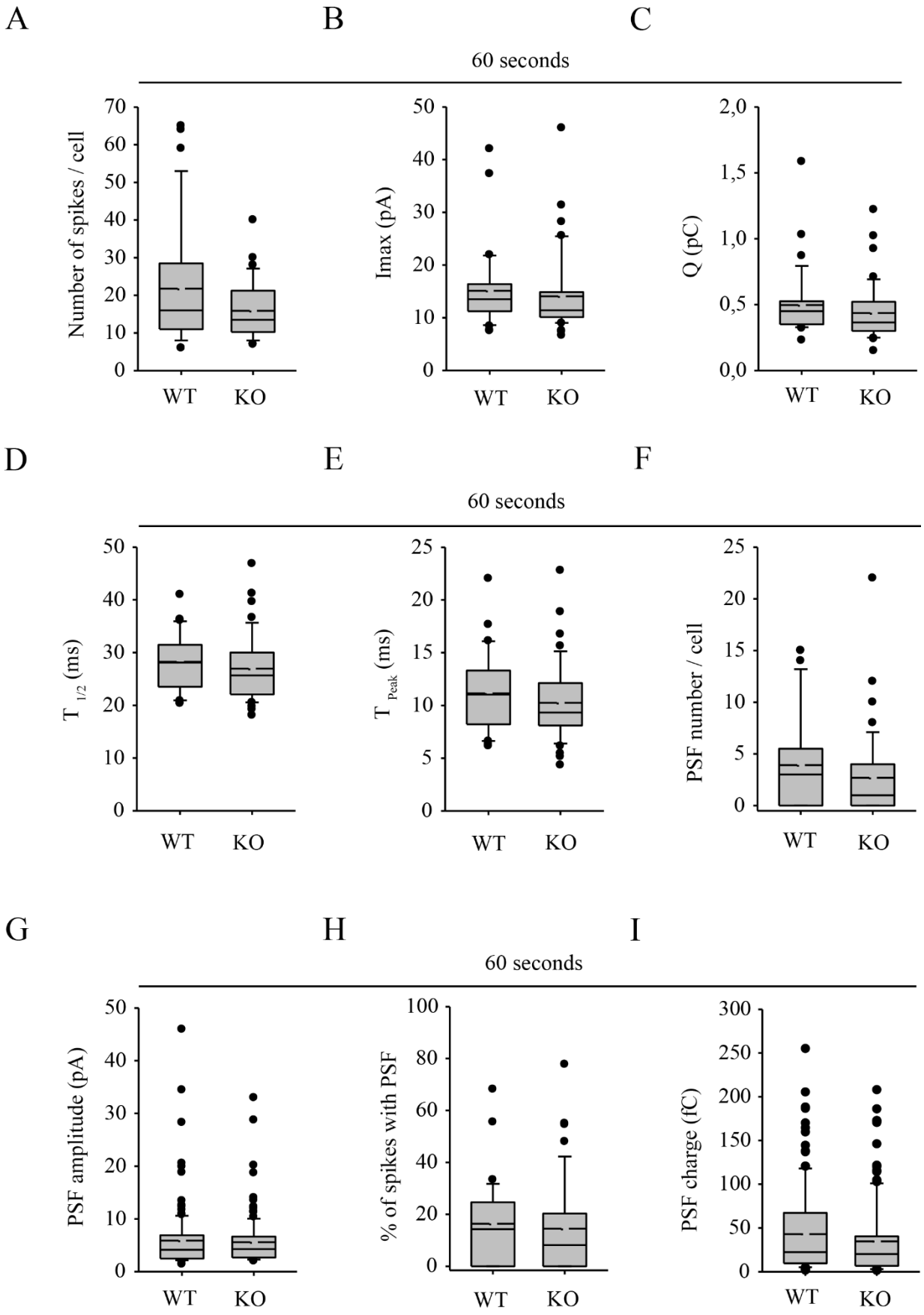
A
B
C
60 seconds
Number of spikes / cell
Imax (pA)
Q (pC)
WT
KO
D
E
F
60 seconds
T 1/2 (ms)
T Peak (ms)
PSF number / cell
WT
KO
G
H
I
60 seconds
PSF amplitude (pA)
% of spikes with PSF
PSF charge (fC)
WT
KO

J

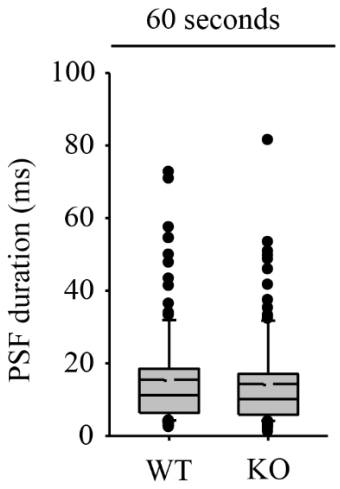

Supplementary Figure 1

S-Figure 1. No difference in CAT release between KO and WT AGCCs from female mice according to amperometry recording. AGCCs were isolated from 3 KO and 3 WT female mice, and their nicotine-stimulated CAT release was registered by amperometry. Box bar graphs show the medium (solid horizontal line in the box), mean (dashed horizontal line in the box), the 75th percentile (up part of the box), 25th percentile (lower part of the box), 95th percentile (upper whisker), 5th percentile (lower whisker), and outliners (dots beyond the 95th and 5th percentile) of each parameter. The number of total AGCCs tested or total pre-spike feet (PSF) analyzed are indicated. The Mann-Whitney Rank Sum tests were conducted for statistical analysis due to failed normality tests of the data. None of the comparisons of the parameters between the female KO and WT AGCCs was significantly different. The number of spikes observed in the 60 second period after nicotine stimulation (**A**), spike peak height (Imax) (**B**), charge of the spikes (Q) (**C**), half time to reach the spikes peak ($T_{½}$) (**D**), time to reach the peak (T_{peak}) (**E**), number of PSF observed per cell (**F**), PSF amplitude (**G**), percentage of spikes with PSF (**H**), PSF charge (fC) (**I**), and PSF duration (**J**) are illustrated. For **A-F and H**, 33 WT cells and 48 KO cells were analyzed; for **G** and **I**, 129 PSF of WT cells and 129 PSF of KO cells.

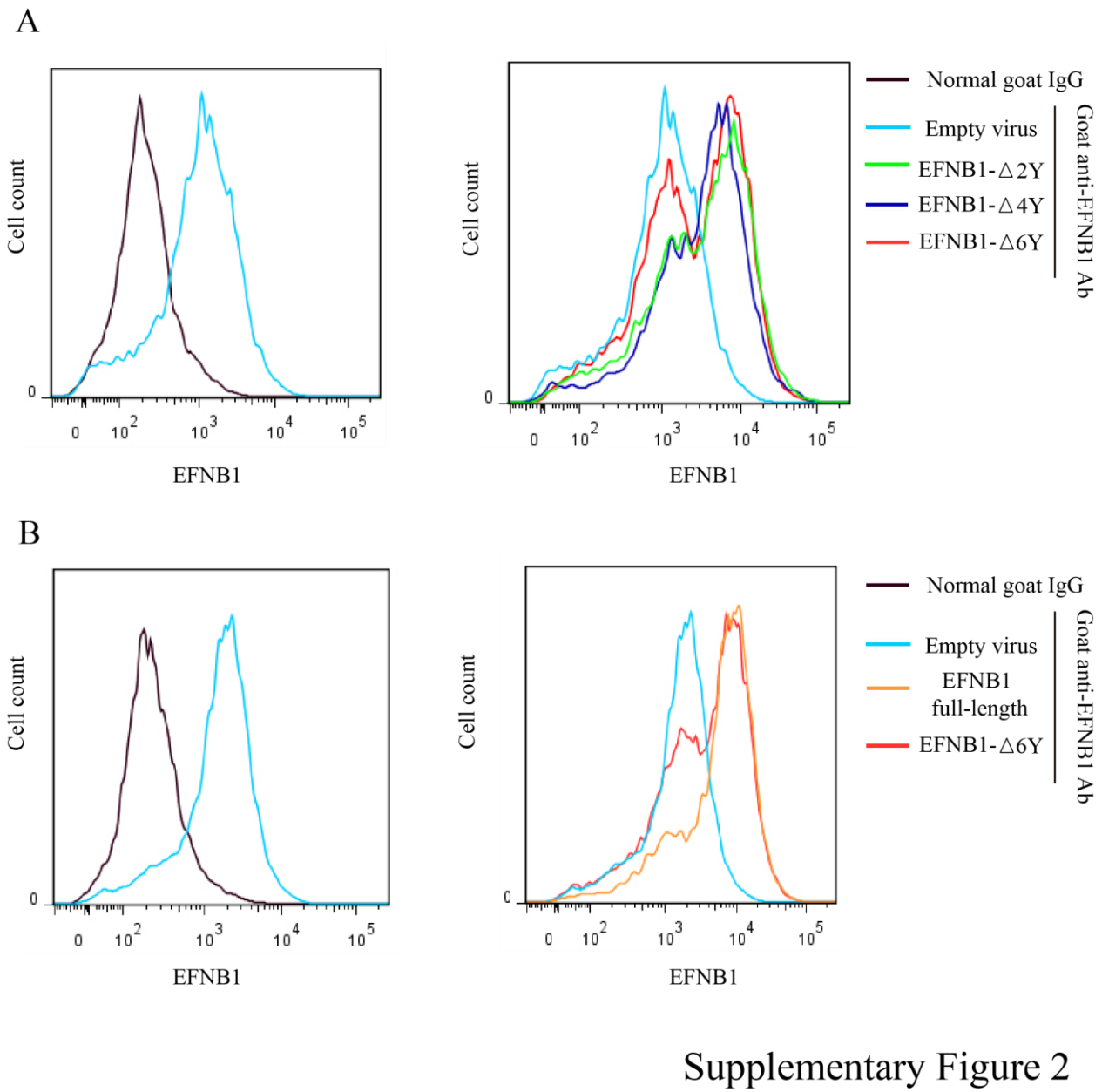

Supplementary Figure 2

S-Figure 2. Similar levels of cell surface EFNB1 expression in tsAM5NE AGCCs infected with lentiviruses expressing different EFNB1 intracellular domain deletion mutants. tsAM5NE cells were transfected with lentiviruses expressing different intracellular domain deletion mutants. After 72 hours, their expression was assessed by flow cytometry. **A**. The similar cell surface overexpression of *EFNB1Δ2Y*, *EFNB1Δ4Y,* and *EFNB1Δ6Y*. The expression of the endogenous *EFNB1* (light blue) in empty virus-transfected cells is shown in the left histogram. The similar levels of *Efnb1Δ2Y* (green), *EFNB1Δ4Y* (dark blue) and *EFNB1Δ6Y* (red) overexpression above the

endogenous EFNB1 level are shown in the right histogram. **B**. The similar cell surface overexpression of the full-length exogenous *EFNB1* and *EFNB1Δ6Y* in the lentivirus-transfected cells. The expression of the endogenous *EFNB1* (light blue) in empty virus-transfected cells is shown in the left histogram. The similar levels of the full-length exogenous EFNB1 (orange) and EFNB1Δ6Y (red) above the endogenous EFNB1 level are shown in the right histogram.

Supplementary Table

		0 s vs. 20 s	0 s vs. 40 s	0 s vs. 60 s	No stimulation vs. stimulation
Figure 2B	Male WT	0.0155	0.004	0.012	<0.001
	Male KO	0.0137	0.001	0.001	0.003
	Castrated male KO	0.001	<0.001	<0.001	<0.001
Figure 2C	Male WT	0.016	0.004	0.012	<0.001
	Castrated male WT	0.002	0.001	0.001	<0.001
Figure 2D	Female WT	0.003	<0.001	<0.001	<0.001
	Female KO	<0.001	<0.001	<0.001	<0.001
Figure 2E	Female KO + vehicle	<0.001	<0.001	<0.001	<0.001
	Female KO + testosterone-BSA	0.071	0.001	0.229	0.0041
Figure 2F	Female WT + vehicle	<0.001	<0.001	<0.001	<0.001
	Female WT + testosterone-BSA	0.001	<0.001	<0.001	<0.001
Figure 2G	Male WT + vehicle	<0.001	<0.001	<0.001	<0.001
	Male WT + estrogen	<0.001	<0.001	<0.001	<0.001
Figure 2H	Male KO + vehicle	0.092	0.005	0.008	0.001

	Male KO + estrogen	0.065	0.004	0.006	0.003

S-Table 1. The detailed statistical analysis of percentages of KO and WT AGCCs with cortical F-actin disassembly for Figure 2

The changes of cortical F-actin disassembly of a given type of AGCCs or a given treatment between two points in time during stimulation, or between being unstimulated (0 s) versus all those being stimulated (20 s + 40 s+ 60 s) were analyzed by two-way paired Student's *t*-test. *P*-values are presented.

Chapitre 6 – General Discussion

The adrenal gland chromaffin cells are the main source of circulating catecholamines during physiological stress conditions. They are activated by stimulating with acetylcholine released from preganglionic splanchnic fibers. Due to the important roles of the catecholamines in the maintenance of homeostasis, the study on chromaffin cell biology has been going on for decades (Borges et al., 2018). In this study, we report for the first time to our knowledge on the biological functions of the EPH/EFN family in AGCCs. EPHB6 knockout in the AGCCs leads to the increased outwards BK channel currents, which causes the VGCC early closure reducing the ACh-triggered calcium influx. While the absence of EPHB6 impairs the reverse signaling from EPHB6 to EFNB1, and further compromises the strength of RAC1/MKK7/JNK/JUN/AP1/EGR1/TH pathway, leading to decreased catecholamine synthesis. In addition, the defective EPHB6/EFNB1 reverse signaling also compromises the signaling pathway FYN/C-ABL/MICAL1, thereby restricting the F-actin disassembly and resulting in the defective catecholamine secretion. These signaling pathways overlay with the Ca^{2+}-dependent signaling induced by ACh receptor activation in AGCCs and are essential for the optimal function of catecholamine synthesis and secretion.
It is noteworthy that the role of EPHB6/EFNB1 in chromaffin cell biology requires the presence of testosterone. As a new player in the modulation of chromaffin cell function, EPH/EFN family may play a role in some catecholamine-related cardiovascular and neurodegenerative diseases and become a potential therapeutic target in the future.

One of the intriguing findings in this study is the reverse signaling from EPHB6 to EFNB1, but not the forward signaling, is responsible for the chromaffin cell function regulation. As a pseudokinase, EPHB6 has no kinase activity to directly catalyze the downstream molecules. However, it can be phosphorylated by cross-linking with other EPHs or SRFs and exert regulatory properties via scaffolding or recruiting downstream molecules upon the EFNs ligation (Liang et al., 2019). In addition, the interaction between EPHB6 and EFNBs will form a tetrameric complex exerting bidirectional signaling to regulate cell function, which is a unique feature of the EPH/EFN signaling (Kullander and Klein, 2002). In our case, EPHB6 acts as a “ligand”, while EFNB1 acts as a “receptor”. Their ligation induces reverse signaling through EFNB1. Such reverse signaling

triggered by EPHB6 was also reported to contribute to VSMC contraction regulation (Luo et al., 2012). In the adrenal medulla, both EPHB6 and EFNB1 are highly expressed on the surface of chromaffin cells. The direct interaction of the adjacent cells provides the basis for the formation of the EPHB6/EFNB1 tetrameric complex to transduce the reverse signaling to the interior of the cell. Our research provides another piece of evidence for the mode of kinase-null EPHB6 receptor's action in regulating cell function.

In the research of catecholamine secretion regulation, we found the EPHB6 was involved in Ca^{2+} influx regulation in AGCCs upon ACh stimulation. The presence of EPHB6 might interfere with the positive effect of testosterone on BK channel activity and prevent excessive outward K^+ currents. The relationship between testosterone and BK channel, testosterone and EPHB6, both require further clarification. Then we revealed the EPHB6/EFNB1 reverse signaling regulates the F-actin disassembly via MICAL-1 activation, which further controls the catecholamine secretion in AGCCs. Mical-1 is an oxidoreductase enzyme, which specifically mediates oxidation of Met44 and Met77 of F-actin, resulting to F-actin depolymerization (Grintsevich et al., 2017). The phosphorylation of Mical is essential for its optimal activity on F-actin disassembly (Yoon et al., 2017). It has been reported that the MICAL-1-induced oxidation of actin could be regulated by the Semaphorin/Plexin signaling (Schmidt et al., 2008; Hung et al., 2010), growth factor signaling (Yoon et al., 2017), and Rab GTPases (Fremont et al., 2017). It's a novel finding that the EPH/EFN signaling is involved in regulating MICAL-1 activity for F-actin disassembly through the FYN/c-ABL/MICAL-1 pathway. The application of either FYN inhibitor or c-ABL inhibitor significantly reduces the phosphorylation of MICAL-1 in AGCCs, which indicates the activities of FYN and c-ABL are critical for MICAL-1 activity. However, it's still not clear how the EPHB6/EFNB1 reverse signaling transduces to the activity of FYN. Many studies have demonstrated that the reverse signaling can recruit SFKs to the EFNB1-containing membrane cluster and phosphorylate the tyrosine residues at the cytoplasmic domain of EFNB1, which then serves as a docking site for SH2-containing proteins to transduce the signal into the cell (Palmer et al., 2002; Vermeer et al., 2012). Thus, FYN could be immediately downstream of EFNB1. Further research is needed to confirm whether FYN is indeed physically associated with EFNB1. We can overexpress the EFNB1 and FYN in our tsAM5NE cells and perform affinity purifications after EPHB6-FC stimulation. The

lysates can also be used in an in vitro kinase assay to identify the activity of FYN. In our study, a 7-aa sequence between residues 322 and 328 (containing Y323 and Y328) at the intracellular domain of EFNB1 is critical for catecholamine secretion regulation. It can be inferred that this sequence may be the binding site of FYN on EFNB1. These deletion mutations of EFNB1 intracellular tails can be introduced into the above system to prove this hypothesis. What's more, GST-purified EFNB1 cytoplasmic domain with different deletion mutants can be used as a substrate in the *in vitro* kinase assay to further identify whether the tyrosine residue at the binding site is phosphorylated by the FYN activation. These experiments will help us understand the link between EFNB1 and FYN more clearly.

While in the research of catecholamine synthesis regulation, we found the transcription of TH enzyme in AGCCs was mediated by EPHB6/EFNB1 reverse signaling via EGR1, which is an important transcription factor for TH transcription (Nakashima et al., 2003). Molecules in the signaling pathway RAC1/MKK7/JNK/JUN/AP1 were proved essential for EGR1 transcription in the study. It's an interesting finding that the strength of this pathway can be regulated by EPH/EFN signaling. Same as in the catecholamine secretion study, the detailed signaling between EFNB1 and RAC1 is still not clear. Some studies have provided evidence for the interaction between EFNBs and RAC1. For instance, the stimulation of EPHB2-Fc on the primary cortical neurons triggered the reverse signaling through EFNB1, resulting in the colocalization of EFNB1 and Tiam1, a Rac1-specific guanine nucleotide-exchanging factor, and further activated the Rac1 (Tanaka et al., 2004). The colocalization of EFNB3 with RAC1 was also observed in human glioma cells (Nakada et al., 2006). Some SH2/SH3 adaptors, such as Grb4, could bind to the tyrosine-phosphorylated sites of EFNBs and recruit RAC exchange factors to activate RAC (Noren and Pasquale, 2004). Thus, the interaction of EFNB1 and RAC1 during catecholamine synthesis in AGCCs should also require the participation of some SH2/SH3 adaptors and RAC GEFs. Some high-throughput approaches, such as affinity purification coupled to mass spectrometry and proximity labeling approach combined to mass spectrometry, can help us to identify the transient or stable protein-protein interactions in the AGCCs, which provide reliable clues for us to further study the precise signaling between EFNB1 and RAC1 in our system.

Based on the results found in this study, we revealed the previously unknown function of EPH/EFN family on catecholamine synthesis and secretion in AGCCs. Since the circulated catecholamines are critical for blood pressure regulation, we will further discuss the contribution of this work to the role of the EPH/EFN family on blood pressure regulation.

Hypertension is one of the most critical risks for morbidity and mortality worldwide. With the increasing aging of the population, the incidence of hypertension and its related cardiovascular adverse events has risen sharply. Our research on the role of the EPH/EFN family on blood pressure regulation has enriched the understanding of hypertension pathogenesis. Our lab has previously found that EPHB6, EFNB1, and EFNB3 deletion results in blood pressure elevation, while EPHB4 and EFNB2 deletion reduces it. These effects depend on the joint action of these molecules and sex hormones. In this study, we revealed that EPHB6 positively regulates catecholamine synthesis and secretion in mouse AGCCs in the presence of sufficient testosterone via reverse signaling through EFNB1. Therefore, when EPHB6 was deleted, catecholamine secretion was reduced. In the castrated KO mice, due to insufficient testosterone, the catecholamine secretion by the KO AGCC returned to a normal level. Since EPHB6 deletion also caused increased VSMC contractility when testosterone was insufficient, the net result of EPHB6 deletion and insufficient testosterone was augmented blood pressure. This implies that the hypogonadal men with deleterious variants in EPHB6 or molecules in the EPHB6 signaling pathway (such as EFNBs, BK channel, and ACh receptor) will lose the protective effect of the reduced catecholamine level and lead to hypertension (Fig.1).

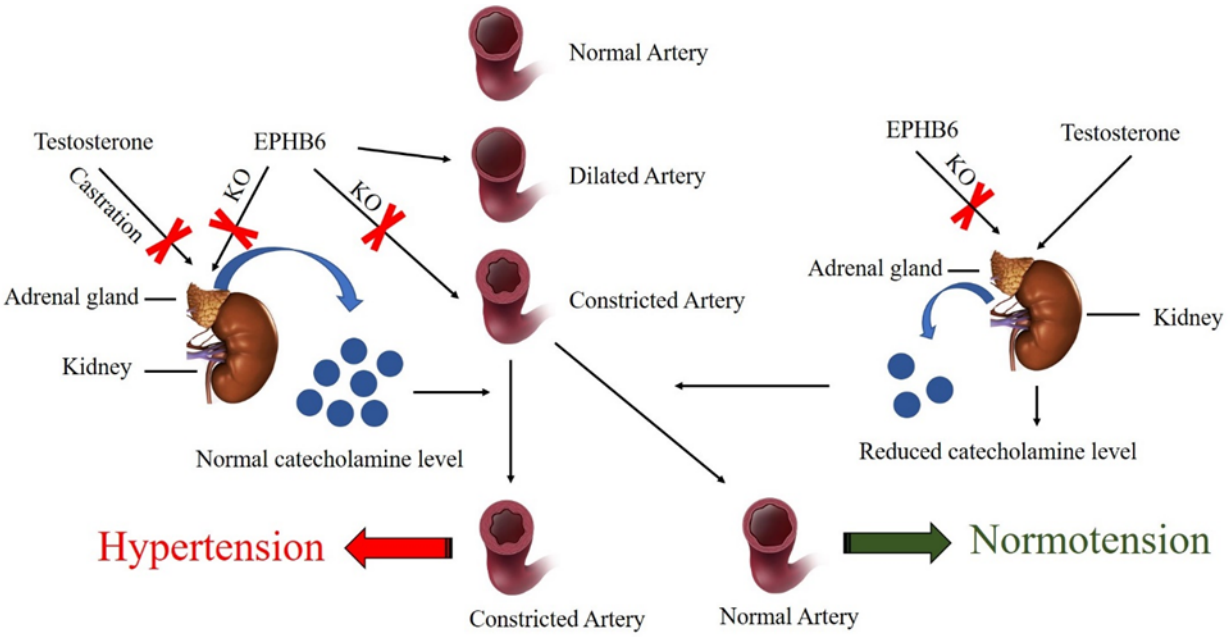

Figure 1. A diagram depicting the regulation of blood pressure by EPHB6 signaling and testosterone

This model is very meaningful for the study of the mechanism of hypertension in a subpopulation of aging males with hypogonadism. Hypogonadism in men is characterized by diminished production of androgens due to the decreased functional activity of the testes. This leads to a series of symptoms, including sexual dysfunction, cardiovascular disease, weakness, decreased bone density, and so on. According to statistics, the age-related decline of testosterone in men begins in their mid-30s and continues at an average annual rate of 1.6% (Qaseem et al., 2020). The prevalence rate of hypogonadism in men in the US aged ⩾45 years is about 38.7%. Sixty-five percent of hypogonadal patients have hypertension, while the proportion in eugonadal patients is 51%. Conversely, the odds ratios of hypogonadism are significantly higher in men with hypertension compared to men with normal blood pressure (Mulligan et al., 2006). In the European Male Aging Study, hypogonadism's prevalence rate in men aged 40-80 is 23% (Wu et al., 2010a). The level of systolic blood pressure is revealed to be inversely associated with the total testosterone level in older men (Laughlin et al., 2008). Based on novel findings in our studies on the role of EPH/EFN family and sex hormones in blood pressure regulation, we can reasonably

speculate on one of the mechanisms of hypertension in hypogonadal men. A subpopulation of this group might have some deleterious variants in EPHB6 or molecules in its signaling pathway (such as EFNBs, BK channel, ACh receptor). Such mutations augment the VSMCs contraction and the vascular tone due to the loss of the negative effects of EPHB6/EFNBs reverse signaling on vasoconstriction. When they are young with sufficient testosterone, the protective effect of the reduced catecholamine level caused by impaired catecholamine synthesis and secretion of AGCCs neutralizes the above-described effect of increased vascular tone. Thus, their blood pressure is kept in a normal range. As they grow older, their testosterone levels progressively decrease. The reduced testosterone levels in combination with the impaired EPHB6/EFNBs reverse signaling cascades restore catecholamine levels, and hence these older men lose the protective effect of the mutated EPHB6 against hypertension. As a consequence, for these patients, there is an relatively increased hypertension risk, compared to those their counterpart without EPHB6 mutations, in the presence of other genetic and environmental factors.

To demonstrate this possible hypertension pathogenesis in men with hypogonadism, we need to get more evidence of the variants of EPHB6 or its signaling molecules in this subpopulation. We also need to test the catecholamines levels in 24-hour urine or in the blood of the adult male humans containing these variants with normal testosterone levels. If their catecholamines levels are significantly reduced compared to other males without such kind of variants, it will give us strong support for our speculation.

To evaluate our hypothesis about the role of the EPH/EFN family in human hypertension, our lab has conducted some human genetic studies on the molecules involved in the EPH/EFN signaling pathway. We analyzed single nucleotide polymorphisms (SNP) in the *EPHB6* gene and its main relevant ligands, *EFNB1* and *EFNB3,* genes in 4,480 Han Chinese males with hypogonadism (Wu et al., 2018). Three SNPs in the 5` upstream of the *EFNB3* gene were detected to be significantly associated with hypertension in this cohort, whereas no meaningful discovery in the *EFNB1* and *EPHB6* SNPs. We assumed these three *EFNB3* SNPs found in hypogonadal males were lose-of-function mutations so that in aged men with low testosterone levels, the occurrence of hypertension would associate with the lose-of-EFNB3-function caused by these SNPs. This finding was consistent with the evidence in our animal experiment that castrated EFNB3 KO mice had

higher blood pressure than their WT counterparts and also supported our explanation about the association of the *EFNB3* mutant to hypertension in the population of the *ADVANCE* study (Wang et al., 2016c;Tremblay et al., 2017).

The catecholamine synthesis and release in AGCCs are majorly triggered by the activation of the nicotinic ACh receptor (nAChR). nAChR is a ligand-gated ion channel made up of five subunits, who have five different types (α, β, δ, ε, and γ), and the composition varies according to the species and cell type. The α3 (CHRNA3) and β4 (CHRNB4) subunits are most abundant in the mouse AGCCs, while they are also expressed and function in human AGCCs (Mousavi et al., 2001;Wu et al., 2010b). The function of nAChR can be modulated by many proteins interacting with it, including SFKs, Abl kinases, Calnexin, and others. (Jones et al., 2010). EPHB6 may also interact with nAChR and incorporate it into the EPHB6 reverse signaling on catecholamine production regulation in AGCCs. Indeed, the physical interaction between EPHB6 and nAChR subunit CHRNA3 in mouse AGCCs was revealed by three different methods (co-immunoprecipitation, colocalization, and FRET) (Wu et al., 2020). We further tried to explore whether such interaction regulated nAChR activity. We hypothesized that the compromised EPHB6 signaling might suppress the initial currents through nAChR upon neurotransmitter stimulation, leading to the reduced catecholamine synthesis and secretion in male EPHB6 KO AGCCs. Due to technical difficulties, we failed to detect a clear nAChR current when patching primary AGCCs. However, if our hypothesis was valid, the nAChR should be one of the molecules involved in the EPHB6 signaling pathway on blood pressure regulation. Thus, we analyzed SNPs in the major nAChR subunit *CHRNA3* in 4,480 Han Chinese males with hypogonadism and found one SNP (*rs3743706*) within *CHRNA3* was significantly related to hypertension risks in this cohort (Wu et al., 2020). This SNP was in the fourth intron of *CHRNA3*. It could be part of a cis-regulatory sequence. Enhancers could exist in introns. For example, the expression of the human growth hormone gene is directly regulated by a functional SNP buried deep within intron 4 (Millar et al., 2010). An SNP rs1635852 in *JAZF1* intron 1 forms a cis-regulatory complex with other functional elements to regulate the transcription of *JAZF1* in insulinoma cells (Fogarty et al., 2013). Alternatively, this SNP might be in linkage disequilibrium (LD) with other functional SNPs. The exact action mechanism is worth further studying. If this SNP indeed has a loss-of-function role

for *CHRNA3*, the mutation will impair the function of EPHB6 signaling in AGCCs, and reduce the catecholamine secretion from AGCCs when sufficient androgen is present. The reduced catecholamine level is considered a protective factor against hypertension. Once the androgen level is significantly reduced in the hypogonadal males, catecholamines will return to a normal level and thus lose the protective effect. In this case, the enhanced vasoconstriction due to compromised EPHB6 signaling in VSMCs by any defect of EPHB6 signaling molecules will raise the blood pressure and subsequently leads to hypertension in the hypogonadal male patients.

Although no EPHB6 SNP was significantly associated with hypertension in our genetic study of the hypogonadal patients, we did find significant hypertension association of SNPs of several molecules (*e.g.,* SNPs in *EFNB3*, *GRIP1*, and *CHRNA3*) in the EPHB6 signaling pathway. There could be several reasons that no significant EPHB6 SNPs were detected in our patient genetic study. First, it could be due to insufficient sample size. Secondly, it could be due to the test group's genetic background, as we only examined Han Chinese patients. Thirdly, it is entirely possible that in humans, the responsible genetic defect lies with other EPHB6 signaling molecules, some of which we discovered and reported (Wang et al., 2016b; Tremblay et al., 2017), but not with EPHB6 *per se*.

With the increase of population aging, hypertension and its related cardiovascular adverse events have increasingly become a major challenge endangering the quality of human life. The extensive global research on the pathogenesis of hypertension allows us to understand it more deeply and comprehensively. Our research suggests that low testosterone levels may lead to hypertension in males with the variants of EPHB6 signaling molecules.

Although there are many powerful anti-hypertensive drugs in the market currently, including diuretics, beta-blockers, alpha-blockers, ACE inhibitors, angiotensin II receptor blockers, calcium channel blockers, et al., they mostly regulate the symptoms of elevated blood pressure rather than treat specific causes. Our research indicates that testosterone replacement therapy (TRT) may be a good personalized treatment for the root cause of hypertension for patients whose hypertension is caused by compromised EPHB6 signaling and hypogonadism. In addition, TRT in

hypogonadal men can also bring other benefits to improve other symptoms besides lowering blood pressure.

There are still some controversies about the benefits and adverse effects of TRT. The biggest concern about TRT is testosterone treatment may promote prostate cancer growth. This concept stems from the research of two Nobel Prize winners, Huggins and Hodges, in the 1940s. They found the incidence of prostate cancer is related to androgen activity since androgen elimination could restrain the progression of metastatic prostate cancer, while injection of androgen promotes the progression of prostate cancer (Huggins and Hodges, 2002;Morgentaler and Traish, 2009). In the following years, surgical castration or androgen deprivation therapy has shown significant effects on the reduction of PSA, which is a very sensitive indicator of prostate cancer, and on the treatment of prostate cancer.

However, since the late 1990s, more and more retrospective or prospective studies have shown that there was no clear relationship between the serum testosterone levels and PSA level, prostate size, or risk of developing prostate cancer in normal men (Monath et al., 1995; Bhasin et al., 1996; Cooper et al., 1998). These two seemingly opposite views are well explained by a saturation model, which states that the growth of prostate cancer has a testosterone-dependent phase at low testosterone levels but becomes insensitive to variation of testosterone concentration at higher levels. This is because the maximal androgen-AR binding has been achieved in the prostate at a very low testosterone concentration, much lower than its physiological concentration (Morgentaler and Traish, 2009). Wright et al. revealed that the serum testosterone concentration of the half-maximal androgen-AR binding in rat prostate is about 36 ng/dl, which is near the range of that in the castrated animals (Wright et al., 1999). This testosterone level corresponds to about 50 ng/dl in humans, while the physiological concentration range of human serum testosterone is 300–1000 ng/dl. This saturation model negates the previous cognition of the absolute adverse effect of testosterone on prostate cancer and has been further continuously proved by mountains of human studies. The TRT for hypogonadal patients induces a very short increase or no increase of PSA levels, but has no association with any increase in prostate cancer risks compared to the patients without TRT (Guay et al., 2000;Endogenous et al., 2008;McLaren et al., 2008;Coward et al., 2009;Debruyne et al.,

2017). The safety of TRT in hypogonadal patients is proved in the patients with untreated prostate cancer or with definitive prostate cancer treatment (Agarwal and Oefelein, 2005;Pastuszak et al., 2013;San Francisco et al., 2014;Kacker et al., 2016). Thus, the risk of TRT on prostate cancer growth in the subpopulation of hypogonadal males with hypertension is manageable by monitoring the testosterone level, PSA level, and prostate cancer grade before or during the application.

In addition to the risk of promoting prostate cancer growth, the cardiovascular risk of TRT is also controversial. Many cohort studies reveal increased risks of cardiovascular diseases in the older men with low plasma testosterone levels (Yeap et al., 2009; Haring et al., 2010;Soisson et al., 2013), and the treatment of testosterone in these cohorts showed a beneficial effect on reducing the cardiovascular risks and adverse consequences (Shores et al., 2012;Muraleedharan et al., 2013; Traish et al., 2017). However, an increased number of cardiovascular events, such as myocardial infarction and stroke after the TRT, was also reported in some retrospective studies, which prompted FDA to issue a safety warning to the TRT in 2014 (Vigen et al., 2013; Finkle et al., 2014). Nevertheless, more subsequent retrospective studies and randomized controlled trials support the benefit and safety of the TPT in men with hypogonadism (Basaria et al., 2015; Maggi et al., 2016; Snyder et al., 2016; Budoff et al., 2017). Lately, Farid Saad reported long-term testosterone therapy in hypogonadal men significantly reduces elevated blood pressure and improves mortality due to major adverse cardiovascular events compared to the hypogonadal men without testosterone treatment (5.4% vs. 19.5%), according to an 11-year controlled registry study of hypogonadal men (Saad et al., 2020). The American College of Physicians provided the newest clinical guideline for testosterone treatment in aged men with hypogonadism in 2020. They reported that testosterone treatment in this subpopulation did not increase the risk of death, cardiovascular events, prostate cancer, or pulmonary embolism, according to 20 randomized controlled trials with an average follow-up time of 0.73 to 10.3 years (Qaseem et al., 2020). A large randomized controlled trial to evaluate the impact of TRT on the incidence of major adverse cardiovascular events in men with hypogonadism and the measurement of its efficacy (TRAVERSE) has been ongoing since 2018 in the US, which will provide much stronger and clearer evidence for the safety of TPT in cardiovascular risk (Gagliano-Juca and Basaria, 2019). Before reaching a

certain result, the clinicians are suggested to have a full discussion of the potential benefits and harms of TPT with their patients before the treatment.

Academic contribution and future research directions

This research reveals the previously unknown function of the EPH/EFN family on blood pressure regulation, especially on the regulation and mechanisms of CAT secretion by AGCCs. The blood pressure-related phenotype found in EPHB6 KO mice and the human genetic studies about the EPHB6 signaling molecules provides a novel explanation for the pathogenesis of hypertension in some men with hypogonadism. We propose that testosterone replacement therapy could be a causal treatment for hypertension in this particular subpopulation in the era of personalized medicine. In the future, we need to verify the effect of the EPHB6 signaling on the nAChR, BK channel, and androgen receptor. We have detected several SNPs in the molecules involved in the EPHB6 signaling pathway in human genetic studies. The function validation of these SNPs is a crucial task to establish whether the variants are simply non-functional polymorphisms or truly functional mutations.

Références bibliographiques

Niels Grabe [Online]. Available: http://gene-regulation.com/pub/programs/alibaba2/index.html [Accessed].

Agarwal, P.K., and Oefelein, M.G. (2005). Testosterone replacement therapy after primary treatment for prostate cancer. *J Urol* 173**,** 533-536.

Alfaro, D., Rodriguez-Sosa, M.R., and Zapata, A.G. (2020). Eph/ephrin Signaling and Biology of Mesenchymal Stromal/Stem Cells. *J Clin Med* 9.

Alvarez, Y.D., Belingheri, A.V., Perez Bay, A.E., Javis, S.E., Tedford, H.W., Zamponi, G., and Marengo, F.D. (2013). The immediately releasable pool of mouse chromaffin cell vesicles is coupled to P/Q-type calcium channels via the synaptic protein interaction site. *PLoS One* 8**,** e54846.

Alvarez, Y.D., Ibanez, L.I., Uchitel, O.D., and Marengo, F.D. (2008). P/Q Ca2+ channels are functionally coupled to exocytosis of the immediately releasable pool in mouse chromaffin cells. *Cell Calcium* 43**,** 155-164.

Alvarez, Y.D., and Marengo, F.D. (2011). The immediately releasable vesicle pool: highly coupled secretion in chromaffin and other neuroendocrine cells. *J Neurochem* 116**,** 155-163.

Anaissie, J., Roberts, N.H., Wang, P., and Yafi, F.A. (2017). Testosterone Replacement Therapy and Components of the Metabolic Syndrome. *Sex Med Rev* 5**,** 200-210.

Anggard, E., Lewander, T., and Sjoquist, B. (1974). Determination of homovanillic acid turnover in man. *Life Sci* 15**,** 111-122.

Aranyi, T., Sarkis, C., Berrard, S., Sardin, K., Siron, V., Khalfallah, O., and Mallet, J. (2007). Sodium butyrate modifies the stabilizing complexes of tyrosine hydroxylase mRNA. *Biochem Biophys Res Commun* 359**,** 15-19.

Armando, I., Jezova, M., Juorio, A.V., Terron, J.A., Falcon-Neri, A., Semino-Mora, C., Imboden, H., and Saavedra, J.M. (2002). Estrogen upregulates renal angiotensin II AT(2) receptors. *Am J Physiol Renal Physiol* 283**,** F934-943.

Astin, J.W., Batson, J., Kadir, S., Charlet, J., Persad, R.A., Gillatt, D., Oxley, J.D., and Nobes, C.D. (2010). Competition amongst Eph receptors regulates contact inhibition of locomotion and invasiveness in prostate cancer cells. *Nat Cell Biol* 12**,** 1194-1204.

Aunis, D. (1998). Exocytosis in chromaffin cells of the adrenal medulla. *Int Rev Cytol* 181**,** 213-320.

Axelrod, J. (1976). Catecholamines and hypertension. *Clin Sci Mol Med Suppl* 3**,** 415s-421s.

Azziz, R., Carmina, E., Dewailly, D., Diamanti-Kandarakis, E., Escobar-Morreale, H.F., Futterweit, W., Janssen, O.E., Legro, R.S., Norman, R.J., Taylor, A.E., Witchel, S.F., and Androgen Excess, S. (2006). Positions statement: criteria for defining polycystic ovary syndrome as a predominantly hyperandrogenic syndrome: an Androgen Excess Society guideline. *J Clin Endocrinol Metab* 91**,** 4237-4245.

Bader, M.F., Doussau, F., Chasserot-Golaz, S., Vitale, N., and Gasman, S. (2004). Coupling actin and membrane dynamics during calcium-regulated exocytosis: a role for Rho and ARF GTPases. *Biochim Biophys Acta* 1742**,** 37-49.

Barton, M., Filardo, E.J., Lolait, S.J., Thomas, P., Maggiolini, M., and Prossnitz, E.R. (2018). Twenty years of the G protein-coupled estrogen receptor GPER: Historical and personal perspectives. *J Steroid Biochem Mol Biol* 176**,** 4-15.

Basaria, S., Harman, S.M., Travison, T.G., Hodis, H., Tsitouras, P., Budoff, M., Pencina, K.M., Vita, J., Dzekov, C., Mazer, N.A., Coviello, A.D., Knapp, P.E., Hally, K., Pinjic, E., Yan, M., Storer, T.W., and Bhasin, S. (2015). Effects of Testosterone Administration for 3 Years on Subclinical Atherosclerosis Progression in Older Men With Low or Low-Normal Testosterone Levels: A Randomized Clinical Trial. *JAMA* 314**,** 570-581.

Batson, J., Maccarthy-Morrogh, L., Archer, A., Tanton, H., and Nobes, C.D. (2014). EphA receptors regulate prostate cancer cell dissemination through Vav2-RhoA mediated cell-cell repulsion. *Biol Open* 3**,** 453-462.

Beaulieu, J.M., and Gainetdinov, R.R. (2011). The physiology, signaling, and pharmacology of dopamine receptors. *Pharmacol Rev* 63**,** 182-217.

Bennesch, M.A., and Picard, D. (2015). Minireview: Tipping the balance: ligand-independent activation of steroid receptors. *Mol Endocrinol* 29**,** 349-363.

Benten, W.P., Lieberherr, M., Giese, G., Wrehlke, C., Stamm, O., Sekeris, C.E., Mossmann, H., and Wunderlich, F. (1999a). Functional testosterone receptors in plasma membranes of T cells. *FASEB J* 13**,** 123-133.

Benten, W.P., Lieberherr, M., Stamm, O., Wrehlke, C., Guo, Z., and Wunderlich, F. (1999b). Testosterone signaling through internalizable surface receptors in androgen receptor-free macrophages. *Mol Biol Cell* 10**,** 3113-3123.

Best, J.A., and Tank, A.W. (1998). The THCRE2 site in the rat tyrosine hydroxylase gene promoter is responsive to phorbol ester. *Neurosci Lett* 258**,** 131-134.

Beuming, T., Skrabanek, L., Niv, M.Y., Mukherjee, P., and Weinstein, H. (2005). PDZBase: a protein-protein interaction database for PDZ-domains. *Bioinformatics* 21**,** 827-828.

Bhasin, S., Storer, T.W., Berman, N., Callegari, C., Clevenger, B., Phillips, J., Bunnell, T.J., Tricker, R., Shirazi, A., and Casaburi, R. (1996). The effects of supraphysiologic doses of testosterone on muscle size and strength in normal men. *N Engl J Med* 335**,** 1-7.

Bhattacharya, R.K., Khera, M., Blick, G., Kushner, H., Nguyen, D., and Miner, M.M. (2011). Effect of 12 months of testosterone replacement therapy on metabolic syndrome components in hypogonadal men: data from the Testim Registry in the US (TRiUS). *BMC Endocr Disord* 11**,** 18.

Binns, K.L., Taylor, P.P., Sicheri, F., Pawson, T., and Holland, S.J. (2000). Phosphorylation of tyrosine residues in the kinase domain and juxtamembrane region regulates the biological and catalytic activities of Eph receptors. *Mol Cell Biol* 20**,** 4791-4805.

Bohme, B., Holtrich, U., Wolf, G., Luzius, H., Grzeschik, K.H., Strebhardt, K., and Rubsamen-Waigmann, H. (1993). PCR mediated detection of a new human receptor-tyrosine-kinase, HEK 2. *Oncogene* 8**,** 2857-2862.

Bong, Y.S., Lee, H.S., Carim-Todd, L., Mood, K., Nishanian, T.G., Tessarollo, L., and Daar, I.O. (2007). ephrinB1 signals from the cell surface to the nucleus by recruitment of STAT3. *Proc Natl Acad Sci U S A* 104**,** 17305-17310.

Bong, Y.S., Park, Y.H., Lee, H.S., Mood, K., Ishimura, A., and Daar, I.O. (2004). Tyr-298 in ephrinB1 is critical for an interaction with the Grb4 adaptor protein. *Biochem J* 377**,** 499-507.

Borges, R., Gandia, L., and Carbone, E. (2018). Old and emerging concepts on adrenal chromaffin cell stimulus-secretion coupling. *Pflugers Arch* 470**,** 1-6.

Borisovska, M., Zhao, Y., Tsytsyura, Y., Glyvuk, N., Takamori, S., Matti, U., Rettig, J., Sudhof, T., and Bruns, D. (2005). v-SNAREs control exocytosis of vesicles from priming to fusion. *EMBO J* 24**,** 2114-2126.

Borkowski, K.R., and Quinn, P. (1984). Adrenaline and the development of genetic hypertension. *J Hypertens Suppl* 2**,** S81-83.

Bosk, S., Braunger, J.A., Gerke, V., and Steinem, C. (2011). Activation of F-actin binding capacity of ezrin: synergism of PIP(2) interaction and phosphorylation. *Biophys J* 100**,** 1708-1717.

Bourdeau, V., Deschenes, J., Metivier, R., Nagai, Y., Nguyen, D., Bretschneider, N., Gannon, F., White, J.H., and Mader, S. (2004). Genome-wide identification of high-affinity estrogen response elements in human and mouse. *Mol Endocrinol* 18**,** 1411-1427.

Boyan, B.D., Sylvia, V.L., Frambach, T., Lohmann, C.H., Dietl, J., Dean, D.D., and Schwartz, Z. (2003). Estrogen-dependent rapid activation of protein kinase C in estrogen receptor-positive MCF-7 breast cancer cells and estrogen receptor-negative HCC38 cells is membrane-mediated and inhibited by tamoxifen. *Endocrinology* 144**,** 1812-1824.

Brantley-Sieders, D.M., and Chen, J. (2004). Eph receptor tyrosine kinases in angiogenesis: from development to disease. *Angiogenesis* 7**,** 17-28.

Breitsprecher, D., and Goode, B.L. (2013). Formins at a glance. *J Cell Sci* 126**,** 1-7.

Brouns, M.R., Matheson, S.F., and Settleman, J. (2001). p190 RhoGAP is the principal Src substrate in brain and regulates axon outgrowth, guidance and fasciculation. *Nat Cell Biol* 3**,** 361-367.

Bruckner, K., Pablo Labrador, J., Scheiffele, P., Herb, A., Seeburg, P.H., and Klein, R. (1999). EphrinB ligands recruit GRIP family PDZ adaptor proteins into raft membrane microdomains. *Neuron* 22**,** 511-524.

Budoff, M.J., Ellenberg, S.S., Lewis, C.E., Mohler, E.R., 3rd, Wenger, N.K., Bhasin, S., Barrett-Connor, E., Swerdloff, R.S., Stephens-Shields, A., Cauley, J.A., Crandall, J.P., Cunningham, G.R., Ensrud, K.E., Gill, T.M., Matsumoto, A.M., Molitch, M.E., Nakanishi, R., Nezarat, N., Matsumoto, S., Hou, X., Basaria, S., Diem, S.J., Wang, C., Cifelli, D., and Snyder, P.J. (2017). Testosterone Treatment and Coronary Artery Plaque Volume in Older Men With Low Testosterone. *JAMA* 317**,** 708-716.

Buhler, F.R., Amann, F.W., Bolli, P., Hulthen, L., Kiowski, W., Landmann, R., and Burgisser, E. (1982). Elevated adrenaline and increased alpha-adrenoceptor-mediated vasoconstriction in essential hypertension. *J Cardiovasc Pharmacol* 4 Suppl 1**,** S134-138.

Bush, J.O., and Soriano, P. (2010). Ephrin-B1 forward signaling regulates craniofacial morphogenesis by controlling cell proliferation across Eph-ephrin boundaries. *Genes Dev* 24**,** 2068-2080.

Buvat, J., Maggi, M., Guay, A., and Torres, L.O. (2013). Testosterone deficiency in men: systematic review and standard operating procedures for diagnosis and treatment. *J Sex Med* 10**,** 245-284.

Byrne, C.J., Khurana, S., Kumar, A., and Tai, T.C. (2018). Inflammatory Signaling in Hypertension: Regulation of Adrenal Catecholamine Biosynthesis. *Front Endocrinol (Lausanne)* 9**,** 343.

Cai, J., Hong, Y., Weng, C., Tan, C., Imperato-Mcginley, J., and Zhu, Y.S. (2011). Androgen stimulates endothelial cell proliferation via an androgen receptor/VEGF/cyclin A-mediated mechanism. *Am J Physiol Heart Circ Physiol* 300**,** H1210-1221.

Cairrao, E., Alvarez, E., Carvas, J.M., Santos-Silva, A.J., and Verde, I. (2012). Non-genomic vasorelaxant effects of 17beta-estradiol and progesterone in rat aorta are mediated by L-type Ca2+ current inhibition. *Acta Pharmacol Sin* 33**,** 615-624.

Campos, C., Sartorio, C.L., Casali, K.R., Fernandes, R.O., Llesuy, S., Da Rosa Araujo, A.S., Bello-Klein, A., and Rigatto, K.V. (2014). Low-dose estrogen is as effective as high-dose treatment in rats with postmenopausal hypertension. *J Cardiovasc Pharmacol* 63**,** 144-151.

Carey, R.M. (2013). The intrarenal renin-angiotensin and dopaminergic systems: control of renal sodium excretion and blood pressure. *Hypertension* 61**,** 673-680.

Cerretti, D.P., Vanden Bos, T., Nelson, N., Kozlosky, C.J., Reddy, P., Maraskovsky, E., Park, L.S., Lyman, S.D., Copeland, N.G., Gilbert, D.J., and Et Al. (1995). Isolation of LERK-5: a ligand of the eph-related receptor tyrosine kinases. *Mol Immunol* 32**,** 1197-1205.

Chambliss, K.L., Yuhanna, I.S., Mineo, C., Liu, P., German, Z., Sherman, T.S., Mendelsohn, M.E., Anderson, R.G., and Shaul, P.W. (2000). Estrogen receptor alpha and endothelial nitric oxide synthase are organized into a functional signaling module in caveolae. *Circ Res* 87**,** E44-52.

Chan, C., Beltzner, C.C., and Pollard, T.D. (2009). Cofilin dissociates Arp2/3 complex and branches from actin filaments. *Curr Biol* 19**,** 537-545.

Chang, C., Saltzman, A., Yeh, S., Young, W., Keller, E., Lee, H.J., Wang, C., and Mizokami, A. (1995). Androgen receptor: an overview. *Crit Rev Eukaryot Gene Expr* 5**,** 97-125.

Chang, C.W., Hui, E., Bai, J., Bruns, D., Chapman, E.R., and Jackson, M.B. (2015). A structural role for the synaptobrevin 2 transmembrane domain in dense-core vesicle fusion pores. *J Neurosci* 35**,** 5772-5780.

Chang, Q., Jorgensen, C., Pawson, T., and Hedley, D.W. (2008). Effects of dasatinib on EphA2 receptor tyrosine kinase activity and downstream signalling in pancreatic cancer. *Br J Cancer* 99**,** 1074-1082.

Chen, F., Liu, Z., Peng, W., Gao, Z., Ouyang, H., Yan, T., Ding, S., Cai, Z., Zhao, B., Mao, L., and Cao, Z. (2018). Activation of EphA4 induced by EphrinA1 exacerbates disruption of the blood-brain barrier following cerebral ischemia-reperfusion via the Rho/ROCK signaling pathway. *Exp Ther Med* 16**,** 2651-2658.

Chen, X., Mcclusky, R., Chen, J., Beaven, S.W., Tontonoz, P., Arnold, A.P., and Reue, K. (2012). The number of x chromosomes causes sex differences in adiposity in mice. *PLoS Genet* 8**,** e1002709.

Chen, Y.F., and Meng, Q.C. (1991). Sexual dimorphism of blood pressure in spontaneously hypertensive rats is androgen dependent. *Life Sci* 48**,** 85-96.

Chen, Y.F., Naftilan, A.J., and Oparil, S. (1992). Androgen-dependent angiotensinogen and renin messenger RNA expression in hypertensive rats. *Hypertension* 19**,** 456-463.

Chignalia, A.Z., Schuldt, E.Z., Camargo, L.L., Montezano, A.C., Callera, G.E., Laurindo, F.R., Lopes, L.R., Avellar, M.C., Carvalho, M.H., Fortes, Z.B., Touyz, R.M., and Tostes, R.C. (2012). Testosterone induces vascular smooth muscle cell migration by NADPH oxidase and c-Src-dependent pathways. *Hypertension* 59**,** 1263-1271.

Cho, H.J., Hwang, Y.S., Yoon, J., Lee, M., Lee, H.G., and Daar, I.O. (2018). EphrinB1 promotes cancer cell migration and invasion through the interaction with RhoGDI1. *Oncogene* 37**,** 861-872.

Chou, T.M., Sudhir, K., Hutchison, S.J., Ko, E., Amidon, T.M., Collins, P., and Chatterjee, K. (1996). Testosterone induces dilation of canine coronary conductance and resistance arteries in vivo. *Circulation* 94**,** 2614-2619.

Choudhury, A., Solanki, B., Singh, S., Sahu, U., Parvez, S., Kar, S., and Ganguly, S. (2019). Persistent peripheral presence of Staphylococcus aureus promotes histone H3 hypoacetylation and decreases tyrosine hydroxylase protein level in rat brain tissues. *Neuroreport* 30**,** 1087-1094.

Cleutjens, K.B., Van Der Korput, H.A., Van Eekelen, C.C., Van Rooij, H.C., Faber, P.W., and Trapman, J. (1997). An androgen response element in a far upstream enhancer region is essential for high, androgen-regulated activity of the prostate-specific antigen promoter. *Mol Endocrinol* 11**,** 148-161.

Cleutjens, K.B., Van Eekelen, C.C., Van Der Korput, H.A., Brinkmann, A.O., and Trapman, J. (1996). Two androgen response regions cooperate in steroid hormone regulated activity of the prostate-specific antigen promoter. *J Biol Chem* 271**,** 6379-6388.

Colafella, K.M.M., and Denton, K.M. (2018). Sex-specific differences in hypertension and associated cardiovascular disease. *Nat Rev Nephrol* 14**,** 185-201.

Colomer, C., Desarmenien, M.G., and Guerineau, N.C. (2009). Revisiting the stimulus-secretion coupling in the adrenal medulla: role of gap junction-mediated intercellular communication. *Mol Neurobiol* 40**,** 87-100.

Committee, E.N. (1997). Unified nomenclature for Eph family receptors and their ligands, the ephrins. *Cell* 90**,** 403-404.

Cooper, C.S., Perry, P.J., Sparks, A.E., Macindoe, J.H., Yates, W.R., and Williams, R.D. (1998). Effect of exogenous testosterone on prostate volume, serum and semen prostate specific antigen levels in healthy young men. *J Urol* 159**,** 441-443.

Corssmit, E.P., Heijligenberg, R., Endert, E., Ackermans, M.T., Sauerwein, H.P., and Romijn, J.A. (1996). Endocrine and metabolic effects of interferon-alpha in humans. *J Clin Endocrinol Metab* 81**,** 3265-3269.

Cotecchia, S. (2010). The alpha1-adrenergic receptors: diversity of signaling networks and regulation. *J Recept Signal Transduct Res* 30**,** 410-419.

Couchonnal, L.F., and Anderson, M.E. (2008). The role of calmodulin kinase II in myocardial physiology and disease. *Physiology (Bethesda)* 23**,** 151-159.

Cowan, C.W., Shao, Y.R., Sahin, M., Shamah, S.M., Lin, M.Z., Greer, P.L., Gao, S., Griffith, E.C., Brugge, J.S., and Greenberg, M.E. (2005). Vav family GEFs link activated Ephs to endocytosis and axon guidance. *Neuron* 46**,** 205-217.

Coward, R.M., Simhan, J., and Carson, C.C., 3rd (2009). Prostate-specific antigen changes and prostate cancer in hypogonadal men treated with testosterone replacement therapy. *BJU Int* 103**,** 1179-1183.

Cruzalegui, F.H., Cano, E., and Treisman, R. (1999). ERK activation induces phosphorylation of Elk-1 at multiple S/T-P motifs to high stoichiometry. *Oncogene* 18**,** 7948-7957.

Czyzyk-Krzeska, M.F., and Beresh, J.E. (1996). Characterization of the hypoxia-inducible protein binding site within the pyrimidine-rich tract in the 3'-untranslated region of the tyrosine hydroxylase mRNA. *J Biol Chem* 271**,** 3293-3299.

Czyzyk-Krzeska, M.F., Dominski, Z., Kole, R., and Millhorn, D.E. (1994a). Hypoxia stimulates binding of a cytoplasmic protein to a pyrimidine-rich sequence in the 3'-untranslated region of rat tyrosine hydroxylase mRNA. *J Biol Chem* 269**,** 9940-9945.

Czyzyk-Krzeska, M.F., Furnari, B.A., Lawson, E.E., and Millhorn, D.E. (1994b). Hypoxia increases rate of transcription and stability of tyrosine hydroxylase mRNA in pheochromocytoma (PC12) cells. *J Biol Chem* 269**,** 760-764.

Dalton, S., and Treisman, R. (1992). Characterization of SAP-1, a protein recruited by serum response factor to the c-fos serum response element. *Cell* 68**,** 597-612.

Daubner, S.C., Lauriano, C., Haycock, J.W., and Fitzpatrick, P.F. (1992). Site-directed mutagenesis of serine 40 of rat tyrosine hydroxylase. Effects of dopamine and cAMP-dependent phosphorylation on enzyme activity. *J Biol Chem* 267**,** 12639-12646.

Daubner, S.C., Le, T., and Wang, S. (2011). Tyrosine hydroxylase and regulation of dopamine synthesis. *Arch Biochem Biophys* 508**,** 1-12.

Davey, R.A., and Grossmann, M. (2016). Androgen Receptor Structure, Function and Biology: From Bench to Bedside. *Clin Biochem Rev* 37**,** 3-15.

Davis, S., Gale, N.W., Aldrich, T.H., Maisonpierre, P.C., Lhotak, V., Pawson, T., Goldfarb, M., and Yancopoulos, G.D. (1994). Ligands for EPH-related receptor tyrosine kinases that require membrane attachment or clustering for activity. *Science* 266**,** 816-819.

Davy, A., Gale, N.W., Murray, E.W., Klinghoffer, R.A., Soriano, P., Feuerstein, C., and Robbins, S.M. (1999). Compartmentalized signaling by GPI-anchored ephrin-A5 requires the Fyn tyrosine kinase to regulate cellular adhesion. *Genes Dev* 13**,** 3125-3135.

Davy, A., and Robbins, S.M. (2000). Ephrin-A5 modulates cell adhesion and morphology in an integrin-dependent manner. *EMBO J* 19**,** 5396-5405.

Dawidowski, D., and Cafiso, D.S. (2016). Munc18-1 and the Syntaxin-1 N Terminus Regulate Open-Closed States in a t-SNARE Complex. *Structure* 24**,** 392-400.

De Gooijer, M.C., Guillen Navarro, M., Bernards, R., Wurdinger, T., and Van Tellingen, O. (2018). An Experimenter's Guide to Glioblastoma Invasion Pathways. *Trends Mol Med* 24**,** 763-780.

De Miguel, C., Rudemiller, N.P., Abais, J.M., and Mattson, D.L. (2015). Inflammation and hypertension: new understandings and potential therapeutic targets. *Curr Hypertens Rep* 17**,** 507.

De Vries, G.J., Rissman, E.F., Simerly, R.B., Yang, L.Y., Scordalakes, E.M., Auger, C.J., Swain, A., Lovell-Badge, R., Burgoyne, P.S., and Arnold, A.P. (2002). A model system for study of sex chromosome effects on sexually dimorphic neural and behavioral traits. *J Neurosci* 22**,** 9005-9014.

Debruyne, F.M., Behre, H.M., Roehrborn, C.G., Maggi, M., Wu, F.C., Schroder, F.H., Jones, T.H., Porst, H., Hackett, G., Wheaton, O.A., Martin-Morales, A., Meuleman, E., Cunningham, G.R., Divan, H.A., Rosen, R.C., and Investigators, R. (2017). Testosterone treatment is not associated with increased risk of prostate cancer or worsening of lower urinary tract symptoms: prostate health outcomes in the Registry of Hypogonadism in Men. *BJU Int* 119**,** 216-224.

Deenadayalu, V.P., White, R.E., Stallone, J.N., Gao, X., and Garcia, A.J. (2001). Testosterone relaxes coronary arteries by opening the large-conductance, calcium-activated potassium channel. *Am J Physiol Heart Circ Physiol* 281**,** H1720-1727.

Dehm, S.M., and Tindall, D.J. (2006). Molecular regulation of androgen action in prostate cancer. *J Cell Biochem* 99**,** 333-344.

Dominiak, P., and Grobecker, H. (1982). Elevated plasma catecholamines in young hypertensive and hyperkinetic patients: effect of pindolol. *Br J Clin Pharmacol* 13**,** 381S-390S.

Dos Remedios, C.G., Chhabra, D., Kekic, M., Dedova, I.V., Tsubakihara, M., Berry, D.A., and Nosworthy, N.J. (2003). Actin binding proteins: regulation of cytoskeletal microfilaments. *Physiol Rev* 83**,** 433-473.

Douglas, W.W., and Rubin, R.P. (1961). The role of calcium in the secretory response of the adrenal medulla to acetylcholine. *J Physiol* 159**,** 40-57.

Dravis, C., and Henkemeyer, M. (2011). Ephrin-B reverse signaling controls septation events at the embryonic midline through separate tyrosine phosphorylation-independent signaling avenues. *Dev Biol* 355**,** 138-151.

Dravis, C., Wu, T., Chumley, M.J., Yokoyama, N., Wei, S., Wu, D.K., Marcus, D.C., and Henkemeyer, M. (2007). EphB2 and ephrin-B2 regulate the ionic homeostasis of vestibular endolymph. *Hear Res* 223**,** 93-104.

Drescher, U. (2000). Excitation at the synapse: Eph receptors team up with NMDA receptors. *Cell* 103**,** 1005-1008.

Du Rusquec, P., Blonz, C., Frenel, J.S., and Campone, M. (2020). Targeting the PI3K/Akt/mTOR pathway in estrogen-receptor positive HER2 negative advanced breast cancer. *Ther Adv Med Oncol* 12**,** 1758835920940939.

Dubois, V., Laurent, M.R., Jardi, F., Antonio, L., Lemaire, K., Goyvaerts, L., Deldicque, L., Carmeliet, G., Decallonne, B., Vanderschueren, D., and Claessens, F. (2016). Androgen Deficiency Exacerbates High-Fat Diet-Induced Metabolic Alterations in Male Mice. *Endocrinology* 157**,** 648-665.

Dumitrescu Pene, T., Rose, S.D., Lejen, T., Marcu, M.G., and Trifaro, J.M. (2005). Expression of various scinderin domains in chromaffin cells indicates that this protein acts as a molecular switch in the control of actin filament dynamics and exocytosis. *J Neurochem* 92**,** 780-789.

Dunkley, P.R., Bobrovskaya, L., Graham, M.E., Von Nagy-Felsobuki, E.I., and Dickson, P.W. (2004). Tyrosine hydroxylase phosphorylation: regulation and consequences. *J Neurochem* 91**,** 1025-1043.

Eiden, L.E., Emery, A.C., Zhang, L., and Smith, C.B. (2018). PACAP signaling in stress: insights from the chromaffin cell. *Pflugers Arch* 470**,** 79-88.

Eisenhofer, G., Kopin, I.J., and Goldstein, D.S. (2004). Catecholamine metabolism: a contemporary view with implications for physiology and medicine. *Pharmacol Rev* 56**,** 331-349.

El Zawily, A., Mcewen, E., Toosi, B., Vizeacoumar, F.S., Freywald, T., Vizeacoumar, F.J., and Freywald, A. (2017). The EphB6 receptor is overexpressed in pediatric T cell acute lymphoblastic leukemia and increases its sensitivity to doxorubicin treatment. *Scientific Reports* 7.

Elowe, S., Holland, S.J., Kulkarni, S., and Pawson, T. (2001). Downregulation of the Ras-mitogen-activated protein kinase pathway by the EphB2 receptor tyrosine kinase is required for ephrin-induced neurite retraction. *Mol Cell Biol* 21**,** 7429-7441.

Ely, D., Boehme, S., Dunphy, G., Hart, M., Chiarappa, F., Miller, B., Martins, A.S., Turner, M., and Milsted, A. (2011). The Sry3 Y chromosome locus elevates blood pressure and renin-angiotensin system indexes. *Gend Med* 8**,** 126-138.

Ely, D.L., and Turner, M.E. (1990). Hypertension in the spontaneously hypertensive rat is linked to the Y chromosome. *Hypertension* 16**,** 277-281.

Endogenous, H., Prostate Cancer Collaborative, G., Roddam, A.W., Allen, N.E., Appleby, P., and Key, T.J. (2008). Endogenous sex hormones and prostate cancer: a collaborative analysis of 18 prospective studies. *J Natl Cancer Inst* 100**,** 170-183.

English, K.M., Steeds, R.P., Jones, T.H., Diver, M.J., and Channer, K.S. (2000). Low-dose transdermal testosterone therapy improves angina threshold in men with chronic stable angina: A randomized, double-blind, placebo-controlled study. *Circulation* 102**,** 1906-1911.

Erraji-Benchekroun, L., Couton, D., Postic, C., Borde, I., Gaston, J., Guillet, J.G., and Andre, C. (2005). Overexpression of beta2-adrenergic receptors in mouse liver alters the expression of gluconeogenic and glycolytic enzymes. *Am J Physiol Endocrinol Metab* 288**,** E715-722.

Esler, M., Eikelis, N., Schlaich, M., Lambert, G., Alvarenga, M., Kaye, D., El-Osta, A., Guo, L., Barton, D., Pier, C., Brenchley, C., Dawood, T., Jennings, G., and Lambert, E. (2008). Human sympathetic nerve biology: parallel influences of stress and epigenetics in essential hypertension and panic disorder. *Ann N Y Acad Sci* 1148**,** 338-348.

Estrada, M., Espinosa, A., Muller, M., and Jaimovich, E. (2003). Testosterone stimulates intracellular calcium release and mitogen-activated protein kinases via a G protein-coupled receptor in skeletal muscle cells. *Endocrinology* 144**,** 3586-3597.

Fahed, A.C., Gholmieh, J.M., and Azar, S.T. (2012). Connecting the Lines between Hypogonadism and Atherosclerosis. *Int J Endocrinol* 2012**,** 793953.

Fan, Y., Arif, A., Gong, Y., Jia, J., Eswarappa, S.M., Willard, B., Horowitz, A., Graham, L.M., Penn, M.S., and Fox, P.L. (2012). Stimulus-dependent phosphorylation of profilin-1 in angiogenesis. *Nat Cell Biol* 14**,** 1046-1056.

Fang, Q., Zhao, Y., and Lindau, M. (2013). Juxtamembrane tryptophans of synaptobrevin 2 control the process of membrane fusion. *FEBS Lett* 587**,** 67-72.

Fang, W.B., Brantley-Sieders, D.M., Hwang, Y., Ham, A.J., and Chen, J. (2008). Identification and functional analysis of phosphorylated tyrosine residues within EphA2 receptor tyrosine kinase. *J Biol Chem* 283**,** 16017-16026.

Fardoun, M., Dehaini, H., Shaito, A., Mesmar, J., El-Yazbi, A., Badran, A., Beydoun, E., and Eid, A.H. (2020). The hypertensive potential of estrogen: An untold story. *Vascul Pharmacol* 124**,** 106600.

Fehon, R.G., Mcclatchey, A.I., and Bretscher, A. (2010). Organizing the cell cortex: the role of ERM proteins. *Nat Rev Mol Cell Biol* 11**,** 276-287.

Fenwick, E.M., Marty, A., and Neher, E. (1982). Sodium and calcium channels in bovine chromaffin cells. *J Physiol* 331**,** 599-635.

Ferrer-Lorente, R., Cabot, C., Fernandez-Lopez, J.A., and Alemany, M. (2005). Combined effects of oleoyl-estrone and a beta3-adrenergic agonist (CL316,243) on lipid stores of diet-induced overweight male Wistar rats. *Life Sci* 77**,** 2051-2058.

Finkle, W.D., Greenland, S., Ridgeway, G.K., Adams, J.L., Frasco, M.A., Cook, M.B., Fraumeni, J.F., Jr., and Hoover, R.N. (2014). Increased risk of non-fatal myocardial infarction following testosterone therapy prescription in men. *PLoS One* 9**,** e85805.

Flanagan, J.G., and Vanderhaeghen, P. (1998). The ephrins and Eph receptors in neural development. *Annu Rev Neurosci* 21**,** 309-345.

Fletcher, D.S., Candelore, M.R., Grujic, D., Lowell, B.B., Luell, S., Susulic, V.S., and Macintyre, D.E. (1998). Beta-3 adrenergic receptor agonists cause an increase in gastrointestinal transit time in wild-type mice, but not in mice lacking the beta-3 adrenergic receptor. *J Pharmacol Exp Ther* 287**,** 720-724.

Foltz, I.N., Gerl, R.E., Wieler, J.S., Luckach, M., Salmon, R.A., and Schrader, J.W. (1998). Human mitogen-activated protein kinase kinase 7 (MKK7) is a highly conserved c-Jun N-terminal kinase/stress-activated protein kinase (JNK/SAPK) activated by environmental stresses and physiological stimuli. *J Biol Chem* 273**,** 9344-9351.

Fossom, L.H., Sterling, C.R., and Tank, A.W. (1992). Regulation of tyrosine hydroxylase gene transcription rate and tyrosine hydroxylase mRNA stability by cyclic AMP and glucocorticoid. *Mol Pharmacol* 42**,** 898-908.

Fox, B.P., and Kandpal, R.P. (2009). EphB6 receptor significantly alters invasiveness and other phenotypic characteristics of human breast carcinoma cells. *Oncogene* 28**,** 1706-1713.

Fox, B.P., and Kandpal, R.P. (2011). A paradigm shift in EPH receptor interaction: biological relevance of EPHB6 interaction with EPHA2 and EPHB2 in breast carcinoma cell lines. *Cancer Genomics Proteomics* 8**,** 185-193.

Fox, G.M., Holst, P.L., Chute, H.T., Lindberg, R.A., Janssen, A.M., Basu, R., and Welcher, A.A. (1995). cDNA cloning and tissue distribution of five human EPH-like receptor protein-tyrosine kinases. *Oncogene* 10**,** 897-905.

Fremont, S., Romet-Lemonne, G., Houdusse, A., and Echard, A. (2017). Emerging roles of MICAL family proteins - from actin oxidation to membrane trafficking during cytokinesis. *J Cell Sci* 130**,** 1509-1517.

Freshour, J.R., Chase, S.E., and Vikstrom, K.L. (2002). Gender differences in cardiac ACE expression are normalized in androgen-deprived male mice. *Am J Physiol Heart Circ Physiol* 283**,** H1997-2003.

Fuentes, N., and Silveyra, P. (2019). Estrogen receptor signaling mechanisms. *Adv Protein Chem Struct Biol* 116**,** 135-170.

Fukai, J., Yokote, H., Yamanaka, R., Arao, T., Nishio, K., and Itakura, T. (2008). EphA4 promotes cell proliferation and migration through a novel EphA4-FGFR1 signaling pathway in the human glioma U251 cell line. *Mol Cancer Ther* 7**,** 2768-2778.

Gagliano-Juca, T., and Basaria, S. (2019). Testosterone replacement therapy and cardiovascular risk. *Nat Rev Cardiol* 16**,** 555-574.

Gai, Y., Zhang, J., Wei, C., Cao, W., Cui, Y., and Cui, S. (2017). miR-375 negatively regulates the synthesis and secretion of catecholamines by targeting Sp1 in rat adrenal medulla. *Am J Physiol Cell Physiol* 312**,** C663-C672.

Gaitanos, T.N., Koerner, J., and Klein, R. (2016). Tiam-Rac signaling mediates trans-endocytosis of ephrin receptor EphB2 and is important for cell repulsion. *J Cell Biol* 214**,** 735-752.

Gale, N.W., Baluk, P., Pan, L., Kwan, M., Holash, J., Dechiara, T.M., Mcdonald, D.M., and Yancopoulos, G.D. (2001). Ephrin-B2 selectively marks arterial vessels and neovascularization sites in the adult, with expression in both endothelial and smooth-muscle cells. *Developmental biology* 230**,** 151-160.

Gao, S., Lee, P., Wang, H., Gerald, W., Adler, M., Zhang, L., Wang, Y.F., and Wang, Z. (2005). The androgen receptor directly targets the cellular Fas/FasL-associated death domain protein-like inhibitory protein gene to promote the androgen-independent growth of prostate cancer cells. *Mol Endocrinol* 19**,** 1792-1802.

Garcia-Cruz, E., Piqueras, M., Huguet, J., Perez-Marquez, M., Gosalbez, D., Peri, L., Izquierdo, L., Luque, P., Ribal, M.J., and Alcaraz, A. (2012). Hypertension, dyslipidemia and overweight are related to lower testosterone levels in a cohort of men undergoing prostate biopsy. *Int J Impot Res* 24**,** 110-113.

Garcia, A.G., Garcia-De-Diego, A.M., Gandia, L., Borges, R., and Garcia-Sancho, J. (2006). Calcium signaling and exocytosis in adrenal chromaffin cells. *Physiol Rev* 86**,** 1093-1131.

Gasman, S., Chasserot-Golaz, S., Bader, M.F., and Vitale, N. (2003). Regulation of exocytosis in adrenal chromaffin cells: focus on ARF and Rho GTPases. *Cell Signal* 15**,** 893-899.

Gasman, S., Chasserot-Golaz, S., Malacombe, M., Way, M., and Bader, M.F. (2004). Regulated exocytosis in neuroendocrine cells: a role for subplasmalemmal Cdc42/N-WASP-induced actin filaments. *Mol Biol Cell* 15**,** 520-531.

Gasman, S., Chasserot-Golaz, S., Popoff, M.R., Aunis, D., and Bader, M.F. (1997). Trimeric G proteins control exocytosis in chromaffin cells. Go regulates the peripheral actin network and catecholamine secretion by a mechanism involving the small GTP-binding protein Rho. *J Biol Chem* 272**,** 20564-20571.

Geneste, O., Copeland, J.W., and Treisman, R. (2002). LIM kinase and Diaphanous cooperate to regulate serum response factor and actin dynamics. *J Cell Biol* 157**,** 831-838.

Gerdts, E., Okin, P.M., De Simone, G., Cramariuc, D., Wachtell, K., Boman, K., and Devereux, R.B. (2008). Gender differences in left ventricular structure and function during antihypertensive treatment: the Losartan Intervention for Endpoint Reduction in Hypertension Study. *Hypertension* 51**,** 1109-1114.

Ginnan, R., Zou, X., Pfleiderer, P.J., Mercure, M.Z., Barroso, M., and Singer, H.A. (2013). Vascular smooth muscle cell motility is mediated by a physical and functional interaction of Ca2+/calmodulin-dependent protein kinase IIdelta2 and Fyn. *J Biol Chem* 288**,** 29703-29712.

Giovannitti, J.A., Jr., Thoms, S.M., and Crawford, J.J. (2015). Alpha-2 adrenergic receptor agonists: a review of current clinical applications. *Anesth Prog* 62**,** 31-39.

Gizang-Ginsberg, E., and Ziff, E.B. (1990). Nerve growth factor regulates tyrosine hydroxylase gene transcription through a nucleoprotein complex that contains c-Fos. *Genes Dev* 4**,** 477-491.

Gizang-Ginsberg, E., and Ziff, E.B. (1994). Fos family members successively occupy the tyrosine hydroxylase gene AP-1 site after nerve growth factor or epidermal growth factor stimulation and can repress transcription. *Mol Endocrinol* 8**,** 249-262.

Go, S., Kurita, H., Matsumoto, K., Hatano, M., Inden, M., and Hozumi, I. (2018). Methylmercury causes epigenetic suppression of the tyrosine hydroxylase gene in an in vitro neuronal differentiation model. *Biochem Biophys Res Commun* 502**,** 435-441.

Goldstein, D.S. (1983). Arterial baroreflex sensitivity, plasma catecholamines, and pressor responsiveness in essential hypertension. *Circulation* 68**,** 234-240.

Gong, L.W., De Toledo, G.A., and Lindau, M. (2007). Exocytotic catecholamine release is not associated with cation flux through channels in the vesicle membrane but Na+ influx through the fusion pore. *Nat Cell Biol* 9**,** 915-922.

Gonzalez-Jamett, A.M., Guerra, M.J., Olivares, M.J., Haro-Acuna, V., Baez-Matus, X., Vasquez-Navarrete, J., Momboisse, F., Martinez-Quiles, N., and Cardenas, A.M. (2017). The F-Actin Binding Protein Cortactin Regulates the Dynamics of the Exocytotic Fusion Pore through its SH3 Domain. *Front Cell Neurosci* 11**,** 130.

Gordon, S.L., Quinsey, N.S., Dunkley, P.R., and Dickson, P.W. (2008). Tyrosine hydroxylase activity is regulated by two distinct dopamine-binding sites. *J Neurochem* 106**,** 1614-1623.

Grace, A.A., Floresco, S.B., Goto, Y., and Lodge, D.J. (2007). Regulation of firing of dopaminergic neurons and control of goal-directed behaviors. *Trends Neurosci* 30**,** 220-227.

Grady, D., Herrington, D., Bittner, V., Blumenthal, R., Davidson, M., Hlatky, M., Hsia, J., Hulley, S., Herd, A., Khan, S., Newby, L.K., Waters, D., Vittinghoff, E., Wenger, N., and Group, H.R. (2002). Cardiovascular disease outcomes during 6.8 years of hormone therapy: Heart and Estrogen/progestin Replacement Study follow-up (HERS II). *JAMA* 288**,** 49-57.

Graham, R.M., Perez, D.M., Hwa, J., and Piascik, M.T. (1996). alpha 1-adrenergic receptor subtypes. Molecular structure, function, and signaling. *Circ Res* 78**,** 737-749.

Gregg, J., and Fraizer, G. (2011). Transcriptional Regulation of EGR1 by EGF and the ERK Signaling Pathway in Prostate Cancer Cells. *Genes Cancer* 2**,** 900-909.

Grintsevich, E.E., Ge, P., Sawaya, M.R., Yesilyurt, H.G., Terman, J.R., Zhou, Z.H., and Reisler, E. (2017). Catastrophic disassembly of actin filaments via Mical-mediated oxidation. *Nat Commun* 8**,** 2183.

Grintsevich, E.E., Yesilyurt, H.G., Rich, S.K., Hung, R.J., Terman, J.R., and Reisler, E. (2016). F-actin dismantling through a redox-driven synergy between Mical and cofilin. *Nat Cell Biol* 18**,** 876-885.

Grynkiewicz, G., Poenie, M., and Tsien, R.Y. (1985). A new generation of Ca2+ indicators with greatly improved fluorescence properties. *J Biol Chem* 260**,** 3440-3450.

Guay, A.T., Perez, J.B., Fitaihi, W.A., and Vereb, M. (2000). Testosterone treatment in hypogonadal men: prostate-specific antigen level and risk of prostate cancer. *Endocr Pract* 6**,** 132-138.

Gueorguiev, V.D., Zeman, R.J., Hiremagalur, B., Menezes, A., and Sabban, E.L. (1999). Differing temporal roles of Ca2+ and cAMP in nicotine-elicited elevation of tyrosine hydroxylase mRNA. *Am J Physiol* 276**,** C54-65.

Guo, Z., Du, X., and Iacovitti, L. (1998). Regulation of tyrosine hydroxylase gene expression during transdifferentiation of striatal neurons: changes in transcription factors binding the AP-1 site. *J Neurosci* 18**,** 8163-8174.

Gurniak, C.B., and Berg, L.J. (1996). A new member of the Eph family of receptors that lacks protein tyrosine kinase activity. *Oncogene* 13**,** 777-786.

Gutierrez, L.M., and Villanueva, J. (2018). The role of F-actin in the transport and secretion of chromaffin granules: an historic perspective. *Pflugers Arch* 470**,** 181-186.

Haase, M., Dringenberg, T., Allelein, S., Willenberg, H.S., and Schott, M. (2017). Excessive Catecholamine Secretion and the Activation of the Renin-Angiotensin-Aldosterone-System in Patients with Pheochromocytoma: A Single Center Experience and Overview of the Literature. *Horm Metab Res* 49**,** 748-754.

Hafner, C., Schmitz, G., Meyer, S., Bataille, F., Hau, P., Langmann, T., Dietmaier, W., Landthaler, M., and Vogt, T. (2004). Differential gene expression of Eph receptors and ephrins in benign human tissues and cancers. *Clin Chem* 50**,** 490-499.

Hai, T., and Curran, T. (1991). Cross-family dimerization of transcription factors Fos/Jun and ATF/CREB alters DNA binding specificity. *Proc Natl Acad Sci U S A* 88**,** 3720-3724.

Haider, A., Saad, F., Doros, G., and Gooren, L. (2014). Hypogonadal obese men with and without diabetes mellitus type 2 lose weight and show improvement in cardiovascular risk factors when treated with testosterone: an observational study. *Obes Res Clin Pract* 8**,** e339-349.

Han, D.H., Chae, M.R., Jung, J.H., So, I., Park, J.K., and Lee, S.W. (2008). Effect of testosterone on potassium channel opening in human corporal smooth muscle cells. *The journal of sexual medicine* 5**,** 822-832.

Han, Y., Li, X., Zhou, S., Meng, G., Xiao, Y., Zhang, W., Wang, Z., Xie, L., Liu, Z., Lu, H., and Ji, Y. (2012). 17ss-estradiol antagonizes the down-regulation of ERalpha/NOS-3 signaling in vascular endothelial dysfunction of female diabetic rats. *PLoS One* 7**,** e50402.

Han, Y., Wang, X., Chen, J., and Sha, S.H. (2015). Noise-induced cochlear F-actin depolymerization is mediated via ROCK2/p-ERM signaling. *J Neurochem* 133**,** 617-628.

Haring, R., Volzke, H., Steveling, A., Krebs, A., Felix, S.B., Schofl, C., Dorr, M., Nauck, M., and Wallaschofski, H. (2010). Low serum testosterone levels are associated with increased risk of mortality in a population-based cohort of men aged 20-79. *Eur Heart J* 31**,** 1494-1501.

Hashimoto, T., Karasawa, T., Saito, A., Miyauchi, N., Han, G.D., Hayasaka, K., Shimizu, F., and Kawachi, H. (2007). Ephrin-B1 localizes at the slit diaphragm of the glomerular podocyte. *Kidney Int* 72**,** 954-964.

Haupaix, N., Stolfi, A., Sirour, C., Picco, V., Levine, M., Christiaen, L., and Yasuo, H. (2013). p120RasGAP mediates ephrin/Eph-dependent attenuation of FGF/ERK signals during cell fate specification in ascidian embryos. *Development* 140**,** 4347-4352.

Haycock, J.W., Ahn, N.G., Cobb, M.H., and Krebs, E.G. (1992). ERK1 and ERK2, two microtubule-associated protein 2 kinases, mediate the phosphorylation of tyrosine hydroxylase at serine-31 in situ. *Proc Natl Acad Sci U S A* 89**,** 2365-2369.

Haycock, J.W., Lew, J.Y., Garcia-Espana, A., Lee, K.Y., Harada, K., Meller, E., and Goldstein, M. (1998). Role of serine-19 phosphorylation in regulating tyrosine hydroxylase studied with site- and phosphospecific antibodies and site-directed mutagenesis. *J Neurochem* 71**,** 1670-1675.

Haycock, J.W., Meligeni, J.A., Bennett, W.F., and Waymire, J.C. (1982). Phosphorylation and activation of tyrosine hydroxylase mediate the acetylcholine-induced increase in catecholamine biosynthesis in adrenal chromaffin cells. *J Biol Chem* 257**,** 12641-12648.

Heemers, H.V., and Tindall, D.J. (2007). Androgen receptor (AR) coregulators: a diversity of functions converging on and regulating the AR transcriptional complex. *Endocr Rev* 28**,** 778-808.

Heinemann, C., Von Ruden, L., Chow, R.H., and Neher, E. (1993). A two-step model of secretion control in neuroendocrine cells. *Pflugers Arch* 424**,** 105-112.

Henriques, T., Zhang, X., Yiannikouris, F.B., Daugherty, A., and Cassis, L.A. (2008). Androgen increases AT1a receptor expression in abdominal aortas to promote angiotensin II-induced AAAs in apolipoprotein E-deficient mice. *Arterioscler Thromb Vasc Biol* 28**,** 1251-1256.

Hernandez, I., Delgado, J.L., Diaz, J., Quesada, T., Teruel, M.J., Llanos, M.C., and Carbonell, L.F. (2000). 17beta-estradiol prevents oxidative stress and decreases blood pressure in ovariectomized rats. *Am J Physiol Regul Integr Comp Physiol* 279**,** R1599-1605.

Hertzog, M., Van Heijenoort, C., Didry, D., Gaudier, M., Coutant, J., Gigant, B., Didelot, G., Preat, T., Knossow, M., Guittet, E., and Carlier, M.F. (2004). The beta-thymosin/WH2 domain; structural basis for the switch from inhibition to promotion of actin assembly. *Cell* 117**,** 611-623.

Hess, J., Angel, P., and Schorpp-Kistner, M. (2004). AP-1 subunits: quarrel and harmony among siblings. *J Cell Sci* 117**,** 5965-5973.

Hille, B. (1992). G protein-coupled mechanisms and nervous signaling. *Neuron* 9**,** 187-195.

Himanen, J.P., Rajashankar, K.R., Lackmann, M., Cowan, C.A., Henkemeyer, M., and Nikolov, D.B. (2001). Crystal structure of an Eph receptor-ephrin complex. *Nature* 414**,** 933-938.

Himanen, J.P., Yermekbayeva, L., Janes, P.W., Walker, J.R., Xu, K., Atapattu, L., Rajashankar, K.R., Mensinga, A., Lackmann, M., Nikolov, D.B., and Dhe-Paganon, S. (2010). Architecture of Eph receptor clusters. *Proc Natl Acad Sci U S A* 107**,** 10860-10865.

Hinojosa-Laborde, C., Lange, D.L., and Haywood, J.R. (2000). Role of female sex hormones in the development and reversal of dahl hypertension. *Hypertension* 35**,** 484-489.

Hirai, H., Maru, Y., Hagiwara, K., Nishida, J., and Takaku, F. (1987). A novel putative tyrosine kinase receptor encoded by the eph gene. *Science* 238**,** 1717-1720.

Hiremagalur, B., Nankova, B., Nitahara, J., Zeman, R., and Sabban, E.L. (1993). Nicotine increases expression of tyrosine hydroxylase gene. Involvement of protein kinase A-mediated pathway. *J Biol Chem* 268**,** 23704-23711.

Hoffmann, E., Ashouri, J., Wolter, S., Doerrie, A., Dittrich-Breiholz, O., Schneider, H., Wagner, E.F., Troppmair, J., Mackman, N., and Kracht, M. (2008). Transcriptional regulation of EGR-1 by the interleukin-1-JNK-MKK7-c-Jun pathway. *J Biol Chem* 283**,** 12120-12128.

Hohmann, N., Xia, N., Steinkamp-Fenske, K., Forstermann, U., and Li, H. (2016). Estrogen Receptor Signaling and the PI3K/Akt Pathway Are Involved in Betulinic Acid-Induced eNOS Activation. *Molecules* 21.

Holen, H.L., Shadidi, M., Narvhus, K., Kjosnes, O., Tierens, A., and Aasheim, H.C. (2008). Signaling through ephrin-A ligand leads to activation of Src-family kinases, Akt phosphorylation, and inhibition of antigen receptor-induced apoptosis. *J Leukoc Biol* 84**,** 1183-1191.

Holland, P.M., Suzanne, M., Campbell, J.S., Noselli, S., and Cooper, J.A. (1997). MKK7 is a stress-activated mitogen-activated protein kinase kinase functionally related to hemipterous. *J Biol Chem* 272**,** 24994-24998.

Holmberg, J., Genander, M., Halford, M.M., Anneren, C., Sondell, M., Chumley, M.J., Silvany, R.E., Henkemeyer, M., and Frisen, J. (2006). EphB receptors coordinate migration and proliferation in the intestinal stem cell niche. *Cell* 125**,** 1151-1163.

Holtmann, H., Winzen, R., Holland, P., Eickemeier, S., Hoffmann, E., Wallach, D., Malinin, N.L., Cooper, J.A., Resch, K., and Kracht, M. (1999). Induction of interleukin-8 synthesis integrates effects on transcription and mRNA degradation from at least three different cytokine- or stress-activated signal transduction pathways. *Mol Cell Biol* 19**,** 6742-6753.

Hong, K., and Choi, Y. (2018). Role of estrogen and RAS signaling in repeated implantation failure. *BMB Rep* 51**,** 225-229.

Hristov, K.L., Cui, X., Brown, S.M., Liu, L., Kellett, W.F., and Petkov, G.V. (2008). Stimulation of beta3-adrenoceptors relaxes rat urinary bladder smooth muscle via activation of the large-conductance Ca2+-activated K+ channels. *Am J Physiol Cell Physiol* 295**,** C1344-1353.

Hsu, W.H., Xiang, H.D., Rajan, A.S., and Boyd, A.E., 3rd (1991). Activation of alpha 2-adrenergic receptors decreases Ca2+ influx to inhibit insulin secretion in a hamster beta-cell line: an action mediated by a guanosine triphosphate-binding protein. *Endocrinology* 128**,** 958-964.

Hu, Y., Wang, X., Wu, Y., Jin, W., Cheng, B., Fang, X., Martel‐Pelletier, J., Kapoor, M., Peng, J., and Qi, S. (2015). Role of EFNB1 and EFNB2 in Mouse Collagen‐Induced Arthritis and Human Rheumatoid Arthritis. *Arthritis & Rheumatology* 67**,** 1778-1788.

Huggins, C., and Hodges, C.V. (2002). Studies on prostatic cancer: I. The effect of castration, of estrogen and of androgen injection on serum phosphatases in metastatic carcinoma of the prostate. 1941. *J Urol* 168**,** 9-12.

Hughes, G.S., Mathur, R.S., and Margolius, H.S. (1989). Sex steroid hormones are altered in essential hypertension. *J Hypertens* 7**,** 181-187.

Hung, R.J., Pak, C.W., and Terman, J.R. (2011). Direct redox regulation of F-actin assembly and disassembly by Mical. *Science* 334**,** 1710-1713.

Hung, R.J., Yazdani, U., Yoon, J., Wu, H., Yang, T., Gupta, N., Huang, Z., Van Berkel, W.J., and Terman, J.R. (2010). Mical links semaphorins to F-actin disassembly. *Nature* 463**,** 823-827.

Inoue, M., Harada, K., Matsuoka, H., and Warashina, A. (2010). Paracrine role of GABA in adrenal chromaffin cells. *Cell Mol Neurobiol* 30**,** 1217-1224.

Ip, Y.T., and Davis, R.J. (1998). Signal transduction by the c-Jun N-terminal kinase (JNK)--from inflammation to development. *Curr Opin Cell Biol* 10**,** 205-219.

Jablonskis, L.T., and Howe, P.R. (1994). Elevated plasma adrenaline in spontaneously hypertensive rats. *Blood Press* 3**,** 106-111.

Jaffe, A., Chen, Y., Kisch, E.S., Fischel, B., Alon, M., and Stern, N. (1996). Erectile dysfunction in hypertensive subjects. Assessment of potential determinants. *Hypertension* 28**,** 859-862.

Janes, P.W., Griesshaber, B., Atapattu, L., Nievergall, E., Hii, L.L., Mensinga, A., Chheang, C., Day, B.W., Boyd, A.W., Bastiaens, P.I., Jorgensen, C., Pawson, T., and Lackmann, M. (2011). Eph receptor function is modulated by heterooligomerization of A and B type Eph receptors. *J Cell Biol* 195**,** 1033-1045.

Jeong, H., Kim, M.S., Kwon, J., Kim, K.S., and Seol, W. (2006). Regulation of the transcriptional activity of the tyrosine hydroxylase gene by androgen receptor. *Neurosci Lett* 396**,** 57-61.

Ji, H., Menini, S., Zheng, W., Pesce, C., Wu, X., and Sandberg, K. (2008). Role of angiotensin-converting enzyme 2 and angiotensin(1-7) in 17beta-oestradiol regulation of renal pathology in renal wrap hypertension in rats. *Exp Physiol* 93**,** 648-657.

Ji, H., Zheng, W., Wu, X., Liu, J., Ecelbarger, C.M., Watkins, R., Arnold, A.P., and Sandberg, K. (2010). Sex chromosome effects unmasked in angiotensin II-induced hypertension. *Hypertension* 55**,** 1275-1282.

Jiang, J., Wang, Z.H., Qu, M., Gao, D., Liu, X.P., Zhu, L.Q., and Wang, J.Z. (2015). Stimulation of EphB2 attenuates tau phosphorylation through PI3K/Akt-mediated inactivation of glycogen synthase kinase-3beta. *Sci Rep* 5**,** 11765.

Jin, W., Luo, H., and Wu, J. (2014). Effect of reduced EPHB4 expression in thymic epithelial cells on thymocyte development and peripheral T cell function. *Molecular immunology* 58**,** 1-9.
Jones, A.K., Buckingham, S.D., and Sattelle, D.B. (2010). Proteins interacting with nicotinic acetylcholine receptors: expanding functional and therapeutic horizons. *Trends Pharmacol Sci* 31**,** 455-462.
Jones, T.H., and Saad, F. (2009). The effects of testosterone on risk factors for, and the mediators of, the atherosclerotic process. *Atherosclerosis* 207**,** 318-327.
Juarez Olguin, H., Calderon Guzman, D., Hernandez Garcia, E., and Barragan Mejia, G. (2016). The Role of Dopamine and Its Dysfunction as a Consequence of Oxidative Stress. *Oxid Med Cell Longev* 2016**,** 9730467.
Jurney, W.M., Gallo, G., Letourneau, P.C., and Mcloon, S.C. (2002). Rac1-mediated endocytosis during ephrin-A2- and semaphorin 3A-induced growth cone collapse. *J Neurosci* 22**,** 6019-6028.
Kacker, R., Hult, M., San Francisco, I.F., Conners, W.P., Rojas, P.A., Dewolf, W.C., and Morgentaler, A. (2016). Can testosterone therapy be offered to men on active surveillance for prostate cancer? Preliminary results. *Asian J Androl* 18**,** 16-20.
Kallio, P.J., Poukka, H., Moilanen, A., Janne, O.A., and Palvimo, J.J. (1995). Androgen receptor-mediated transcriptional regulation in the absence of direct interaction with a specific DNA element. *Mol Endocrinol* 9**,** 1017-1028.
Kannan, H., Tanaka, Y., Kunitake, T., Ueta, Y., Hayashida, Y., and Yamashita, H. (1996). Activation of sympathetic outflow by recombinant human interleukin-1 beta in conscious rats. *Am J Physiol* 270**,** R479-485.
Kansy, J.W., Daubner, S.C., Nishi, A., Sotogaku, N., Lloyd, M.D., Nguyen, C., Lu, L., Haycock, J.W., Hope, B.T., Fitzpatrick, P.F., and Bibb, J.A. (2004). Identification of tyrosine hydroxylase as a physiological substrate for Cdk5. *J Neurochem* 91**,** 374-384.
Kilbourne, E.J., Nankova, B.B., Lewis, E.J., Mcmahon, A., Osaka, H., Sabban, D.B., and Sabban, E.L. (1992). Regulated expression of the tyrosine hydroxylase gene by membrane depolarization. Identification of the responsive element and possible second messengers. *J Biol Chem* 267**,** 7563-7569.
Kim, A.H., Reimers, M., Maher, B., Williamson, V., Mcmichael, O., Mcclay, J.L., Van Den Oord, E.J., Riley, B.P., Kendler, K.S., and Vladimirov, V.I. (2010). MicroRNA expression profiling in the prefrontal cortex of individuals affected with schizophrenia and bipolar disorders. *Schizophr Res* 124**,** 183-191.
Kim, S.M., Chen, L., Faulhaber-Walter, R., Oppermann, M., Huang, Y., Mizel, D., Briggs, J.P., and Schnermann, J. (2007). Regulation of renin secretion and expression in mice deficient in beta1- and beta2-adrenergic receptors. *Hypertension* 50**,** 103-109.
King, D.E. (2014). Acute DSS colitis alters EphB6 receptor expression in neurons of the spinal dorsal horn. *Neurosci Lett* 559**,** 105-110.
Klein, M.O., Battagello, D.S., Cardoso, A.R., Hauser, D.N., Bittencourt, J.C., and Correa, R.G. (2019). Dopamine: Functions, Signaling, and Association with Neurological Diseases. *Cell Mol Neurobiol* 39**,** 31-59.
Klingauf, J., and Neher, E. (1997). Modeling buffered Ca2+ diffusion near the membrane: implications for secretion in neuroendocrine cells. *Biophys J* 72**,** 674-690.
Kohno, S., Murata, T., Koide, N., Hikita, K., and Kaneda, N. (2011). Establishment and characterization of a noradrenergic adrenal chromaffin cell line, tsAM5NE, immortalized with the temperature-sensitive SV40 T-antigen. *Cell Biol Int* 35**,** 325-334.
Kolski-Andreaco, A., Cai, H., Currle, D.S., Chandy, K.G., and Chow, R.H. (2007). Mouse adrenal chromaffin cell isolation. *J Vis Exp***,** 129.
Konstantinova, I., Nikolova, G., Ohara-Imaizumi, M., Meda, P., Kucera, T., Zarbalis, K., Wurst, W., Nagamatsu, S., and Lammert, E. (2007). EphA-Ephrin-A-mediated beta cell communication regulates insulin secretion from pancreatic islets. *Cell* 129**,** 359-370.
Kotlikoff, M.I., and Kamm, K.E. (1996). Molecular mechanisms of beta-adrenergic relaxation of airway smooth muscle. *Annu Rev Physiol* 58**,** 115-141.
Kouzarides, T., and Ziff, E. (1988). The role of the leucine zipper in the fos-jun interaction. *Nature* 336**,** 646-651.
Kullander, K., and Klein, R. (2002). Mechanisms and functions of Eph and ephrin signalling. *Nat Rev Mol Cell Biol* 3**,** 475-486.
Kumai, T., Tanaka, M., Watanabe, M., Nakura, H., and Kobayashi, S. (1995). Influence of androgen on tyrosine hydroxylase mRNA in adrenal medulla of spontaneously hypertensive rats. *Hypertension* 26**,** 208-212.
Kumer, S.C., and Vrana, K.E. (1996). Intricate regulation of tyrosine hydroxylase activity and gene expression. *J Neurochem* 67**,** 443-462.

Laughlin, G.A., Barrett-Connor, E., and Bergstrom, J. (2008). Low serum testosterone and mortality in older men. *J Clin Endocrinol Metab* 93**,** 68-75.

Le Bourdelles, B., Horellou, P., Le Caer, J.P., Denefle, P., Latta, M., Haavik, J., Guibert, B., Mayaux, J.F., and Mallet, J. (1991). Phosphorylation of human recombinant tyrosine hydroxylase isoforms 1 and 2: an additional phosphorylated residue in isoform 2, generated through alternative splicing. *J Biol Chem* 266**,** 17124-17130.

Leal, R.B., Sim, A.T., Goncalves, C.A., and Dunkley, P.R. (2002). Tyrosine hydroxylase dephosphorylation by protein phosphatase 2A in bovine adrenal chromaffin cells. *Neurochem Res* 27**,** 207-213.

Ledoux, J., Bonev, A.D., and Nelson, M.T. (2008). Ca2+-activated K+ channels in murine endothelial cells: block by intracellular calcium and magnesium. *The Journal of general physiology* 131**,** 125-135.

Ledoux, J., Greenwood, I., Villeneuve, L.R., and Leblanc, N. (2003). Modulation of Ca2+ ‐ dependent Cl− channels by calcineurin in rabbit coronary arterial myocytes. *The Journal of physiology* 552**,** 701-714.

Lee, A.M., Navaratnam, D., Ichimiya, S., Greene, M.I., and Davis, J.G. (1996). Cloning of m-ehk2 from the murine inner ear, an eph family receptor tyrosine kinase expressed in the developing and adult cochlea. *DNA Cell Biol* 15**,** 817-825.

Lee, H.S., Nishanian, T.G., Mood, K., Bong, Y.S., and Daar, I.O. (2008). EphrinB1 controls cell-cell junctions through the Par polarity complex. *Nature Cell Biology* 10**,** 979-986.

Lee, S.H., and Dominguez, R. (2010). Regulation of actin cytoskeleton dynamics in cells. *Mol Cells* 29**,** 311-325.

Lehmann, I.T., Bobrovskaya, L., Gordon, S.L., Dunkley, P.R., and Dickson, P.W. (2006). Differential regulation of the human tyrosine hydroxylase isoforms via hierarchical phosphorylation. *J Biol Chem* 281**,** 17644-17651.

Lenartowski, R., and Goc, A. (2011). Epigenetic, transcriptional and posttranscriptional regulation of the tyrosine hydroxylase gene. *Int J Dev Neurosci* 29**,** 873-883.

Li, L., Hisamoto, K., Kim, K.H., Haynes, M.P., Bauer, P.M., Sanjay, A., Collinge, M., Baron, R., Sessa, W.C., and Bender, J.R. (2007). Variant estrogen receptor-c-Src molecular interdependence and c-Src structural requirements for endothelial NO synthase activation. *Proc Natl Acad Sci U S A* 104**,** 16468-16473.

Li, L., Wu, J., Pu, D., Zhao, Y., Wan, C., Sun, L., Shen, C.E., Sun, W., Yuan, Z., Shen, Q., He, X., Jiang, J., Luo, N., He, Y., Qian, Q., Cai, P., and Zhang, M. (2012). Factors associated with the age of natural menopause and menopausal symptoms in Chinese women. *Maturitas* 73**,** 354-360.

Li, Y., Luo, Z.Y., Hu, Y.Y., Bi, Y.W., Yang, J.M., Zou, W.J., Song, Y.L., Li, S., Shen, T., Li, S.J., Huang, L., Zhou, A.J., Gao, T.M., and Li, J.M. (2020). The gut microbiota regulates autism-like behavior by mediating vitamin B6 homeostasis in EphB6-deficient mice. *Microbiome* 8**,** 120.

Li, Y.W., and Bayliss, D.A. (1998). Activation of alpha 2-adrenoceptors causes inhibition of calcium channels but does not modulate inwardly-rectifying K+ channels in caudal raphe neurons. *Neuroscience* 82**,** 753-765.

Liang, L.Y., Patel, O., Janes, P.W., Murphy, J.M., and Lucet, I.S. (2019). Eph receptor signalling: from catalytic to non-catalytic functions. *Oncogene* 38**,** 6567-6584.

Liao, R.S., Ma, S., Miao, L., Li, R., Yin, Y., and Raj, G.V. (2013). Androgen receptor-mediated non-genomic regulation of prostate cancer cell proliferation. *Transl Androl Urol* 2**,** 187-196.

Lim, Y.S., Mclaughlin, T., Sung, T.C., Santiago, A., Lee, K.F., and O'leary, D.D. (2008). p75(NTR) mediates ephrin-A reverse signaling required for axon repulsion and mapping. *Neuron* 59**,** 746-758.

Lin, B., Ferguson, C., White, J.T., Wang, S., Vessella, R., True, L.D., Hood, L., and Nelson, P.S. (1999). Prostate-localized and androgen-regulated expression of the membrane-bound serine protease TMPRSS2. *Cancer Res* 59**,** 4180-4184.

Lin, B., Yin, T., Wu, Y.I., Inoue, T., and Levchenko, A. (2015). Interplay between chemotaxis and contact inhibition of locomotion determines exploratory cell migration. *Nat Commun* 6**,** 6619.

Lindberg, R.A., and Hunter, T. (1990). cDNA cloning and characterization of eck, an epithelial cell receptor protein-tyrosine kinase in the eph/elk family of protein kinases. *Mol Cell Biol* 10**,** 6316-6324.

Linnemann, T., Geyer, M., Jaitner, B.K., Block, C., Kalbitzer, H.R., Wittinghofer, A., and Herrmann, C. (1999). Thermodynamic and kinetic characterization of the interaction between the Ras binding domain of AF6 and members of the Ras subfamily. *J Biol Chem* 274**,** 13556-13562.

Lisabeth, E.M., Falivelli, G., and Pasquale, E.B. (2013). Eph receptor signaling and ephrins. *Cold Spring Harb Perspect Biol* 5.

Liu, B., and Ely, D. (2011). Testosterone increases: sodium reabsorption, blood pressure, and renal pathology in female spontaneously hypertensive rats on a high sodium diet. *Adv Pharmacol Sci* 2011**,** 817835.

Liu, D., Qiu, H.M., Fei, H.Z., Hu, X.Y., Xia, H.J., Wang, L.J., Qin, L.J., Jiang, X.H., and Zhou, Q.X. (2014a). Histone acetylation and expression of mono-aminergic transmitters synthetases involved in CUS-induced depressive rats. *Exp Biol Med (Maywood)* 239**,** 330-336.

Liu, P.Y., Death, A.K., and Handelsman, D.J. (2003). Androgens and cardiovascular disease. *Endocr Rev* 24**,** 313-340.

Liu, R., Ding, L., Yu, M.H., Wang, H.Q., Li, W.C., Cao, Z., Zhang, P., Yao, B.C., Tang, J., Ke, Q., and Huang, T.Z. (2014b). Effects of dihydrotestosterone on adhesion and proliferation via PI3-K/Akt signaling in endothelial progenitor cells. *Endocrine* 46**,** 634-643.

Liu, Y., Schirra, C., Stevens, D.R., Matti, U., Speidel, D., Hof, D., Bruns, D., Brose, N., and Rettig, J. (2008). CAPS facilitates filling of the rapidly releasable pool of large dense-core vesicles. *J Neurosci* 28**,** 5594-5601.

Liu, Y.Z., Wang, Y.X., and Jiang, C.L. (2017). Inflammation: The Common Pathway of Stress-Related Diseases. *Front Hum Neurosci* 11**,** 316.

Lopes, R.A., Neves, K.B., Pestana, C.R., Queiroz, A.L., Zanotto, C.Z., Chignalia, A.Z., Valim, Y.M., Silveira, L.R., Curti, C., and Tostes, R.C. (2014). Testosterone induces apoptosis in vascular smooth muscle cells via extrinsic apoptotic pathway with mitochondria-generated reactive oxygen species involvement. *Am J Physiol Heart Circ Physiol* 306**,** H1485-1494.

Lorin, T., Salzburger, W., and Bohne, A. (2015). Evolutionary Fate of the Androgen Receptor-Signaling Pathway in Ray-Finned Fishes with a Special Focus on Cichlids. *G3 (Bethesda)* 5**,** 2275-2283.

Lu, Q., Sun, E.E., Klein, R.S., and Flanagan, J.G. (2001). Ephrin-B reverse signaling is mediated by a novel PDZ-RGS protein and selectively inhibits G protein-coupled chemoattraction. *Cell* 105**,** 69-79.

Lubahn, D.B., Joseph, D.R., Sar, M., Tan, J., Higgs, H.N., Larson, R.E., French, F.S., and Wilson, E.M. (1988). The human androgen receptor: complementary deoxyribonucleic acid cloning, sequence analysis and gene expression in prostate. *Mol Endocrinol* 2**,** 1265-1275.

Luo, H., Broux, B., Wang, X., Hu, Y., Ghannam, S., Jin, W., Larochelle, C., Prat, A., and Wu, J. (2016). EphrinB1 and EphrinB2 regulate T cell chemotaxis and migration in experimental autoimmune encephalomyelitis and multiple sclerosis. *Neurobiology of disease* 91**,** 292-306.

Luo, H., Charpentier, T., Wang, X., Qi, S., Han, B., Wu, T., Terra, R., Lamarre, A., and Wu, J. (2011a). Efnb1 and Efnb2 proteins regulate thymocyte development, peripheral T cell differentiation, and antiviral immune responses and are essential for interleukin-6 (IL-6) signaling. *Journal of Biological Chemistry* 286**,** 41135-41152.

Luo, H., Qi, S., Wu, Z., Han, B., Wang, X., and Wu, J. (2011b). EFNB1 and EFNB2 physically bind to IL-7R-alpha and retard its internalization from the cell surface (57.2). *The Journal of Immunology* 186**,** 57.52-57.52.

Luo, H., Wan, X., Wu, Y., and Wu, J. (2001). Cross-linking of EphB6 resulting in signal transduction and apoptosis in Jurkat cells. *The Journal of Immunology* 167**,** 1362-1370.

Luo, H., Wu, Z., Tremblay, J., Thorin, E., Peng, J., Lavoie, J.L., Hu, B., Stoyanova, E., Cloutier, G., and Qi, S. (2012). Receptor tyrosine kinase Ephb6 regulates vascular smooth muscle contractility and modulates blood pressure in concert with sex hormones. *Journal of Biological Chemistry* 287**,** 6819-6829.

Luo, H., Yu, G., Tremblay, J., and Wu, J. (2004). EphB6-null mutation results in compromised T cell function. *The Journal of clinical investigation* 114**,** 1762-1773.

Luo, H., Yu, G., Wu, Y., and Wu, J. (2002). EphB6 crosslinking results in costimulation of T cells. *The Journal of clinical investigation* 110**,** 1141-1150.

Lyons, L.S., Rao, S., Balkan, W., Faysal, J., Maiorino, C.A., and Burnstein, K.L. (2008). Ligand-independent activation of androgen receptors by Rho GTPase signaling in prostate cancer. *Mol Endocrinol* 22**,** 597-608.

Ma, C., Li, W., Xu, Y., and Rizo, J. (2011). Munc13 mediates the transition from the closed syntaxin-Munc18 complex to the SNARE complex. *Nat Struct Mol Biol* 18**,** 542-549.

Maggi, M., Wu, F.C., Jones, T.H., Jackson, G., Behre, H.M., Hackett, G., Martin-Morales, A., Balercia, G., Dobs, A.S., Arver, S.T., Maggio, M., Cunningham, G.R., Isidori, A.M., Quinton, R., Wheaton, O.A., Siami, F.S., Rosen, R.C., and Investigators, R. (2016). Testosterone treatment is not associated with increased risk of adverse cardiovascular events: results from the Registry of Hypogonadism in Men (RHYME). *Int J Clin Pract* 70**,** 843-852.

Maharjan, S., Serova, L., and Sabban, E.L. (2005). Transcriptional regulation of tyrosine hydroxylase by estrogen: opposite effects with estrogen receptors alpha and beta and interactions with cyclic AMP. *J Neurochem* 93**,** 1502-1514.

Maharjan, S., Serova, L.I., and Sabban, E.L. (2010). Membrane-initiated estradiol signaling increases tyrosine hydroxylase promoter activity with ER alpha in PC12 cells. *J Neurochem* 112**,** 42-55.

Malkin, C.J., Pugh, P.J., Jones, R.D., Kapoor, D., Channer, K.S., and Jones, T.H. (2004). The effect of testosterone replacement on endogenous inflammatory cytokines and lipid profiles in hypogonadal men. *J Clin Endocrinol Metab* 89**,** 3313-3318.

Mangelsdorf, D.J., Thummel, C., Beato, M., Herrlich, P., Schutz, G., Umesono, K., Blumberg, B., Kastner, P., Mark, M., Chambon, P., and Evans, R.M. (1995). The nuclear receptor superfamily: the second decade. *Cell* 83**,** 835-839.

Maranon, R., and Reckelhoff, J.F. (2013). Sex and gender differences in control of blood pressure. *Clin Sci (Lond)* 125**,** 311-318.

Marengo, F.D., and Cardenas, A.M. (2018). How does the stimulus define exocytosis in adrenal chromaffin cells? *Pflugers Arch* 470**,** 155-167.

Marin, P., Holmang, S., Gustafsson, C., Jonsson, L., Kvist, H., Elander, A., Eldh, J., Sjostrom, L., Holm, G., and Bjorntorp, P. (1993). Androgen treatment of abdominally obese men. *Obes Res* 1**,** 245-251.

Marjoram, R.J., Lessey, E.C., and Burridge, K. (2014). Regulation of RhoA activity by adhesion molecules and mechanotransduction. *Curr Mol Med* 14**,** 199-208.

Marsick, B.M., San Miguel-Ruiz, J.E., and Letourneau, P.C. (2012). Activation of ezrin/radixin/moesin mediates attractive growth cone guidance through regulation of growth cone actin and adhesion receptors. *J Neurosci* 32**,** 282-296.

Martinez-Espinosa, P.L., Yang, C., Gonzalez-Perez, V., Xia, X.M., and Lingle, C.J. (2014). Knockout of the BK beta2 subunit abolishes inactivation of BK currents in mouse adrenal chromaffin cells and results in slow-wave burst activity. *J Gen Physiol* 144**,** 275-295.

Mason, E.O., Goldgur, Y., Robev, D., Freywald, A., Nikolov, D.B., and Himanen, J.P. (2021). Structure of the EphB6 receptor ectodomain. *PLoS One* 16**,** e0247335.

Masubuchi, Y., Kumai, T., Uematsu, A., Komoriyama, K., and Hirai, M. (1982). Gonadectomy-induced reduction of blood pressure in adult spontaneously hypertensive rats. *Acta Endocrinol (Copenh)* 101**,** 154-160.

Mateo-Lozano, S., Bazzocco, S., Rodrigues, P., Mazzolini, R., Andretta, E., Dopeso, H., Fernandez, Y., Del Llano, E., Bilic, J., Suarez-Lopez, L., Macaya, I., Carton-Garcia, F., Nieto, R., Jimenez-Flores, L.M., De Marcondes, P.G., Nunez, Y., Afonso, E., Cacci, K., Hernandez-Losa, J., Landolfi, S., Abasolo, I., Ramon, Y.C.S., Mariadason, J.M., Schwartz, S., Jr., Matsui, T., and Arango, D. (2017). Loss of the EPH receptor B6 contributes to colorectal cancer metastasis. *Sci Rep* 7**,** 43702.

Mathar, I., Vennekens, R., Meissner, M., Kees, F., Van Der Mieren, G., Camacho Londono, J.E., Uhl, S., Voets, T., Hummel, B., Van Den Bergh, A., Herijgers, P., Nilius, B., Flockerzi, V., Schweda, F., and Freichel, M. (2010). Increased catecholamine secretion contributes to hypertension in TRPM4-deficient mice. *J Clin Invest* 120**,** 3267-3279.

Matsuoka, H., Obama, H., Kelly, M.L., Matsui, T., and Nakamoto, M. (2005). Biphasic functions of the kinase-defective Ephb6 receptor in cell adhesion and migration. *J Biol Chem* 280**,** 29355-29363.

Maturana, M.A., Breda, V., Lhullier, F., and Spritzer, P.M. (2008). Relationship between endogenous testosterone and cardiovascular risk in early postmenopausal women. *Metabolism* 57**,** 961-965.

Mcglynn, L.M., Kirkegaard, T., Edwards, J., Tovey, S., Cameron, D., Twelves, C., Bartlett, J.M., and Cooke, T.G. (2009). Ras/Raf-1/MAPK pathway mediates response to tamoxifen but not chemotherapy in breast cancer patients. *Clin Cancer Res* 15**,** 1487-1495.

Mclaren, D., Siemens, D.R., Izard, J., Black, A., and Morales, A. (2008). Clinical practice experience with testosterone treatment in men with testosterone deficiency syndrome. *BJU Int* 102**,** 1142-1146.

Medina, D., Mehay, D., and Arnold, A.C. (2020). Sex differences in cardiovascular actions of the renin-angiotensin system. *Clin Auton Res* 30**,** 393-408.

Menezes, A., Zeman, R., and Sabban, E. (1996). Involvement of intracellular or extracellular calcium in activation of tyrosine hydroxylase gene expression in PC12 cells. *J Neurochem* 67**,** 2316-2324.

Miao, H., Li, D.Q., Mukherjee, A., Guo, H., Petty, A., Cutter, J., Basilion, J.P., Sedor, J., Wu, J., Danielpour, D., Sloan, A.E., Cohen, M.L., and Wang, B. (2009). EphA2 mediates ligand-dependent inhibition and ligand-independent promotion of cell migration and invasion via a reciprocal regulatory loop with Akt. *Cancer Cell* 16**,** 9-20.

Miao, H., Wei, B.R., Peehl, D.M., Li, Q., Alexandrou, T., Schelling, J.R., Rhim, J.S., Sedor, J.R., Burnett, E., and Wang, B. (2001). Activation of EphA receptor tyrosine kinase inhibits the Ras/MAPK pathway. *Nat Cell Biol* 3**,** 527-530.

Miklavc, P., Ehinger, K., Sultan, A., Felder, T., Paul, P., Gottschalk, K.E., and Frick, M. (2015). Actin depolymerisation and crosslinking join forces with myosin II to contract actin coats on fused secretory vesicles. *J Cell Sci* 128**,** 1193-1203.

Miller, W.L. (2017). Steroidogenesis: Unanswered Questions. *Trends Endocrinol Metab* 28**,** 771-793.

Minami, M., Koyama, T., Wakayama, Y., Fukuhara, S., and Mochizuki, N. (2011). EphrinA/EphA signal facilitates insulin-like growth factor-I-induced myogenic differentiation through suppression of the Ras/extracellular signal-regulated kinase 1/2 cascade in myoblast cell lines. *Mol Biol Cell* 22**,** 3508-3519.

Miner, M., Barkin, J., and Rosenberg, M.T. (2014). Testosterone deficiency: myth, facts, and controversy. *Can J Urol* 21 Suppl 2**,** 39-54.

Mishra, J.S., Hankins, G.D., and Kumar, S. (2016). Testosterone downregulates angiotensin II type-2 receptor via androgen receptor-mediated ERK1/2 MAP kinase pathway in rat aorta. *J Renin Angiotensin Aldosterone Syst* 17.

Missale, C., Nash, S.R., Robinson, S.W., Jaber, M., and Caron, M.G. (1998). Dopamine receptors: from structure to function. *Physiol Rev* 78**,** 189-225.

Mohrmann, R., De Wit, H., Connell, E., Pinheiro, P.S., Leese, C., Bruns, D., Davletov, B., Verhage, M., and Sorensen, J.B. (2013). Synaptotagmin interaction with SNAP-25 governs vesicle docking, priming, and fusion triggering. *J Neurosci* 33**,** 14417-14430.

Molinari, C., Battaglia, A., Grossini, E., Mary, D.A., Vassanelli, C., and Vacca, G. (2002). The effect of testosterone on regional blood flow in prepubertal anaesthetized pigs. *J Physiol* 543**,** 365-372.

Monath, J.R., Mccullough, D.L., Hart, L.J., and Jarow, J.P. (1995). Physiologic variations of serum testosterone within the normal range do not affect serum prostate-specific antigen. *Urology* 46**,** 58-61.

Montenegro, M., Bayones, L., Moya-Diaz, J., Borassi, C., Martin Toscani, A., Gallo, L.I., and Marengo, F.D. (2020). Rapid vesicle replenishment after the immediately releasable pool exocytosis is tightly linked to fast endocytosis, and depends on basal calcium and cortical actin in chromaffin cells. *J Neurochem*.

Moosmann, B., and Behl, C. (1999). The antioxidant neuroprotective effects of estrogens and phenolic compounds are independent from their estrogenic properties. *Proc Natl Acad Sci U S A* 96**,** 8867-8872.

Moretti, C., Lanzolla, G., Moretti, M., Gnessi, L., and Carmina, E. (2017). Androgens and Hypertension in Men and Women: a Unifying View. *Curr Hypertens Rep* 19**,** 44.

Morgentaler, A., and Traish, A.M. (2009). Shifting the paradigm of testosterone and prostate cancer: the saturation model and the limits of androgen-dependent growth. *Eur Urol* 55**,** 310-320.

Mosharov, E.V., and Sulzer, D. (2005). Analysis of exocytotic events recorded by amperometry. *Nat Methods* 2**,** 651-658.

Mousavi, M., Hellstrom-Lindahl, E., Guan, Z.Z., Bednar, I., and Nordberg, A. (2001). Expression of nicotinic acetylcholine receptors in human and rat adrenal medulla. *Life Sci* 70**,** 577-590.

Moya-Diaz, J., Alvarez, Y.D., Montenegro, M., Bayones, L., Belingheri, A.V., Gonzalez-Jamett, A.M., Cardenas, A.M., and Marengo, F.D. (2016). Sustained Exocytosis after Action Potential-Like Stimulation at Low Frequencies in Mouse Chromaffin Cells Depends on a Dynamin-Dependent Fast Endocytotic Process. *Front Cell Neurosci* 10**,** 184.

Muller-Tidow, C., Diederichs, S., Bulk, E., Pohle, T., Steffen, B., Schwable, J., Plewka, S., Thomas, M., Metzger, R., Schneider, P.M., Brandts, C.H., Berdel, W.E., and Serve, H. (2005). Identification of metastasis-associated receptor tyrosine kinases in non-small cell lung cancer. *Cancer Res* 65**,** 1778-1782.

Mulligan, T., Frick, M.F., Zuraw, Q.C., Stemhagen, A., and Mcwhirter, C. (2006). Prevalence of hypogonadism in males aged at least 45 years: the HIM study. *Int J Clin Pract* 60**,** 762-769.

Mund, R.A., and Frishman, W.H. (2013). Brown adipose tissue thermogenesis: beta3-adrenoreceptors as a potential target for the treatment of obesity in humans. *Cardiol Rev* 21**,** 265-269.

Murai, K.K., and Pasquale, E.B. (2003). 'Eph'ective signaling: forward, reverse and crosstalk. *J Cell Sci* 116**,** 2823-2832.

Murai, K.K., and Pasquale, E.B. (2004). Eph receptors, ephrins, and synaptic function. *Neuroscientist* 10**,** 304-314.

Muraleedharan, V., Marsh, H., Kapoor, D., Channer, K.S., and Jones, T.H. (2013). Testosterone deficiency is associated with increased risk of mortality and testosterone replacement improves survival in men with type 2 diabetes. *Eur J Endocrinol* 169**,** 725-733.

Najafi, A., Sequeira, V., Kuster, D.W., and Van Der Velden, J. (2016). beta-adrenergic receptor signalling and its functional consequences in the diseased heart. *Eur J Clin Invest* 46**,** 362-374.

Nakabeppu, Y., Ryder, K., and Nathans, D. (1988). DNA binding activities of three murine Jun proteins: stimulation by Fos. *Cell* 55**,** 907-915.

Nakada, M., Drake, K.L., Nakada, S., Niska, J.A., and Berens, M.E. (2006). Ephrin-B3 ligand promotes glioma invasion through activation of Rac1. *Cancer Res* 66**,** 8492-8500.

Nakashima, A., Ota, A., and Sabban, E.L. (2003). Interactions between Egr1 and AP1 factors in regulation of tyrosine hydroxylase transcription. *Brain Res Mol Brain Res* 112**,** 61-69.

Nakayama, A., Nakayama, M., Turner, C.J., Hoing, S., Lepore, J.J., and Adams, R.H. (2013). Ephrin-B2 controls PDGFRbeta internalization and signaling. *Genes Dev* 27**,** 2576-2589.

Nakhla, A.M., Leonard, J., Hryb, D.J., and Rosner, W. (1999). Sex hormone-binding globulin receptor signal transduction proceeds via a G protein. *Steroids* 64**,** 213-216.

Nankova, B., Hiremagalur, B., Menezes, A., Zeman, R., and Sabban, E. (1996). Promoter elements and second messenger pathways involved in transcriptional activation of tyrosine hydroxylase by ionomycin. *Brain Res Mol Brain Res* 35**,** 164-172.

Nateri, A.S., Riera-Sans, L., Da Costa, C., and Behrens, A. (2004). The ubiquitin ligase SCFFbw7 antagonizes apoptotic JNK signaling. *Science* 303**,** 1374-1378.

Nateri, A.S., Spencer-Dene, B., and Behrens, A. (2005). Interaction of phosphorylated c-Jun with TCF4 regulates intestinal cancer development. *Nature* 437**,** 281-285.

Neco, P., Gil, A., Del Mar Frances, M., Viniegra, S., and Gutierrez, L.M. (2002). The role of myosin in vesicle transport during bovine chromaffin cell secretion. *Biochem J* 368**,** 405-413.

Neco, P., Giner, D., Viniegra, S., Borges, R., Villarroel, A., and Gutierrez, L.M. (2004). New roles of myosin II during vesicle transport and fusion in chromaffin cells. *J Biol Chem* 279**,** 27450-27457.

Nickenig, G., Baumer, A.T., Grohe, C., Kahlert, S., Strehlow, K., Rosenkranz, S., Stablein, A., Beckers, F., Smits, J.F., Daemen, M.J., Vetter, H., and Bohm, M. (1998). Estrogen modulates AT1 receptor gene expression in vitro and in vivo. *Circulation* 97**,** 2197-2201.

Niggli, V., and Rossy, J. (2008). Ezrin/radixin/moesin: versatile controllers of signaling molecules and of the cortical cytoskeleton. *Int J Biochem Cell Biol* 40**,** 344-349.

Noren, N.K., and Pasquale, E.B. (2004). Eph receptor-ephrin bidirectional signals that target Ras and Rho proteins. *Cell Signal* 16**,** 655-666.

North, R.A. (1989). Twelfth Gaddum memorial lecture. Drug receptors and the inhibition of nerve cells. *Br J Pharmacol* 98**,** 13-28.

O'neill, A.K., Kindberg, A.A., Niethamer, T.K., Larson, A.R., Ho, H.H., Greenberg, M.E., and Bush, J.O. (2016). Unidirectional Eph/ephrin signaling creates a cortical actomyosin differential to drive cell segregation. *J Cell Biol* 215**,** 217-229.

Okamoto, K., Bosch, M., and Hayashi, Y. (2009). The roles of CaMKII and F-actin in the structural plasticity of dendritic spines: a potential molecular identity of a synaptic tag? *Physiology (Bethesda)* 24**,** 357-366.

Olivares, M.J., Gonzalez-Jamett, A.M., Guerra, M.J., Baez-Matus, X., Haro-Acuna, V., Martinez-Quiles, N., and Cardenas, A.M. (2014). Src kinases regulate de novo actin polymerization during exocytosis in neuroendocrine chromaffin cells. *PLoS One* 9**,** e99001.

Ong, L.K., Page, S., Briggs, G.D., Guan, L., Dun, M.D., Verrills, N.M., Dunkley, P.R., and Dickson, P.W. (2017). Peripheral Lipopolysaccharide Challenge Induces Long-Term Changes in Tyrosine Hydroxylase Regulation in the Adrenal Medulla. *J Cell Biochem* 118**,** 2096-2107.

Ory, S., Ceridono, M., Momboisse, F., Houy, S., Chasserot-Golaz, S., Heintz, D., Calco, V., Haeberle, A.M., Espinoza, F.A., Sims, P.J., Bailly, Y., Bader, M.F., and Gasman, S. (2013). Phospholipid scramblase-1-induced lipid reorganization regulates compensatory endocytosis in neuroendocrine cells. *J Neurosci* 33**,** 3545-3556.

Osborn, J.L., Dibona, G.F., and Thames, M.D. (1981). Beta-1 receptor mediation of renin secretion elicited by low-frequency renal nerve stimulation. *J Pharmacol Exp Ther* 216**,** 265-269.

Palmer, A., Zimmer, M., Erdmann, K.S., Eulenburg, V., Porthin, A., Heumann, R., Deutsch, U., and Klein, R. (2002). EphrinB phosphorylation and reverse signaling: regulation by Src kinases and PTP-BL phosphatase. *Mol Cell* 9**,** 725-737.

Pandini, G., Mineo, R., Frasca, F., Roberts, C.T., Jr., Marcelli, M., Vigneri, R., and Belfiore, A. (2005). Androgens up-regulate the insulin-like growth factor-I receptor in prostate cancer cells. *Cancer Res* 65**,** 1849-1857.

Pantaloni, D., and Carlier, M.F. (1993). How profilin promotes actin filament assembly in the presence of thymosin beta 4. *Cell* 75**,** 1007-1014.

Papanikolaou, N.A., and Sabban, E.L. (1999). Sp1/Egr1 motif: a new candidate in the regulation of rat tyrosine hydroxylase gene transcription by immobilization stress. *J Neurochem* 73**,** 433-436.

Papanikolaou, N.A., and Sabban, E.L. (2000). Ability of Egr1 to activate tyrosine hydroxylase transcription in PC12 cells. Cross-talk with AP-1 factors. *J Biol Chem* 275**,** 26683-26689.

Paradiso, K., and Brehm, P. (1998). Long-term desensitization of nicotinic acetylcholine receptors is regulated via protein kinase A-mediated phosphorylation. *J Neurosci* 18**,** 9227-9237.

Parsaud, L., Li, L., Jung, C.H., Park, S., Saw, N.M., Park, S., Kim, M.Y., and Sugita, S. (2013). Calcium-dependent activator protein for secretion 1 (CAPS1) binds to syntaxin-1 in a distinct mode from Munc13-1. *J Biol Chem* 288**,** 23050-23063.

Pasquale, E.B. (2005). Eph receptor signalling casts a wide net on cell behaviour. *Nat Rev Mol Cell Biol* 6**,** 462-475.

Pasquale, E.B. (2008). Eph-ephrin bidirectional signaling in physiology and disease. *Cell* 133**,** 38-52.

Pastuszak, A.W., Pearlman, A.M., Lai, W.S., Godoy, G., Sathyamoorthy, K., Liu, J.S., Miles, B.J., Lipshultz, L.I., and Khera, M. (2013). Testosterone replacement therapy in patients with prostate cancer after radical prostatectomy. *J Urol* 190**,** 639-644.

Patankar, S., Lazaroff, M., Yoon, S.O., and Chikaraishi, D.M. (1997). A novel basal promoter element is required for expression of the rat tyrosine hydroxylase gene. *J Neurosci* 17**,** 4076-4086.

Pende, A., Musso, N.R., Vergassola, C., Puppo, F., Ioverno, A., Criscuolo, D., Indiveri, F., and Lotti, G. (1990). Neuroendocrine effects of interferon alpha 2-a in healthy human subjects. *J Biol Regul Homeost Agents* 4**,** 67-72.

Penzes, P., Beeser, A., Chernoff, J., Schiller, M.R., Eipper, B.A., Mains, R.E., and Huganir, R.L. (2003). Rapid induction of dendritic spine morphogenesis by trans-synaptic ephrinB-EphB receptor activation of the Rho-GEF kalirin. *Neuron* 37**,** 263-274.

Perusquia, M., Navarrete, E., Gonzalez, L., and Villalon, C.M. (2007). The modulatory role of androgens and progestins in the induction of vasorelaxation in human umbilical artery. *Life Sci* 81**,** 993-1002.

Perusquia, M., and Stallone, J.N. (2010). Do androgens play a beneficial role in the regulation of vascular tone? Nongenomic vascular effects of testosterone metabolites. *Am J Physiol Heart Circ Physiol* 298**,** H1301-1307.

Phillips, G.B., Jing, T.Y., Resnick, L.M., Barbagallo, M., Laragh, J.H., and Sealey, J.E. (1993). Sex hormones and hemostatic risk factors for coronary heart disease in men with hypertension. *J Hypertens* 11**,** 699-702.

Piech-Dumas, K.M., Best, J.A., Chen, Y., Nagamoto-Combs, K., Osterhout, C.A., and Tank, A.W. (2001). The cAMP responsive element and CREB partially mediate the response of the tyrosine hydroxylase gene to phorbol ester. *J Neurochem* 76**,** 1376-1385.

Piech-Dumas, K.M., and Tank, A.W. (1999). CREB mediates the cAMP-responsiveness of the tyrosine hydroxylase gene: use of an antisense RNA strategy to produce CREB-deficient PC12 cell lines. *Brain Res Mol Brain Res* 70**,** 219-230.

Plattner, R., Kadlec, L., Demali, K.A., Kazlauskas, A., and Pendergast, A.M. (1999). c-Abl is activated by growth factors and Src family kinases and has a role in the cellular response to PDGF. *Genes Dev* 13**,** 2400-2411.

Poea-Guyon, S., Ammar, M.R., Erard, M., Amar, M., Moreau, A.W., Fossier, P., Gleize, V., Vitale, N., and Morel, N. (2013). The V-ATPase membrane domain is a sensor of granular pH that controls the exocytotic machinery. *J Cell Biol* 203**,** 283-298.

Poitz, D.M., Ende, G., Stutz, B., Augstein, A., Friedrichs, J., Brunssen, C., Werner, C., Strasser, R.H., and Jellinghaus, S. (2015). EphrinB2/EphA4-mediated activation of endothelial cells increases monocyte adhesion. *Mol Immunol* 68**,** 648-656.

Pollard, T.D. (2007). Regulation of actin filament assembly by Arp2/3 complex and formins. *Annu Rev Biophys Biomol Struct* 36**,** 451-477.

Prakash, Y.S., Togaibayeva, A.A., Kannan, M.S., Miller, V.M., Fitzpatrick, L.A., and Sieck, G.C. (1999). Estrogen increases Ca2+ efflux from female porcine coronary arterial smooth muscle. *Am J Physiol* 276**,** H926-934.

Prossnitz, E.R., and Barton, M. (2014). Estrogen biology: new insights into GPER function and clinical opportunities. *Mol Cell Endocrinol* 389**,** 71-83.

Qaseem, A., Horwitch, C.A., Vijan, S., Etxeandia-Ikobaltzeta, I., Kansagara, D., and Clinical Guidelines Committee of the American College Of, P. (2020). Testosterone Treatment in Adult Men With Age-Related Low Testosterone: A Clinical Guideline From the American College of Physicians. *Ann Intern Med* 172**,** 126-133.

Qiao, M., Jiang, Q.S., Liu, Y.J., Hu, X.Y., Wang, L.J., Zhou, Q.X., and Qiu, H.M. (2019). Antidepressant mechanisms of venlafaxine involving increasing histone acetylation and modulating tyrosine hydroxylase and tryptophan hydroxylase expression in hippocampus of depressive rats. *Neuroreport* 30**,** 255-261.

Rabi, D.M., Khan, N., Vallee, M., Hladunewich, M.A., Tobe, S.W., and Pilote, L. (2008). Reporting on sex-based analysis in clinical trials of angiotensin-converting enzyme inhibitor and angiotensin receptor blocker efficacy. *Can J Cardiol* 24**,** 491-496.

Rana, K., Davey, R.A., and Zajac, J.D. (2014). Human androgen deficiency: insights gained from androgen receptor knockout mouse models. *Asian J Androl* 16**,** 169-177.

Rao, V.N., Huebner, K., Isobe, M., Ar-Rushdi, A., Croce, C.M., and Reddy, E.S. (1989). elk, tissue-specific ets-related genes on chromosomes X and 14 near translocation breakpoints. *Science* 244**,** 66-70.

Reckelhoff, J.F. (2019). Androgens and Blood Pressure Control: Sex Differences and Mechanisms. *Mayo Clin Proc* 94**,** 536-543.

Reckelhoff, J.F., and Roman, R.J. (2011). Androgens and hypertension: role in both males and females? *Hypertension* 57**,** 681-682.

Reckelhoff, J.F., Zhang, H., and Granger, J.P. (1998). Testosterone exacerbates hypertension and reduces pressure-natriuresis in male spontaneously hypertensive rats. *Hypertension* 31**,** 435-439.

Richter, M., Murai, K.K., Bourgin, C., Pak, D.T., and Pasquale, E.B. (2007). The EphA4 receptor regulates neuronal morphology through SPAR-mediated inactivation of Rap GTPases. *J Neurosci* 27**,** 14205-14215.

Riedl, J.A., Brandt, D.T., Batlle, E., Price, L.S., Clevers, H., and Bos, J.L. (2005). Down-regulation of Rap1 activity is involved in ephrinB1-induced cell contraction. *Biochem J* 389**,** 465-469.

Rivier, C., Vale, W., and Brown, M. (1989). In the rat, interleukin-1 alpha and -beta stimulate adrenocorticotropin and catecholamine release. *Endocrinology* 125**,** 3096-3102.

Roe, D.F., Craviso, G.L., and Waymire, J.C. (2004). Nicotinic stimulation modulates tyrosine hydroxylase mRNA half-life and protein binding to the 3'UTR in a manner that requires transcription. *Brain Res Mol Brain Res* 120**,** 91-102.

Rokhlin, O.W., Taghiyev, A.F., Guseva, N.V., Glover, R.A., Chumakov, P.M., Kravchenko, J.E., and Cohen, M.B. (2005). Androgen regulates apoptosis induced by TNFR family ligands via multiple signaling pathways in LNCaP. *Oncogene* 24**,** 6773-6784.

Role, L.W., Leeman, S.E., and Perlman, R.L. (1981). Somatostatin and substance P inhibit catecholamine secretion from isolated cells of guinea-pig adrenal medulla. *Neuroscience* 6**,** 1813-1821.

Romano, G., Macaluso, M., Lucchetti, C., and Iacovitti, L. (2007). Transcription and epigenetic profile of the promoter, first exon and first intron of the human tyrosine hydroxylase gene. *J Cell Physiol* 211**,** 431-438.

Rosano, G.M., Vitale, C., and Fini, M. (2006). Hormone replacement therapy and cardioprotection: what is good and what is bad for the cardiovascular system? *Ann N Y Acad Sci* 1092**,** 341-348.

Rose, S.D., Lejen, T., Casaletti, L., Larson, R.E., Pene, T.D., and Trifaro, J.M. (2002). Molecular motors involved in chromaffin cell secretion. *Ann N Y Acad Sci* 971**,** 222-231.

Rotty, J.D., Wu, C., and Bear, J.E. (2013). New insights into the regulation and cellular functions of the ARP2/3 complex. *Nat Rev Mol Cell Biol* 14**,** 7-12.

Rowland, N.E., and Fregly, M.J. (1992). Role of gonadal hormones in hypertension in the Dahl salt-sensitive rat. *Clin Exp Hypertens A* 14**,** 367-375.

Ruehlmann, D.O., Steinert, J.R., Valverde, M.A., Jacob, R., and Mann, G.E. (1998). Environmental estrogenic pollutants induce acute vascular relaxation by inhibiting L-type Ca2+ channels in smooth muscle cells. *FASEB J* 12**,** 613-619.

Saad, F., Doros, G., Haider, K.S., and Haider, A. (2020). Differential effects of 11 years of long-term injectable testosterone undecanoate therapy on anthropometric and metabolic parameters in hypogonadal men

with normal weight, overweight and obesity in comparison with untreated controls: real-world data from a controlled registry study. *Int J Obes (Lond)* 44**,** 1264-1278.
Sajjadi, F.G., Pasquale, E.B., and Subramani, S. (1991). Identification of a new eph-related receptor tyrosine kinase gene from mouse and chicken that is developmentally regulated and encodes at least two forms of the receptor. *New Biol* 3**,** 769-778.
Sakamoto, A., Sugamoto, Y., Tokunaga, Y., Yoshimuta, T., Hayashi, K., Konno, T., Kawashiri, M.A., Takeda, Y., and Yamagishi, M. (2011). Expression profiling of the ephrin (EFN) and Eph receptor (EPH) family of genes in atherosclerosis-related human cells. *J Int Med Res* 39**,** 522-527.
Sala, F., Nistri, A., and Criado, M. (2008). Nicotinic acetylcholine receptors of adrenal chromaffin cells. *Acta Physiol (Oxf)* 192**,** 203-212.
Salhab, W.A., Shaul, P.W., Cox, B.E., and Rosenfeld, C.R. (2000). Regulation of types I and III NOS in ovine uterine arteries by daily and acute estrogen exposure. *Am J Physiol Heart Circ Physiol* 278**,** H2134-2142.
Salvucci, O., De La Luz Sierra, M., Martina, J.A., Mccormick, P.J., and Tosato, G. (2006). EphB2 and EphB4 receptors forward signaling promotes SDF-1-induced endothelial cell chemotaxis and branching remodeling. *Blood* 108**,** 2914-2922.
San Francisco, I.F., Rojas, P.A., Dewolf, W.C., and Morgentaler, A. (2014). Low free testosterone levels predict disease reclassification in men with prostate cancer undergoing active surveillance. *BJU Int* 114**,** 229-235.
Santulli, G., Lombardi, A., Sorriento, D., Anastasio, A., Del Giudice, C., Formisano, P., Beguinot, F., Trimarco, B., Miele, C., and Iaccarino, G. (2012). Age-related impairment in insulin release: the essential role of beta(2)-adrenergic receptor. *Diabetes* 61**,** 692-701.
Saras, J., Franzen, P., Aspenstrom, P., Hellman, U., Gonez, L.J., and Heldin, C.H. (1997). A novel GTPase-activating protein for Rho interacts with a PDZ domain of the protein-tyrosine phosphatase PTPL1. *J Biol Chem* 272**,** 24333-24338.
Sato, S., Vasaikar, S., Eskaros, A., Kim, Y., Lewis, J.S., Zhang, B., Zijlstra, A., and Weaver, A.M. (2019). EPHB2 carried on small extracellular vesicles induces tumor angiogenesis via activation of ephrin reverse signaling. *JCI Insight* 4.
Savica, R., and Benarroch, E.E. (2014). Dopamine receptor signaling in the forebrain: recent insights and clinical implications. *Neurology* 83**,** 758-767.
Schaub, J.R., Lu, X., Doneske, B., Shin, Y.K., and Mcnew, J.A. (2006). Hemifusion arrest by complexin is relieved by Ca2+-synaptotagmin I. *Nat Struct Mol Biol* 13**,** 748-750.
Schiffelers, S.L., Saris, W.H., Boomsma, F., and Van Baak, M.A. (2001). beta(1)- and beta(2)-Adrenoceptor-mediated thermogenesis and lipid utilization in obese and lean men. *J Clin Endocrinol Metab* 86**,** 2191-2199.
Schmidt, E.F., Shim, S.O., and Strittmatter, S.M. (2008). Release of MICAL autoinhibition by semaphorin-plexin signaling promotes interaction with collapsin response mediator protein. *J Neurosci* 28**,** 2287-2297.
Schnell, P.O., Ignacak, M.L., Bauer, A.L., Striet, J.B., Paulding, W.R., and Czyzyk-Krzeska, M.F. (2003). Regulation of tyrosine hydroxylase promoter activity by the von Hippel-Lindau tumor suppressor protein and hypoxia-inducible transcription factors. *J Neurochem* 85**,** 483-491.
Schreck, I., Al-Rawi, M., Mingot, J.M., Scholl, C., Diefenbacher, M.E., O'donnell, P., Bohmann, D., and Weiss, C. (2011). c-Jun localizes to the nucleus independent of its phosphorylation by and interaction with JNK and vice versa promotes nuclear accumulation of JNK. *Biochem Biophys Res Commun* 407**,** 735-740.
Seyrek, M., Yildiz, O., Ulusoy, H.B., and Yildirim, V. (2007). Testosterone relaxes isolated human radial artery by potassium channel opening action. *J Pharmacol Sci* 103**,** 309-316.
Shamah, S.M., Lin, M.Z., Goldberg, J.L., Estrach, S., Sahin, M., Hu, L., Bazalakova, M., Neve, R.L., Corfas, G., Debant, A., and Greenberg, M.E. (2001). EphA receptors regulate growth cone dynamics through the novel guanine nucleotide exchange factor ephexin. *Cell* 105**,** 233-244.
Shi, W., Wang, Y., Peng, J., Qi, S., Vitale, N., Kaneda, N., Murata, T., Luo, H., and Wu, J. (2019). EPHB6 controls catecholamine biosynthesis by up-regulating tyrosine hydroxylase transcription in adrenal gland chromaffin cells. *J Biol Chem* 294**,** 6871-6887.
Shi, X., and Wang, B. (2018). Caught in the "Akt": Cross-talk between EphA2 and EGFR through the Akt-PIKfyve axis maintains cellular sensitivity to EGF. *Sci Signal* 11.
Shimizu, N., Ohta, M., Fujiwara, C., Sagara, J., Mochizuki, N., Oda, T., and Utiyama, H. (1992). A gene coding for a zinc finger protein is induced during 12-O-tetradecanoylphorbol-13-acetate-stimulated HL-60 cell differentiation. *J Biochem* 111**,** 272-277.

Shin, J., Gu, C., Kim, J., and Park, S. (2008). Transient activation of the MAP kinase signaling pathway by the forward signaling of EphA4 in PC12 cells. *BMB Rep* 41**,** 479-484.

Shores, M.M., Smith, N.L., Forsberg, C.W., Anawalt, B.D., and Matsumoto, A.M. (2012). Testosterone treatment and mortality in men with low testosterone levels. *J Clin Endocrinol Metab* 97**,** 2050-2058.

Skruber, K., Read, T.A., and Vitriol, E.A. (2018). Reconsidering an active role for G-actin in cytoskeletal regulation. *J Cell Sci* 131.

Smith, C.B., and Eiden, L.E. (2012). Is PACAP the major neurotransmitter for stress transduction at the adrenomedullary synapse? *J Mol Neurosci* 48**,** 403-412.

Snyder, P.J., Bhasin, S., Cunningham, G.R., Matsumoto, A.M., Stephens-Shields, A.J., Cauley, J.A., Gill, T.M., Barrett-Connor, E., Swerdloff, R.S., Wang, C., Ensrud, K.E., Lewis, C.E., Farrar, J.T., Cella, D., Rosen, R.C., Pahor, M., Crandall, J.P., Molitch, M.E., Cifelli, D., Dougar, D., Fluharty, L., Resnick, S.M., Storer, T.W., Anton, S., Basaria, S., Diem, S.J., Hou, X., Mohler, E.R., 3rd, Parsons, J.K., Wenger, N.K., Zeldow, B., Landis, J.R., Ellenberg, S.S., and Testosterone Trials, I. (2016). Effects of Testosterone Treatment in Older Men. *N Engl J Med* 374**,** 611-624.

Soisson, V., Brailly-Tabard, S., Helmer, C., Rouaud, O., Ancelin, M.L., Zerhouni, C., Guiochon-Mantel, A., and Scarabin, P.Y. (2013). A J-shaped association between plasma testosterone and risk of ischemic arterial event in elderly men: the French 3C cohort study. *Maturitas* 75**,** 282-288.

Sokolova, O.S., Chemeris, A., Guo, S., Alioto, S.L., Gandhi, M., Padrick, S., Pechnikova, E., David, V., Gautreau, A., and Goode, B.L. (2017). Structural Basis of Arp2/3 Complex Inhibition by GMF, Coronin, and Arpin. *J Mol Biol* 429**,** 237-248.

Solaro, C.R., Prakriya, M., Ding, J.P., and Lingle, C.J. (1995). Inactivating and noninactivating Ca(2+)- and voltage-dependent K+ current in rat adrenal chromaffin cells. *J Neurosci* 15**,** 6110-6123.

Sontag, J.M., Sanderson, P., Klepper, M., Aunis, D., Takeda, K., and Bader, M.F. (1990). Modulation of secretion by dopamine involves decreases in calcium and nicotinic currents in bovine chromaffin cells. *J Physiol* 427**,** 495-517.

Sparrenberger, F., Cichelero, F.T., Ascoli, A.M., Fonseca, F.P., Weiss, G., Berwanger, O., Fuchs, S.C., Moreira, L.B., and Fuchs, F.D. (2009). Does psychosocial stress cause hypertension? A systematic review of observational studies. *J Hum Hypertens* 23**,** 12-19.

Spiering, D., and Hodgson, L. (2011). Dynamics of the Rho-family small GTPases in actin regulation and motility. *Cell Adh Migr* 5**,** 170-180.

Stallaert, W., Bruggemann, Y., Sabet, O., Baak, L., Gattiglio, M., and Bastiaens, P.I.H. (2018). Contact inhibitory Eph signaling suppresses EGF-promoted cell migration by decoupling EGFR activity from vesicular recycling. *Sci Signal* 11.

Stein, E., Cerretti, D.P., and Daniel, T.O. (1996). Ligand activation of ELK receptor tyrosine kinase promotes its association with Grb10 and Grb2 in vascular endothelial cells. *J Biol Chem* 271**,** 23588-23593.

Stevens, D.R., Schirra, C., Becherer, U., and Rettig, J. (2011). Vesicle pools: lessons from adrenal chromaffin cells. *Front Synaptic Neurosci* 3**,** 2.

Strakova, Z., Reed, J., and Ihnatovych, I. (2010). Human transcriptional coactivator with PDZ-binding motif (TAZ) is downregulated during decidualization. *Biol Reprod* 82**,** 1112-1118.

Suárez, L., Bilal, U., Bordallo, J., Cantabrana, B., and Sánchez, M. (2015). Androgens block outward potassium currents and decrease spontaneous action potentials in GH3 cells. *Naunyn-Schmiedeberg's archives of pharmacology* 388**,** 67-78.

Suzuki, T., Kurahashi, H., and Ichinose, H. (2004). Ras/MEK pathway is required for NGF-induced expression of tyrosine hydroxylase gene. *Biochem Biophys Res Commun* 315**,** 389-396.

Takeuchi, S., Katoh, H., and Negishi, M. (2015). Eph/ephrin reverse signalling induces axonal retraction through RhoA/ROCK pathway. *J Biochem* 158**,** 245-252.

Tanaka, M., Kamata, R., Yanagihara, K., and Sakai, R. (2010). Suppression of gastric cancer dissemination by ephrin-B1-derived peptide. *Cancer Sci* 101**,** 87-93.

Tanaka, M., Kamo, T., Ota, S., and Sugimura, H. (2003). Association of Dishevelled with Eph tyrosine kinase receptor and ephrin mediates cell repulsion. *EMBO J* 22**,** 847-858.

Tanaka, M., Nakaya, S., Watanabe, M., Kumai, T., Tateishi, T., and Kobayashi, S. (1997). Effects of ovariectomy and estrogen replacement on aorta angiotensin-converting enzyme activity in rats. *Jpn J Pharmacol* 73**,** 361-363.

Tanaka, M., Ohashi, R., Nakamura, R., Shinmura, K., Kamo, T., Sakai, R., and Sugimura, H. (2004). Tiam1 mediates neurite outgrowth induced by ephrin-B1 and EphA2. *EMBO J* 23**,** 1075-1088.

Tanaka, M., Sasaki, K., Kamata, R., and Sakai, R. (2007). The C-terminus of ephrin-B1 regulates metalloproteinase secretion and invasion of cancer cells. *J Cell Sci* 120**,** 2179-2189.

Tang, X.X., Zhao, H., Robinson, M.E., Cohen, B., Cnaan, A., London, W., Cohn, S.L., Cheung, N.K., Brodeur, G.M., Evans, A.E., and Ikegaki, N. (2000). Implications of EPHB6, EFNB2, and EFNB3 expressions in human neuroblastoma. *Proc Natl Acad Sci U S A* 97**,** 10936-10941.

Tank, A.W., and Lee Wong, D. (2015). Peripheral and central effects of circulating catecholamines. *Compr Physiol* 5**,** 1-15.

Tekin, I., Roskoski, R., Jr., Carkaci-Salli, N., and Vrana, K.E. (2014). Complex molecular regulation of tyrosine hydroxylase. *J Neural Transm (Vienna)* 121**,** 1451-1481.

Thomas, P., Converse, A., and Berg, H.A. (2017). ZIP9, a novel membrane androgen receptor and zinc transporter protein. *Gen Comp Endocrinol*.

Tomatis, V.M., Papadopulos, A., Malintan, N.T., Martin, S., Wallis, T., Gormal, R.S., Kendrick-Jones, J., Buss, F., and Meunier, F.A. (2013). Myosin VI small insert isoform maintains exocytosis by tethering secretory granules to the cortical actin. *J Cell Biol* 200**,** 301-320.

Tomlinson, A., Durbin, J., and Coupland, R.E. (1987). A quantitative analysis of rat adrenal chromaffin tissue: morphometric analysis at tissue and cellular level correlated with catecholamine content. *Neuroscience* 20**,** 895-904.

Toosi, B.M., El Zawily, A., Truitt, L., Shannon, M., Allonby, O., Babu, M., Decoteau, J., Mousseau, D., Ali, M., Freywald, T., Gall, A., Vizeacoumar, F.S., Kirzinger, M.W., Geyer, C.R., Anderson, D.H., Kim, T., Welm, A.L., Siegel, P., Vizeacoumar, F.J., Kusalik, A., and Freywald, A. (2018). EPHB6 augments both development and drug sensitivity of triple-negative breast cancer tumours. *Oncogene* 37**,** 4073-4093.

Torres, R., Firestein, B.L., Dong, H., Staudinger, J., Olson, E.N., Huganir, R.L., Bredt, D.S., Gale, N.W., and Yancopoulos, G.D. (1998). PDZ proteins bind, cluster, and synaptically colocalize with Eph receptors and their ephrin ligands. *Neuron* 21**,** 1453-1463.

Toth, J., Cutforth, T., Gelinas, A.D., Bethoney, K.A., Bard, J., and Harrison, C.J. (2001). Crystal structure of an ephrin ectodomain. *Dev Cell* 1**,** 83-92.

Toth, M., and Zakar, T. (1982). Relative binding affinities of testosterone, 19-nortestosterone and their 5 alpha-reduced derivatives to the androgen receptor and to other androgen-binding proteins: a suggested role of 5 alpha-reductive steroid metabolism in the dissociation of "myotropic" and "androgenic" activities of 19-nortestosterone. *J Steroid Biochem* 17**,** 653-660.

Traish, A.M., Abdou, R., and Kypreos, K.E. (2009). Androgen deficiency and atherosclerosis: The lipid link. *Vascul Pharmacol* 51**,** 303-313.

Traish, A.M., Haider, A., Doros, G., and Saad, F. (2014). Long-term testosterone therapy in hypogonadal men ameliorates elements of the metabolic syndrome: an observational, long-term registry study. *Int J Clin Pract* 68**,** 314-329.

Traish, A.M., Haider, A., Haider, K.S., Doros, G., and Saad, F. (2017). Long-Term Testosterone Therapy Improves Cardiometabolic Function and Reduces Risk of Cardiovascular Disease in Men with Hypogonadism: A Real-Life Observational Registry Study Setting Comparing Treated and Untreated (Control) Groups. *J Cardiovasc Pharmacol Ther* 22**,** 414-433.

Traish, A.M., Moreland, R.B., Huang, Y.H., and Goldstein, I. (1997). Expression of functional alpha2-adrenergic receptor subtypes in human corpus cavernosum and in cultured trabecular smooth muscle cells. *Recept Signal Transduct* 7**,** 55-67.

Tremblay, J., Wang, Y., Raelson, J., Marois-Blanchet, F.C., Wu, Z., Luo, H., Bradley, E., Chalmers, J., Woodward, M., Harrap, S., Hamet, P., and Wu, J. (2017). Evidence from single nucleotide polymorphism analyses of ADVANCE study demonstrates EFNB3 as a hypertension risk gene. *Sci Rep* 7**,** 44114.

Trifaro, J., Rose, S.D., Lejen, T., and Elzagallaai, A. (2000). Two pathways control chromaffin cell cortical F-actin dynamics during exocytosis. *Biochimie* 82**,** 339-352.

Trifaro, J.M., Gasman, S., and Gutierrez, L.M. (2008). Cytoskeletal control of vesicle transport and exocytosis in chromaffin cells. *Acta Physiol (Oxf)* 192**,** 165-172.

Truitt, L., and Freywald, A. (2011). Dancing with the dead: Eph receptors and their kinase-null partners. *Biochem Cell Biol* 89**,** 115-129.

Truitt, L., Freywald, T., Decoteau, J., Sharfe, N., and Freywald, A. (2010). The EphB6 receptor cooperates with c-Cbl to regulate the behavior of breast cancer cells. *Cancer Res* 70**,** 1141-1153.

Udenfriend, S. (1966). Tyrosine hydroxylase. *Pharmacol Rev* 18**,** 43-51.

Ueda, T., Bruchovsky, N., and Sadar, M.D. (2002). Activation of the androgen receptor N-terminal domain by interleukin-6 via MAPK and STAT3 signal transduction pathways. *J Biol Chem* 277**,** 7076-7085.

Um, K., Niu, S., Duman, J.G., Cheng, J.X., Tu, Y.K., Schwechter, B., Liu, F., Hiles, L., Narayanan, A.S., Ash, R.T., Mulherkar, S., Alpadi, K., Smirnakis, S.M., and Tolias, K.F. (2014). Dynamic control of excitatory synapse development by a Rac1 GEF/GAP regulatory complex. *Dev Cell* 29**,** 701-715.

Unni, E., Sun, S., Nan, B., Mcphaul, M.J., Cheskis, B., Mancini, M.A., and Marcelli, M. (2004). Changes in androgen receptor nongenotropic signaling correlate with transition of LNCaP cells to androgen independence. *Cancer Res* 64**,** 7156-7168.

Uray, K., Major, E., and Lontay, B. (2020). MicroRNA Regulatory Pathways in the Control of the Actin-Myosin Cytoskeleton. *Cells* 9.

Valente, M.A., Voors, A.A., Damman, K., Van Veldhuisen, D.J., Massie, B.M., O'connor, C.M., Metra, M., Ponikowski, P., Teerlink, J.R., Cotter, G., Davison, B., Cleland, J.G., Givertz, M.M., Bloomfield, D.M., Fiuzat, M., Dittrich, H.C., and Hillege, H.L. (2014). Diuretic response in acute heart failure: clinical characteristics and prognostic significance. *Eur Heart J* 35**,** 1284-1293.

Vegh, A.M.D., Duim, S.N., Smits, A.M., Poelmann, R.E., Ten Harkel, A.D.J., Deruiter, M.C., Goumans, M.J., and Jongbloed, M.R.M. (2016). Part and Parcel of the Cardiac Autonomic Nerve System: Unravelling Its Cellular Building Blocks during Development. *J Cardiovasc Dev Dis* 3.

Venihaki, M., Gravanis, A., and Margioris, A.N. (1996). Opioids inhibit dopamine secretion from PC12 rat pheochromocytoma cells in a naloxone-reversible manner. *Life Sci* 58**,** 75-82.

Vermeer, P.D., Bell, M., Lee, K., Vermeer, D.W., Wieking, B.G., Bilal, E., Bhanot, G., Drapkin, R.I., Ganesan, S., Klingelhutz, A.J., Hendriks, W.J., and Lee, J.H. (2012). ErbB2, EphrinB1, Src kinase and PTPN13 signaling complex regulates MAP kinase signaling in human cancers. *PLoS One* 7**,** e30447.

Vigen, R., O'donnell, C.I., Baron, A.E., Grunwald, G.K., Maddox, T.M., Bradley, S.M., Barqawi, A., Woning, G., Wierman, M.E., Plomondon, M.E., Rumsfeld, J.S., and Ho, P.M. (2013). Association of testosterone therapy with mortality, myocardial infarction, and stroke in men with low testosterone levels. *JAMA* 310**,** 1829-1836.

Vikan, T., Schirmer, H., Njolstad, I., and Svartberg, J. (2009). Endogenous sex hormones and the prospective association with cardiovascular disease and mortality in men: the Tromso Study. *Eur J Endocrinol* 161**,** 435-442.

Villanueva, M., Thornley, K., Augustine, G.J., and Wightman, R.M. (2006). Synapsin II negatively regulates catecholamine release. *Brain Cell Biol* 35**,** 125-136.

Vindis, C., Cerretti, D.P., Daniel, T.O., and Huynh-Do, U. (2003). EphB1 recruits c-Src and p52Shc to activate MAPK/ERK and promote chemotaxis. *J Cell Biol* 162**,** 661-671.

Virani, S.S., Alonso, A., Benjamin, E.J., Bittencourt, M.S., Callaway, C.W., Carson, A.P., Chamberlain, A.M., Chang, A.R., Cheng, S., Delling, F.N., Djousse, L., Elkind, M.S.V., Ferguson, J.F., Fornage, M., Khan, S.S., Kissela, B.M., Knutson, K.L., Kwan, T.W., Lackland, D.T., Lewis, T.T., Lichtman, J.H., Longenecker, C.T., Loop, M.S., Lutsey, P.L., Martin, S.S., Matsushita, K., Moran, A.E., Mussolino, M.E., Perak, A.M., Rosamond, W.D., Roth, G.A., Sampson, U.K.A., Satou, G.M., Schroeder, E.B., Shah, S.H., Shay, C.M., Spartano, N.L., Stokes, A., Tirschwell, D.L., Vanwagner, L.B., Tsao, C.W., American Heart Association Council On, E., Prevention Statistics, C., and Stroke Statistics, S. (2020). Heart Disease and Stroke Statistics-2020 Update: A Report From the American Heart Association. *Circulation* 141**,** e139-e596.

Vitale, M.L., Seward, E.P., and Trifaro, J.M. (1995). Chromaffin cell cortical actin network dynamics control the size of the release-ready vesicle pool and the initial rate of exocytosis. *Neuron* 14**,** 353-363.

Vollmer, R.R., Baruchin, A., Kolibal-Pegher, S.S., Corey, S.P., Stricker, E.M., and Kaplan, B.B. (1992). Selective activation of norepinephrine- and epinephrine-secreting chromaffin cells in rat adrenal medulla. *Am J Physiol* 263**,** R716-721.

Vyas, S., Faucon Biguet, N., and Mallet, J. (1990). Transcriptional and post-transcriptional regulation of tyrosine hydroxylase gene by protein kinase C. *EMBO J* 9**,** 3707-3712.

Wagner, M.J., Hsiung, M.S., Gish, G.D., Bagshaw, R.D., Doodnauth, S.A., Soliman, M.A., Jorgensen, C., Tucholska, M., and Rottapel, R. (2020). The Shb scaffold binds the Nck adaptor protein, p120 RasGAP, and Chimaerins and thereby facilitates heterotypic cell segregation by the receptor EphB2. *J Biol Chem* 295**,** 3932-3944.

Wahl, S., Barth, H., Ciossek, T., Aktories, K., and Mueller, B.K. (2000). Ephrin-A5 induces collapse of growth cones by activating Rho and Rho kinase. *J Cell Biol* 149**,** 263-270.

Walsh, D.A., and Van Patten, S.M. (1994). Multiple pathway signal transduction by the cAMP-dependent protein kinase. *FASEB J* 8**,** 1227-1236.

Wang, X., Destrument, A., and Tournier, C. (2007). Physiological roles of MKK4 and MKK7: insights from animal models. *Biochim Biophys Acta* 1773**,** 1349-1357.

Wang, Y., Hamet, P., Thorin, E., Tremblay, J., Raelson, J., Wu, Z., Luo, H., Jin, W., Lavoie, J.L., and Peng, J. (2016a). Reduced blood pressure after smooth muscle EFNB2 deletion and the potential association of EFNB2 mutation with human hypertension risk. *European Journal of Human Genetics 24, 1817-1825*.

Wang, Y., Shi, W., Blanchette, A., Peng, J., Qi, S., Luo, H., Ledoux, J., and Wu, J. (2018). EPHB6 and testosterone in concert regulate epinephrine release by adrenal gland chromaffin cells. *Sci Rep* 8**,** 842.

Wang, Y., Thorin, E., Luo, H., Tremblay, J., Lavoie, J.L., Wu, Z., Peng, J., Qi, S., and Wu, J. (2015). EPHB4 protein expression in vascular smooth muscle cells regulates their contractility, and EPHB4 deletion leads to hypotension in mice. *Journal of Biological Chemistry* 290**,** 14235-14244.

Wang, Y., Wu, Z., Luo, H., Peng, J., Raelson, J., Ehret, G.B., Munroe, P.B., Stoyanova, E., Qin, Z., Cloutier, G., Bradley, W.E., Wu, T., Shen, J.Z., Hu, S., and Wu, J. (2016b). The role of GRIP1 and ephrin B3 in blood pressure control and vascular smooth muscle cell contractility. *Sci Rep* 6**,** 38976.

Wang, Y., Wu, Z., Thorin, E., Tremblay, J., Lavoie, J.L., Luo, H., Peng, J., Qi, S., Wu, T., and Chen, F. (2016c). Estrogen and testosterone in concert with EFNB3 regulate vascular smooth muscle cell contractility and blood pressure. *American Journal of Physiology-Heart and Circulatory Physiology* 310**,** H861-H872.

Wang, Z., Liu, H., Gu, Y., and Chapman, E.R. (2011). Reconstituted synaptotagmin I mediates vesicle docking, priming, and fusion. *J Cell Biol* 195**,** 1159-1170.

Weiss, C., Schneider, S., Wagner, E.F., Zhang, X., Seto, E., and Bohmann, D. (2003). JNK phosphorylation relieves HDAC3-dependent suppression of the transcriptional activity of c-Jun. *EMBO J* 22**,** 3686-3695.

Wen, P.J., Grenklo, S., Arpino, G., Tan, X., Liao, H.S., Heureaux, J., Peng, S.Y., Chiang, H.C., Hamid, E., Zhao, W.D., Shin, W., Nareoja, T., Evergren, E., Jin, Y., Karlsson, R., Ebert, S.N., Jin, A., Liu, A.P., Shupliakov, O., and Wu, L.G. (2016). Actin dynamics provides membrane tension to merge fusing vesicles into the plasma membrane. *Nat Commun* 7**,** 12604.

White, R.E., Han, G., Maunz, M., Dimitropoulou, C., El-Mowafy, A.M., Barlow, R.S., Catravas, J.D., Snead, C., Carrier, G.O., Zhu, S., and Yu, X. (2002). Endothelium-independent effect of estrogen on Ca(2+)-activated K(+) channels in human coronary artery smooth muscle cells. *Cardiovasc Res* 53**,** 650-661.

Wimalasena, K. (2011). Vesicular monoamine transporters: structure-function, pharmacology, and medicinal chemistry. *Med Res Rev* 31**,** 483-519.

Wimmer-Kleikamp, S.H., Janes, P.W., Squire, A., Bastiaens, P.I., and Lackmann, M. (2004). Recruitment of Eph receptors into signaling clusters does not require ephrin contact. *J Cell Biol* 164**,** 661-666.

Wioland, H., Guichard, B., Senju, Y., Myram, S., Lappalainen, P., Jegou, A., and Romet-Lemonne, G. (2017). ADF/Cofilin Accelerates Actin Dynamics by Severing Filaments and Promoting Their Depolymerization at Both Ends. *Curr Biol* 27**,** 1956-1967 e1957.

Wong, D.L., and Tank, A.W. (2007). Stress-induced catecholaminergic function: transcriptional and post-transcriptional control. *Stress* 10**,** 121-130.

Wong, S.L., Leung, F.P., Lau, C.W., Au, C.L., Yung, L.M., Yao, X., Chen, Z.Y., Vanhoutte, P.M., Gollasch, M., and Huang, Y. (2009). Cyclooxygenase-2-derived prostaglandin F2alpha mediates endothelium-dependent contractions in the aortae of hamsters with increased impact during aging. *Circ Res* 104**,** 228-235.

Wright, A.S., Douglas, R.C., Thomas, L.N., Lazier, C.B., and Rittmaster, R.S. (1999). Androgen-induced regrowth in the castrated rat ventral prostate: role of 5alpha-reductase. *Endocrinology* 140**,** 4509-4515.

Wu, C.C., and Schwartzman, M.L. (2011). The role of 20-HETE in androgen-mediated hypertension. *Prostaglandins Other Lipid Mediat* 96**,** 45-53.

Wu, F.C., Tajar, A., Beynon, J.M., Pye, S.R., Silman, A.J., Finn, J.D., O'neill, T.W., Bartfai, G., Casanueva, F.F., Forti, G., Giwercman, A., Han, T.S., Kula, K., Lean, M.E., Pendleton, N., Punab, M., Boonen, S., Vanderschueren, D.,

Labrie, F., Huhtaniemi, I.T., and Group, E. (2010a). Identification of late-onset hypogonadism in middle-aged and elderly men. *N Engl J Med* 363**,** 123-135.

Wu, J., and Luo, H. (2005). Recent advances on T-cell regulation by receptor tyrosine kinases. *Current opinion in hematology* 12**,** 292-297.

Wu, P.C., Fann, M.J., and Kao, L.S. (2010b). Characterization of Ca2+ signaling pathways in mouse adrenal medullary chromaffin cells. *J Neurochem* 112**,** 1210-1222.

Wu, T., Wang, Y., Shi, W., Zhang, B.Q., Raelson, J., Yao, Y.M., Wu, H.D., Xu, Z.X., Marois-Blanchet, F.C., Ledoux, J., Blunck, R., Sheng, J.Z., Hu, S.J., Luo, H., and Wu, J. (2020). A Variant in the Nicotinic Acetylcholine Receptor Alpha 3 Subunit Gene Is Associated With Hypertension Risks in Hypogonadic Patients. *Front Genet* 11**,** 539862.

Wu, T., Zhang, B.Q., Raelson, J., Yao, Y.M., Wu, H.D., Xu, Z.X., Marois-Blanchet, F.C., Tahir, M.R., Wang, Y., Bradley, W.E., Luo, H., Wu, J., Sheng, J.Z., and Hu, S.J. (2018). Analysis of the association of EPHB6, EFNB1 and EFNB3 variants with hypertension risks in males with hypogonadism. *Sci Rep* 8**,** 14497.

Wu, Z., Luo, H., Thorin, E., Tremblay, J., Peng, J., Lavoie, J.L., Wang, Y., Qi, S., Wu, T., and Wu, J. (2012). Possible role of Efnb1 protein, a ligand of Eph receptor tyrosine kinases, in modulating blood pressure. *Journal of Biological Chemistry* 287**,** 15557-15569.

Wybenga-Groot, L.E., Baskin, B., Ong, S.H., Tong, J., Pawson, T., and Sicheri, F. (2001). Structural basis for autoinhibition of the Ephb2 receptor tyrosine kinase by the unphosphorylated juxtamembrane region. *Cell* 106**,** 745-757.

Xing, W., Kim, J., Wergedal, J., Chen, S.T., and Mohan, S. (2010). Ephrin B1 regulates bone marrow stromal cell differentiation and bone formation by influencing TAZ transactivation via complex formation with NHERF1. *Mol Cell Biol* 30**,** 711-721.

Xu, K., Tzvetkova-Robev, D., Xu, Y., Goldgur, Y., Chan, Y.P., Himanen, J.P., and Nikolov, D.B. (2013). Insights into Eph receptor tyrosine kinase activation from crystal structures of the EphA4 ectodomain and its complex with ephrin-A5. *Proc Natl Acad Sci U S A* 110**,** 14634-14639.

Xu, L., Chen, X., Sun, B., Sterling, C., and Tank, A.W. (2007). Evidence for regulation of tyrosine hydroxylase mRNA translation by stress in rat adrenal medulla. *Brain Res* 1158**,** 1-10.

Xu, L., Sterling, C.R., and Tank, A.W. (2009). cAMP-mediated stimulation of tyrosine hydroxylase mRNA translation is mediated by polypyrimidine-rich sequences within its 3'-untranslated region and poly(C)-binding protein 2. *Mol Pharmacol* 76**,** 872-883.

Xu, N.J., and Henkemeyer, M. (2009). Ephrin-B3 reverse signaling through Grb4 and cytoskeletal regulators mediates axon pruning. *Nat Neurosci* 12**,** 268-276.

Xu, N.J., and Henkemeyer, M. (2012). Ephrin reverse signaling in axon guidance and synaptogenesis. *Semin Cell Dev Biol* 23**,** 58-64.

Xu, Y., Moseley, J.B., Sagot, I., Poy, F., Pellman, D., Goode, B.L., and Eck, M.J. (2004). Crystal structures of a Formin Homology-2 domain reveal a tethered dimer architecture. *Cell* 116**,** 711-723.

Xue, B., Leyrat, C., Grimes, J.M., and Robinson, R.C. (2014). Structural basis of thymosin-beta4/profilin exchange leading to actin filament polymerization. *Proc Natl Acad Sci U S A* 111**,** E4596-4605.

Xue, B., Zhao, Y., Johnson, A.K., and Hay, M. (2008). Central estrogen inhibition of angiotensin II-induced hypertension in male mice and the role of reactive oxygen species. *Am J Physiol Heart Circ Physiol* 295**,** H1025-H1032.

Yanes, L.L., Romero, D.G., Moulana, M., Lima, R., Davis, D.D., Zhang, H., Lockhart, R., Racusen, L.C., and Reckelhoff, J.F. (2011). Cardiovascular-renal and metabolic characterization of a rat model of polycystic ovary syndrome. *Gend Med* 8**,** 103-115.

Yang, C., Kim, H.S., Seo, H., and Kim, K.S. (1998). Identification and characterization of potential cis-regulatory elements governing transcriptional activation of the rat tyrosine hydroxylase gene. *J Neurochem* 71**,** 1358-1368.

Yang, N.Y., Fernandez, C., Richter, M., Xiao, Z., Valencia, F., Tice, D.A., and Pasquale, E.B. (2011). Crosstalk of the EphA2 receptor with a serine/threonine phosphatase suppresses the Akt-mTORC1 pathway in cancer cells. *Cell Signal* 23**,** 201-212.

Yang, S.H., Jaffray, E., Hay, R.T., and Sharrocks, A.D. (2003). Dynamic interplay of the SUMO and ERK pathways in regulating Elk-1 transcriptional activity. *Mol Cell* 12**,** 63-74.

Yassin, D.J., Doros, G., Hammerer, P.G., and Yassin, A.A. (2014). Long-term testosterone treatment in elderly men with hypogonadism and erectile dysfunction reduces obesity parameters and improves metabolic syndrome and health-related quality of life. *J Sex Med* 11**,** 1567-1576.

Yeap, B.B., Hyde, Z., Almeida, O.P., Norman, P.E., Chubb, S.A., Jamrozik, K., Flicker, L., and Hankey, G.J. (2009). Lower testosterone levels predict incident stroke and transient ischemic attack in older men. *J Clin Endocrinol Metab* 94**,** 2353-2359.

Yoon, J., Kim, S.B., Ahmed, G., Shay, J.W., and Terman, J.R. (2017). Amplification of F-Actin Disassembly and Cellular Repulsion by Growth Factor Signaling. *Dev Cell* 42**,** 117-129 e118.

Yoon, S.O., and Chikaraishi, D.M. (1994). Isolation of two E-box binding factors that interact with the rat tyrosine hydroxylase enhancer. *J Biol Chem* 269**,** 18453-18462.

Yu, G., Luo, H., Wu, Y., and Wu, J. (2003a). Ephrin B2 induces T cell costimulation. *The Journal of Immunology* 171**,** 106-114.

Yu, G., Luo, H., Wu, Y., and Wu, J. (2003b). Mouse ephrinB3 augments T-cell signaling and responses to T-cell receptor ligation. *Journal of Biological Chemistry* 278**,** 47209-47216.

Yu, G., Luo, H., Wu, Y., and Wu, J. (2004). EphrinB1 is essential in T-cell-T-cell co-operation during T-cell activation. *Journal of Biological Chemistry* 279**,** 55531-55539.

Yu, G., Mao, J., Wu, Y., Luo, H., and Wu, J. (2006). Ephrin-B1 is critical in T-cell development. *Journal of Biological Chemistry* 281**,** 10222-10229.

Yu, J., Akishita, M., Eto, M., Koizumi, H., Hashimoto, R., Ogawa, S., Tanaka, K., Ouchi, Y., and Okabe, T. (2012). Src kinase-mediates androgen receptor-dependent non-genomic activation of signaling cascade leading to endothelial nitric oxide synthase. *Biochem Biophys Res Commun* 424**,** 538-543.

Yu, J., Bulk, E., Ji, P., Hascher, A., Tang, M., Metzger, R., Marra, A., Serve, H., Berdel, W.E., Wiewroth, R., Koschmieder, S., and Muller-Tidow, C. (2010). The EPHB6 Receptor Tyrosine Kinase Is a Metastasis Suppressor That Is Frequently Silenced by Promoter DNA Hypermethylation in Non-Small Cell Lung Cancer. *Clinical Cancer Research* 16**,** 2275-2283.

Yu, X., Li, F., Klussmann, E., Stallone, J.N., and Han, G. (2014). G protein-coupled estrogen receptor 1 mediates relaxation of coronary arteries via cAMP/PKA-dependent activation of MLCP. *Am J Physiol Endocrinol Metab* 307**,** E398-407.

Yuan, P., Leonetti, M.D., Pico, A.R., Hsiung, Y., and Mackinnon, R. (2010). Structure of the human BK channel Ca2+-activation apparatus at 3.0 A resolution. *Science* 329**,** 182-186.

Yue, P., Chatterjee, K., Beale, C., Poole-Wilson, P.A., and Collins, P. (1995). Testosterone relaxes rabbit coronary arteries and aorta. *Circulation* 91**,** 1154-1160.

Zabransky, D.J., and Park, B.H. (2014). Estrogen receptor and receptor tyrosine kinase signaling: use of combinatorial hormone and epidermal growth factor receptor/human epidermal growth factor receptor 2-targeted therapies for breast cancer. *J Clin Oncol* 32**,** 1084-1086.

Zanchetti, A., Facchetti, R., Cesana, G.C., Modena, M.G., Pirrelli, A., Sega, R., and Participants, S. (2005). Menopause-related blood pressure increase and its relationship to age and body mass index: the SIMONA epidemiological study. *J Hypertens* 23**,** 2269-2276.

Zhang, D., Kanthasamy, A., Anantharam, V., and Kanthasamy, A. (2011). Effects of manganese on tyrosine hydroxylase (TH) activity and TH-phosphorylation in a dopaminergic neural cell line. *Toxicol Appl Pharmacol* 254**,** 65-71.

Zhang, X., Ge, Y., Bukhari, A.A., Zhu, Q., Shen, Y., Li, M., Sun, H., Su, D., and Liang, X. (2019a). Estrogen negatively regulates the renal epithelial sodium channel (ENaC) by promoting Derlin-1 expression and AMPK activation. *Exp Mol Med* 51**,** 1-12.

Zhang, Z., Tremblay, J., Raelson, J., Sofer, T., Du, L., Fang, Q., Argos, M., Marois-Blanchet, F.C., Wang, Y., Yan, L., Chalmers, J., Woodward, M., Harrap, S., Hamet, P., Luo, H., and Wu, J. (2019b). EPHA4 regulates vascular smooth muscle cell contractility and is a sex-specific hypertension risk gene in individuals with type 2 diabetes. *J Hypertens* 37**,** 775-789.

Zhao, C., Irie, N., Takada, Y., Shimoda, K., Miyamoto, T., Nishiwaki, T., Suda, T., and Matsuo, K. (2006). Bidirectional ephrinB2-EphB4 signaling controls bone homeostasis. *Cell Metab* 4**,** 111-121.

Zhao, T.J., Sakata, I., Li, R.L., Liang, G., Richardson, J.A., Brown, M.S., Goldstein, J.L., and Zigman, J.M. (2010). Ghrelin secretion stimulated by {beta}1-adrenergic receptors in cultured ghrelinoma cells and in fasted mice. *Proc Natl Acad Sci U S A* 107**,** 15868-15873.

Zitzmann, M. (2007). Mechanisms of disease: pharmacogenetics of testosterone therapy in hypogonadal men. *Nat Clin Pract Urol* 4**,** 161-166.
Zitzmann, M. (2009). Testosterone deficiency, insulin resistance and the metabolic syndrome. *Nat Rev Endocrinol* 5**,** 673-681.
Zukowska-Grojec, Z. (1995). Neuropeptide Y. A novel sympathetic stress hormone and more. *Ann N Y Acad Sci* 771**,** 219-233.